Influence of material conditioning on tools wear of EPBS machines using different laboratory test

Doctoral Dissertation
Doctoral Program in Environmental Engineering (30th Cycle)

Influence of material conditioning on tools wear of EPBS machines using different laboratory test.

Cristina Gabriela Oñate Salazar

* * * * * *

Supervisor

Prof. Daniele Peila

Doctoral Examination Committee:

Prof. Domenico Antonio De Luca, Università di Torino
Prof. Monica Barbero, Politecnico di Torino
Prof. Anna Siemińska – Lewandowska, University of Warsaw
Prof. Andrè Assis, Universidade de Brasília
Prof. Maria Migliazza, Politecnico di Torino
Eng. Daniele Martinelli, Politecnico di Torino

May 7, 2018

I hereby declare that, the contents and organisation of this dissertation constitute my own original work and does not compromise in any way the rights of third parties, including those relating to the security of personal data.

Cristina Gabriela Oñate Salazar

Turin, May 7, 2018

A mis padres

"El mundo pertenece a quien sale a buscarlo" es una frase que se escucha mucho en mi hogar. He salido a buscarlo, pero mi corazón nunca ha dejado de estar ahí con ellos. Mis padres me han inspirado e impulsado siempre a ser la mejor versión de mí, por eso me encuentro aquí, culminando otro objetivo, que sin su apoyo y amor no hubiese sido posible.

Acknowledgment

Quisiera agradecer a mis padres y hermanos porque su amor me mantiene de pie y me hace fuerte ante cualquier obstáculo, con ustedes no hay imposibles y por ustedes todo vale la pena. Gracias por la confianza, el amor y el apoyo.

Gracias a la mejor barra y mejor equipo de mi vida: mi familia Salazar. Su amor me llega y colma dondequiera que esté, sus oraciones me acompañan y el deseo de volverlos a ver me inspira y me impulsa cada día.

Ringrazio i miei colleghi Carmine, Andrea, Liliana e Daniele, per le tante prove realizzate insieme, per i consigli e il supporto, ma soprattutto per aver fatto sì che da un rapporto lavorativo potesse nascere un'amicizia così salda e sincera. Tra questi nella fattispecie rivolgo un ringraziamento speciale a Carmine, che mi ha supportata dal primo all'ultimo giorno nello svolgimento di questa Tesi di dottorato. Senza di te la strada sarebbe diventata troppo lunga e complicata.

Grazie a Daniele Peila per avermi ispirata a scoprire il mondo delle gallerie attraverso il suo entusiasmo e amore verso ciò che fa. Grazie per tutte le opportunità che mi ha offerto fino ad oggi.

Grazie alla Prof.ssa Marini, al Sig. Claudio, a Mureu, a La Placa, a Rino, ai tecnici del Laboratorio di Strade del DIATI, ai tecnici del Laboratorio di Caratterizzazione Meccanica del DISAT, alla MAPEI S.p.A. e a tutti quelli che hanno reso possibile la realizzazione delle 474 prove di usura e altrettante analisi per questo lavoro di ricerca.

Gracias infinitas a Pachi y a Dai por cubrir mis limitaciones lingüísticas con tanta paciencia y esfuerzo, ahora son casi ingenieras.

Grazie alla famiglia Politeam estesa, a Dona ed Andrea, a Hilmar e a tutti quelli (anche quelli nominati precedentemente) che mi hanno fatta sentire a casa gli ultimi sei anni della mia vita. Grazie a voi mi porto l'Italia nel cuore.

Gracias a mis amigas Caro y Gie, por los más de 15 años de cariño y apoyo.

Agradezco a Dios por guiarme y protegerme siempre y por premiarme con todas estas maravillosas personas a quien hoy tengo la dicha de agradecer.

Summary

Underground construction in urban areas that need more efficient transportation systems, energy and water supplies is a very challenging task, due to the complexity of the work itself and because surface disturbances and subsidences require to be minimized. In order to face the challenge and allow the excavation of tunnels even with low overburdens, Earth Pressure Balance Shields (EPBS) technology has been increasingly used in the recent years.

EPBS is a type of tunnel boring machine (TBM) with earth pressure support. By transforming the excavated material into a soft paste that has plastic properties to be used as support medium, it is possible to balance the pressure conditions at the tunnel face allowing minimum settlement. In addition, uncontrolled inflow of soil and water into the machine is avoided and tunnelling process becomes more effective.

In order to better understand soil behaviour and improve the performance of the EPBS machine, two variables are studied: soil conditioning and tools wear.

During excavation with EPB machines the correct soil conditioning is a very important parameter to be controlled. For this reason, it is critical to perform preliminary tests with different conditioning agents in order to determine the most suitable reference dosage for an excavation project. Currently, soil conditioning is evaluated by performing slump tests and plasticity and homogeneity checks of the dough at laboratory scale. There is also the Extraction Test used to evaluate material extraction that is one of the most realistic tests to know the behaviour that soil could develop during excavation process.

On the other hand, a very important but still less studied variable is the wear of EPBS metal parts like excavation tools, rotating head, shield and screw conveyor. Wear leads to a reduction in working yield due to the mentioned machine components lose their optimum properties and have to be replaced; consequently, downtime is required in order to execute proper maintenance, which is difficult and dangerous.

Many aspects play key roles in the wear process like excavated medium, water content, applied pressure, soil conditioning and type of metal used for machine tools manufacturing. In fact, rocks and soil excavated during EPB work can be composed from any kind of minerals. Hard minerals increase the wear phenomenon that concerns all parts of the machine where there is friction between

metallic part and the medium. For this reason, study of wear phenomenon is an extremely important issue for new projects with EPB excavation technology.

Therefore, the objective of this work is to study of the influence of soil conditioning on tools wear and the relationship of the main factors associated to this phenomenon. In order to accomplish this goal, about 26150 kg of different soils were studied using 4 different wear test methods.

These tests were based on the application of a test methodology already used in the Tunnels and Underground Works Laboratory of Politecnico di Torino and other new methodologies and equipment, developed with the aim of deepening the study of wear taking into account several variables that concern the construction of tunnels. Each methodology implemented has different benefits, limitations and scopes, but provides congruent technical results.

Finally, prediction indexes were proposed in order to evaluate tool wear phenomenon and compare the effects of different soil conditioning. As a result, better decisions are made when choosing the ideal conditioning for EPB tunnelling, maximizing projects effectiveness and success.

Contents

List of Tables

List of Figures

Chapter 1

Introduction

The constant growth of the population has led to the continuous search for technologies and techniques of construction that allow the execution of increasingly complex and innovative engineering works. In urban areas, engineering projects and works have to be build underground due to the lack of space on the surface. In order to reduce environmental impact and avoid connection problems with old works, many new projects are planned to be realized in underground spaces.

Technically, underground construction in urban areas is a big challenge, especially because surface disturbances, including subsidence, vibration and noise, must be minimized. In order to solve these problems and allow the excavation of tunnels even with low overburdens, EPB (Earth Pressure Balance) technology has been implemented with greater diffusion in recent years.

1.1 Construction of tunnels with EPB

The full section excavation machines, called TBM (Tunnel-Boring Machines), of EPB type are increasingly used and currently represent the most advanced common tunnel excavation technology in urban areas, especially in the presence of granular soils.

The EPB excavation technique is based on the ability to counterbalance the geostatic pressure of the front TBM face using the same excavated soil and to adapt to excavation conditions in the presence of water.

The machine has a rotating head and it is equipped with cutting knives and/or discs or rippers in function of the geology.

Once excavated, the soil enters into a chamber behind the cutting head where it is properly conditioned and mixed until reaching a soft and pasty consistency, suitable for the transmission of pressure from the head to the tunnel face.

The excavated material is extracted by means of a screw conveyor, which extracts the material from the storage chamber and transfers it by conveyor belts onto muck wagons or other conveyors belts for transport.

The pressure on the excavation face is maintained by balancing the volume of material excavated in function of the machine thrust towards the ground and the volume of material inside the storage chamber, which is regulated by the extraction of the soil through the screw conveyor. The conditioned soil inside the excavation chamber ensures the application of back-pressure to the excavation face. Furthermore, it creates a “seal” that protect the screw conveyor from water of any crossed aquifer.

Then, conditioning is used to modify the physical and chemical properties of the soil making it plastic, pasty and impermeable so as to allow the most accurate control of the pressure at the excavation face, avoiding superficial subsidence, caused by water inside the machine, facilitating the extraction of the muck and reducing tool wear.

An important parameter to control during excavation is the correct soil conditioning. For this reason, it is essential to carry out a prior study of the soil with different conditioning agents, in order to choose the most suitable reference dosage for excavation. Moreover, engineer experience can lead to a good control of conditioning process also for geology changes where adaptations of conditioning parameters could be required.

Nowadays, at laboratory level, soil conditioning is evaluated by performing slump tests and plasticity and homogeneity checks of the dough. There is also a test to evaluate material extraction, which is currently one of the most realistic tests on the performance that soil could have during excavation.

1.2 Wear

A very important but still less studied variable is the wear of the TBM metal parts, such as excavation tools, the rotating head, the shield and the extraction screw conveyor. Wear leads to a reduction in working yield due to the above machine components lose their optimum properties and have to be replaced, so downtime is required in order to allow proper maintenance, which is difficult and dangerous.

The study of wear phenomenon is an extremely important issue for new projects with EPB excavation technology. Many aspects play key roles in the abrasion process like the type excavated medium, water content, applied pressure, air conditioning and type of metal used for the machine. In fact, rocks and soil excavated during EPB work can be composed from any kind of minerals. Hard minerals increase the wear phenomenon that concerns all parts of the machine where there is friction between metallic part and excavated / to excavate medium.

Several research centers worldwide are interested in the technical hitches related to EPB excavation. The aim of the research projects is to understand the

excavation mechanism and the wear phenomenon due to the contact between the soil and the metallic parts, rotating to perform the excavation.

The operation of replacement of machine components every time that are consumed is performed by operators who work in hyperbaric conditions. This type of operation is technically complex and requires long operating periods. Therefore, the minimization of the number of interventions related to part changes is a central prerogative in order to reduce the associated risks, as well as optimize the economic resources on the total cost of the work.

It would be important to have a reliable estimate of the wear of excavation components or at least a solid knowledge of what factors could increase or decrease this phenomenon. This awareness would bring economic advantages, a better organization to carry out the work and technological and productive improvements.

The presence of foaming agents and polymers on the excavation face together with highly heterogeneous soil conditions make it difficult to apply the known predictive models on wear that are used in literature for other types of soil.

1.3 Objectives

This thesis is based on the application of a test methodology used in the Tunnels and Underground Works Laboratory of Politecnico di Torino and developed in other methodologies and equipment, with the aim of deepening the study of wear, taking into account several variables that concern the construction of tunnels.

The aim of the developed laboratory tests is to study the interaction between the metal used for original machine tool, the soil and the operative parameters like pressure, conditioning design and water content. Two procedures were suggested based on the existing equipment and a new and innovative machine was designed and built with the purpose of simulate the chamber at laboratory scale.

The objective of this thesis, in addition to the presentation of four (4) test methods, is to establish a relationship among the main factors that influence wear, such as conditioning agents, presence of water and soil pressure. In addition, prediction indexes will be proposed in order to evaluate tool wear phenomenon and compare the effects of different soil conditioning; as a result, better decisions can be made when choosing the ideal optimal conditioning set for EPB tunnelling.

Chapter 2

EPB machines

In general, EPBS machines are mechanical devices which work by applying a pressure at the face of the tunnel to counterbalance earth pressures. They operate as follows: excavation face is supported by pressurizing earth inside the cutterhead chamber. Earth pressure in the chamber is regulated by the rate of material discharge through the screw conveyor. In other words, the material is extracted by means of the screw conveyor. By varying the thrust force and the screw conveyor removal speed, the ground balancing pressure is controlled ensuring the stability of the front face and minimizing settling on the surface.

Functions of the Earth Pressure Balance Shield (EPBS) machine can be summarized in four main steps:

1. Excavating the Ground
2. Supporting the Ground
3. Removing and disposal of the excavated materials
4. Advancing

They operate in the following modalities:

- **Open:** Used when the tunnel face is stable. The excavation system can be manual with an excavation arm or a rotating head.
- **Closed:** Used when the tunnel face is significantly unstable. There are described other closed modes that include different elements such as piston pumps and slurryfying box for transport.

The EPBS machine is able to operate in both modes, the open mode (non-pressurized excavation chamber) and the closed mode (pressurized excavation chamber). It has several components. The rotating cutterhead equipped with several cutting/crushing elements, the protective shield, the screw conveyor, which removes the earth from the pressurized chamber as the excavation progresses, allowing the pressure inside the chamber to be controlled. For the

advance phase there is the thrust system, composed by longitudinal hydraulic jacks supported against the lining of prefabricated segments.

2.1 Operational principles

The need to excavate tunnels without causing surface damage or disturbance to the groundwater system has attracted the interest of engineers for over 150 years and continues to do so.

Urbanized areas are a particularly difficult space for the excavation of tunnels due to the high presence of infrastructures, services and numerous problems that can be encountered, such as (Kovari, 2004):

- low overburdens;
- existing structures in surface;
- forced trajectories;
- presence of unknown elements along the tunnel route;
- restrictions of alignment, access to the tunnel and site investigations;
- high impact and potential damage to surface structures;
- complexity on improve the quality of the overburden soil from the surface;
- poor mechanical resistance of the soil that, in the case of surface tunnels, could cause: superficial collapses, excessive surface subsidences.

In order to face these problems, a machine that applies a counterbalance pressing force in the front face can be used. This is possible by using an EPB shield.

EPB machines support the excavation face with the soil already excavated subjected to pressure in the excavation chamber, thus preventing uncontrolled entry of the excavated soil into the chamber. The soil is then pulled out through a screw conveyor from the pressure chamber to the area under atmospheric pressure. To balance the pressure difference, there must be a suitable pressure gradient over the entire length of the screw conveyor.

The operation of the active excavation face support in EPB machines is described in Figure 1. The ground is excavated by the cutterhead and transported into the excavation chamber (bulk chamber), at the back of which there is the pressure bulkhead. The support pressure in the excavation chamber is regulated through the control of supply (advance rate of the jacks of advancement that generates a rise of pressure ahead the cutterhead; addition of conditioning agent at the injection point) and removal (volume of spoil transported by the screw conveyor). After the required stroke length of the advancement jacks has been reached, the erector is used to install the segments (modified from Peila, et al., 2009).

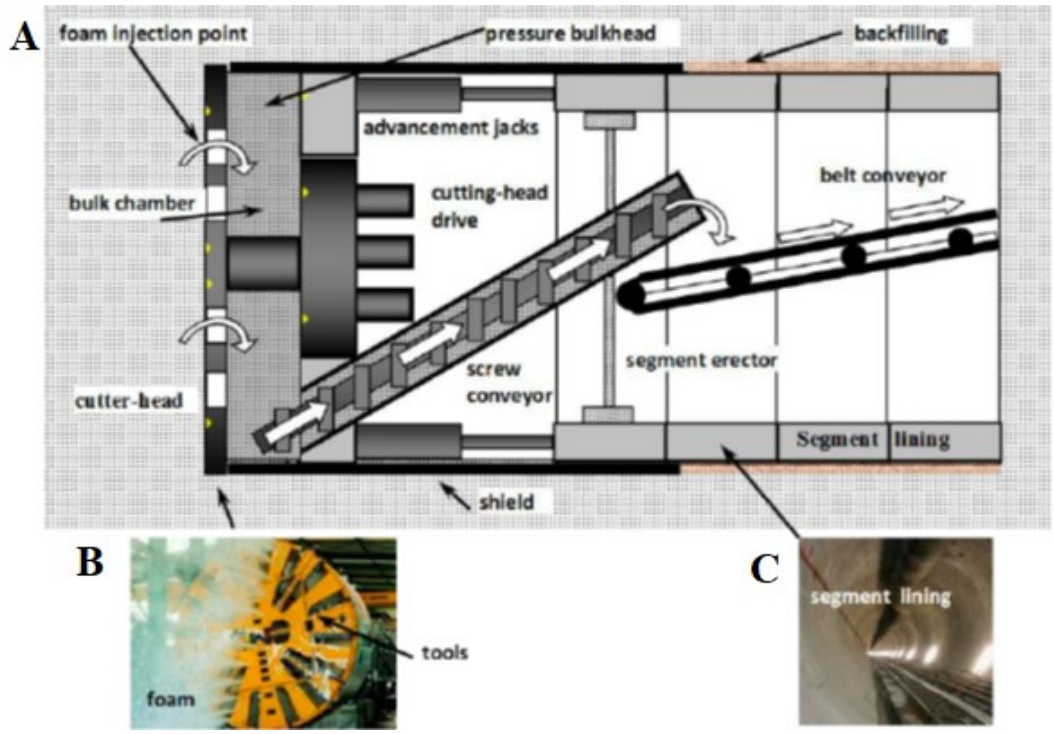

Figure 1. Schematic drawing of EPB shield machine elements: A) Transversal section with main components. B) Cutting tools and Foam injection point on the Cutterhead. C) Installed segment lining. (modified from Peila et al., 2009).

The EPB working operational principle is to fill the pressure chamber with the excavated soil. Properties of ground are changed by the conditioning process and by the application of pressurization that make the so obtained material able to withstand excavation face collapses or movements.

The advancement of the machine blocks the material in the diaphragm that is created between the excavation face and the head, allowing the transfer of the thrust of hydraulic pistons of the shield to the material contained in the diaphragm, exerting on the excavation face the pressure necessary to counterbalance that exerted by the excavated soil. Therefore, the excavation operation must be carried out in such a way that, by operating on the hydraulic pistons and on the screw conveyor discharge speed, the pressure exerted is able to counterbalance, straightaway, the pressure present at the front face.

The essential condition for a regular operation is that the soil removed at the front face moves uniformly from the pressure chamber to the discharge point of the screw conveyor. Therefore, the basic principles of the balanced pressure discharge system can be deduced. According to what has been said, the excavated soil must be removed and then continuously unloaded through the screw conveyor, while maintaining sufficient pressure on the ground at the excavation face.

Using a screw conveyor as mean of transportation and discharge and, since the diameter of the screw conveyor is smaller than the cutterhead one, it is necessary that the soil has adequate fluidity and plasticity to allow itself a uniform movement towards the entrance of the discharge point. If the material to be

excavated does not reach these requirements, the muck will not be able to move uniformly, causing an arc effect and producing inhomogeneties inside the diaphragm through which the water present at the front face would be able to flow freely inside the machine, causing a potential collapse of the front face.

It is also essential to provide a system able to controlling the water present at the front face while working in the excavation phase. In fact, even if the ground completely fills the excavation chamber and the discharge conveyor belt, it also must have enough strength to hold the front face. If the material is so permeable that water flows through the conveyor belt until reaching the machine, it may be able to flood it. It is evident from these considerations, that it is crucial to guarantee the impermeability of conditioned soil.

Operationally, when the machine moves forward must be able to keep the pressure chamber completely full, support the front face and dig up the muck.

The best way in order to do this operation is to constantly check the volume of excavated material and the volume of the material that has been dug up, in order to guarantee the same value between them.

There are two ways of achieving this goal:

- The volumes are balanced between excavated and unloaded materials; i. e. the machine is moved forward at a speed that excavates a volume of soil equivalent to the one extracted from the screw conveyor in a specific interval of time (1 min.). With this method it is difficult to have real time control, since there is a physical delay between excavation and unloading operations.
- The quantity of material excavated is evaluated by calculating the volume of material removed and correlated with the number of revolutions of the discharge screw conveyor. Frequently, it is used a formula (1) that defines the direct proportionality between the cross section of the screw conveyor (A), the number of screw conveyor revolutions (N), the pitch between the screw conveyor blades (P) and the discharge coefficient of the screw conveyor (ε):

$$Q = \varepsilon \cdot A \cdot N \cdot P \qquad \text{Equation (1)}$$

As previously mentioned, the purpose of the counterbalanced pressure excavation method is to give stability to the excavation face. The applied pressure must be enough in order to control ground and water, if present.

In general, the pressure on the excavated ground, which does not determine any variation on the front face, is that established by the following formula:

$$P_A + P_W < P < P_P + P_W \qquad \text{Equation (2)}$$

Where P_a represents the active pressure of the soil, P_p is the passive pressure of the soil and P_w is the pressure of the water flow. The two pressures, P_a and P_p, are obtained by calculation, based on the initial conditions of the soil, i. e. the soil conditions before the drill process. By keeping the applied pressure in the aforementioned range, it is possible to use EPB technology without problem of collapse. In other words, the thrust of the pistons and the screw conveyor speed

must be controlled so that the shield always operates by providing a front face pressure between the active and passive pressure values.

This pressure is generated inside the chamber and is evenly spread to all the excavation face through suitable openings (muck buckets).

2.2 Description of the machine

As previously mentioned, the operating drilling principle is based on the concept that the machine proceeds in the excavation process by means of the tools placed on the cutterhead. The excavated material is introduced into the space behind the head and there it is properly mixed with the additive in a suitable quantity according to the characteristics of the soil. In the most modern machines proposed by Herrenknecht, et al., 2011, the additive is injected into the front of head and then mixed with the soil in the chamber (Figure 2). The used additive is foam and consists of a solution of water, foaming agent and polymers that are used for changing the properties of the soil in order to make it able to stabilize the excavation face.

The injection volume of the additive can surpass 100% of the excavated volume, if the tunnel face conditions are particularly problematic. At this point, an amalgam with an adequate degree of viscosity is obtained; it possesses different characteristics from the excavation soil. A conditioned soil has different specific weight (usually lighter than unconditioned ones) and it is less permeable and with higher plasticity than in situ ones. This conditioned soil continuously fills the chamber and the screw conveyor, also if the machine is stopped.

Figure 2. Foam production during works assembly, EPB shield Metro Valencia, 1995 (Herrenknecht, et al., 2011).

The required pressure is given by the conditioned soil, which push the shield of the machine forward. This is achieved by means of the full face cutterhead of the machine. The correct pressure to be applied is obtained when the machine starts the excavation operations, and the measured soil values are obtained and confirmed, taking into account overburdens, water inflow if present, and other factors.

The pressure on the conditioned soil can be easily varied by working on the hydraulic cylinders and the discharge screw conveyor. In summary, the functioning mechanism of EPBS lies on three key operations:

(a) Creation of conditioned soil;

(b) Stabilization of the excavation face by exerting pressure on the conditioned soil;

(c) Control of the excavation by working simultaneously on the screw conveyor rotation speed and the thrust system.

2.2.1 Cutterhead

The cutterhead has a different configuration from the Slurry Shield one. In general, the cutterhead has a "star" conformation made up of tooling arms that define a larger free surface area (Figure 3). The openings generally have a width of 0.2–0.3 m, so the ratio between free and total surface ranges from 15–40%, compared to Slurry Shields. This feature facilitates the entrance of the soil into the excavation chamber, and consequently more the front face stability possible. The shape and size of the head depends on the geological conditions as well as the type, the number and shape of tools. In principle, the cutterhead can have four different configurations. Below is a brief classification.

Figure 3. Cutterhead of EPB machine.

- ***Central shaft system*** (Figure 4) - has a single sealing gasket on the central shaft. This configuration has been studied to operate in the most abrasive soils, in fact the bearing is unique and the number of sealing gaskets is limited to the shaft area only. The screw conveyor is positioned at the bottom, ensuring an efficient removal of spoil.

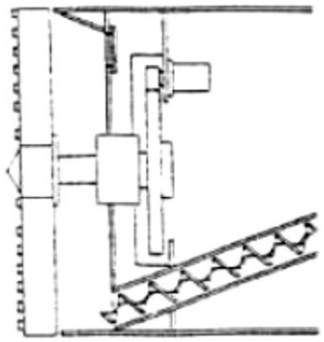

Figure 4. Cutterhead central shaft system.

- ***Central cone system*** (Figure 5) - there is no central shaft but a peripheral support, a sort of circular crown, to which the rotation is transmitted by the peripheral gears. This is a system that maximizes the volume in the excavation chamber; it is very easy to replace the mixing blades and is used in soils with high adhesion problems.

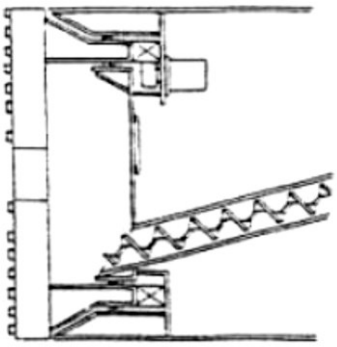

Figure 5. Cutterhead central cone system

- **Intermediate system** (Figure 6) - is a system that targets to increase the available volume within the chamber by using a small central shaft and peripheral supports. It is easy to assemble, making it suitable when problems of ground adhesion to the chamber walls are anticipated. This configuration allows a significantly higher torque to be applied to the head.

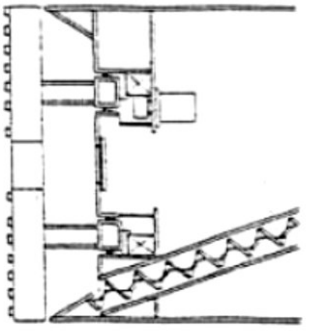

Figure 6. Cutterhead intermediate system

- ***Drum system*** (Figure 7) – it is similar to the one used for hard rock TBMs. It allows the installation of a large diameter screw conveyor placed at the centre of the excavation chamber. As a result, the screw conveyor has a low inclination, which is considered an unfavourable factor when there is very high water pressure. In this system is also impossible to prevent soil from adhering to the bottom of the chamber.

The counter-pressure shield works by loading the excavated soil into the chamber until it is completely filled. This combined volume of soil prevents the front collapses and creates an impermeable wall inside the screw conveyor that counteracts the possible inflow of water. The shield head forms an independent body; in fact, it is the first to be built and the last to be installed during the assembly phase.

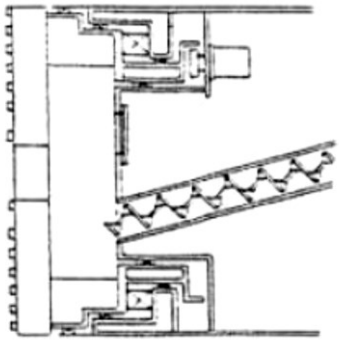

Figure 7. Cutterhead drum system

2.2.2 Cutting Tools

In addition to conventional cutting tools, TBM EPBS are also equipped with:

1. ***Fishtail bit***: it is a particular tool that has two curved steel blades shaped like a fish tail. It is placed on the hub in which the mixing blades are located. Its central position on the head is intended to excavate deeper in the front face centre, before the other bit tools act, facilitating the excavation, as they crack the area adjacent to that affected by the fishtail bit. Depending on the characteristics of the soil, these bits protrude more or less. The theory, on which its purpose is based, is equivalent to the theory applied to explosive excavation, on which is often predicted the presence of a discharge borehole on the front.
2. ***Reamer tools***: these are used for the excavation of gravel layers, with particularly hard material insertions. They are characterized by widia inserts, fixed by a reinforced welding.
3. ***External bits***: they have a particular geometry. They are placed on the external circumference and their goal is to ensure that the diameter of the excavated borehole meet the specifications, even if the tools are worn.

Their peculiar characteristic is that they can attack the immediate soil and at the same time push it evenly towards the mixing chamber. They are useful for very dense clays.

This method of excavation (in which the centre of the front face is attacked by the fishtail bit and successive extensions are made with the reamer tools) allows an excavation that goes from the centre to the outer circumference, and makes it possible to attack more effectively even the most difficult soils.

All bits used have tungsten carbide inserts and are resistant and suitable for use in gravel soils. The tools can be rotated by oscillating motion to reduce the number of replacements caused by wear of metallic parts.

2.2.3 Excavation chamber

It is the space between the cutterhead or cutting wheel and the bulkhead. It is the machine part that is filled with soil or slurry to stabilize the front under soil pressure.

It is not possible to give a precise definition of the support medium of an EPB, since the latter is a mixture of excavated soil and additives, which can be foaming and/or polymeric agents that condition the excavated material. This material is contained in the excavation chamber, which takes on different names depending on the terminology used.

The conditioned soil, thanks to the rotating action of the cutting wheel and the thrusting action of the hydraulic jacks, is introduced into the chamber in question, from which it is extracted by means of the screw conveyor located at the base of the chamber. The action of the screw conveyor allows the continuous support of the front due to its rotation proper for the extraction of the conditioned soil.

2.2.4 Control system

Controlling the ground pressure in the chamber has a fundamental importance. Pressure data is monitored by using a series of sensors installed in the closing bulkhead of the excavation chamber and in the cutterhead (usually for a shield of 6-8 m in diameter there are three sensors in the cutterhead and 4-6 in the bulkhead, but they can be increased according to the needs and dimensions of each machine). The operating principle is based on the Weatstone's bridge. If they are in direct contact with the ground, they can be easily damaged. For replacement (to avoid having to intervene directly in the camera) an automatic replacement system has been designed by simple rotation of the support on which these sensors are fixed.

The pressure values recorded in the chamber are transmitted to the control central unit, which allows adjusting the thrusting speed of the jacks, the rotation speed of the screw conveyor and the cutting wheel. Pressure controls on the front and parity between weight and volume of removed and excavated spoil are of major importance.

- ***Measurement of excavated volume***: the theoretical volume of soil excavated in a fixed period of time is obtained by multiplying the advancement of the shield at that time by the surface of the head. This parameter is used to check that the volumes are balanced. The theoretical and real values are continuously compared to avoid subsidences.
- ***Measurement of removed volume***: The rotation speed of the screw conveyor, used to control the pressure, is measured with a transducer and the volume of soil removed can be calculated. When the rotation speed of the screw conveyor has been measured, the excavated volume is calculated using the discharge capacity of the screw conveyor per turn, multiplied by the speed.

The discharge capacity is subject to several factors, such as the physical properties of the excavated soil, the pressure difference between inlet and outlet of the screw conveyor, the degree of filling of the screw conveyor, the adhesion of the spoil within the screw conveyor, its deep angle and the abrasion of the propeller.

The main purpose of the screw conveyor rotation speed monitoring is to keep the pressure in the excavation chamber at the wanted value.

The described method for measuring the volume of soil removed is suitable for weak clays, where the disturbing factors previously examined are not relevant.

In other cases, it is preferable to use an ultrasonic wave conveyor system. The amount of spoil carried by a belt, installed at the screw conveyor outlet, is measured continuously by calculating the distance between a sensor and the surface of the spoil. The ultrasonic ray is reflected from the surface of the spoil, and the distance between the spoil surface and the ultrasonic source is calculated. The area of the accumulation section of transported spoil is calculated based on this data and according to the design of the conveyor belt.

2.2.5 Screw Conveyor

Archimedes screw or screw conveyor plays a fundamental role in the management of excavation. In fact, varying its speed increases or decreases the amount of soil removed, while varying its inclination or length directly affects the pressure of the water in the discharge.

There are three types of screw conveyor: central shaft system, shaftless system and a mixed alternative between these two types.

The central shaft screw conveyor is successfully used in the presence of strong water pressure, due to its superior structural strength. The movement is transmitted directly to the shaft by a helical geared motor system located on the screw conveyor head. This type of screw conveyor ensures high transmission efficiency but requires more space on the construction site as the discharge must be performed laterally.

The shaftless system ensures a larger volume for the spoil, since it offers the extra space that is occupied by the shaft in the central shaft system. This system is

suitable for the excavation of sands and gravels with rock blocks but, without high water pressure. If D is the diameter of the screw conveyor, the size of the rock blocks passing through it must be about 2/3 D, while the central shaft system can removed rock blocks not larger than 1/3 D.

The screw conveyor movement is transmitted by a complex system of gearwheels and sprockets, outlining a performance significantly inferior than central shaft system. The discharge can take place along the shaftless zone and therefore requires less space on the construction site.

The mixed system is mainly used with rock blocks presence. The first part of the screw conveyor has not a shaft in order to transport the blocks to a special outlet, from which they are discharged. When this auxiliary outlet opens, the main outlet on the screw conveyor head is automatically closed to guarantee its inner pressure.

Maintaining the pressure inside the screw conveyor is a very delicate topic. The aim is to reduce the pressure as gradually as possible, estimating a drop of approximately 0.2 bar per pitch of the propeller. Therefore, once the thrust to be applied to the front has been established, it must be increased proportionally to the pressure drop in the screw conveyor, due to the opening of the auxiliary outlet.

The diameter of the screw conveyor is closely related to the diameter of the shield, usually at a ratio of 1/5.

The number of revolutions depends on the volume to be removed. This is certainly a critical point in the management of the EPBS. In fact, the pressure at the front and the volume excavated are a function of the advance speed, while the volume extracted depends on the revolutions of the screw conveyors. Since parity between these volumes must be maintained, within the range of 95% excavated volume and 105% removed volume to ensure a tolerance of ±5%, it will be necessary to correlate the thrust velocity and rotation speed among them.

When the weights and volumes of excavated and removed soil are well balanced, there is no risk of collapse or extrusion of the front, but if the removed volume is greater than the excavated volume, undesirable subsidences may occur due to excessive disposal. If the volume is less than necessary, there is an overpressure in the surrounding soil that can lead to high consolidation.

The ratio between the volume removed *Vs* and the theoretical volume excavated *Vt* is equal to a percentage α value; the variation range of this parameter is determined by evaluating the shear limit on the front. The shear stress of the tunnel front for weak clays is given by Nishitake (1990) formula, equation (3):

$$\frac{P-P_0}{C_u} \geq 5.5 \qquad \text{Equation (3)}$$

Where, P is the total geostatic pressure; P_0 is the pressure acting on the front and C_u the undrained shear stress.

In the front, the difference in pressure is almost proportional to the volume of soil removed V_s and as a result it can be assumed that:

$$\alpha - 100 = \alpha \cdot (P - P_0) \qquad \text{Equation (4)}$$

Some experiments have shown that the coefficient α is inversely proportional to Young's elastic modulus (E) of the soil according to the following equation:

$$\alpha = \frac{50}{E} \qquad \text{Equation (5)}$$

Module E can be experimentally derived from the undrained shear strength:

$$E = 100 \cdot C_U \qquad \text{Equation (6)}$$

When excavation work is in soil with high permeability and consequently with high water pressures, suitable devices are used at the screw conveyor outlet to prevent unexpected entrance of soil and water. These systems allow the intermittent discharge by connecting the interior of the screw conveyor alternatively with the external environment.

The soil pressurization action is ensured inside the chamber by the accurate synchronism between the rotation speed of the Archimedes screw and the opening device.

2.2.6 Mixing blades

The mixing blades, assembled if necessary in the pressure chamber, are placed behind the spokes on which the tools are affixed. Their main task is to mix properly the conditioned soil created by the combination of excavated soil and additives.

The blades have different sections which are determined taking into account the type of soil, the shield diameter and other characteristics that should be evaluated in the laboratory.

Once the need of these blades has been studied in the laboratory, the design and the assembling phase can take place. When the design of the machine allows it, rotating blades can also be incorporated replacing the static ones.

2.2.7 Torque

Accurate prediction of cutterhead torque is crucial to the design and operation of an EPBM.

Using the Slurry Shield (SS) as a reference, it can be said that Earth Pressure Balanced Shield uses a much higher torque, as the spoil inside the chamber has higher friction resistance than the mud and ground suspension of the SS, with 80% muck.

The torque is empirically determined based on the diameter of the machine according to the following formula:

$$T = x \cdot D \cdot (t \cdot m) \qquad \text{Equation (7)}$$

Where D, is the shield diameter; x, t, m are variable coefficients ranging from 1 to 2.5, according to a study of Naitoh (1985).

Optimal pressure and torque values are determined during the execution phase by means of an experimental procedure at the beginning of the work project. This procedure is carried out on the basis of the experience acquired in previous works and operator's experience.

Optimal pressure and torque values are determined during the execution phase by means of an experimental procedure at the beginning of the work project. This procedure is carried out on the basis of the experience acquired in previous works and operator's experience.

Chapter 3

Wear Phenomenon

3.1 Wear mechanisms

Excavation process involves different types of motion contact between different types of soil and tools of the EPBS machine, causing damage to the cutting tools. As stated by Zum Gahr (1987), the mechanisms causing damage are plastic deformation, corrosion, cracks and wear. For the purposes of this work only wear will be considered.

According to the definition provided in DIN 50320 (acronym for Deutsches Institut für Normung - German Institute for Standardization) wear is "the progressive loss of material from the surface of a solid body due to mechanical action, i.e. the contact and relative motion against a solid, liquid or gaseous counterbody". In other words, it is the removal of material from one body when subjected to contact and relative motion with another body. Therefore, wear implies that the tool loses its volume and its geometrical properties. In general, tool wear depends on the following parameters: tool and work piece material, tool shape, cutting speed, feed, depth of cut, among others, and the characteristics of the surface where the tool is used.

To describe the different wear processes, wear type classifications are made. In this study, the wear-type classifications described by Zum Gahr (1987) and identified by the DIN have been used as a basis to determine what types of wear might be relevant to the wear of cutting tools.

Wear mechanisms describe the energetic and material interactions between the elements of a tribological system (known as *tribosystem*). A tribosystem consists of four principal elements: a body, a counterbody (opponent body), an interfacial medium (particles, lubricants, water, contaminants) and an environment (temperature, relative humidity, pressure) as shown in Figure 8. All these elements can affect each other and change the mechanism of interaction (KEY, 2016).

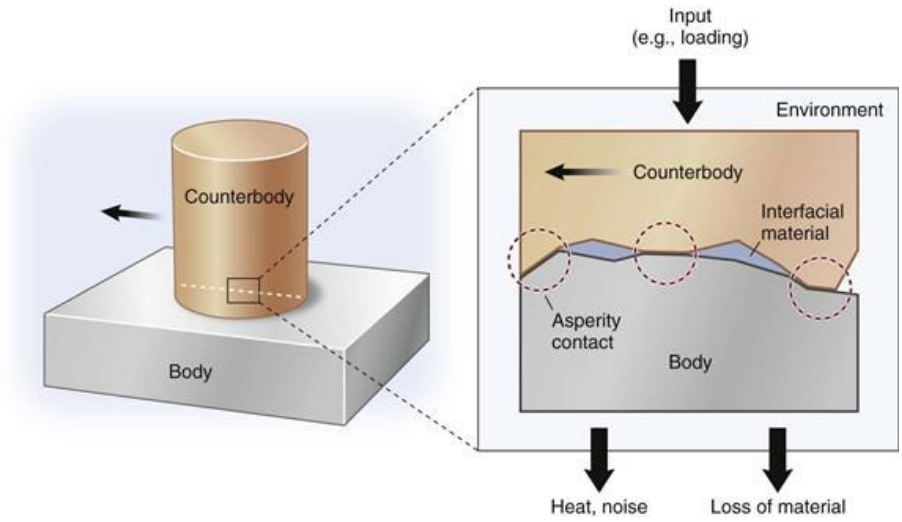

Figure 8. General description of a tribosystem, which consists of four elements: the two bodies in contact, the interfacial material, and the environment (KEY, 2016).

Depending on the parameters of a tribosystem, different wear mechanisms may occur. Each wear mechanism generates a characteristic wear appearance, also known as "wear pattern", observed through visible changes in surface structure. There are four main types of wear mechanisms based on DIN standards: adhesion, abrasion, tribochemical reaction and surface fatigue. The wear mechanisms are illustrated in Figure 9 (Zum Gahr, 1987) and explained in more detail below.

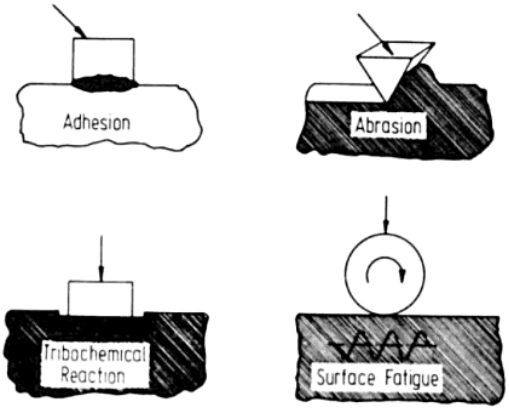

Figure 9. Schematic description of the four main wear mechanisms

Wear mechanisms are described by considering complex changes during friction. In general, wear does not take place through a single wear mechanism, so understanding each wear mechanism in each mode of wear becomes important (Kato & Adachi, 2000).

3.1.1 Adhesion

It is a wear mechanism described between two sliding bodies with plastic deformation phenomena occurring to one of the two bodies. This type of wear appears when surfaces slide against each other (Zum Gahr, 1987).

When two surfaces are brought together under load, asperities of those surfaces adhere to each other. Adhesion appears at low cutting temperatures (or cutting speeds) and high pressures cause pressure welds on tops of the surface irregularities (Figure 10).

There are several types of adhesive wear:

Galling wear: it is the extreme adhesive wear. Metal removal occurs due to tearing, breaking and melting of the metallic junctions;

Scuffing wear: characterized by the formation of grooves and scratches in the sliding direction;

Sliding wear: when one solid slides over another solid;

Oxidative wear: wear in un-lubricated ferrous systems.

Below, an illustration of the adhesion wear mechanism is shown.

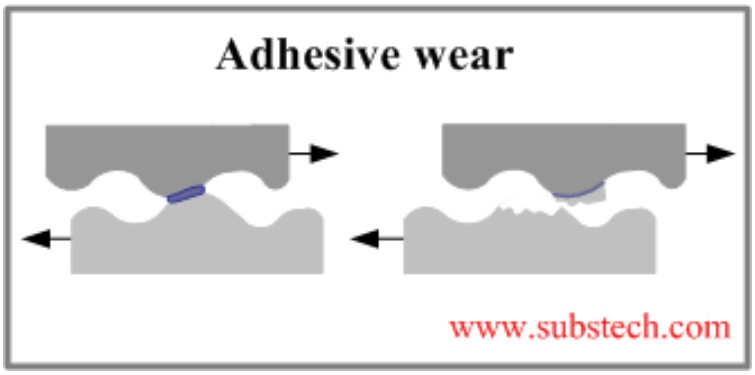

Figure 10. Adhesive wear (substech, n.d.)

Adhesive wear is generated due to several factors such as temperature, load, materials nature and shape, among others. According to Zum Gahr (1987), contributions to adhesion that can be expected for the different groups of materials are:

- Metals: primary bonds, namely metallic and covalent and secondary bonds such as van der Waals;

- Polymers: van der Waals bonds, electrostatic bonds due to electrically charged double-layers, and hydrogen bonding by polar molecules;

- Ceramics: primary bonds, van der Waals bonds and electrostatic bonds.

These adhesions produce cold welding, scoring, seizing, built-up edges, and tool breakage. Measures that can be implemented in order to minimize or prevent such problems should be pointed at tool selection, taking into account the surface characteristics on which the tool will act, making tool surface-working surface as compatible as possible, the hardness of the material, and the surface energy of the material.

3.1.2 Abrasion

Abrasive wear is defined as the displacement that occurs when a rough, hard surface glides across a surface that is relatively softer. Also it is defined as the displacement of material caused by the presence of hard particles between or

embedded in one or both of the two surfaces in relative motion, or by the presence of hard protuberances on one or both of the relative moving surfaces (Zum Gahr, 1987). Abrasion is therefore produced by hard particles in the tool material, by hard particles of the built-up edge and by a hardened surface.

There are two types of abrasion wear: Two-body abrasion and three-body abrasion (Figure 11). The first interaction is between two bodies, where hard particles are embedded in one of the two bodies. This type of abrasion is produced when hard particles remove material from the opposing surface. Abrasion also takes place between three bodies, where particles are free to circulate between the contact bodies. This type occurs when the particles are unconfined and are able to slide down rolling on a surface. Below, an illustration of the adhesion wear mechanism is shown.

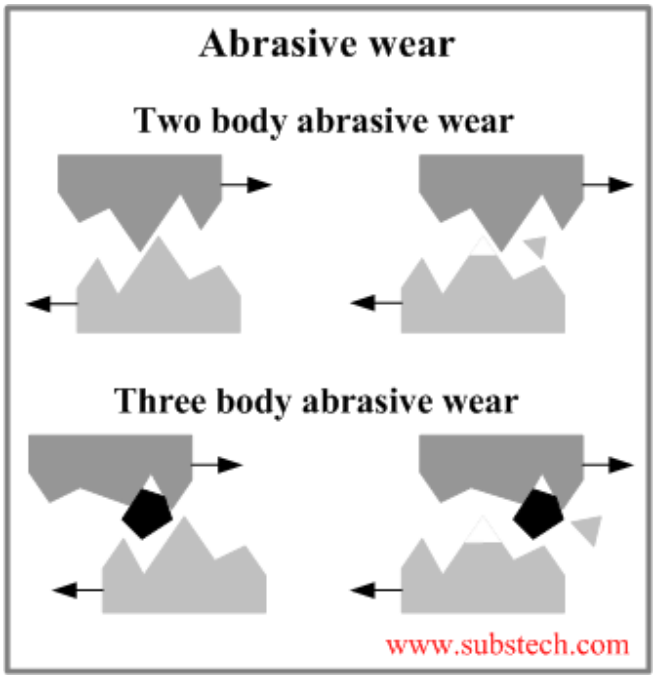

Figure 11. Types of abrasion wear (substech, n.d.).

There are several factors that affect the incidence of abrasive wear and the way the material is separated. The three most important mechanisms related to abrasive wear are:

- Cutting: occurs when a material is separated from a surface in chips or debris in front of the cutting edge. There is a minimal displacement and the material is removed from the surface proportionally to the groove volume. In some cases there is no displacement.

- Plowing: occurs when the material undergone displacement sideways and results in groove formation where no removal of the material is produced.

- Cracking (fragmentation): occurs when part of the material is removed from the surface by the cutting forces, resulting in a volume of the lost material higher than that of the wear tracks. The cracks spread freely throughout the wear, leading to further material removal.

The intensity of abrasion depends on factors such as material's hardness and strength and speed and mass of the moving particles. Usually abrasion can be controlled working on the root cause. Other solutions for the abrasion wear that can be implemented are the use of suitable lubricants and abrasion-resistant materials.

3.1.3 Tribochemical reaction

Chemical stability is the tendency of a material to resist change or decomposition due to internal reaction, or due to the action of environmental factors like air, heat, light, pressure, or others. Chemically stable materials are less reactive and thereby more corrosion resistant.

The tribochemical reaction is a case of corrosive wear, i.e. wear caused by the interaction of surfaces in contact with an aggressive environment. It is a chemical material reaction that takes place on a surface. According to Zum Gahr (1987), tribochemical wear is characterized by rubbing contact between two solid surfaces that react with the corrosive environment, which may be liquid or gaseous. The wear process is the continual removal and new formation of reaction layers on the contacting surfaces. In Figure 12 an illustration of this mechanism is shown.

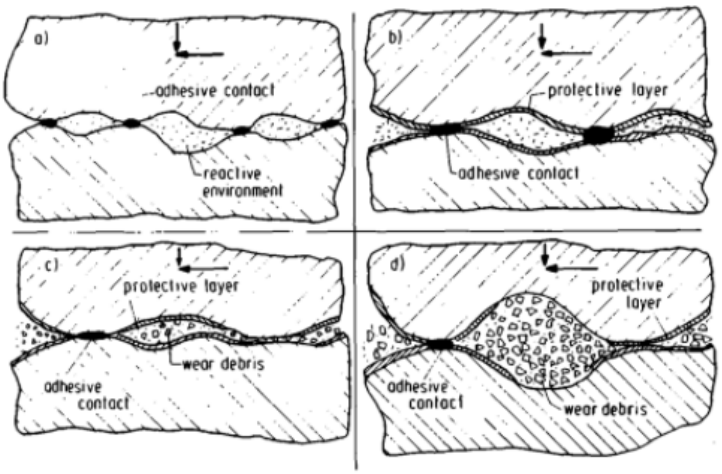

Figure 12. Mechanisms involved in Tribochemical Wear (Zum Gahr, 1987).

The central cause of these forms of wear is chemical reaction between the worn material and the corroding medium. This kind of wear is a mixture of corrosion, wear and the material degradation process due to the combined effect of corrosion and wear, called tribocorrosion. Corrosion may accelerate wear and wear may accelerate corrosion. In corrosive wear, tribochemical reaction produces a reaction layer on the surface. At the same time, such layer is removed by friction. Therefore, relative growth rate and removal rate determine the wear rate of the reaction layers and, as a result, of the bulk material. The material removal in corrosive wear is governed by the growth of chemical reaction film or its chisolution on wear surface, where chemical reactions are highly activated and

accelerated by frictional deformation, frictional heating, microfracture, and successive removal of reaction products (Kato & Adachi, 2000).

Tribochemical wear in cutting operations results from diffusion. In general, tribochemical wear increases with rising temperature. A frequent cause of tribochemical wear is oxidation, due to the presence of oxygen from the air. Avoiding this type of wear can be accomplished by reducing temperature, speed and load, employing compatible materials and using surface coatings.

3.1.4 Surface Fatigue

According to Kato & Adachi, repeated cycles of contact are not necessary in adhesive and abrasive wear for the generation of wear particles. There are other cases of wear where a certain number of repeated contacts are essential for the generation of wear particles. Wear generated after such contact cycles is called fatigue wear. When the number of contact cycles is high, the high-cycle fatigue mechanism is expected to be the wear mechanism. When it is low, the low-cycle fatigue mechanism is expected.

Surface fatigue is the localized fracture of material from a solid surface caused by the action of repeated compressive stressing (load) of a surface. In Figure 13 is a graphic representation of this wear mode.

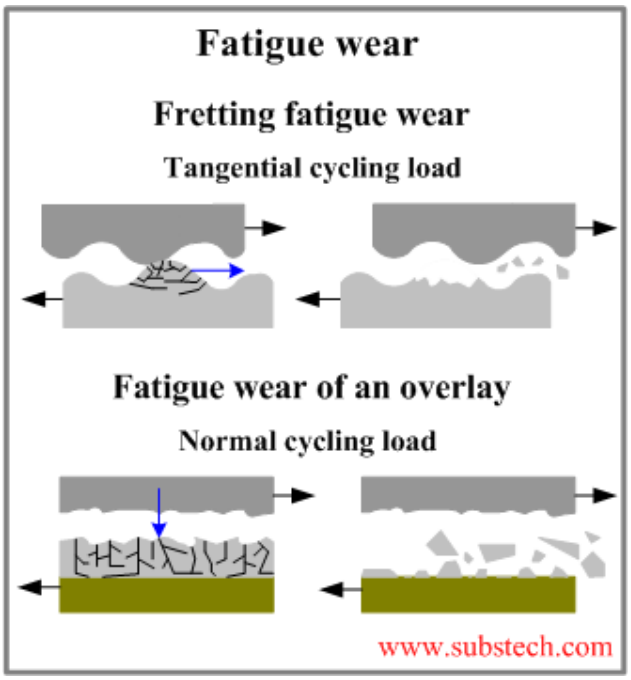

Figure 13. Fatigue wear (substech, n.d.).

Fatigue wear is produced when the wear particles are detached by cyclic crack growth of microcracks on the surface. These microcracks are either superficial cracks or subsurface cracks.

Repeated friction under elastic or elastoplastic contact causes the accumulation of local plastic strain around some stress concentration points, and cracks are generated after reaching a certain number of frictional cycles. The

mechanism of crack initiation and propagation in such a situation is same as fatigue fracture one, which is a kind of rate process controlled by the inhomogeneity of the microstructure of a material. Under plastic contact, a wear particle is not generated by a single pass of sliding and only a shallow, conformable groove is formed (Kato & Adachi, 2000).

Some of the consequences of surface fatigue wear are transverse and crest cracks, pitting and micro-pitting (especially in rolling contact), tool breakage.

The wear modes are defined by the characteristics of the relative motion between the contacting bodies. Information of the wear mode is important for a suitable replication of the wear conditions in laboratory tests. According to Kato & Adachi (2000), these descriptions of wear are all technical and based on the appearance of the contact type. They do not represent wear mechanisms in a scientific way but they explain the different contact configurations. This modes are described herein:

- **Sliding Wear**: in this mode, the mechanisms that determine the surface damage of two contacting bodies and their reciprocal sliding are adhesion and triboxydization. In addition, if the tribological system is characterized by the presence of hard particles, abrasion may also occur. The presence of a interfacial lubricating film considerably reduces the wear of the tribological system, the lubricant prevents direct contact and reduces the cutting forces; there is a particular form of sliding wear that occurs when the relative motion oscillates between 100 and 300μm called *friction wear*.
- **Fretting Wear**: is a small amplitude oscillatory motion, usually tangential, between two solid surfaces in contact. Fretting wear occurs when repeated loading and unloading causes cyclic stresses which induce surface or subsurface break-up and loss of material. Vibration is a common cause of fretting wear.
- **Rolling wear**: also known as contact fatigue wear. This process may occur on mechanical components such as rolling bearings; is the main configuration for surface fatigue wear.
- **Impact wear:** it is the material loss/damage produced by a solid surface repeatedly impacting another solid surface (ASM, 1992).
- **Slurry wear:** defined as that type of wear, or loss of mass, that is experienced by a material exposed to a high-velocity stream of slurry. This erosion occurs either when the material moves at a certain velocity through the slurry or when the slurry moves past the material at a certain velocity (ASM, 1992).

From the above description of the main wear processes it is possible to deduce that identify the exact phenomenon is a difficult task, since what it's happening at the soil-excavation head interface is a combination of several phenomena.

3.2 Wear in EPB

According to Oñate Salazar, et al. (2018), the wear of the tools and of the mechanical parts of a soil machine is mainly located in the cutterhead and in the screw conveyor. This is an important task to be assessed already at the design stage since it influences the needed stops for maintenance of the machine and the tool replacement. The cutterhead tools and screw conveyor maintenance is an important economical and technical factor that affects the cost and the time of construction.

As described above, wear is the process by which a given material is removed from the surface by the action of particles with high hardness; therefore, it is directly linked to soil properties (hardness, shape and size of the particles) and to the configuration of the contact interface (presence or absence of lubrication).

In rock excavation, the crushing by compression process is applied, producing high stress conditions on machine's excavation tools; in soft soil excavation this process is not used and the tools do not experience this stress. However, considerable damage to excavation tools is produced by abrasive and adhesive wear, which depends largely on the water content of the soil (lubrication) and its particles size.

Soft soil excavation requires a lower thrust force in comparison to rock excavation, but there is high energy dissipation on the cutting tools due to high torque. The torque is basically needed for mixing the soil in the excavation chamber and also, in less extent, because the excavation takes place inside a ductile material.

Soft soil excavation causes moderate wear in comparison to rock excavation when considering the frequency of tool replacement; however, in some cases tool wear in soft soil excavation is higher than that of rock excavation due to extreme working conditions, and numerous problems regarding tool replacement occur.

Wear and abrasion can affect and compromise several components on the excavation machines. In EPBS machines, tools, cutterheads, screw conveyors and even the shields are particularly affected.

The TBMs offer a wide range of wear definitions; they can be classified in primary and secondary wear.

Primary wear is referred to wear on excavation components such as discs, cutting tools, milling machines, among others, that must be replaced as a preventive measure at specified intervals. Primary wear is quantified as the loss of the cutter ring diameter due to the contact of the component with the excavation front. In primary wear surfaces adapt to each other and the wear-rate might vary between high and low.

Secondary wear occurs when there is excessive primary wear and even the structures designed to support the tools are compromised. Secondary wear is quantified as the loss of metallic material over the entire cutting head area due to rock block impact or the abrasive action of the “muck”. This type of wear is very dangerous, because it causes damages that require an extraordinary maintenance

intervention; it can develop very quickly and cause structural damage to the machine. The secondary wear is shortened with increasing severity of environmental conditions such as higher temperatures, strain rates, stress and sliding velocities, among others.

In conclusion, wear rate is strongly influenced by the operating and environmental conditions.

3.3 Importance of the wear study

Wear in tunnel construction with EPBS machines is directly related to excavation costs and time, as the advancement of the machine is limited by the integrity of all its components.

The presence of wear problems leads to excavation downtimes as the machine must be stopped for inspection and replacement of the worn components. This problem has a crucial impact on the advancements of unstable excavation fronts, since the replacement of cutting tools is not only a difficult task, but also risky due to the hyperbaric conditions in which is done. For example, a repairing work in a mixing chamber at a pressure of 3 bar could not last longer than 2.8 hours and should be followed by 2 consecutive hours in a decompression chamber. An experienced mechanic under these working conditions is able to replace 1-2 discs and up to 6 rippers per hour, causing a significant downtime.

Studies have shown that the replacement of cutting elements in some rock excavations can reach 15% of the total tunnelling budget, underlining the need to increase material performance in order to reduce construction time and cost.

Another problem resulting from wear in soft soil excavation is the reduction of the excavation head diameter. This causes complications during segment lining operations and decreases the yield of the entire construction process. The solution to this problem requires several months, causing delays in the delivery of work and an exponential increase in terms of costs.

Chapter 4

Conditioning

4.1 Soil Properties

EPBS machine ideally works with specific type of soils (silty and clayey). For this reason, the application range of EPBS method can be hugely improved by affecting soil critical aspects: *plasticity, texture* and *permeability*.

- **Plasticity**: The consistency of the soil defines its state. According to the Swedish engineer Albert Mauritz Atterberg, soil can be in four (4) states of consistency: liquid, plastic, semi-solid and solid. The EPBS machine works with soils ranging from liquid to plastic consistency. In plastic state, soil has plasticity, a property that allows the soil to be deformed without breaking. It is directly related to water content: while water content is reduced, volume of the soil lessens and soil increases its plasticity. If water content is extra reduced, the soil becomes semi-solid, which is a state not suitable for EPBS machines. In Figure 14 the described relationship between soil volume and water contents is shown.

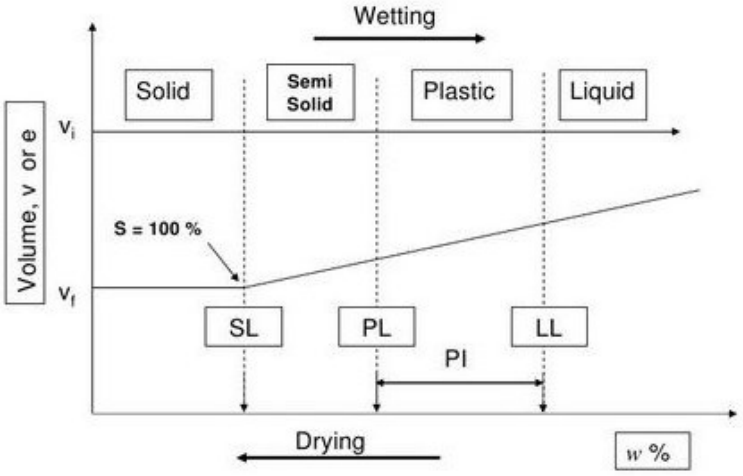

Figure 14. Volume and water content of soils (Atterberg).

The Plasticity Index (PI) is a measure of the range of water contents where the soil displays plastic properties. It denotes the difference between the liquid limit and the plastic limit in percentage. It is used to provide an idea on how the soil should be modified, by wetting or drying the soil or using other conditioning options, to enhance its plasticity and therefore, enabling the soil to transmit a given pressure.

Below it is shown soil classification based on its PI (Sowers, 1979):

- Nonplastic (PI = 0)
- Slightly plastic (PI < 7)
- Medium plastic (PI = 7-17)
- Highly plastic (PI >17)

Soils with high PI tend to be clay, while soils with lower PI tend to be silt. In the case of soils with a PI equal to 0, they have little or no silt or clay.

In EPBS machines, the pressure needs to be transmitted from the cutterhead, as smooth as possible, in order to obtain a minimal internal friction in all the mechanical parts, a minimized torque of the cutting wheel and finally, a more effective tunnelling process. This can be achieved when soil has a plastic behaviour.

- **Texture**: it refers to the size of the particles that compose the soil. Sand, silt, and clay soils refer to the relative sizes of soil particles. These three groups are called *soil separates*. A textural triangle can be used to determine soil textural class from a mechanical analysis, performed to identify soil separates (Figure 15).

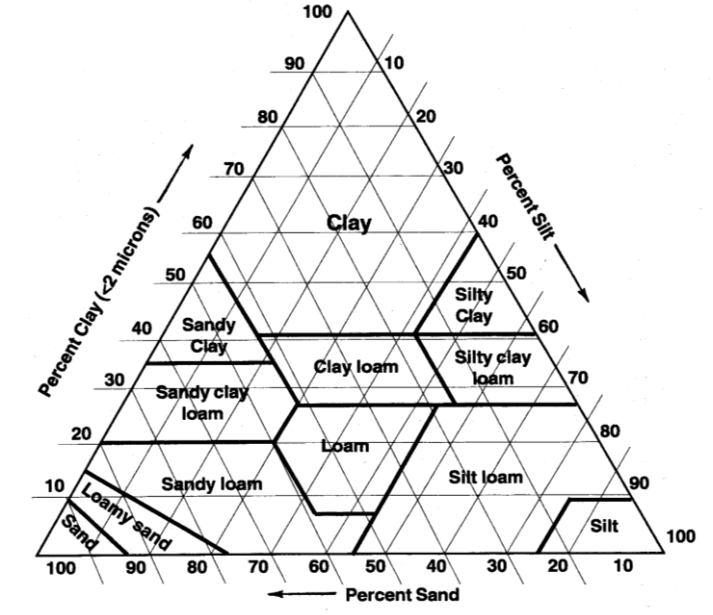

Figure 15. Soil texture triangle

The three sides of the textural triangle represent increasing or decreasing percentages of sand, silt and clay particles and show all probable combinations of soil separates. A coarse-textured or sandy soil is the one comprised primarily of

sand-sized particles. A fine-textured or clayey soil is the one dominated by pint-sized clay particles. Due to the strong physical properties of clay, a soil with only 20% clay particles behaves as sticky, gummy clayey soil, which represents a risk for the machine, due to its clogging potential. The term loam refers to a soil with a combination of sand, silt, and clay sized particles. For example, a soil with 30% clay, 50% sand, and 20% silt is called a sandy clay loam.

By knowing the texture (particle size distribution), a conditioning method can be more accurately chosen, although this is not the only feature to be considered.

- **Permeability**: is defined as the property of a porous material to allow the passage of water through its interconnecting voids. It is usually measured as the rate of water flow through the soil in a given time period. Permeability varies with soil texture and structure. It is generally rated from very rapid to very slow and it is expressed as K (coefficient of permeability), which is calculated by the Darcy's equation:

$$k = \frac{V}{i} \qquad \text{Equation (8)}$$

Where, V is the flow velocity, i is the hydraulic gradient and k is the coefficient, which is influenced by the porosity of the soil, defined as the percentage of soil that is pore space or voids, and the shape and size of those voids.

Soils with large pores are more permeable and soils with smaller pores are less permeable. In Figure 16 are shown the typical values of *k,* as indicator of permeability, for saturated soils (Khna, 2015).

Soil type	Coefficient of permeability, cm/sec
Clean gravel	$1.0 - 100$
Sand gravel (mixture)	$10^{-2} - 10$
Clean sand (coarse)	$10^{-2} - 1.0$
Fine sand	$10^{-3} - 10^{-1}$
Silty sand	$10^{-3} - 10^{-2}$
Clay sand	$10^{-4} - 10^{-2}$
Silt	$10^{-8} - 10^{-3}$
Delhi silt	6×10^{-7}
Clay	$10^{-10} - 10^{-6}$
Boston blue clay	7×10^{-9}
London clay	1.5×10^{-11}

Figure 16. Flow of water through soil – Permeability and factors affecting permeability (Khna, 2015).

According to Martinelli (2016): "the permeability of the ground has to be as lowest as possible in order to prevent the free flow of the water in the excavating chamber and in order to avoid fluctuations on the water table level with relative induced subsidences and destabilizing forces which act on the front and which may cause flows through the machine itself".

When the soil in the excavation chamber has not reached a sufficiently low permeability, excessive flow of water may occur.

All three mentioned aspects, *Plasticity, Texture and Permeability,* can be modified using conditioning agents that include water, bentonite, polymers and foaming agents. *Water* is used as a cohesive agent and to lower shear strength (decreasing the force requires to rearrange soil particles). *Bentonite* is applied in form of suspension for slurry-supported methods. It is useful as a transport medium for excavated soil and as a support medium. *Polymers* are long-chain molecules formed by a large number of monomers. They are used for cohesiveness and consistency control and as anti-clogging agent. Foams are produced by mixing with water and the use of a compressed air system. They are mainly used to keep the particles of the soil apart by reducing internal friction and permeability of the soil.

These agents are basically employed to improve the soil plasticity, obtaining a pasty mass for easier management and better flow, to lubricate the path of the excavated soil through the cutter-head and the screw conveyor sections, to improve the permeability and to improve the performance of the EPBS and other machines.

Therefore, the range of applications of EPBS machine depends on the following main aspects:

- Soil mechanics, to be determined and modified,
- Conditioning additives, to be selected, prepared and implemented and,
- EPBS design, providing better adaptability to different situations.

In conclusion, soils barely have the ideal characteristics of fluidity and structure to use them as a support medium in the EPB-shield machine. As a conclusion, soil requires to be conditioned by adding water, bentonite, polymers or foams to achieve a plastic behaviour (between plastic limit and liquid limit) in the excavation chamber for an easier mixing and removal of the spoil. This soil behaviour allows the machine to work at its best capacity, minimizing wear of metallic parts and the rate of their replacement, avoiding fluctuations and losses of groundwater, improving advance rates and, as a consequence, producing higher effectiveness in the tunnelling process. Also, conditioning agents expand the applicability of EPBS machine into soils that, in past, had required a slurry machine.

4.2 Soil Conditioning in Tunnelling

The world of underground engineering has acquired a growing experience on tunnel construction with new technologies. Currently, there is a huge progress in mechanized tunnelling, an area that is developing fast since use of underground spaces is on the rise and there is a need to work deeper, larger and faster, challenging engineers to improve any knowledge and technology related to this.

Generally, EPBS machines will be used in finer grained soils whilst SPB (Slurry Pressure Balance) machines are preferred in coarser materials. This

criterion has become ambiguous in recent years by the development of improved soil-conditioning additives and additive injection systems, which have broaden the range of ground conditions that each type is able to operate in.

In EPB TBM, soil is the support to the pressure exerted by the ground itself against the machine; therefore, to counterbalance the pressure, soil should behave as a plastic material, having a smooth movement through the machine and out when removing the spoil. Soil should have also low permeability to prevent groundwater flood the machine by defeating its counterpressure force. As an additional problem, some soft soils stick to essential parts of the machine such as the cutter face and the screw conveyor, causing the clogging phenomenon. This produces an increase in working time and wearing of the cutting wheel or the conveyor belts system. For the above reasons, tunnelling engineering has been developing and applying certain additives to minimize or eliminate those problems. They are called *Conditioning Agents*.

In order to understand the use of conditioning agents in EPBS, it is important to mention again that soils should have *suitable properties* for better handling, thus granting an enhanced performance of the EPBS. Adequate soil manageability allows a flawless excavation and protection of the machine. According to Milligan (2000; 2001), critical factors to efficient mixing of spoil and conditioner, include the position and number of injection points, the rotation speed of the cutter head, the shape of the excavation chamber and lead-in to the discharge point, the mixing time in the cutting head, the method of injection and control of the injection rate.

4.3 Use of Conditioning Agents

In tunnelling it is important to take into account the wide variety of soils, ranging from hard rock to soft ground, and groundwater presence when it comes to the selection, design and use of a TBM. It is necessary to perform an extensive ground investigation prior to TBM implementation. Moreover, the range of application of TBMs have been increasing and will continue to do so by the use of conditioning agents and, for that cause, their study has become more significant over the years.

These materials develop different behaviours due to physical-chemical properties of each agent and their interaction with soils and groundwater. Their effect on each soil depends on how they are used (separately or combined), also their concentration, injection ratio and, for foams, its expansion ratio value. These agents are usually introduced to the soil in liquid form as slurries. Slurries have demonstrated the effect known as thixotropy, whereby they ‘set’ to a gel-type material if left undisturbed, but revert to a viscous fluid when sheared. The alternation between fluid and gel may take place any number of times (Milligan (2000; 2001). Conditioning agents modify and control the rheological properties of the soil extracted by the TBMs. They will be described in more detail below, including definition, composition, characteristics and usages of each one.

4.3.1 Foams

4.3.1.1 Definition

Foam is a dispersion of air bubbles in a liquid phase comprising of a water based surfactant solution. Foams are also defined as (Psomas, 2001) a dispersion of gas bubbles in a liquid or solid in which at least one dimension falls within the colloid size range (1-1000 mm). The term “foam” implies the mixture of foam concentrate with water and air.

4.3.1.2 Composition

Generally, in the foam mixture there is a dispersed phase (internal phase) and a continuous phase (external phase). These two phases are distributed as follows: on the bottom, there is bulk liquid and above this, in a second bulk phase, gas. The gas phase is separated from the thin liquid-film by a two-dimensional interface. The region that encompasses the thin film and the two interfaces on either side of the film is conventionally defined as lamella (Psomas, 2001).

Foam concentrate is based on surfactants, which interact with the other foam components: water and air and, in some cases, polymers.

4.3.1.3 Characteristics

The surfactant properties on foam impact the surface tension of a given solution, the interactions with soils, and the properties of the foam.

Surfactants can cause steric interactions and repulsive forces to disperse fine-grained soils due to their molecules with chemical structures made of a hydrophobic chain and a hydrophilic end group. This disposition provides surfactants with anionic, cationic, non-ionic or amphoteric charge properties. The adsorption of surfactants onto steel surfaces of a tunnelling machine is thought to reduce the adhesion of clay soils (Psomas, 2001).

Surface tension is defined as the property of a liquid surface displayed by its acting as if it were a stretched elastic membrane. Also as a chemical phenomenon that happens at the surface of a liquid where the liquid becomes denser than the rest or the elastic tendency of a fluid surface which makes it acquire the least surface area possible. Surface tension depends mainly upon the forces of attraction, called cohesive forces, between the particles within the given liquid and also upon the gas, solid, or liquid in contact with it. The energy responsible for the phenomenon of surface tension may be thought of as approximately equivalent to the work required to remove the surface layer of molecules in a unit area. Surface tension is dimensioned as force (newtons) per unit length (meters) or as energy (joules) per unit area (square meters), also known as surface energy.

The foams (Thewes, et al., 2012) should have a constant and uniform density, which means that liquid and air are completely mixed and that all parts of the produced foam have the same properties, be stable while in the excavation chamber and have a homogenous structure of bubble size. Bubbles in foams are

distributed in different sizes. A bubble size distribution that is weighted toward smaller sizes represents the most stable foams. Foam properties and their interaction with soils and groundwater and the proper behaviour of the soil after the foam is injected are related to foam stability and compressibility. If foams bubbles are stable, their compressibility could increase the compressibility of the foam mixture. Compressibility needs to be controlled to control foam behaviour in the injected mixture. The increase of the compressibility of the soil in the pressure chamber through the addition and mixing of conditioning agents improves the workability and the homogeneity of the spoil. A more compressible and "plastic" material in the pressure chamber behaves as a high viscosity fluid and, as a result, better control of the fluctuations of the pressure distribution at the face can be attained (Psomas & Houlsby, 2002). Stability of the foam is the relative capacity of the finished foam to withstand the impact of heat, spontaneous collapse or rupture due to external factors such as heat, chemical reaction, mechanical agitation or climatic factors. Stabilization of foam is caused by Van der Waals forces between the molecules in the foam, electrical double layers created by surfactants, and the Marangoni effect, which acts as a restoring force to the lamella.

Foam properties are affected by the following parameters:

1- Surfactant dosage expressed in %: concentration of the foaming agent in the generation liquid (c_{foam}). The normal concentrations are between 0,5% and 4,0% (e.g. 4%: 4 parts of liquid foaming agent and 96 parts of water).

2- Foam Expansion Ratio (Air Ratio, known as FER): The proportion by which a given amount of foam solution expands into finished foam. For example, a ratio of 5 to 1 means that one gallon of foam solution will fill a 5-gallon container with expanded foam after being aerated. FER is affected by the foam injection ratio. It represents the ratio between the obtained volume of foam and the volume of generation fluid (water + foaming agent), according to the following formula:

$$FER = \frac{V_{foam}}{V_{generator\ liquid}} \qquad \text{Equation (9)}$$

3- Foam Injection Ratio (known as FIR): represents the volume of foam added to the volume of soil according to the following formula:

$$FIR = 100 * \frac{V_{foam}}{V_{soil}}\ (expressed\ in\ \%) \qquad \text{Equation (10)}$$

The percentage of free water added to the material (w_{add}), represented by the ratio between the mass of free water (M_w) and the mass of material (M_s) is expressed by the following formula:

$$w_{add} = 100 * \frac{M_w}{M_s}\ (expressed\ in\ \%) \qquad \text{Equation (11)}$$

The percentage of total liquid added to the material (w_{tot}), represented by the ratio between the mass of natural water, added free water, liquid generator (M_l) and the mass of material (M_s) is defined by the following formula:

$$w_{tot} = 100 * \frac{M_l}{M_s} \ (expressed\ in\ \%) \qquad \text{Equation (12)}$$

4- Drainage time: 25% to 50%. It is often called a half-life or 50% drain time. The drainage coefficient is one of the qualities of finished foam, it describes how much of the foam solution will drain from the mass of expanded foam, or how long it takes to drain 50% of the solution from the foam. Foam that has a fast draining time is usually very fluid. Foams with longer periods of time are less mobile and fluid.

5- Polymer dosage (when applies) expressed in %. The concentration is usually 0.1 – 5.0% in the foaming solution.

Foams are divided in two groups:

- Protein-based foams.

Agents primarily produced from naturally occurring hydrolyzed proteins that are combined with foam stabilizers (metal salts), bactericide, corrosion inhibitors, freeze protection additives and solvents to create the foam concentrate. These foams usually are 20-40% protein foaming agent and 3-10% glycol-based foam booster. More advanced fluoroprotein foams (FP) and film forming fluoroprotein foams (FFFP) include fluorochemical additives which increase the performance of the foam. Protein foams also exist with alcohol resistant (AR) capabilities. Protein and fluoroprotein concentrates can only be used with air aspirating type discharge devices through most conventional foam equipment.

- Synthetic foams.

This type of foam is composed of a mixture of anionic hydrocarbons, solvents and stabilizers. They usually have low stability due to their relatively rapid drain times that produce bubble collapse. These foams are produced with synthetic concentrates (detergents) generally intended for medium/high type expansions. High expansion foam solution is normally used with discharge devices that produce high expansion ratios.

According to the specifications and guidelines from the European Federation (EFNARC, 2005), the foam type chosen should match the properties of the soil to be excavated. There are three types:

- Foam type A: high dispersing capacity (breaking clay bonds) and/or good coating capacity (reduce swelling effects),
- Foam type B: general purpose, with medium stability,
- Foam type C: high stability and anti-segregation properties to develop and maintain a cohesive soil as impermeable as possible.

4.3.1.4 Usages

As mentioned before, foams contain water and air and, sometimes, polymers. This mix may be applied in different points of the EPB TBM machine in order to meet different objectives, such as reduced wear of machine cutter head face, plate and tools, and all wear parts of the muck removal system, improved stability of tunnel face, with better control of ground movements, improved flow of excavated material (spoil) through the cutter head, reduced friction and heat build-up in the shield, and enhanced properties of soil in the pressure chamber of EPBM machines. In addition, it is important the improved safety for workers operating in tunnels, during cutter changes and cutter head inspections.

4.3.2 Bentonites

4.3.2.1 Definition

They are smectitic materials capable of swelling and increasing several times their volume in contact with water and forming thixotropic gels when added in small quantities, giving a voluminous and gelatinous mass. It was proposed in 1898 by Wilbur C. Knight to designate clayey material from the "Bento Shale" Cretaceous formation in Wyoming, USA.

Bentonites are also called "activated clays" because of their affinity in certain chemical reactions caused by their excessive negative charge.

4.3.2.2 Composition

Bentonite usually forms from weathering of volcanic ash, most regularly in the presence of water. The different types of bentonite are each named after the respective main element, such as potassium (K), sodium (Na), calcium (Ca), and aluminium (Al). The most common bentonites used in the industrial area are Calcium and Sodium bentonites.

4.3.2.3 Characteristics

The properties of bentonites mainly derive from:

1- Small particle size (less than 2 μm).

2- Laminar morphology (phyllosilicates).

3- Isomorphic substitutions:

- Appearance of loads in the laminates
- Presence of cations weakly bound in the inter-laminar space.

Relatively small quantities of bentonite suspended in water form a viscous, shear-thinning material. Majority of bentonite suspensions are also thixotropic, although rare cases of rheopectic behaviour have also been reported. At enough high concentrations (60 g/L), bentonite suspensions begin to take on gel characteristics (a fluid with minimum yield strength required to make it move).

There are several types of commercial Bentonites:

- Montmorillonites: Smectic clays with a layer structure. The aluminium ion predominates in the structure but can be replaced by another metal ion forming a wide variety of minerals.
- Bentonite: In general, this term describes a clay composed essentially of Montmorillonite. Bentonite is composed by absorbent phyllosilicate clay consisting in 2:1 structures of TOT type: Tetrahedral-Octahedral-Tetrahedral.
- Sodium Bentonite: A naturally occurring montmorillonite containing a high level of sodium ions. It swells when mixed with water. It is also known as "Wyoming Bentonite" or "Western Bentonite". It is the preferred one for tunnelling.
- Calcium bentonite: It is a montmorillonite in which the predominant interchangeable cation is calcium. It does not exhibit the swelling capacity of sodium bentonite, but has absorbent properties. It is also called "Southern, Texas or Mississippi Bentonite".

4.3.2.4 Usages

The focal uses of bentonite are for drilling mud, as binder, purifier, absorbent, and as a groundwater barrier. Also as lubrication agent and coating agent that does not allow water to seep into the geological formation.

Bentonite is used in drilling fluids to lubricate and cool the cutting tools, to remove cuttings, and to help prevent blowouts. Much of bentonite's usefulness in the drilling and geotechnical engineering industry comes from its unique rheological properties. It is a common component of drilling mud used to curtail drilling fluid invasion by its propensity for aiding in the formation of mud cake.

4.3.3 Polymers

4.3.3.1 Definition

Polymers are macromolecules consisting of large numbers of repeating smaller molecules, called monomers, chemically bonded into long chains. Polymerisation of a single type of monomer produces a homopolymer, while polymerisation of two or more different monomers produces a copolymer.

4.3.3.2 Composition

Monomers are the basic units of the polymer. A monomer is a molecule that binds chemically or supramolecularly to other molecules. It is a molecule of any of a class of compounds, mostly organic, that can react with other molecules to form very large molecules, or polymers. The essential characteristic of a monomer is polyfunctionality, the ability to form chemical bonds to at least two other monomer molecules. The bifunctional monomers can form only linear chain polymers, but the higher functional monomers produce network crosslinked polymeric products. Polymers are a chain of more than 20 monomers.

4.3.3.3 Characteristics

The properties of polymers vary widely, depending on their chemical composition and structure. The size of polymer molecules (characterized by the molecular weight), branches or groups attached to the polymer chain, cross-linking between chains, and intermolecular forces all influence the physical properties of polymers.

Polymers can be classified according to the following:

- Origin:

a) Natural polymers: originated from living beings. Proteins, polysaccharides and nucleic acids, which are called biopolymers, are examples of it. So are silk, rubber, cotton, wood (cellulose), chitin, etc.

b) Synthetic polymers: obtained by synthesis. They are made up of natural monomers. Some of these polymers are glass, nylon, rayon and adhesives.

c) Semisynthetic polymers: obtained by transformation of monomers or natural polymers. Among the semisynthetic polymers it can be found nitrocellulose or vulcanized rubber.

- Physical properties:

a) Thermostable: polymers that cannot be melted through a simple heating process, since their mass is so hard that they need very high temperatures to undergo some type of damage.

b) Elastomers: although they can be deformed, once the agent that caused the loss of their shape disappears they can return to it. They have the property of recovering their shape when subjected to a deformation force.

c) Thermoplastics: they are easy to melt, and therefore can be molded. If they have a regular and organized structure, they belong to the crystalline subcategory, but if their structure is disorganized and irregular, they are considered as amorphous subcategory.

d) Resins: They are thermostable polymers that suffer a chemical transformation when they melt, becoming a solid that when melted, decomposes.

e) Fibers: They have the shape of filaments. They are produced when the molten polymer is passed through small holes of a suitable matrix and a stretch is applied.

- Production process (polymerization):

a) By condensation: polymers obtained as a result of the union of monomers propitiated by a molecular elimination.

b) By addition: polymers that result from the union of monomers through multiple bonds.

- According to its monomers:

a) Homopolymers: polymers constituted by identical monomers.

b) Copolymers: polymers constituted by several repeated sectors, which are equal to each other, but the chains that form those sectors are different from each other.

- Orientation of its monomers:

a) Linear polymers: those that have a linear structure.

b) Branched polymers: those that, in addition to the main chain, have several secondary characters.

4.3.3.4 Usages

There is a wide variety of polymers and therefore a huge range of use. In case of tunnelling, a large number of polymers are used as soil conditioning agents. Starches and guars (natural polymers), CMC (carboxymethylcellulose) and PAC (polyanionic cellulose) from the modified natural polymers group, and synthetic polymers, particularly derivatives of polyacrylamides, have been used in tunnelling with EPB machines, providing an increased viscosity of water in the soil near the face, an increased stiffness of the ground, more strength to the foam preventing its breakdown, good lubrication of the soil to help with its transfer through the screw conveyor and the working chamber, preventing adhesion to face plates, tools and other metal surfaces, reducing the torque of the cutterhead, and reducing the permeability by binding fine particles of silt and sand.

As an indicator, the parameter that is used to work in tunnelling with polymers is the Polymer Injection Ratio (PIR), which represents the volume of the water-polymer solution added to the soil volume and is defined by the following formula:

$$PIR = 100 * \frac{V_{polymer-water}}{V_{soil}} \ (expressed\ in\ \%) \qquad \text{Equation (13)}$$

4.3.4 Water

Water is essentially a co-component for each of the other conditioning agents. To prepare foam, bentonite or polymer solutions water is the proper coadyuvant, enhancing the performance of the additives. It operates by lubricating and activating the finer grain size fraction of the soil. Additionally, water can be used alone for soft clays that are near to the PL (plastic limit) and to provide better consistency to the soil.

Milligan (2000; 2001), observed that the addition of agents in stiff over-consolidated clays makes them more plastic. However, it is difficult to estimate how much water must be added to reduce the undrained shear strength. If too much is added, then it can turn the clay to slurry whereas insufficient water can make the clay stiffer and would then need extremely high power to remould it. In high plasticity clays, a large quantity of water is required to sufficiently change the water content and therefore, the shear strength. In this case, the danger is the creation of large chunks of clay in a softened soil matrix that will clog up the machine and the conveyor. For intermediate plasticity clays, the best practice is to create a rubble of intact clay blocks in a matrix of polymer foam, which inhibits

water absorption but allows clay blocks to slide around each other (Martinelli, 2016).

4.4 Suitability of the conditioning agent

According to Martinelli (2016), the suitability of the various types of conditioning agents depends on the different ground conditions encountered: In clays, when bentonite slurries are used, the addition of polymers makes them more effective. However, if polymers are used alone, they will disappear into the formation without providing any lubrication. In sands with gravels or poor rock and in sandy-silty soil, foams can be used as conditioning agents. When cobbles and gravel are encountered, polymer additive with foam (0.1 to 3 % per volume) is necessary. The addition of foam offers two major benefits: increased compressibility and reduced permeability. In fine-grained soils, foam can be enhanced with natural polymers, which prevent water absorption. This helps to prevent clogging and balling.

According to Peña Duarte (2007), research into soil conditioning in tunnelling has not established a realistic correlation between the amount of conditioners, such as foams and polymers, and their performance with soils. Most studies have present general guidelines on conditioning treatments and trial and error has been the common practice in tunnelling.

In order to improve the understanding of soil conditioning and its impact on tunnel construction, additional investigation is needed. That is why it is important to provide a wider range of tests for soil conditioning and their effect on the machine performance. If EPBS technique has been chosen it is very difficult to change it throughout the tunnelling process. Hence, a proper analysis of the different related parameters is needed to choose the correct mechanized tunnelling technique and the conditioning additives to be used.

4.5 Environmental Considerations

Concerning about negative environmental impacts of tunnels has been increasing over the years, so an adequate environmental assessment of tunnels is important. Environmental Impact Assessment (EIA) is a process of evaluating the likely environmental impacts of a proposed project or development, taking into account inter-related socio-economic, cultural and human-health impacts. UNEP (United Nations Environment Programme) defines EIA as a tool used to identify the environmental, social and economic impacts of a project prior to decision-making.

Throughout the development of tunnelling projects, part of its objectives should not be to promote significant environmental alterations that put at risk the preservation of species or the functional integrity of ecosystems. During the tunnelling process, different mitigation measures must be implemented to avoid or reduce the impact on the different environmental components (water, air, soil,

flora, fauna, other surface constructions, etc). According to Namin, et al., (2014), in construction, maintenance and operation of underground systems, all favorable or adverse social-economic effects and environmental impacts should be identified and considered.

According to Milligan (2000), "conditioning agents added in EPB shields will usually remain in the excavated material. Environmental aspects may therefore be very important in determining the costs of disposal, for instance in whether the spoil may be used for engineering or landscaping purposes or would have to be treated as contaminated waste. In addition, tunnelling operatives may have to work in close proximity to soil containing additives, raising questions of toxicity and danger to health. Conditioning agents should therefore generally be non-toxic and biodegradable. However over-rapid biodegradation may itself cause problems, for instance if run-off enters water courses and the degradation reactions de-oxygenate the water. Care therefore may need to be taken with run-off from newly deposited spoil."

In general, toxicity and biodegradation of conditioning agents are as follows:

Foams:

- Present low toxicity. Protein-based foams are in general less toxic than synthetic foams.
- Acceptable biodegradation. Foam biodegradation is variable. In general, Protein-based foams degrade faster than synthetic foams.
- Special caution should be taken with handling and disposal of glycol-based foams.
- It is better not to use foams containing fluorocarbon components.

Polymers:

- Generally, they are non-toxic.
- Biodegradation: semisynthetic polymers degrade faster than synthetic polyacrylamide-based polymers; the latter remain present in the excavated soil. Natural polymers are rapidly and completely biodegradable.

Bentonites:

- Toxicity: Due to its mineral composition, they have been proven not to be toxic when in contact with humans or the environment. Usually, conditioning agents based on naturally occurring materials are safer for the environment.

In soil conditioning operation with EPB machines is important to:

Choose products with minimum toxicity and eco-toxicity values: For foams and polymers it can be performed acute ecotoxicity and/or acute aquatic toxicity tests that apply and are standardized for different species. Generally, the lethal oral dose of 50% of the population (LD50, related to mammals) and the lethal concentration for 50% of the population (LC50 or EC50, related to aquatic organisms) product data shall be as high as possible. For all types of Polymers the LC50 data for Daphnids and Algues shall be preferably > 100mg/l water in order to be not classified for acute toxicity. Foams, due to their reduction of surface tension, should reach LC50 data of >10mg/l concerning fish (class acute III)

(Langmaack & Feng, 2005). The above tests are in accordance to the OECD guidelines 201 to 203.

Choose products with high biodegradation or inert components (if the bioaccumulation risk is low): Ready biodegradation and Inherent biodegradation tests need to be performed to obtain data that characterize the ecological properties of the conditioner. Soil conditioning additives should be readily biodegradable or not biodegradable (inert material) and non-toxic. These tests are in accordance to the OECD guidelines 301B and 301B.

Minimize the quantity of injection materials: This is related to achieve the best soil conditioning possible and the capacity of the conditioning agent to be as effective as possible with the smaller amount of it. Additionally, this implies a reduction in costs.

Suitable soil conditioning products should be those that show the desired functional properties and in the same time are as save as possible for the workers and the environment (Langmaack & Feng, 2005).

4.6 Laboratory tests applied to soil conditioning.

There are a large amount of tests used to evaluate soil conditioning. In order to simplify and to perform a general analysis of soil conditioning suitable to this work, some of those laboratory tests were selected.

Laboratory tests as well as the site experience show, that often each soil type, from stiff clay to sandy gravel, requires more or less an own type of foam to reach its best effectiveness (Langmaack & Feng, 2005). Therefore, it is quite important to accurately measure and foresee the most suitable conditioner for a given tunnelling project.

Depending on the soil properties, the key aims of soil conditioning can be detailed as follows (Thewes, et al., 2010):

In coarse-grained soils, temporary changes of muck properties might be necessary to ensure an adequate soil flow, both in the excavation chamber and in the screw conveyor.

In porous soils below the ground-water table, a reduction of the permeability is required to ensure an effective face support maintaining the natural pore pressure at the tunnel face to prevent seepage flow as well as resulting seepage forces and erosion processes.

An increase of the support medium compressibility dampens pressure fluctuations caused by muck volume variations resulting from the actual combination of the cutting wheel rotational speed and the excavation speed of the screw conveyor.

A reduction of the inner friction of the soil decreases the torque of the cutting wheel and the screw conveyor. Thereby, the wear of tools and steel structures in the excavation chamber is reduced, too.

Previous to the execution of the laboratory tests, the foam mixture needs to be produced. There are two alternatives to obtain this. The first is to prepare a mix

with a high speed stirrer by means of a propeller or use a foam generator. The second alternative requires to prepare foams of better quality; it is preferred the foam generator since foam breakdown is slower with respect to that of the propeller method and the quality of the foam produced with the lab scale generator is similar to a TBM generated foam.

The foam generator is a device built in laboratory scale for the tests. It should have the capability to generate foams with a FER from 3 to 20. This can be easily achieved by maintaining a constant liquid volume through the disperser and adjusting the air volume to achieve the FER required (EFNARC, 2003).For the purposes of this work, a lab scale foam generator built at the Politecnico di Torino is used (Figure 17).

The elapsed time between the production and testing of the foam should be kept at minimum (Psomas & Houlsby, 2002). It is important to mention that lab scale foam generator used to deliver the foam to perform early tests of the soil in a given project should be, by design, similar to the foam generator of the selected EPBS machine.

The characterization of conditioned soil is usually obtained using tests derived from geotechnical or concrete measurement technologies; these tests include the mixing test, the cone penetration test, the permeability test, the compressibility test, the shear test, and the slump test (Peila, et al., 2009). Some of the tests already developed are applied to tunnelling projects but there is a substantial gap in the assessment of wear of TBM's components and how this is affected by the use of conditioning agents.

Figure 17. Lab scale foam generator at the Politecnico di Torino Laboratory.

The tests performed in the laboratory to evaluate conditioned soils and conditioning agents, applicable to this work, are:

4.6.1 Slump Test

A slump test is a method used to determine the consistency or the wetness of concrete. This test is empirical and measures the workability of fresh concrete. The stiffness of the concrete mix should be matched to the requirements for the finished product quality. The slump test result is a measure of the behaviour of a compacted inverted cone of concrete under the action of gravity. It has been applied in Tunnelling for more than 30 years. Nowadays it is used to assess the suitability of a given soil conditioned with additives (usually mixtures) that will be managed by mechanized machines. The test is widely held due to the easiness of the apparatus and the procedure.

Equipment and Materials for the Slump Test:

The standard equipment used for this test, according to ASTM International C 143/C 143M (2003), is usually composed by the following parts, although some variations are implemented in this work:

- Mould: shaped as the frustum of a cone, open at the bottom and top, with 30 cm height, 20 cm bottom diameter and 10 cm top diameter. It should have foot pieces and handles;
- non-porous base plate;
- temping rod made of steel with 16 mm diameter and 60cm long and rounded at one end,
- measuring scale.

Standard procedure for the Slump Test:

Basically, the procedure follows 6 steps and is illustrated in Figure 18.

1- Place the clean mould on a smooth horizontal non-porous base plate.

2- Fill the mould with the previous prepared mixture in three layers (1/3 each of the volume of the mould). The mould should be firmly held during this step.

3- Tamp each layer with 25 strokes of the rounded end of the tamping rod in a uniform manner over the cross section of the mould. For the subsequent layers, the tamping rod should penetrate into the underlying layer.

4- Remove the excess of mixture and level the surface with a trowel and clean away the mortar or water leaked out between the mould and the base plate.

5- Lift the mould up from the mixture, straightaway but gradually, in vertical direction.

6- Measure the slump by determining the difference between the height of the mold and that of the highest point of the slumped test mixture.

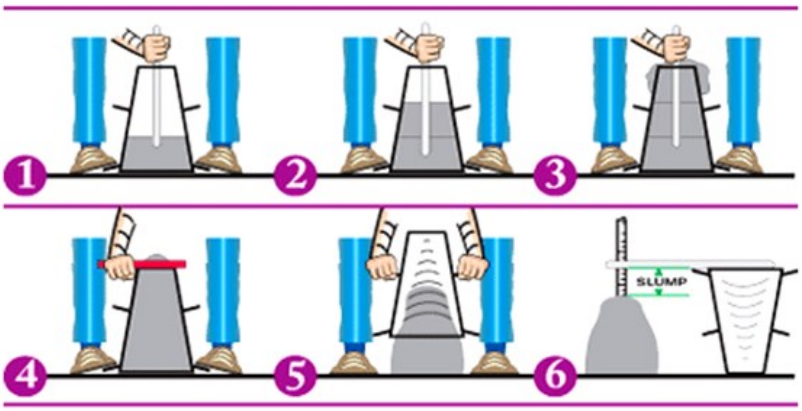

Figure 18. Slump Test Standard Procedure (theconstructor.org, n.d.)

Modification to the standard test procedure:

The use of the temping rod is not applicable for the purposes of this investigation. Instead, the mixture is completely emptied into the mould, then, step 4 is performed and the cone is lifted as described in step 5. Usually, the amount of soil or soil-conditioner mixture to be poured into the cone is 8 to 10 kg. The slump result is compared to the slump matrix, a quality diagram that correlates water content and FIR in %, developed by Peila, et al. (2009) and updated in 2015 by Martinelli, et al. (Figure 19).

This modified slump test can be cost-effectively used for the preliminary phase of tunnelling (previous study of the soil to be excavated and the additives to be used) and during the process with the EPBS technology to control the performance of the conditioned soil.

4.6.2 Half-life Test

Half-life test measures the persistence (texture) of any given foam under atmospheric pressure. The half-life is the time it takes for 50 ml of water to accumulate in the bottom of the graduate. The height of the foam is also helpful when analyzing the foam. This is a test to be applied on foams to determine their stability. It is performed according to EFNARC guidelines (2003). In Figure 20 a standard half-life test is shown.

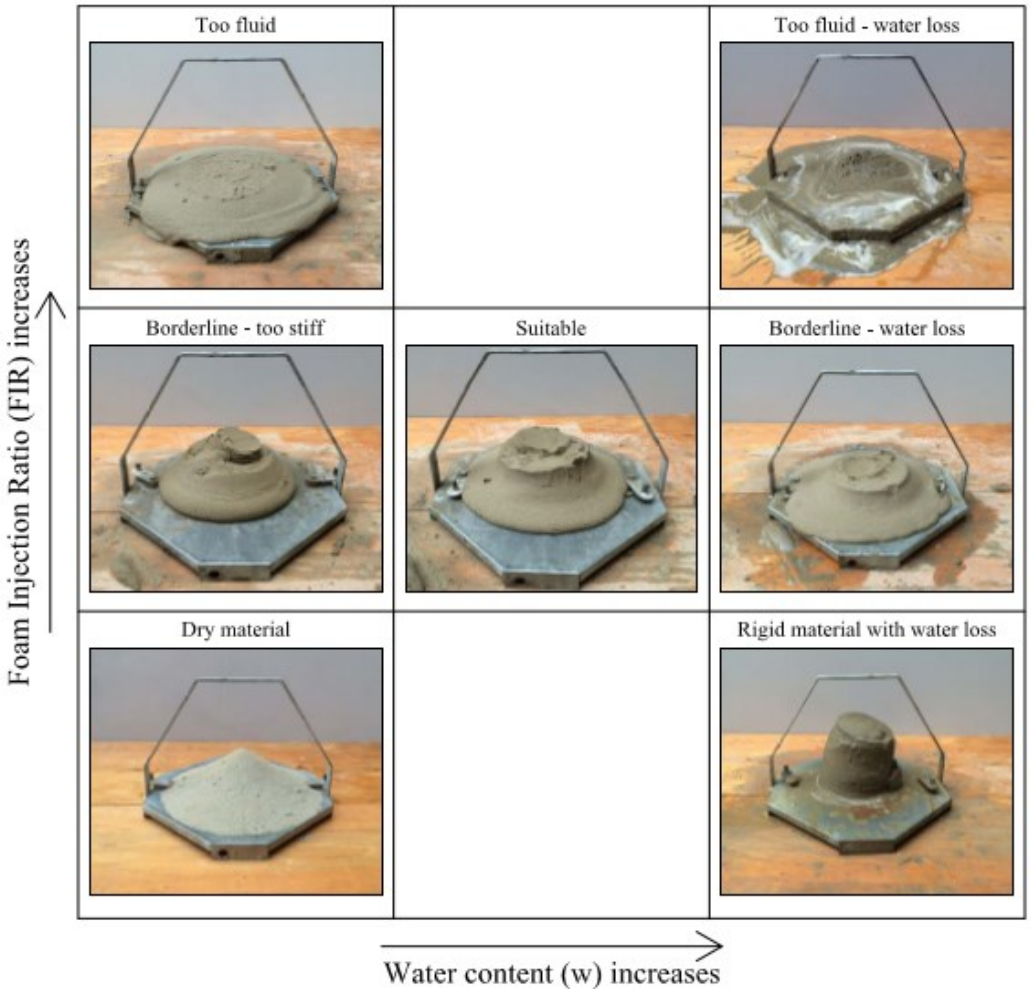

Figure 19. Assessed diagram of slump test quality (Martinelli, et al., 2015)

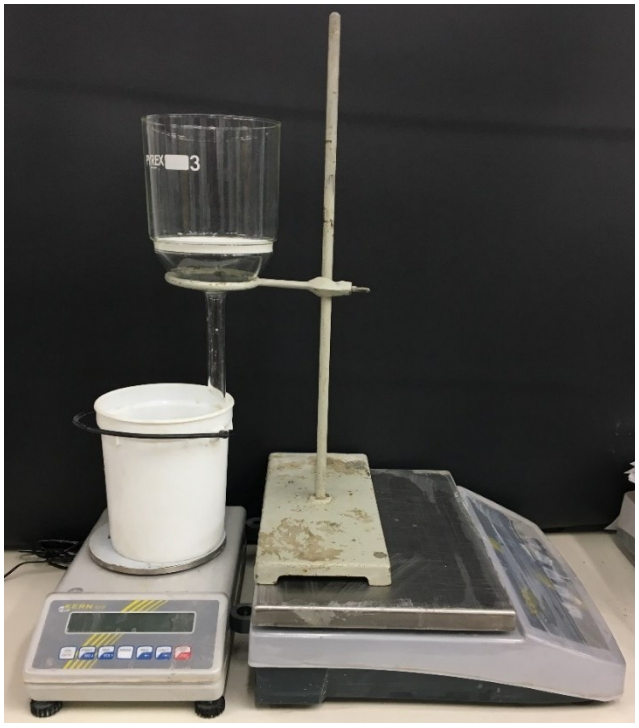

Figure 20. Standard Half-life Test

Equipment and Materials for the Half-life Test:

- A filter – funnel of 1 L capacity with a non-absorbent filter.
- A graduated container of 1 or 2 L capacity made from plastic or non-breakable material.
- A 50 ml graduated cylinder.
- Retort stand.
- A means of making foam with a known expansion ratio (FER) such as a foam generator.
- Weighing balance accurate to 0.1 g.
- Stopwatch.
- Foaming agent plus any polymers (if applicable) to be tested.
- Distilled water.

Standard procedure for the Half-life Test:

- Make a solution of the foaming agent in the distilled water to a fixed concentration.
- Incorporate polymers following manufacturer's recommendations, when applicable.
- Prepare the foam by using the laboratory scale foam generator to the required FER.
- Fill the filter – funnel with 80 g of the foam.
- Measure the time for 40 g of liquid to be collected in the lower cylinder (i.e 50% of the liquid content of the mixture).
- Record the results of the test.

4.6.3 Extraction Test

Extraction test in directed to simulate the situation occurring inside the excavating chamber of the EPBS machine. The device simulates the complex EPB operation that involves the conditioning of the soil and the interaction with machine-member for the extraction operation (Martinelli, 2016).

Equipment and Materials for the Extraction Test:

Peila, et al. (2007) developed a laboratory device made up of a 1500 mm long screw conveyor with an upward inclination of 30° connected to a 800 mm high pressurized tank with an inner diameter of 600 mm. The device was instrumented to measure torque, tank and screw conveyor loads, plate displacement and the weight of the extracted material (Borio & Peila, 2011). The device is shown in Figure 21, where each part is indicated.

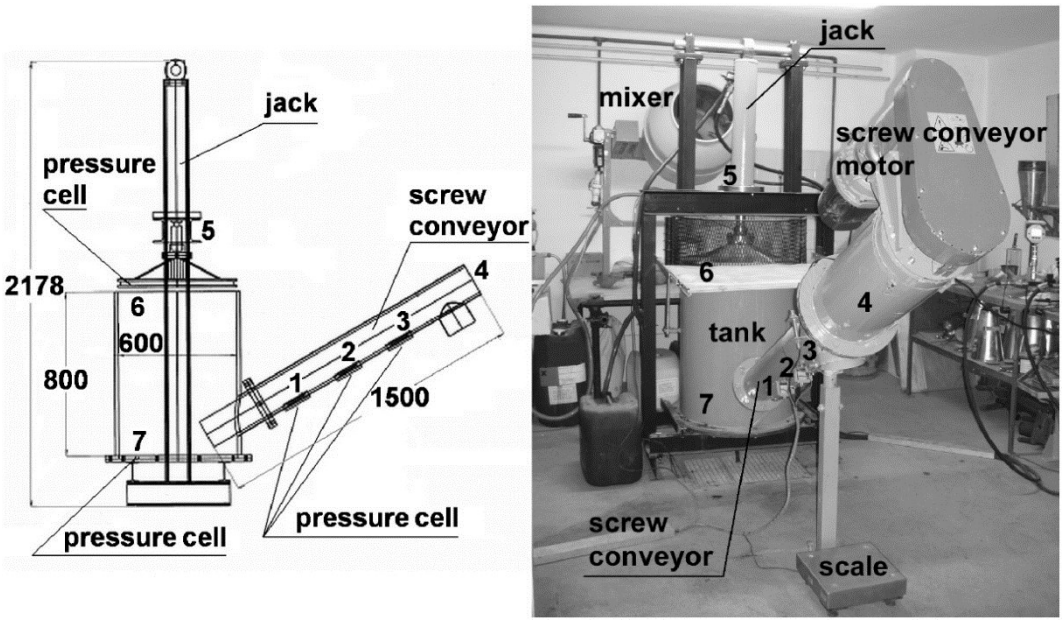

Figure 21. Screw conveyor laboratory device. Installed sensors: 1, 2, 3 are total pressure cells; 4 is the torquemeter; 5 is the displacement wire transducer; 6, 7 are the total pressure cells in the tank (Peila, et al., 2007).

Procedure for the Extraction Test:

According to Borio & Peila (2011), the procedure for the test is as follows:

- The soil sample for the test is prepared by mixing a soil with known moisture in a concrete mixer with the required amount of foam. The conditioned soil is then poured into the tank. This operation is repeated until the tank is full.
- The upper plate is then positioned and pushed down by the jack to reach the test pressure.
- The screw conveyor is then started and the material is collected and weighed at the discharge outlet.
- During the extraction of the material, the upper plate is moved downwards to keep the pressure in the tank constant.
- During the test, the pressure in the tank and along the screw device and the torque are monitored continuously.

Chapter 5

Wear Test

5.1 Bibliographic analysis of pre-existing wear tests in rock excavation

In the case of rocks, different methods have been already implemented to determine the abrasiveness of the metallic material in contact with the ground. These methods are now reliable enough for estimating the wear of cutter discs, as they have been extensively tested on laboratory and real scales.

According to Oñate Salazar, et al. (2018), the most commonly used laboratory tests are: the Vickers test, the Cerchar test, the LPCP abrasimeter test and the NTNU abrasion test (Blindheim & Bruland (1998); Ozdemir & Nilsen (1999); Büchi, et al. (1995); Nilsen, et al. (2006a-c); Abu Bakar, et al. (2016), respectively).

5.1.1 Vickers test

The Vickers test provides the Vickers Hardness Number (VHN), which indicates a hardness value. This test allows to establish the material resistance to plastic deformation on the sample surface or section.

It consist on the penetration of a tetrahedral pyramidal diamond, with an angle between opposite edges of 136°, on the surface to be tested (Figure 22), and it is expressed by the numerical value of hardness. This numerical value is obtained by dividing the applied load (kgf) during a fixed period of time, between the lateral surface of the indentations (mm²) calculated by the diagonals (EcuRed, n.d.).

The numerical value for hardness is calculated by the following formula:

$$VHN = \frac{2*P*sen\frac{\alpha}{2}}{d^2} = 1.8544 * \frac{P}{d^2} \qquad \text{Equation (14)}$$

Where:

- P = load on the pyramidal diamond, in kgf

- α = angle between opposite edges of the pyramidal diamond expressed in degrees
- d = arithmetic mean resulting from the two diagonals of the indentation after the load is removed, in mm.

This formula is generally not used in a practical approach, as the numerical values of hardness are determined by using tables prepared according to the diagonal of the indentation.

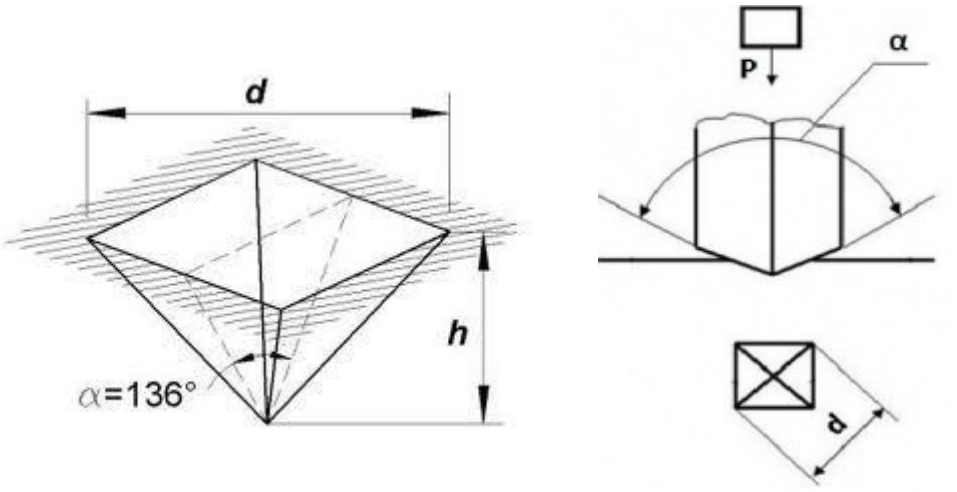

Figure 22. Diamond and schematic of Vickers Hardness test

Different authors have compared and related Vickers hardness values to the more famous Mohs' scale. Young & Millman (1964) proposed a linear relationship in a bi-logarithmic plot Figure 23, which is mathematically expressed by the following equation:

$$VHN = 2.5 \log Mohs + 1.00 \qquad \text{Equation (15)}$$

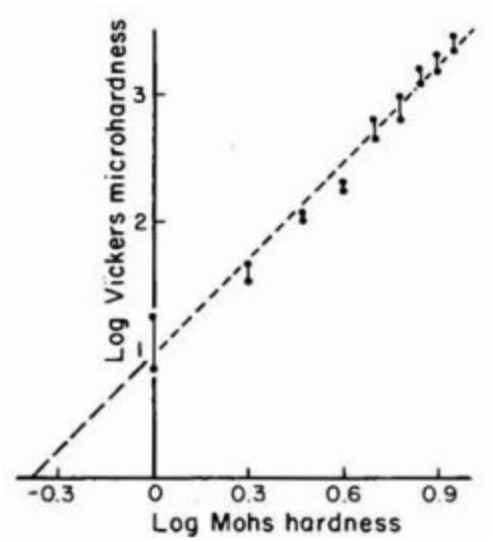

Figure 23. Correlation of Vickers microhardness with Mohs' scale of hardness (Young & Millman, 1964).

5.1.2 Cerchar test

The Cerchar test provides the Cerchar Abrasivity Index (CAI), which represent an abrasivity value. This test was developed by the "Laboratoire du Centre d'Etude et Recherches des Charbonnages" (CERCHAR), located in France, in the 70's, with the objective to measure the abrasivity of the machinery used in the coal industry; nowadays it is widely implemented in tunnel, drilling and mining fields.

As described by Käsling & Thuro (2010), "the testing principle is based on a steel pin with fixed geometry and hardness that is scratches the surface of a rough rock sample over a distance of 10 mm under static load of 70 N". The CAI is dimensionless and is calculated by measuring the diameter of the steel pin after the test (Figure 24) and applying the following formula:

$$CAI = 10\frac{d}{c} \qquad \text{Equation (16)}$$

Where:

- d = diameter of wear flat (mm)
- c = unit correction factor (c=1mm)

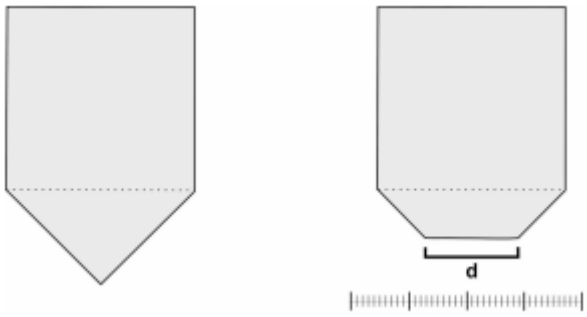

Figure 24. Schematic of the steel pin tip in the Cerchar test before (left) and after (right) (Käsling & Thuro, 2010).

Because of the base principle of the test is simple, there are different devices created for performing this test. Figure 25 represents the diagram designed by the Centre d´Études et des Recherches des Charbonages in France in 1986. As shown in the Figure 25, the device has a dock to place the weight (1) corresponding to the 70 N required and a chuck (2) able to block the bit into the wanted position. (3) All the bits that will be tested, must be previously prepared with an angle of 90°. The rock sample is located in the bottom part (4), clamped tanks of a vice (5). The movement of the sample is possible tanks of a hand lever (6). The bit speed must be of 1 mm/s and the duration of the test must be 10 seconds.

The advantage of this test is that it can be performed also on irregular rock surfaces and it is directly related to the tools life. Table 1 shows an example of classification in terms of abrasivity according to the CAI, for a HRC55 Rockwell Hardness steel pin tip and a rough rock surface.

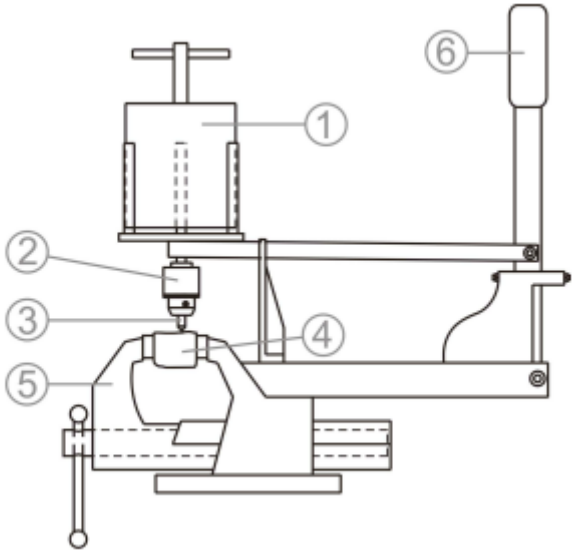

Figure 25. Schematic of Cerchar test proposed by Cerchar (1986). 1 – weight, 2 – pin chuck, 3 – steel pin, 4 – sample, 5 – vice , 6 – hand lever.

Table 1. Classification of CAI (Alber, et al., 2014).

Mean CAI	Classification
0.1–0.4	Extremely low
0.5–0.9	Very low
1.0–1.9	Low
2.0–2.9	Medium
3.0–3.9	High
4.0–4.9	Very high
≥5	Extremely high

In a study carried out by Deliormanli (2011) it is demonstrated that the CAI is conected to the life of the cutter on the field. His study is based on rocks with CAI values ranging from 0.5 to 3.0, explaining that CAI values lower than 0.5 corresponds to soft rocks, which produce little wear to the bit and makes difficult to assess the CAI value. Meanwhile, values above 5.0 correspond to hard rock and the bit jumps on the sample surface due to 70 N are insufficient for the vertical pressure required in hard rocks.

For the mentioned fixed range, Deliormanli establishes a relationship between the resistance to uniaxial compressive strength and the CAI, described by the following formula:

$$UCS = 54{,}47 \cdot CAI + 18{,}26 \qquad \text{Equation (17)}$$

Deliormani also establishes a relationship between the direct shear strength (DSS) and the CAI (Equation 18) and found a multiple regression mathematical relation (Equation 19) from which the CAI can be obtained, using the UCS and DSS values.

$$DSS = 7{,}72 \cdot CAI + 2{,}87 \qquad \text{Equation (18)}$$

$$CAI = 0{,}0410 + 0{,}0224 \cdot UCS - 0{,}0525 \cdot DSS \qquad \text{Equation (19)}$$

On the other hand, a study performed at the Bochum University (Alber, 2017) shows that CAI index depends on the stress of the rock. Thanks to the tests carried out on a triaxial cell, Alber demonstrated that the abrasive effect is different when comparing laboratory results to in situ outcomes, having the latter a higher state of stress. In Figure 26, an example of this study is shown. It is observed that confining is an important factor that needs to be considered in the laboratory tests.

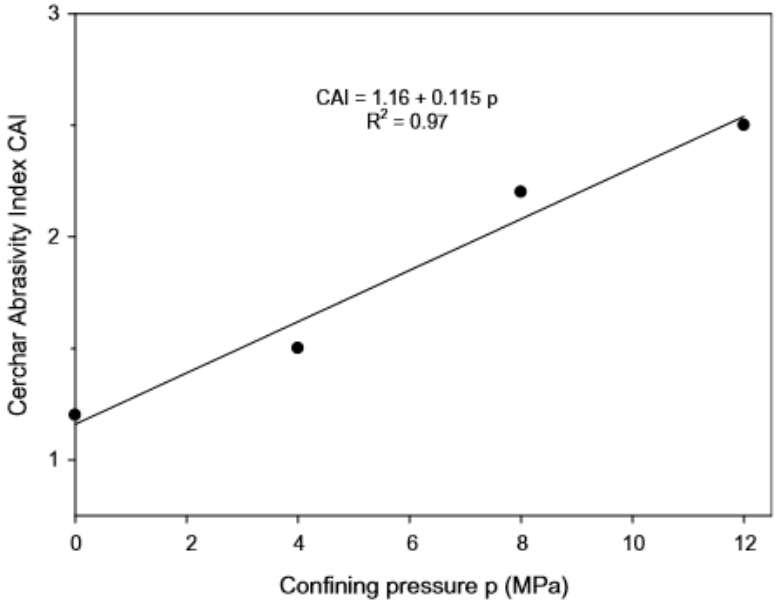

Figure 26. CAI versus confining pressure, test results of one sandstone sample (Alber, 2017).

5.1.3 LPCP abrasimeter test

The LPCP abrasimeter test provides the LCPC abrasivity coefficient (LAC), which is an abrasivity value. This method was developed by the "Laboratoire Central des Ponts et Chausées" (LCPC) in France for testing rock and aggregates and it is described in the French standard P18-579.

The test consists of rotating a rectangular metal impeller, which is inserted in a cylindrical vessel containing 500 g of granular sample, during 5 minutes at a speed of 4500 rpm (Figure 27). As described by Käsling & Thuro (2010), "the rectangular impeller is made of standardized steel with a Rockwell hardness of HRB 60–75. As stated in the standard, the grain size of the rock sample has to be in a range between 4 to 6.3 mm; rock has to be crushed before the test accordingly". Fragments with dimensions lower than 4 mm are discarded.

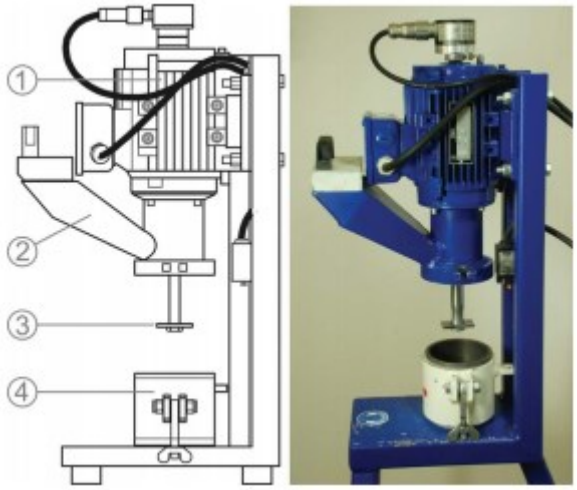

Figure 27. LCPC abrasivity testing device according to the French standard P18-579 (1990). 1 – motor, 2 – funnel tube, 3 – steel impeller, 4 – sample container (Käsling & Thuro, 2010).

Before and after the test the impeller is weighed in order to obtain the LCPC Abrasivity Coefficient (LAC) by using the following formula:

$$LAC = \frac{(m_0 - m)}{M} \qquad \text{Equation (20)}$$

Where:

- m_0 = mass of impeller before test (g)
- m = mass of impeller after test (g)
- M = mass of the sample material (=0.0005t)

As shown in the equation, the LAC is expressed in g/t, representing the amount of metallic material lost per ton of granular sample studied. The typical values of LAC in rock range from 0 to 2000 g/t. In Table 2 a classification of CAI and LAC indexes, published by Käsling & Thuro (2010), is shown. This classification demonstrates a linear relation between both indexes.

Table 2. Classification of the LCPC-Abrasivity-Coefficient (LAC) in connection with the CERCHAR-Abrasivity-Index (CAI) according to Thuro, et al. (2007), Käsling & Thuro (2010).

LAC [g/t]	CAI [0.1]	Abrasivity classification	Examples
0-50	0.0-0.3	not abrasive	organic material
50-100	0.3-0.5	not very abrasive	mudstone, marl
100-250	0.5-1.0	slightly abrasive	slate, limestone
250-500	1.0-2.0	(medium) abrasive	schist, sandstone
500-1250	2.0-4.0	very abrasive	basalt, quartzitic sdst.
1250-2000	4.0-6.0	extremely abrasive	amphibolite, quartzite

According to Käsling & Thuro (2010), the LCPC abrasivity test also allows to quantify the brittleness or breakability of the sample material using the LCPC Breakability Coefficient (LBC), which is calculated with the following equation:

$$LBC = \frac{(M_{1.6} * 100)}{M}$$ Equation (21)

Where:

- $M_{1.6}$ = mass fraction < 1.6 mm after LCPC test (g)
- M = mass of the sample material (=0.0005t)

The LCPC Breakability Coefficient (LBC) is expressed as a percentage (%) and is defined as the fraction below 1.6 mm of the sample material after the test. A modified classification is given in Table 3.

Table 3. Classification of the LCPC-Breakability-Coefficient (LBC) (Käsling & Thuro, 2010).

LBC [%]	Breakability classification
0-25	low
25-50	medium
50-75	high
75-100	very high

5.1.4 NTNU abrasion test

The NTNU abrasion test provides the AV/AVS indexes, which are abrasion values. This method was developed by the Engineering Geology Laboratory of the Norwegian Institute of Technology (NTH). Originally, it was designed for estimating the drillability of rocks by percussive drilling, and then adapted for predicting hard rock TBM wear performance. Currently, there is a version of the test applicable to soft ground and will be further described in Paragraph 5.2.2.

To perform this test a sample of 2 kg of crushed rock powder with granular dimensions < 1 mm (obtained by using standard procedures) is required. The test consists of a steel plate rotating at 20 rpm, on which the rock powder is fed to form a layer. Over this layer, the cutter steel test piece (previously prepared and weighed) is placed with applied a load of 10 kg (Figure 28).

The test specifications propose testing 2 or 4 steel elements, measuring their weight loss and checking that the measured weight loss between them does not differ by more than 5 mg (Nilsen, et al., 2006b). The AV/AVS values will be the average loss of the 2 or 4 elements in milligrams.

The AV and AVS parameters differ in the following details:

- AV (Abrasion value): the studied element is made of tungsten carbide; the test lasts 5 minutes, and therefore, the disc performs 100 revolutions. AV is originally used for drilling tests.
- AVS (Abrasion value steel): the studied element is made of cutter steel; the test lasts 1 minute, and therefore, the disc performs 20 revolutions. The use of AVS was extended to be applied in the assessment of TBM wear performance.

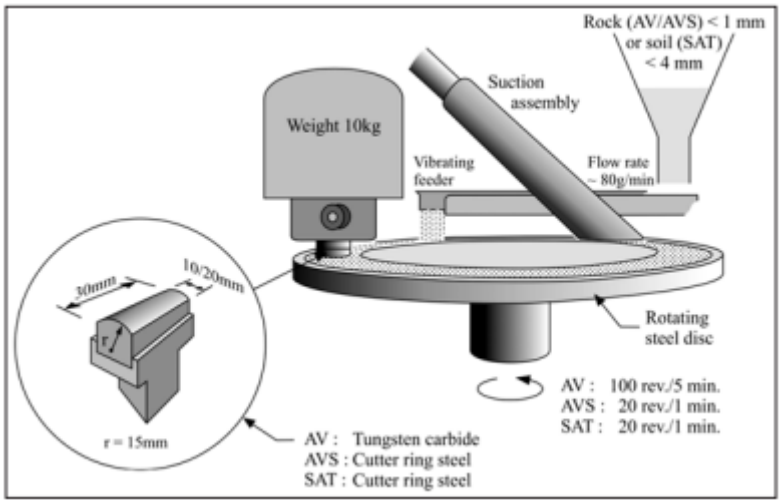

Figure 28. Principle sketch of the NTNU abrasion tests (Nilsen, et al., 2006b).

5.2 Bibliographic analysis of pre-existing wear tests in soft ground excavation

There are different tests for studying the abrasiveness of soils, but they are usually limited to describe the abrasiveness of the mineral, without considering the wear that occurs in metallic components. Such tests are not adaptable for the study of wear in the construction of tunnels where significant wear occurs in machine elements. Nevertheless, a brief description of these tests is herein presented:

- **Los Angeles abrasion test:** This test used for road pavements. A standard size metal cylinder is filled with 5 kg of aggregate and 5 kg of spheroidal graphite iron balls Ø 48 mm; this cylinder is rotated for 500 or 100 revolutions at a speed of 30-33 rpm. The material is then separated into material passing the 1.7 mm sieve and the material retained on the sieve to evaluate the crushing produced on the material.
- **Nordic Ball Mill Test:** The principle is very similar to that of the Los Angeles abrasion test and is mainly used in Scandinavia and Iceland. 1.5 kg of soil or rock fragments and 20 steel bits (16x16mm) are used and on the sample is applied 5400 revolutions in 1 hour.
- **Dorry's abrasion test:** is a test to determine the resistance to surface abrasion of the aggregate used in road paving. Basically, the aggregate is used as an abrasive and is dropped on a steel disc horizontally rotating, on which two specimens are pressed with a force of 0.365 N/cm^2, during 500 disc revolutions; the weight loss of the aggregate is then measured.

In terms of wear, the behavior of the cutting discs in soft ground excavation has a different effect to that exhibited in rock excavation. This difference is more evident in the presence of conditioned soils or with different water contents. The

main reason for this difference is due to the nature of the soil particles and the interaction between them under different environmental conditions.

The problem with abrasive soils and wear of cutter tools and, in general, of all metal components of the excavating machines, has raised much attention worldwide in the recent years. Different research centers have come to be interested in creating tests that allow studying the wear of the tools used in the EPBS. As mentioned by Oñate Salazar, et al. (2018), a good and wide discussion of the available tests can be found in Nilsen, et al. (2007), Gharahbagh, et al. (2011) and Mosleh, et al. (2009).

The most relevant studies carried out so far on soil wear are listed below.

5.2.1 LPCP abrasimeter test

The test method is the same as described in the Paragraph 5.1.3. Originally, the proposed test made by Büchi, et al. (1995) was designed only for rocks, and later on, a variant for soils was suggested in Thuro, et al. (2007) and Thuro & Käsling (2009).

Two of the most important factors to be considered for evaluating soils are shape and grain-size distribution. Regarding the shape, as particles break, it tends to become more angular and the increasing particle angularity could contribute to increasing abrasivity. One method for quantifying changing particle shape is by measuring sphericity and roundness (Gharahbagh, et al., 2011). Regarding grain-size distribution, in the original LPCP test, the grain sizes should range from 4 to 6.3 mm and fragments with dimensions lower than 4 mm or larger than 6 mm are discarded. This is not representative as the real abrasivity for an entire soil sample. Regarding the device, it is not cost effective if considering changing the dimensions of the vessel and/or the impeller, which is exchanged after each test.

According to Käsling & Thuro (2010), "when testing soil material, some considerations have to be done in order to agree with the technical recommendations: maximum grain size 6.3 mm due to the arrangement of the impeller and the capacity of the engine". In LPCP test for soils, grains larger than 6.3 mm can be crushed and sieved to obtain the required size. The grains less than 4 mm in some cases may be used for testing. The fines below 2 mm can be analyzed by X-ray diffractometer, whereas the larger components can be determined manually or optically. According to Thuro, et al. (2006), the wear process on site is crucial for the decision to discard or not the fines. As an example, the fine fraction of soils such as sand and fine gravel, may have a great impact on tool wear e.g. of a TBM shield; in such cases the grain fraction < 4 mm is very important.

There are two modalities for the LPCP test: 1- Testing an entire sample by crushing with a jaw crusher all grains > 6.3 mm until the sample grain-size achieve the suitable range for the device but "the test results have to prove if the obtained abrasivity represents the original grain size distribution of the natural sample" (Thuro, et al., 2006) and 2- Testing separate grain-size fractions, selected

and prepared to perform an LPCP test for each fraction. For soils, grain size distribution (before crushing and after applying the test) and petrologic and mineralogical analysis should be performed as a first step to understand the processes linked to the abrasivity in TBM.

5.2.2 NTNU/SINTEF Soil Abrasion Test

The NTNU/SINTEF Soil Abrasion Test is a variant of the NTNU abrasion test, described in Paragraph 5.1.4 of this thesis but, in this case, the SAT (Soil Abrasion Test) value is obtained instead of the AVS or AV values.

The difference between this variant for soils and the rock test is mainly based on the size of the abrasive grains. Originally, the maximum size was 1mm and now it is 4mm. Consequently, the test piece has also changed, going from 10 mm to 20 mm of width and maintaining the 15 mm curvature radius. In Figure 29 these modifications can be observed (Jakobsen, et al., 2013a), while in Figure 28, the schematic of the test is provided, being the same as that used in the rock test.

The SAT is the mean of weight loss of 2 or 4 steel elements once they have been exposed to the abrasion of the soil powder placed on the cutter ring steel plate. The test lasts 1 minute and the disc performs 20 revolutions.

To reduce and/or avoid changing the shape and size of the grains to be evaluated, it is required to dry the sample in a ventilated oven at a temperature of 30 degrees Celsius for 3 to 4 days. After the drying process, a series of steps, listed below, should be performed:

Disintegration of the material using a soft hammer.

- Sieving the material with steel balls.
- Previous disintegration using a jaw crusher if the sample initially contains very hard lumps of cohesive material. This is to be performed after the drying process. Crushing of intact grains already evaluated should be avoided.

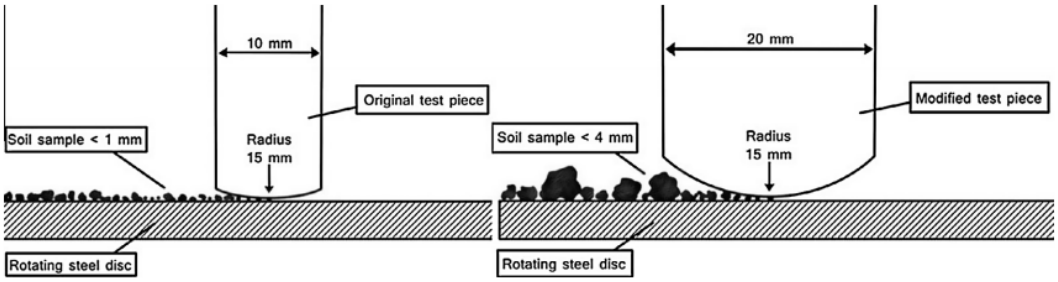

Figure 29. The initial AVS (left) and modified and current SAT™ (right) test pieces (Jakobsen, et al., 2013a)

In Jakobsen, et al. (2013a), some correlations between the SAT index and the parameters indicating the quartz content of the soil (Figure 30) and the Vickers hardness (Figure 31) are available.

Although the available data are based on some types of cutter discs, by relating laboratory data to the actual scale wear of these discs, it was possible to correlate the SAT index value and the tool life, but conditioning and soil density were not considered (Figure 32).

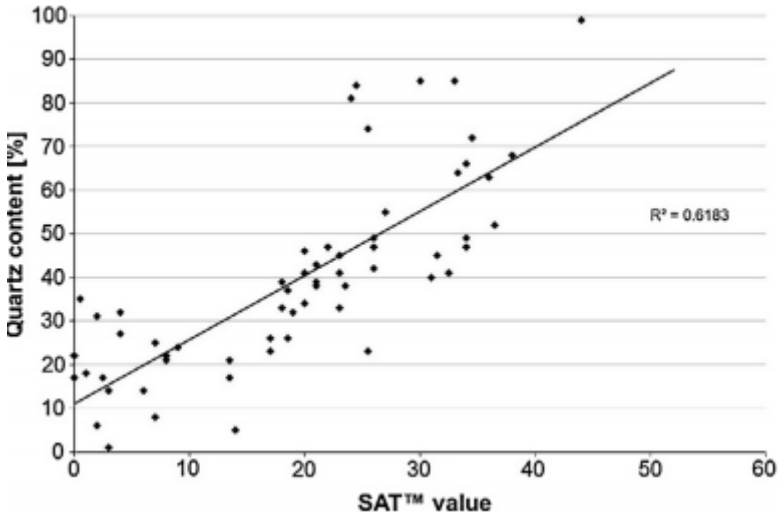

Figure 30. Correlation between SAT™ value and content of quartz. N = 62 (Jakobsen, et al. 2013a).

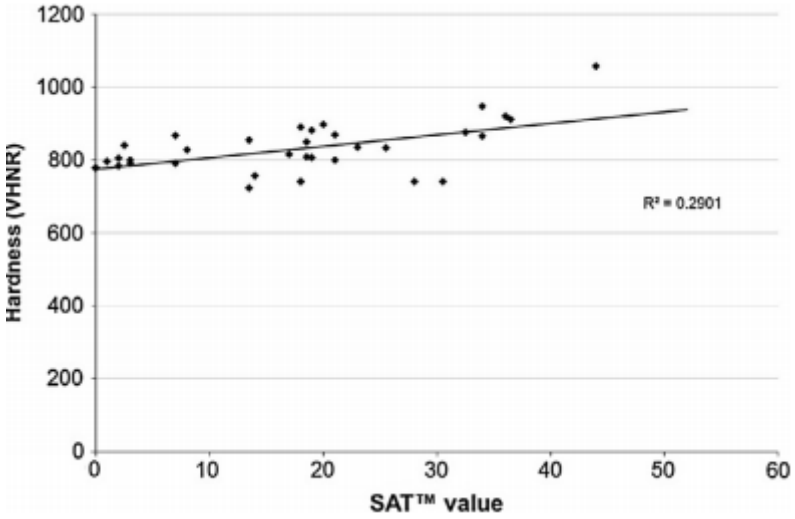

Figure 31. Correlation between SAT™ value and content of quartz. N = 62 (Jakobsen, et al. 2013a).

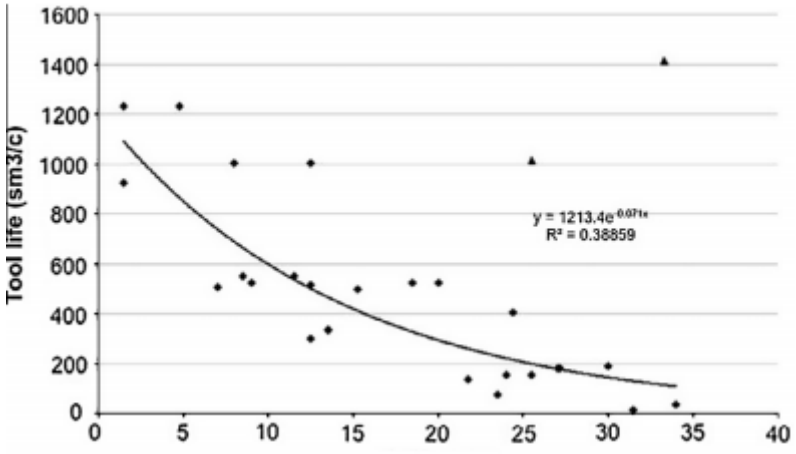

Figure 32. Correlation between SAT values and recorded soft ground tool life (Jakobsen, et al. 2013a).

5.2.3 SGAT - Soft Ground Abrasion Tester

This method, same as the NTNU/SINTEF Soil Abrasion Test (SAT), was developed by the Norwegian University of Science and Technology (NTNU) and SINTEF Rock Engineering, in collaboration with BASF Construction Chemicals. The purpose of this new test device was to better replicate the contact produced between the *in situ* soil and the TBM excavation tool and also adding some conditions not considered in the previous method (such as the use of conditioning agents).

In Jakobsen, et al. (2013b) the test procedure and specifications are described and will be briefly explained below.

As shown in Figure 33, the SGAT apparatus consists of a drive unit. This unit rotates and moves vertically and it is connected to a shaft that has two steel bars at its lower end (Figure 34).

These bars, which are the elements to be studied for assessing wear, penetrate the soil placed in a chamber equipped with an airtight cover that supports up to 6 bar of pressure. The soil is prepared discarding any fractions > 1 cm; depending on the degree of compaction, from 6500 to 8000 grams of soil are used.

Before or during the test, it is possible to inject water, bentonite or soil conditioning additives by using the nozzles positioned in the bars. Rotation speed can vary from 0 to 100 rpm and penetration rate is usually set at 40 mm/min.

Once the rotation and penetration rate values have been set, the torque needed for that rotation speed and the thrust force required for that vertical feed to occur are determined; they will change according to the environment conditions of each test. At the end of the test, the weight loss of the bars is calculated and the torque and thrust force values are recorded.

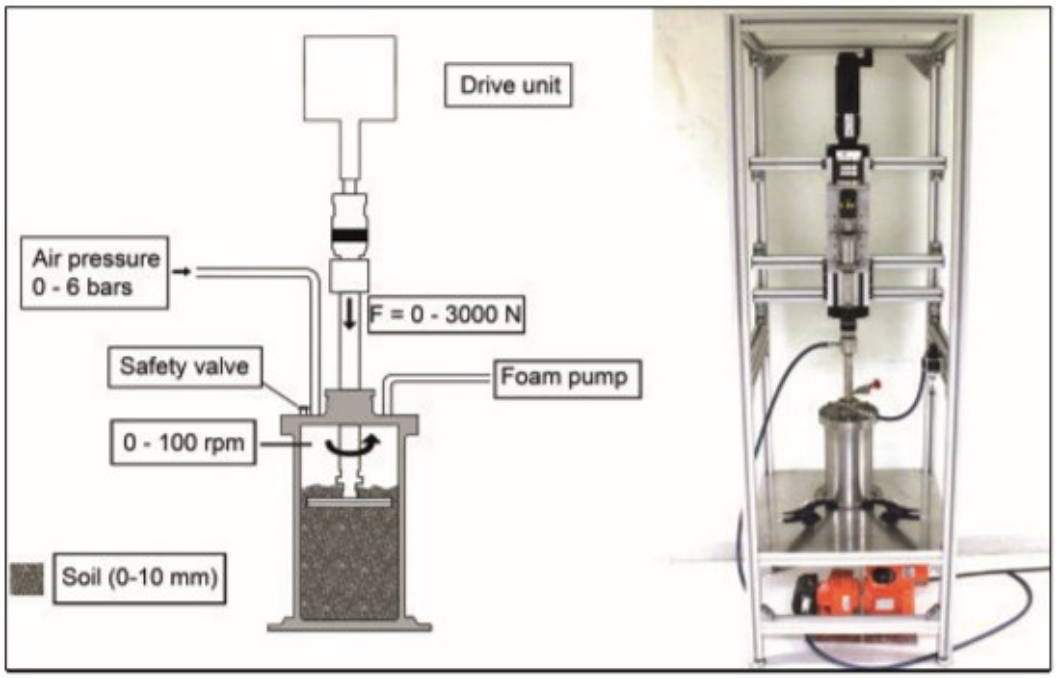

Figure 33. The SGAT apparatus (Jakobsen, et al., 2013b)

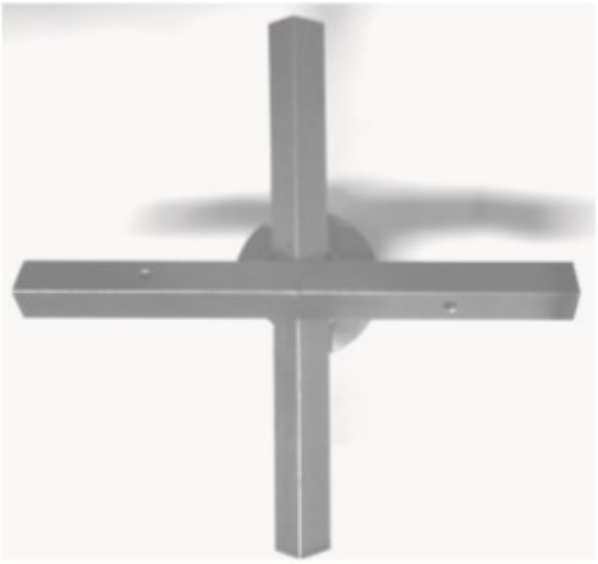

Figure 34. The SGAT drilling tool (Jakobsen, et al. 2013b)

In Figure 35 it can be observed the three techniques that have been tested for additives addition: (a) before the test, the soil is compacted and the additives are then injected, (b) the additives are continuously injected during the test; (c) the soil is mixed with the additives before performing the test. The preferred one is (b) technique, since it fits best to reality.

Some results, presented in Table 4, show that increasing compaction and consequently the density it increases the wear and torque applied under predefined conditions. Figure 36 shows that higher torque results in greater thrust force and Figure 37 displays the relationship between soil density and weight loss and torque.

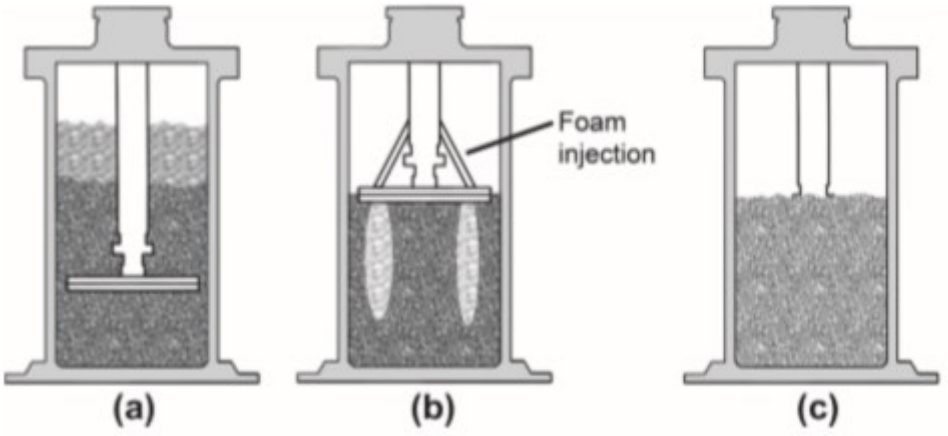

Figure 35. Overview of possibilities to add soil conditioning additives in the SGAT apparatus. (a) Shows addition of foam on top of the soil sample, (b) shows a continuous addition of foam through nozzles, and (c) shows a premix of foam and the soil sample (Jakobsen, et al. 2013b)

Table 4. Example of influence of soil compaction and density on wear and torque (Jakobsen et al. 2013b).

Density (kg/m^3)	Compaction proc.	Wear (mg)	Avg. torque (Nm)
1544	No compaction	52	8.7
1886	5 Blows/4 layers	82	10.7
1958	10 Blows/4 layers	75	11.2
2058	15 Blows/4 layers	92	13.2
2109	20 Blows/4 layers	92	11.4
2228	30 Blows/4 layers	115	17.0

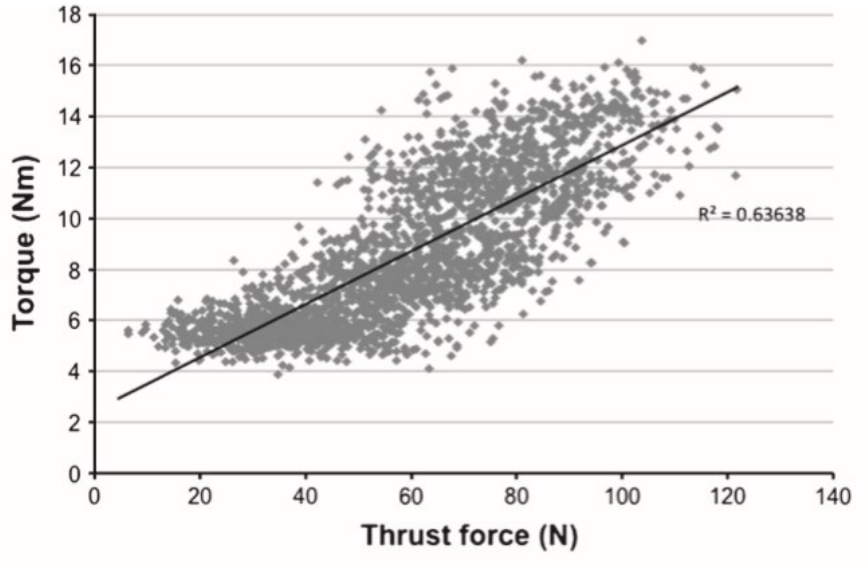

Figure 36. Example of relation between thrust force and required torque for achieving a fixed penetration of 40 mm/min for one soil sample (Jakobsen, et al. 2013b).

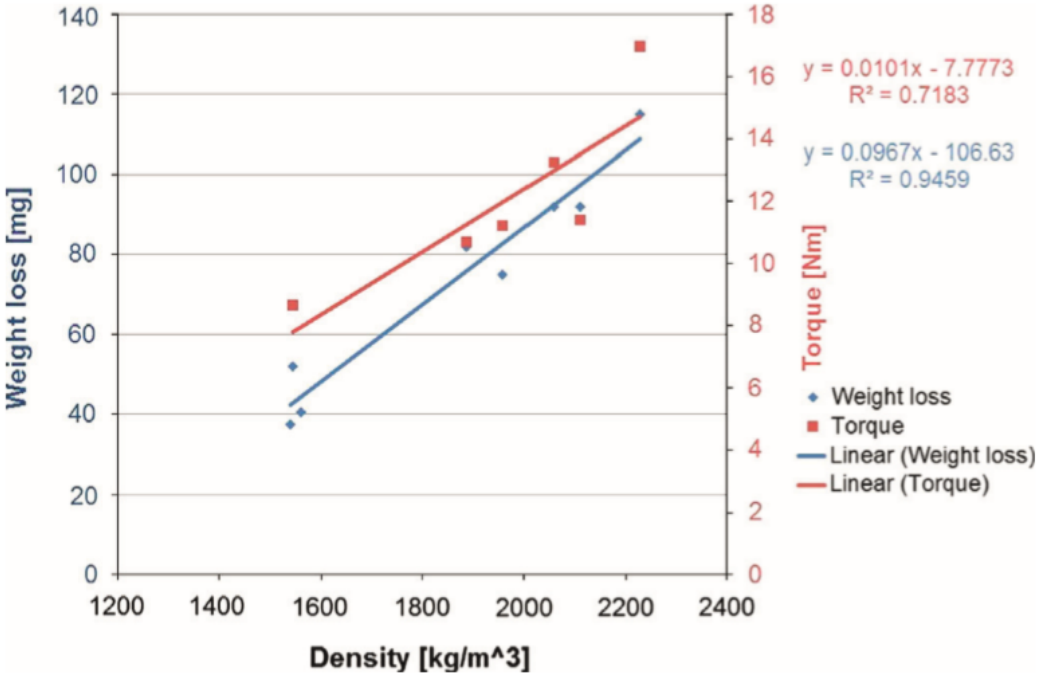

Figure 37. Measured relation between soil compaction grade (density), abrasivity (weight loss) and average torque on one soil sample (Jakobsen & Lohne, 2013).

In relation to soil water content and the use of foams for conditioning, Jakobsen, et al. (2012) published the plot shown in Figure 38, where a "bell" behaviour can be observed as the water content varies and the use of foam results in a lower weight loss for the tool with water contents below 12%.

On the other hand, in Figure 39 some preliminary results related to the minor influence of pressure on steel wear are shown.

Summarizing, the tests performed under this method show that tool wear in soft ground is influenced, in different extent, by:

- Soil Nature (mineralogy, quartz content, particle hardness, distribution and compaction of the soil);
- Soil Moisture;
- Conditioning type and method;
- Application of pressure inside the chamber of the SGAT apparatus.

From all the above studies, it is important to highlight that environment conditions should not be underestimated when evaluating the interaction between soil and metallic elements.

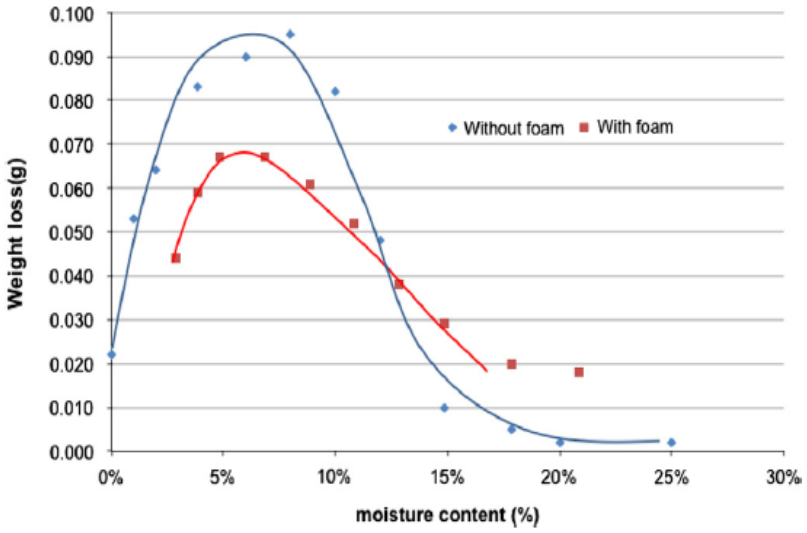

Figure 38. Abrasivity (weight loss on the steel tool) for different moisture contents on one soil sample (Jakobsen, et al., 2012).

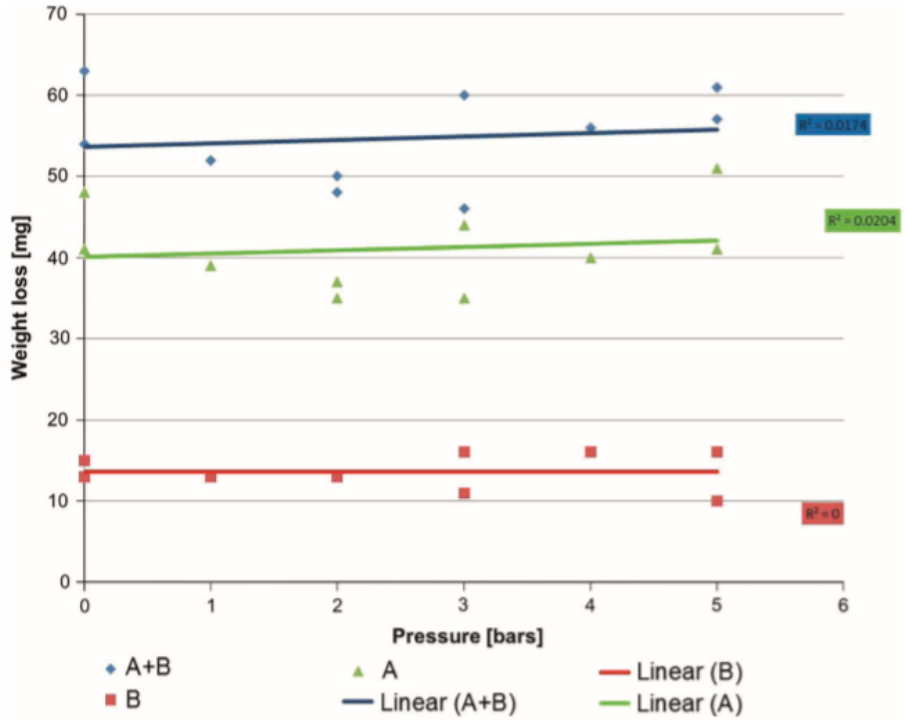

Figure 39. Example of relation between weight loss (abrasion) and face support pressure (bars) for a soil sample (Jakobsen, et al. 2013b).

5.2.4 Penn State Soil Abrasion Testing

This test method was developed by a group of researchers at the Pennsylvania State University, with the objective of building a device to study soil abrasion under conditions more consistent with those obtained in situ.

As described in Gharahbagh, et al. (2011) and Rostami, et al. (2012), the device consists of a cylindrical chamber approximately 350 mm in diameter by 450 mm in length that can bear up to 10 bar of pressure. Such dimensions were

selected to allow the soil samples having large particles as seen in the work field and thus avoid affecting grain size distribution.

The soil to be tested is placed into the cylindrical chamber equipped with a rotating propeller, which is attached to a drive shaft located right in the middle of soil sample. The device works with a drill press equipped with engine of 5 hp and a drive unit that allows shifting between several rotation speeds (Figure 40). The propeller has three triangular blades with a 150 mm radius; they are welded at 120 degrees of angular separation among them, leaving an annular space of about 12 mm between the edge of the blades and the walls of the chamber, which allow the flow of materials. The blades can be placed with different degrees of inclination regarding the rotation axis.

In Figure 41 the details of the propeller and blades are shown, it can be seen that propeller blades are fitted with three steel covers.

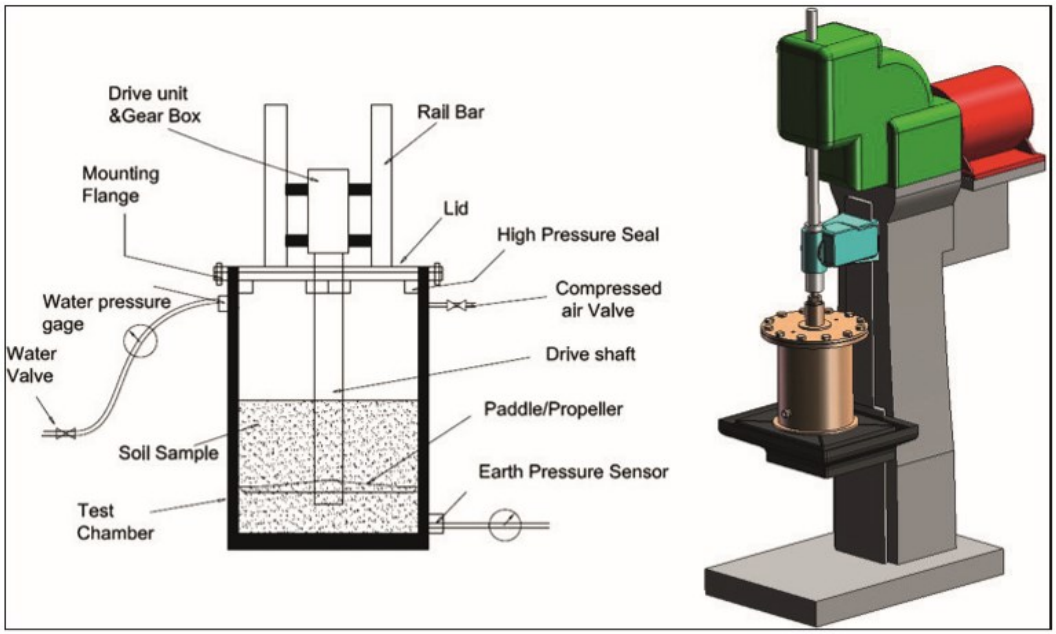

Figure 40. Illustration of the Penn State Abrasion Testing System (Gharahbagh, et al., 2011).

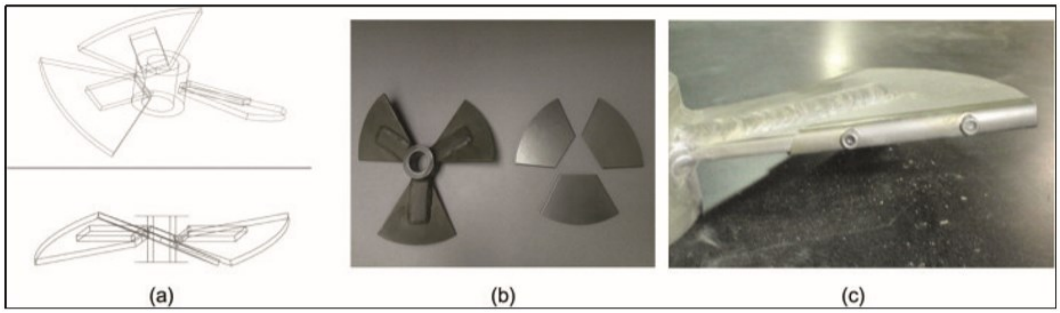

Figure 41. The propeller blade: (a) schematics of the propeller and blades, (b) propeller with three covers, and (c) mounting system of the cover on the propeller blades using two bolts (Rostami, et al., 2012).

Wear is expressed in terms of weight loss. The final weight loss is the cumulative loss of the three covers measured at different time steps (5, 10, 30, 60 minutes).

Below are presented some results from the tests:

- **Effect of pitch angle on abrasion:** lower blade pitch angles resulted in maximum wear values (Figure 42). "This clearly indicates that the 10 degree pitch angle causes the maximum compression and mutual pressure between the soil grains and propeller blades" (Rostami, et al., 2012).

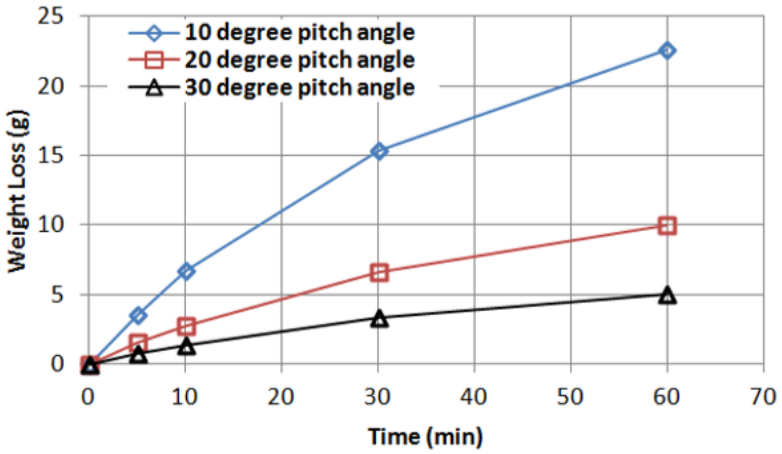

Figure 42. The effect of propeller pitch angle on the weight loss of the covers (Rostami, et al., 2012).

- **Effect of moisture content on abrasion:** by increasing the water content of the soil, the wear of the metallic elements presents "bell" behaviour, being the maximum weight loss value of about 7.5% obtained in silica sand (Figure 43).

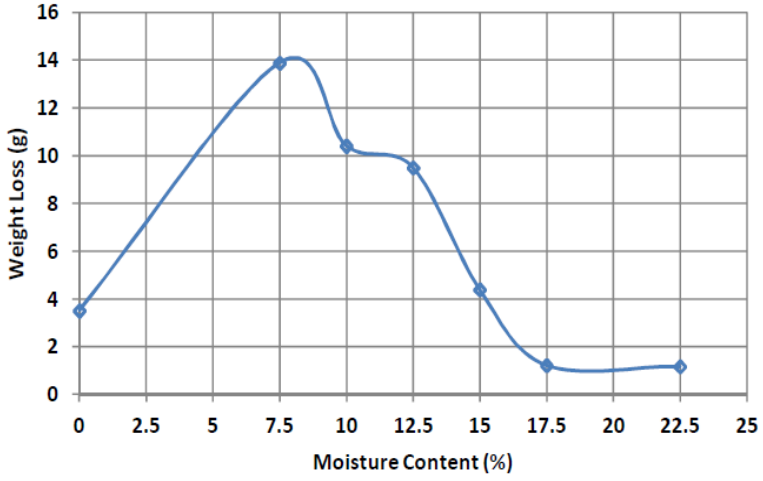

Figure 43. Weight loss, of 17 HRC covers after 5 min of testing with different moisture contents in silica sand (Rostami, et al., 2012).

- **Effect of material hardness on abrasion:** it was observed that "the relationship between tool wear and the surrounding moisture condition is

opposite under dry and wet conditions" (Rostami, et al., 2012). In dry conditions the wear is lower when there is an increase in element hardness; while in conditions of 10% moisture, the wear is larger for the elements with higher hardness (Figure 44).

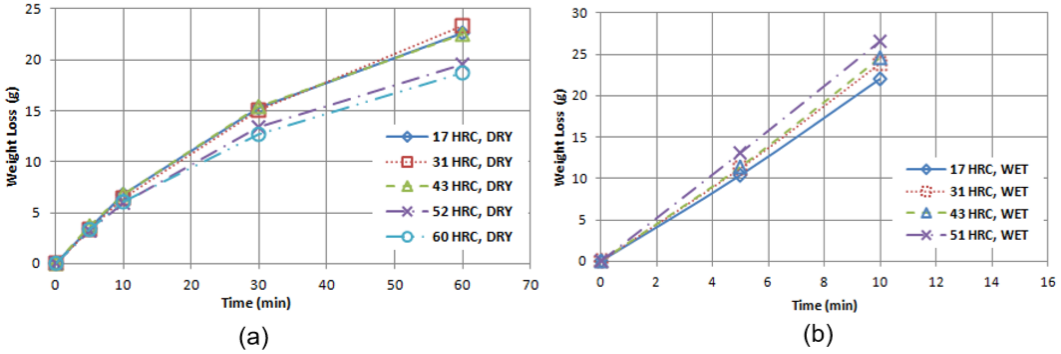

Figure 44. a) Weight loss of different hardened covers with respect to time in dry Silica sand samples b) in 10% moisture content silica sand sample (Rostami, et al., 2012).

- **Effect of ambient** pressure on abrasion: the relationship between the pressure increase and the consequent increase in wear is not particularly evident in the obtained results. During the first minutes of the test, the pressure does not appear to have a significant effect on wear, while after 60 minutes there is a slight increase in wear on tests performed at higher pressures, especially for the lower hardness elements (Figure 45).

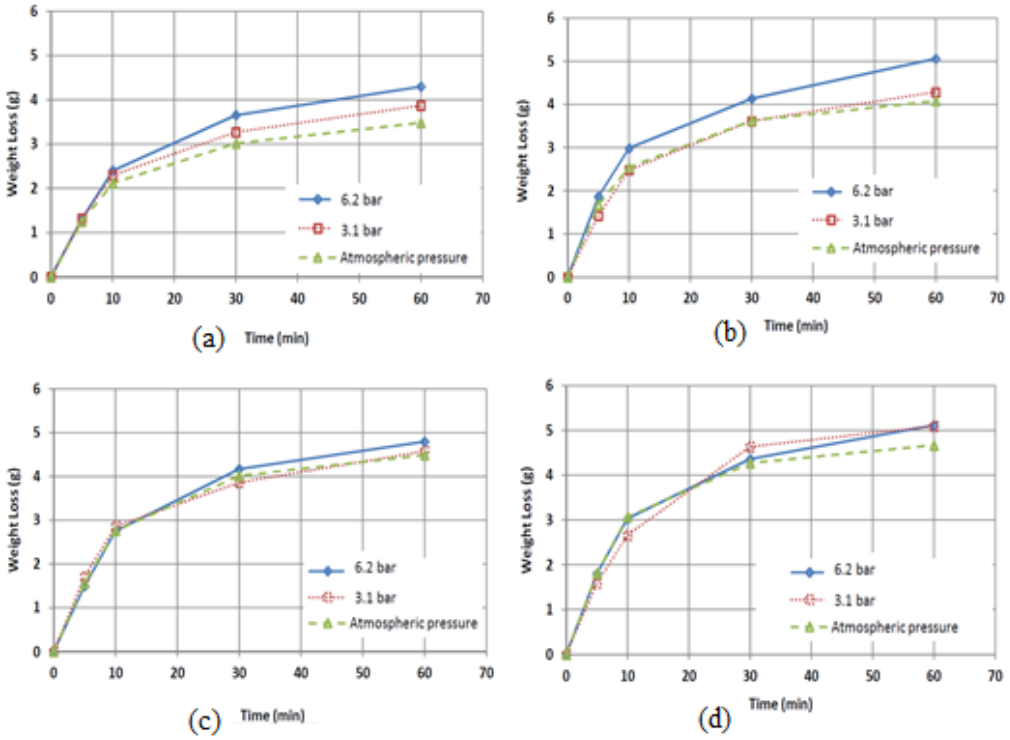

Figure 45. Weight loss in saturated silica sand sample with different applied pressure (a) 17 HRC covers (b) 31 HRC covers (c) 43 HRC covers (d) 51 HRC covers (Rostami, et al., 2012).

- **Effect of relative mineral hardness on tool wear:** some tests were performed using several combinations of silica sand (abrasive soil with high quartz content) and limestone sand (less abrasive soil with low quartz content). In Figure 46, one of the test results is provided; it can be observed that wear increase proportionally to the increase in silica sand quantity, meaning there is larger wear with increasing quartz presence.

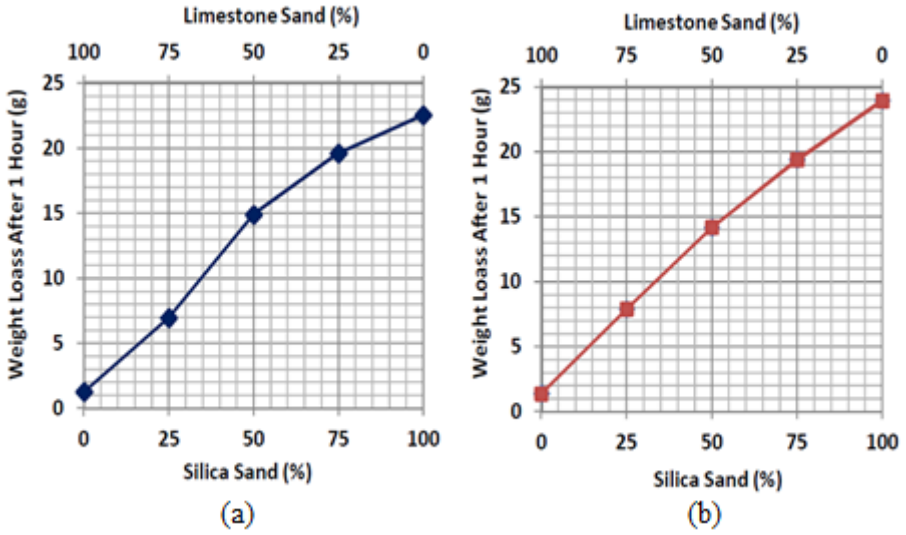

Figure 46. Weight loss of (a) 17HRC and (b) 31 HRC covers after 1 h of testing in dry condition with respect to the percentage of limestone sand and silica sand in the mixture (Rostami, et al., 2012).

5.2.5 Wear Disc Test

This test methodology was designed at the Politecnico di Torino for the purpose of building a testing machine for studying the wear of a disc submerged in soils that could be conditioned (Barbero, et al., 2012). This doctoral thesis is based on the implementation of this methodology; therefore, this test will be explained in depth in the next chapter (Paragraph 6.1).

Chapter 6

Methodology of the performed wear tests

Wear tests were applied using different methodologies by modifying the pre-existing tests or designing and manufacturing new devices, in order to demonstrate and quantify the influence of water content and/or conditioning agents on wear phenomenon. This chapter describes each used test method.

6.1 Wear Disc Test

Wear Disc Test has been extensively used in recent years, so it cannot be considered a novelty. In this thesis it was widely used to deepen the performed studies and it is the basis for the innovative methodologies that will be the real object of this work.

This test allows to quickly and easily assessing the abrasiveness of a given soil under different conditions (dry, wet or conditioned), by rotating a metal disc inserted in a steel vessel that contains the soil to be tested (Barbero, et al., 2012).

The test device (Figure 47) consists of a cylindrical steel tank with 300 mm in height and 308 mm in nominal diameter (Figure 48) and a vertical column drill. Inside the cylinder, the disc rotates (Figure 49) tightly connected to a drive shaft (Figure 50). At the same time, the drive shaft is connected to a torque transducer Lorenz type DR 1221-R for data acquisition, which is assembled to the electric motor drill that produces the rotational torque at 160 rpm.

Traditional wear test (Wear Disc Test) aims at determining the weight loss of the disc rotating on its own axis. This weight value will be the reference for the following results and the different tested conditions.

The disc used to estimate metal wear is circular shaped with 120 mm in diameter and 10 mm in thickness. It has a central opening of 24 mm for inserting the drive shaft and 4 openings for the clamping system (Figure 51). A different

material for the disk can be utilized to obtain data for other kinds of metals. The first tests were conducted on aluminium discs (440 MPa tensile strength and 3.3 GPa elastic modulus) (Barbero, et al., 2012).

Soil abrasiveness can be assessed with this method by varying soil natural conditions with the addition of water and conditioning products. Wear can also be tested using different kinds of soils and different disc materials but all the other parameters, such as disk rotation, durability and confinement, should remain unchanged.

To ensure a constant contact between the ground and the disc, it is possible to fix a higher confinement pressure (about 2 kPa) by putting concrete weights on the ground by means of wooden platforms. The wooden platforms and the concrete weights are design to fit the shape of the container (Figure 52).

Figure 47. Wear Disc Test device

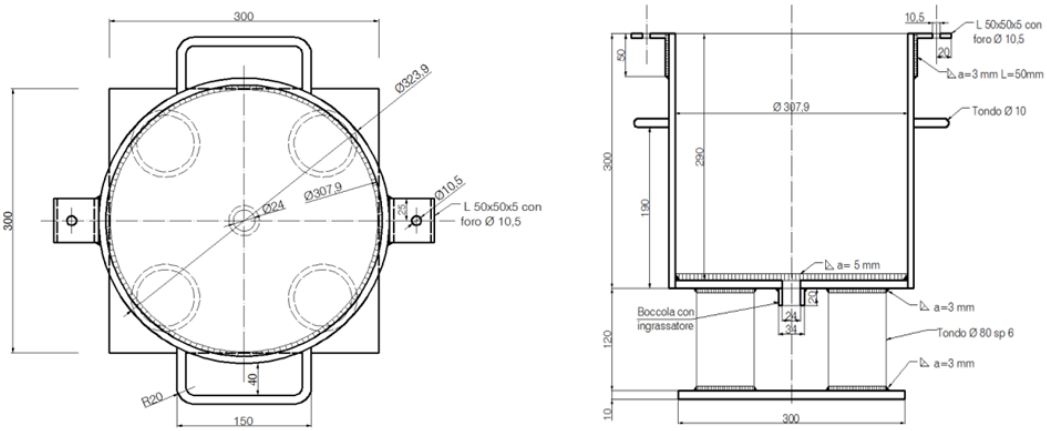

Figure 48. Schematic of the cylindrical steel tank.

Figure 49. Detail of the disc assembled on the drive shaft inside the tank.

Figure 50. Schematic of the Drive Shaft (left) and photograph of the disc on the drive shaft (right).

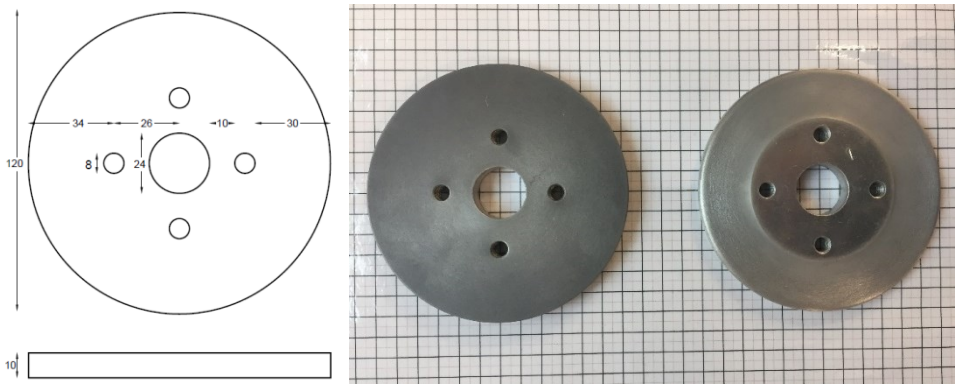

Figure 51. Schematic of disc geometry used for the Wear Disc Test and some discs examples.

Figure 52. Soil confinement

6.1.1 Test Procedure

The operating procedure is herein described:

1. Preparation of about 15 dm^3 of soil (particle size less than 20 mm). According to the test to be performed, natural soil, soil with different percentages of water added or soil conditioned with foaming agents and/or anti-wear agents shall be used.
2. Disc Weighing: before the test, the disc is washed, dried and weighed, and the w_1 value is recorded.
3. Assembly the disc on the drive shaft that is connected to the torque transducer Lorenz type DR 1221-R and then, place it inside the tank at about 80 mm from the bottom. The drive shaft is secure to the tank by using two bushings that fix the mobile bushing on the tank body (Figure 53)
4. Fill the tank with the soil sample: the disc is covered with a layer of soil sample material at approximately 90 mm in height above its position.
5. Application of confinement load, using a wooden platform and concrete weights loads for a confinement of 2 kPa.
6. Run the test by activating the drill at a speed of 160 rpm. Rotate the disc inside the soil sample for 10 minutes. Throughout the test, the torque is measured by the use of the torque transducer Lorenz type DR 1221-R.
7. Disassembling the equipment: empty the tank and remove the disc.
8. Disc Weighing: after the test the disc is washed, dried and weighed, and the w_2 value is recorded.
9. Determination of weight loss on the disc by using the equation: $\Delta w = w_1 - w_2$.
10. The study of torsion trends and mean test torque calculations is performed.

For each of the selected configurations, at least three tests are performed, and the data to be associated with the test is calculated as the average of the three weight loss values of the disc (Oñate Salazar, et al., 2016)

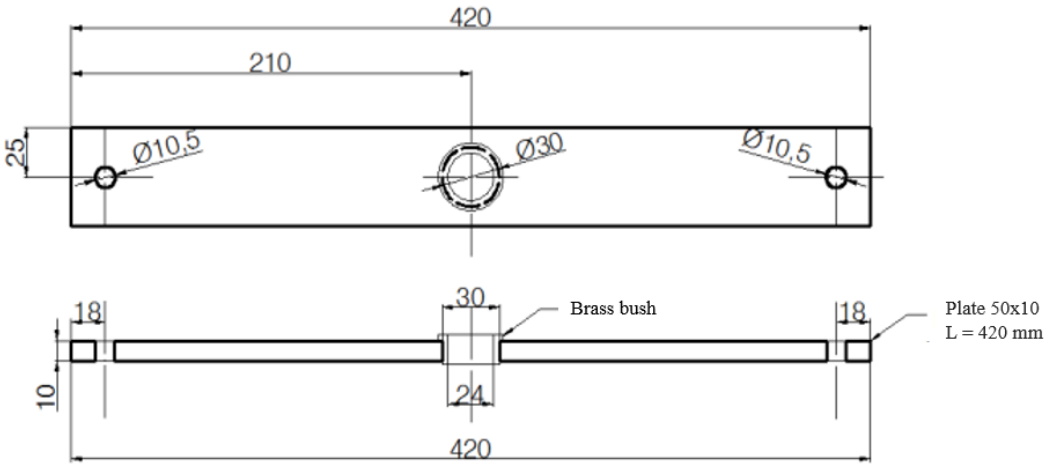

Figure 53. Detail of the mobile bushing.

6.2 Modified Wear Disc Test

A new test procedure has been developed in order to increase the interaction between the ground and the disc. In the previous test, the disc remained stationary at a known fixed depth. In the modified test, it was decided to implement controlled vertical displacements of ±90mm at a vertical speed of about 1 mm/s, allowing the flow of the ground and thus ensuring a greater contact with the disc.

6.2.1 Test Procedure

The new test procedure presents minor modifications regarding the Wear Disc Test described in the Paragraph 6.1.1. The modified procedure is as follows:

1. Preparation of about 15 dm^3 of soil (particle size less than 20 mm). According to the test to be performed, natural soil, soil with different percentages of water added or soil conditioned with foaming agents and/or anti-wear agents shall be used.
2. Disc Weighing (same disc of Wear Disc Test, Figure 51): before the test the disc is washed, dried and weighed, and the w_1 value is recorded.
3. Assembly the disc on the drive shaft that is connected to the torque transducer Lorenz type DR 1221-R and then, place it inside the tank at about 170 mm from the bottom (See Position 1 in Figure 54). The drive shaft is secure to the tank by using two bushings that fix the mobile bushing on the tank body.

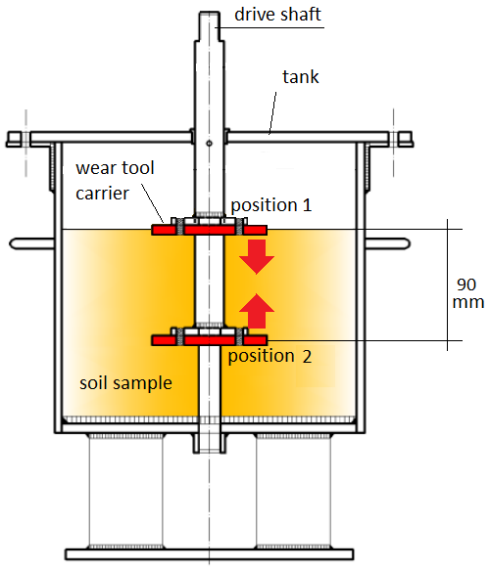

Figure 54. Schematic drawing of the test tank

4. Fill the cylindrical tank with the soil sample; the disc remains at the top of the soil (Position 1, Figure 54).
5. Run the test by activating the drill at a speed of 160 rpm. Rotate the disc inside the soil sample for 10 minutes. The test is carried out with 2 consecutive wear steps of 5 min each from position 1 to position 2 as shown in Figure 54. The elementary wear test is carried out with the following operational scheme (Oñate Salazar, et al., 2018):
   (a) the test starts with the tool carrier in the upper position (i.e. laying on the soil – position 1). The tool is then rotated for 15 s in this position;
   (b) the tool carrier is moved down, inside the soil to the test lower position (2) with an advance speed of about 1.3 mm/s;
   (c) the tool carrier is then kept rotating in the lower position (i.e. at a depth of 90 mm from the surface) for about 180 s;
   (d) the tool carrier in moved up to the upper position with an advancement speed of about 1.3 mm/s;
   (e) when the tool carrier reaches the surface of the soil, immediately steps b, c and d are repeated for a second round and then the test is stopped with the tool totally embedded in the soil.
   The Figure 55 describes the path of the wear tool carrier vs. time.
6. Disassembling the equipment: empty the tank and remove the disc.
7. Disc Weighing: after the test the disc is washed, dried and weighed, and the w_2 value is recorded.
8. Determination of weight loss on the disc by using the equation: $\Delta w = w_1 - w_2$.
9. The study of torsion trends and mean test torque calculations is performed
10. Throughout the test, the torque is measured by the use of the torque transducer Lorenz type DR 1221-R.

As for the previous test procedure, for each of the selected configurations, at least three tests are performed and the data to be associated with the test is calculated as the average of the three weight loss values of the disc.

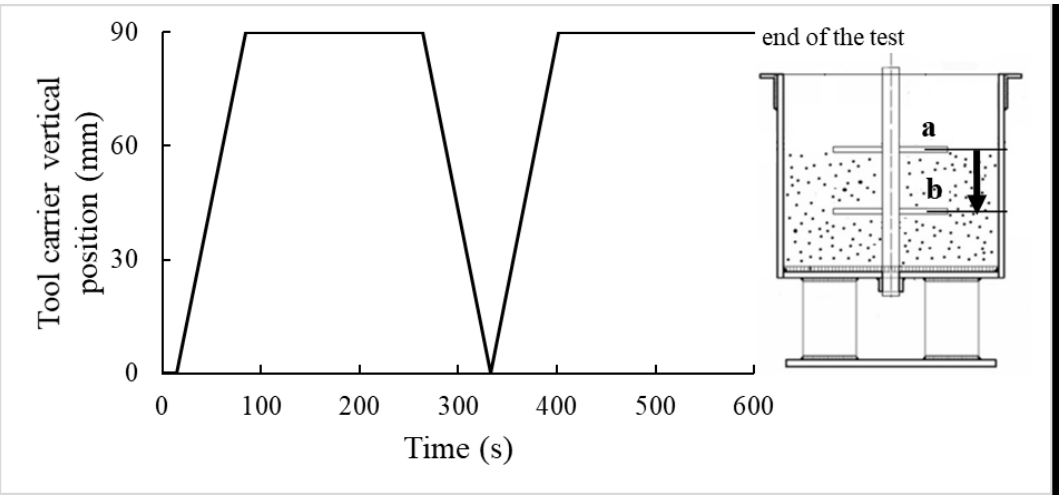

Figure 55. Scheme of the wear test process for the Modified Wear Disc Test. The figure describes the path of the wear tool carrier vs. time.

6.3 Sharp Cutter Test

An additional methodology based on the modified Wear Disc Test has been introduced, shifting from the traditional circular disc shape to a tool carrier disc. This new disc has a 4-pointed star shape, in which it is possible to fix a metal sample for each tip, even of different materials. This new methodology and all preliminary results were published in Oñate Salazar, et al. (2018) and Bosio, et al. (2018).

The tool carrier disc has an external diameter of 160 mm and a thickness of 10 mm (Figure 56). The tools are pyramidal, with about 21 mm in base, 11 mm in height and 40 mm in depth, and they are fixed by bolts (Figure 57).

This new tool carrier disc was designed to allow the use of more resistant and expensive metal alloys samples, optimising the production costs in comparison to the previous test discs. In addition, this test method allows testing different metals simultaneously under the same surrounding conditions (water content, soil grain size distribution, foam conditioning parameters, degree of compaction, etc.).

The parameters to be evaluated, in addition to the weight loss of each tool and the average torque, are the curvature radius of the tips and the area and volume lost. This approach provides more accuracy in wear assessment, especially for resistant metals.

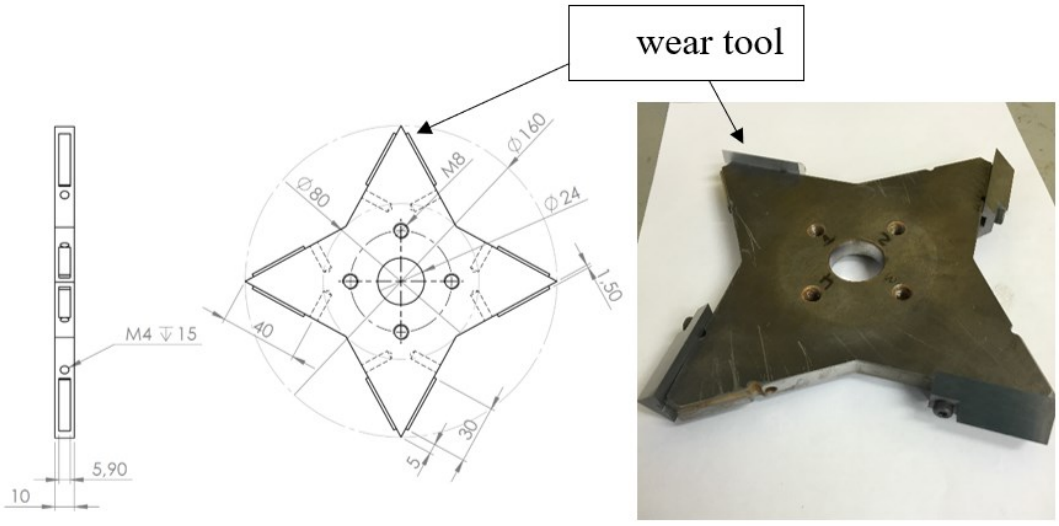

Figure 56. Technical drawing of the wear tool carrier and photo of the arrangement of the wear tools (Oñate Salazar, et al., 2018).

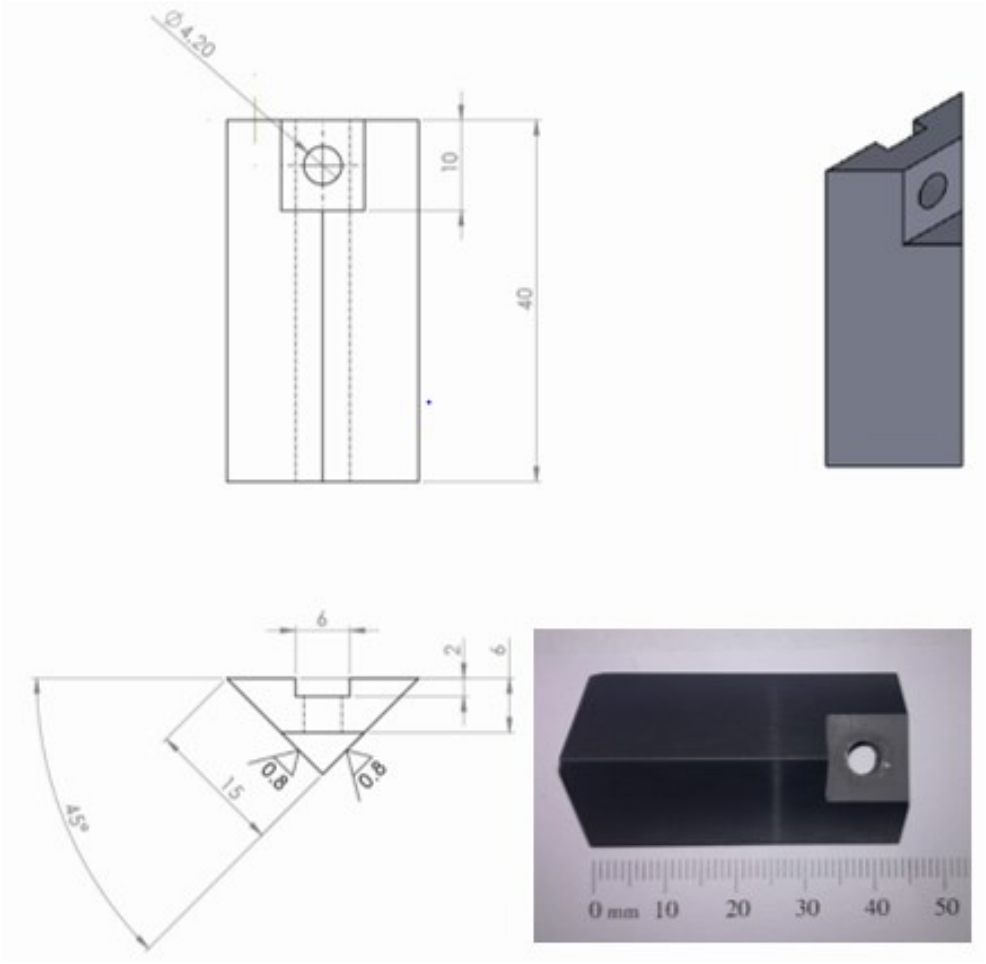

Figure 57. Technical drawing and picture of the wear tool. Units: dimensions (mm), roughness (µm), angle (°).

6.3.1 Test Procedure

The test is carried out under similar conditions to that described in the previous methodology; varying test time from 10 to 15 minutes due to this test is designed to assess wear on hard metals, which have a higher wear resistance. The procedure of the test is described below.

The new test procedure presents minor changes regarding the modified Wear Disc Test described in the Paragraph 6.2.1. The modified procedure is as follows:

1. Preparation of about 15 dm^3 of soil (particle size less than 20 mm). According to the test to be performed, natural soil, soil with different percentages of water added or soil conditioned with foaming agents and/or anti-wear agents shall be used.
2. Tool Weighing (Figure K): before the test the tools are washed, dried and weighed, and the w_1 values for each tool are recorded.
3. Docking the tools to the star disc using bolts.
4. Assembly the disc on the drive shaft that is connected to the torque transducer Lorenz type DR 1221-R and then, place it inside the tank at about 170 mm from the bottom (See Position 1 in Figure 54). The drive shaft is secure to the tank by using two bushings that fix the mobile bushing on the tank body.
5. Fill the cylindrical tank with the soil sample; the disc remains at the top of the soil (Position 1).
6. Run the test by activating the drill at a speed of 160 rpm. Rotate the disc inside the soil sample for 15 minutes. The test is carried out with 3 consecutive wear steps of 5 min each from position 1 to position 2 as shown in Figure 54. The elementary wear test is carried out with the following operational scheme (Oñate Salazar, et al., 2018):
   (a) the test starts with the tool carrier in the upper position (i.e. laying on the soil – position 1). The tool is then rotated for 15 s in this position;
   (b) the tool carrier is moved down, inside the soil to the test lower position (2) with an advance speed of about 1.3 mm/s;
   (c) the tool carrier is then kept rotating in the lower position (i.e. at a depth of 90 mm from the surface) for about 180 s;
   (d) the tool carrier in moved up to the upper position with an advancement speed of about 1.3 mm/s;
   (e) when the tool carrier reaches the surface of the soil, immediately steps b, c and d are repeated for a second round;
   (f) after the second round the steps b and c are repeated and then the test is stopped with the tool totally embedded in the soil
   The Figure 58 describes the path of the wear tool carrier vs. time.
7. The study of profiles and volumes of each tool is conducted (Paragraph 6.3.2)

8. Disassembling the equipment: empty the tank, remove the tool carrier disc and disassemble each tool.
9. Tool Weighing: after the test the tools are washed, dried and weighed, and the w_2 value for each tool are recorded.
10. Determination of weight loss on each tool by using the equation: $\Delta w = w_1 - w_2$.
11. The study of torsion trends and mean test torque calculations is performed
12. Throughout the test, the drill torque is measured by the use of the torque transducer Lorenz type DR 1221-R.

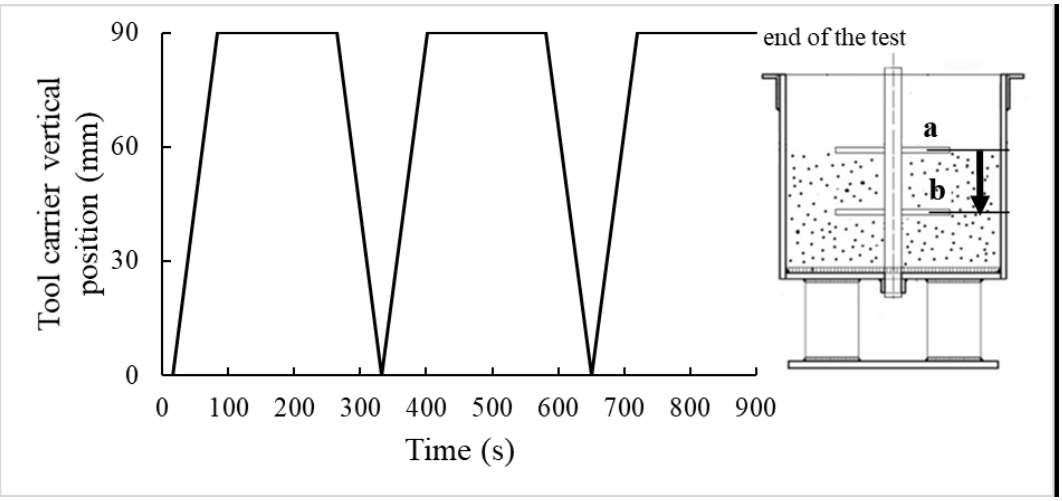

Figure 58. Scheme of the wear test process for the Sharp Cutter Test. The figure describes the path of the wear tool carrier vs. time.

6.3.2 Tribological measurements on the wear tools

Once the test is completed, tribological measurements are performed. Each 15-minute test contains three steps, that correspond to a cycle. These measurements are performed on a one-cycle basis. Each tool will be studied for three cycles, changing the initial wear conditions for each test.

The aims of these measurements are (Oñate Salazar et al., 2018):

- to quantify the volume loss on the wear tools induced by both natural and conditioned soil;
- to identify the tool position where heaviest wear occurs and to investigate the wear mechanisms;
- to characterize the change of geometry of the tool and to verify if these data can become a representative parameter for assessing the action of the soil wear.

In Figure 59, the scheme of the tribological characterization applied is presented. Two analyses were performed: a qualitative assessment on the morphology of the tool surface and a quantitative assessment on wear tool profiles. The first is carried out through the use of a Scanning Electron

Microscopy (SEM-model Leo 1450 MP) and a Field Emission SEM (FESEM) Zeiss Merlin equipped with Gemini column while the evaluation of the tool cutting edge is carried out using a video-microscope LEICA VZ85R (50-400 ×) with a magnification of 200× (Oñate Salazar et al., 2018). The quantitative evaluation consists of recording the profile of the tool in 7 different cross-sections, allowing registering the change of geometry and shape, with the measurements of the curvature radius and the volume loss, calculated on the areas and the separation between the cross-sections.

A specimen sample holder, specifically designed and constructed, was used to ensure a parallelism between tool surface and the positioning table of the microscope, as shown in Figure 60.

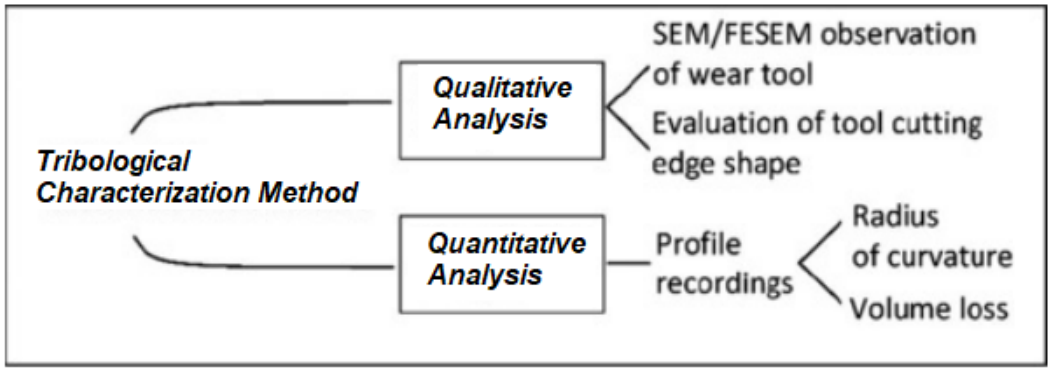

Figure 59. Schematic of the tribological characterization plan for wear tools (Oñate Salazar, et al., 2018).

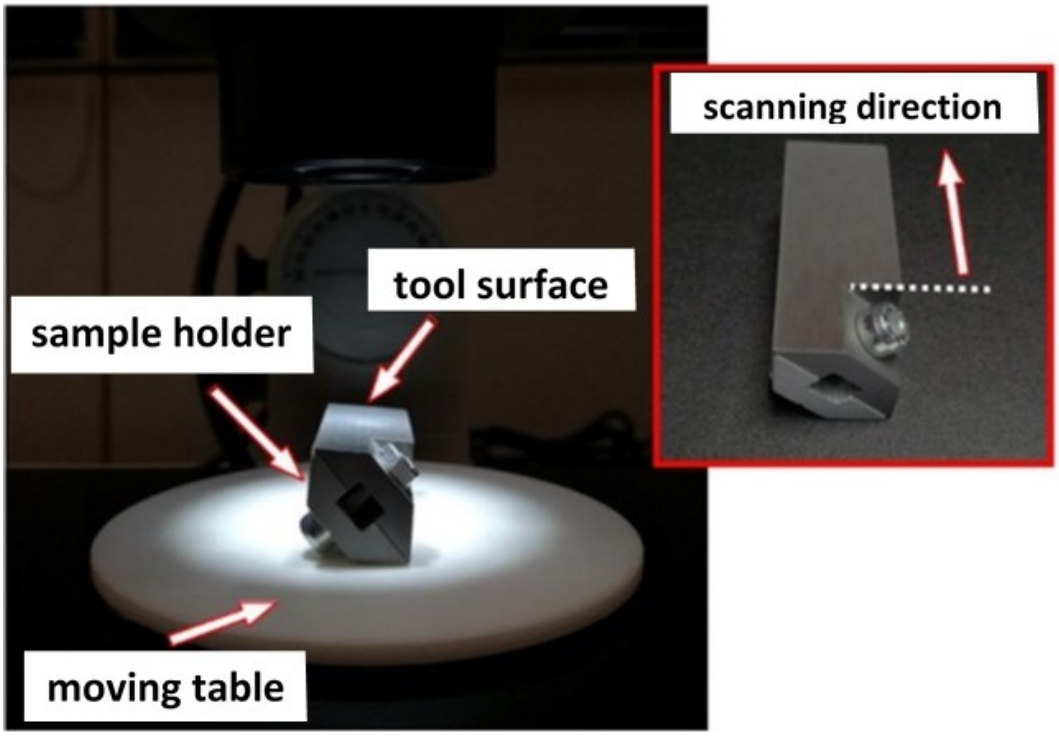

Figure 60. Sample holder developed for cutting edge observation

By using a profilometer (model MarSurf CD 120), a quantitative analysis of edge rounding was performed on the seven measuring locations of the tool sample profiles along the cutting edge as shown in Figure 61. According to Oñate Salazar, et al. (2018), the position of the measuring locations has been chosen to guarantee a complete representation of the worn area along the tool. The radius of curvature of the worn tool is the radius of the osculating circle which best approximates the worn profile at maxima. The volume loss is obtained comparing the original and worn geometries (Figure 62).

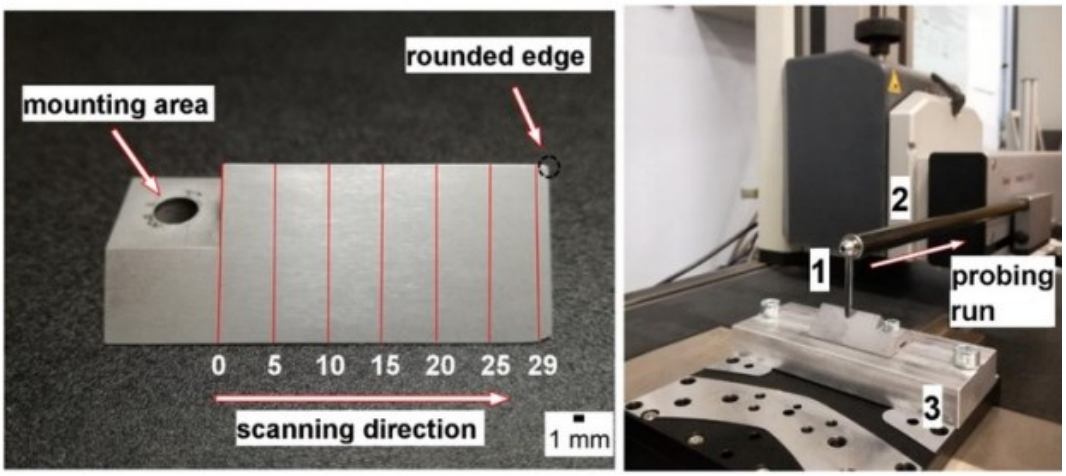

Figure 61. Locations of the recording linescans along the tool cutting edge and photograph of profilometer MarSurf CD 120 set up used for the measurements. Key: probe (1), tracing arm (2), automated micrometrical sled to position the tool correctly (3)

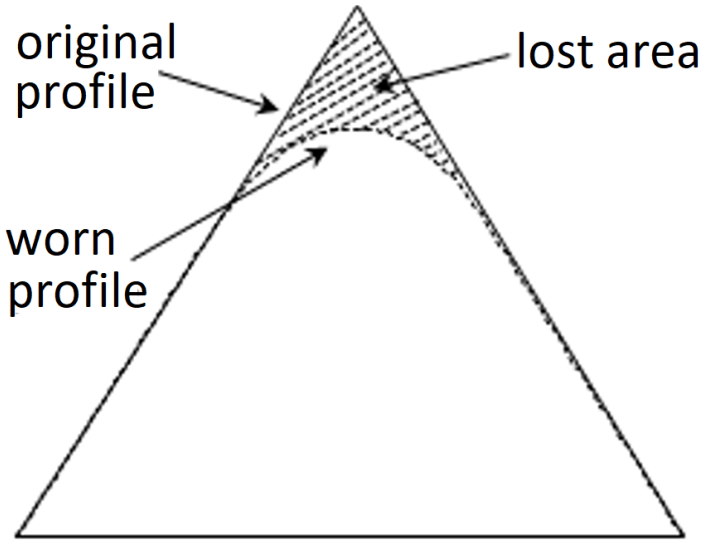

Figure 62. Examples of two measured profiles of a tool: original and worn ones. The dashed area represents the lost area for the studied cross sections

6.4 Pressurized Rotating Mixer

A completely new device has been studied, designed and built with the aim of performing tests on soil conditioning and wear.

This equipment is not based on any existing geotechnical testing, the results indicating the differences between natural and conditioned material, without returning an absolute value of conditioning or wear, were relative. Based on this principle, the purpose of the device is to evaluate the resistance of the soil against mixing blades, by simulating a mechanism similar to that happening in the excavation chamber, as well as to assess wear by rotating the disc against the flow of the soil sample.

This equipment was financed by the Piedmont Region, thanks to a research contract called "HM-TUNES: development of new formulations of hard metal tools and their use in combination with conditioning agents for ground excavation of tunnels". This resulted in the necessity of studying the functionality and wear of the conditioned material under different pressures to better simulate the real behaviour, that can be found during excavation with EPBS. The device (Figure 63) was designed by TUSC and built by Toso Srl.

The most important feature of this equipment is the possibility of applying hydrostatic pressure to the sample in the tank by using compressed air at a maximum pressure of 10 bar, although the excavation machines (EPBs) usually reach a pressure of about 4 bar. In this way it’s possible to study behaviour of both, natural and conditioned soil, at different pressures.

The device can mix the material under defined pressure conditions that better simulate the conditioned soil behaviour in the excavation chamber, and simultaneously record torque values. At the same time, it can also rotate the disc for assessing wear using the same conditions and record rotor torque.

Figure 63. Pressurized Rotating Mixer

The equipment consists of a stainless steel cylinder with 600 mm in internal diameter and 613 mm in height. The cylinder is equipped with balls that rotate to mix the material and keep the sample in constant movement. In addition, it has a wear rotor laterally assembled, with an independent motor that allows the rotation of the wear disc. The large size of the device makes it possible to reduce the surrounding effects that occur in small-scale tests and, therefore, approaches a behaviour more similar to that of a real scale.

The cylinder has several connection points from which foam, water and compressed air can be injected. For this thesis work, the connections placed at the top of the machine were used to inject the conditioned material and the bushings were only used for the application of compressed air.
The main characteristics of the device are herein summarised:

- internal cylinder height: 613 mm;
- internal diameter: 600 mm;
- internal capacity: 170 dm^3;
- cylinder thickness: 15 mm;
- upper closing plate thickness: 25 mm;
- maximum pressure inside the chamber: 10 bar.

Machine geometrical details are represented in Figure 64, Figure 65 and Figure 66.

In order to meet all the requirements, the new machine has been designed in stainless steel to prevent corrosion and resist the 10 bar pressure inside the tank. The cylinder size has also been designed to reduce the surrounding effects that would occur in a small container. The tank is open at the top to allow material filling and has a removable closure plate that is fixed with 20 steel bolts.

The removable upper closing plate (Figure 67) has several openings: a 154 mm porthole for inspection purposes, a connection for the pressure transducer, and two connections for insertion/expulsion of compressed air to balance the internal pressure.

A stainless steel shaft is located inside the cylinder on which propellers are connected. The entire system is capable of rotating around its axis to mix the soil, allowing the discs wear study related to the moving ground (Figure 68).

The rotation of the propellers can be done in both directions. If they rotate in clockwise direction the flow of material is downwards, if they rotate in the opposite direction, the flow of material is upwards.

The rotation system of the propeller is powered by an electric motor, which allows a 10 rpm minimum rotation and a 32 rpm maximum rotation, and a maximum applied torque of 500 KNm.

The following values can be monitored during the test:

- Propeller torque: This parameter is measured through a load cell connected to the motor;

- Wear rotor torque: This parameter is measured through the current consumption of the device motor;
- Internal pressure in the tank: it is measured through two pressure transducers, placed at the bottom and the top (on the closing plate) of the cylinder. They were strategically positioned to be able to assess the conditioned soil ability to transmit the applied pressure.

All machine measured values are recorded by a software specially designed for this machine. The program has a main screen (Figure 69), where the operator programs the test and is able to control in real time all the operating parameters. From the main screen it is possible to open different tabs to see in detail the values recorded for each parameter. Another important screen is shown in Figure 70, where the calibrations of torque are executed before each test, selecting the test configuration that each program will perform for both rotors (direction and speed rotation).

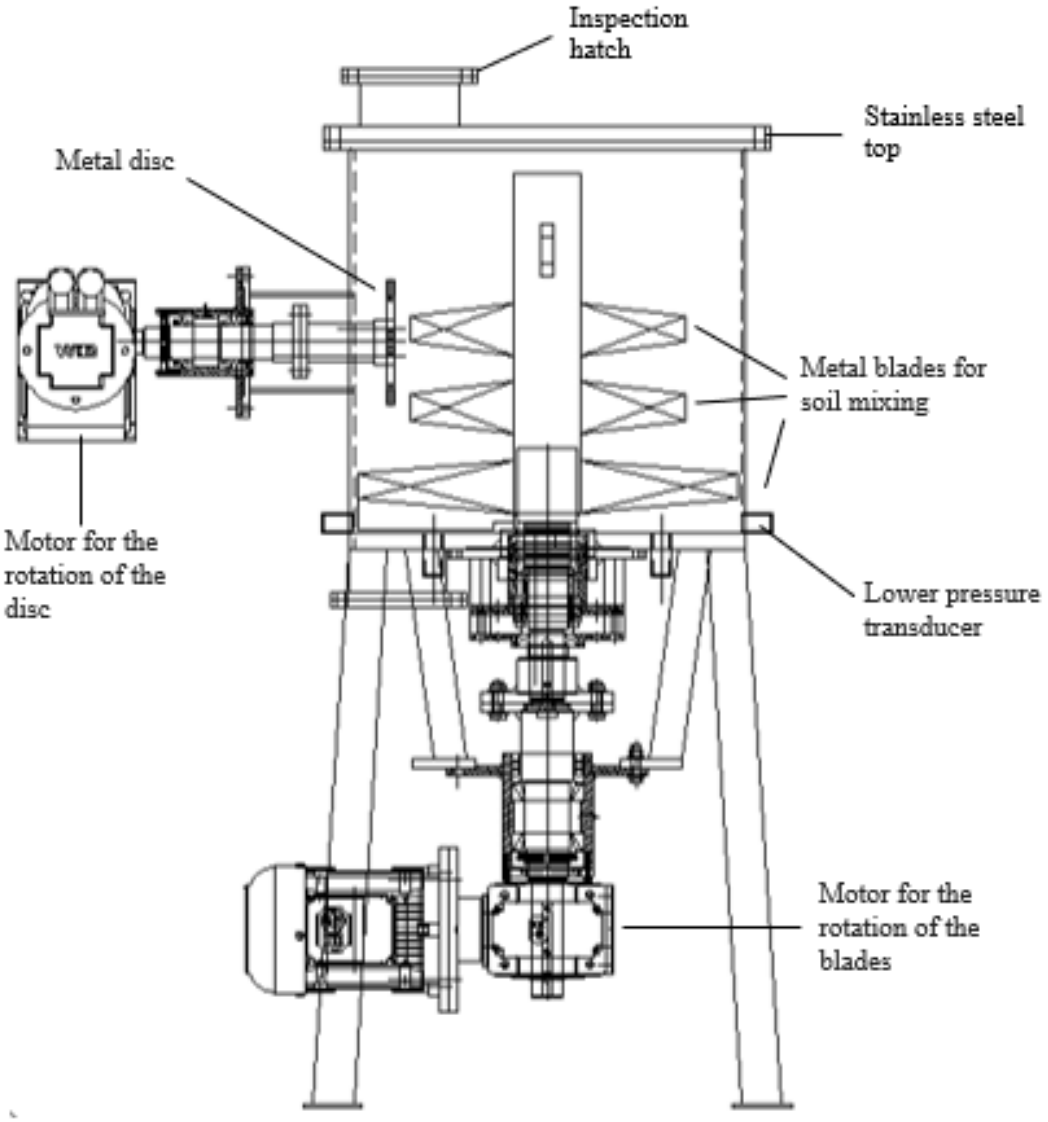

Figure 64. Construction details of the Pressurized Rotating Mixer (lateral view).

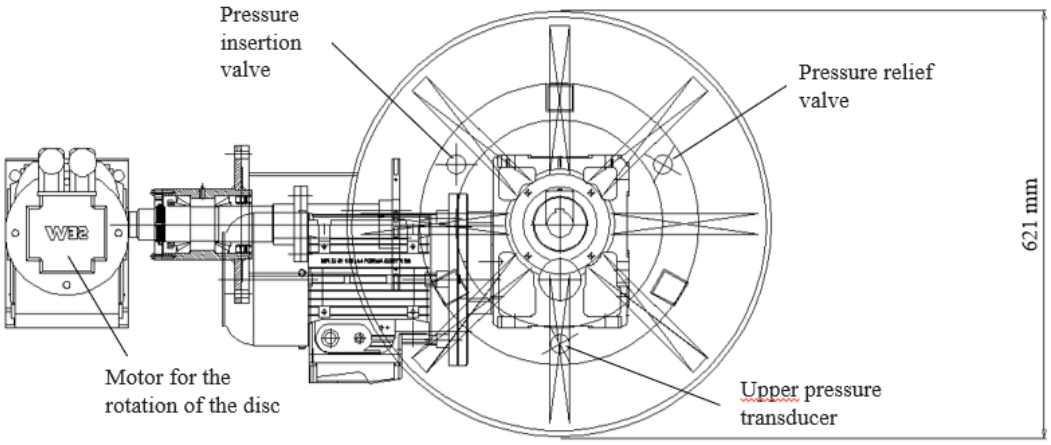

Figure 65. Construction details of the Pressurized Rotating Mixer (top view).

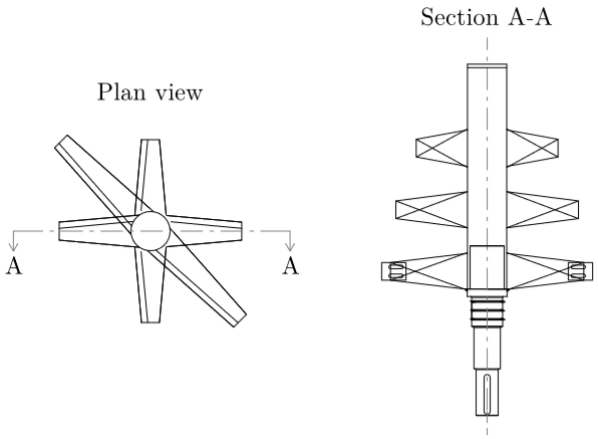

Figure 66. Construction details of the Pressurized Rotating Mixer. Technical drawing of the warped blades.

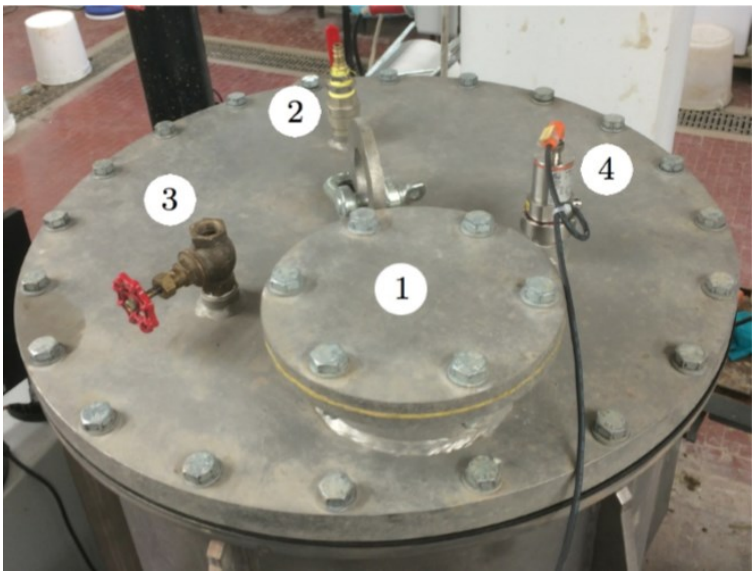

Figure 67. Top removable closing plate with the inspection porthole (1), compressed air connection (2), needle valve (3) and pressure transducer (4) (Martinelli, 2016)

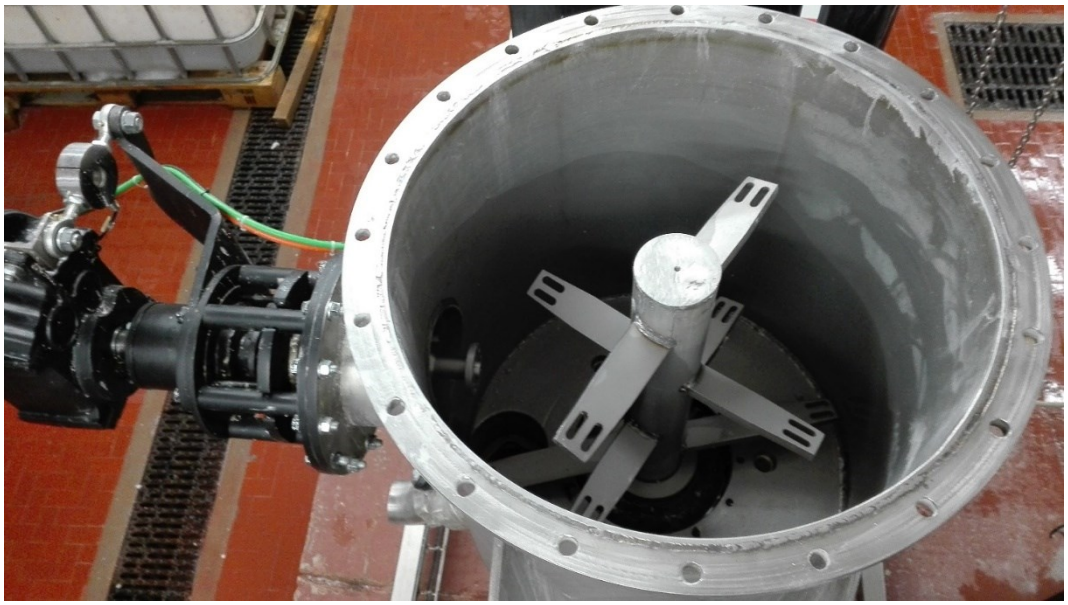

Figure 68. Photograph of the machine interior.

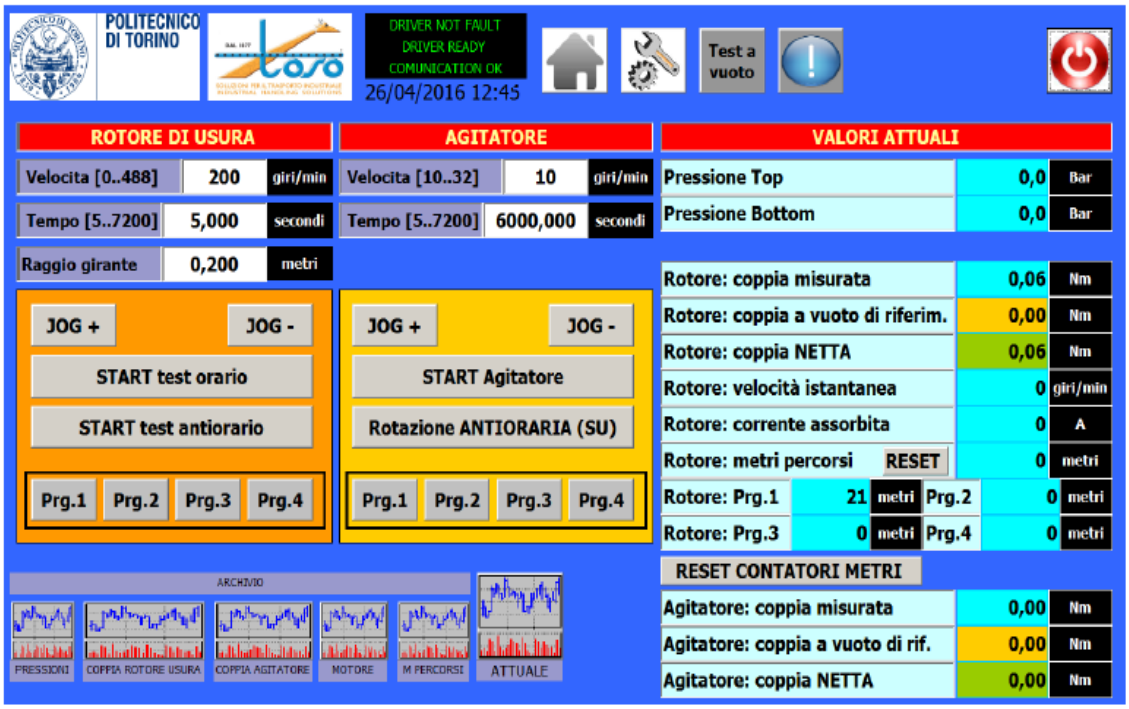

Figure 69. Main control panel of the software

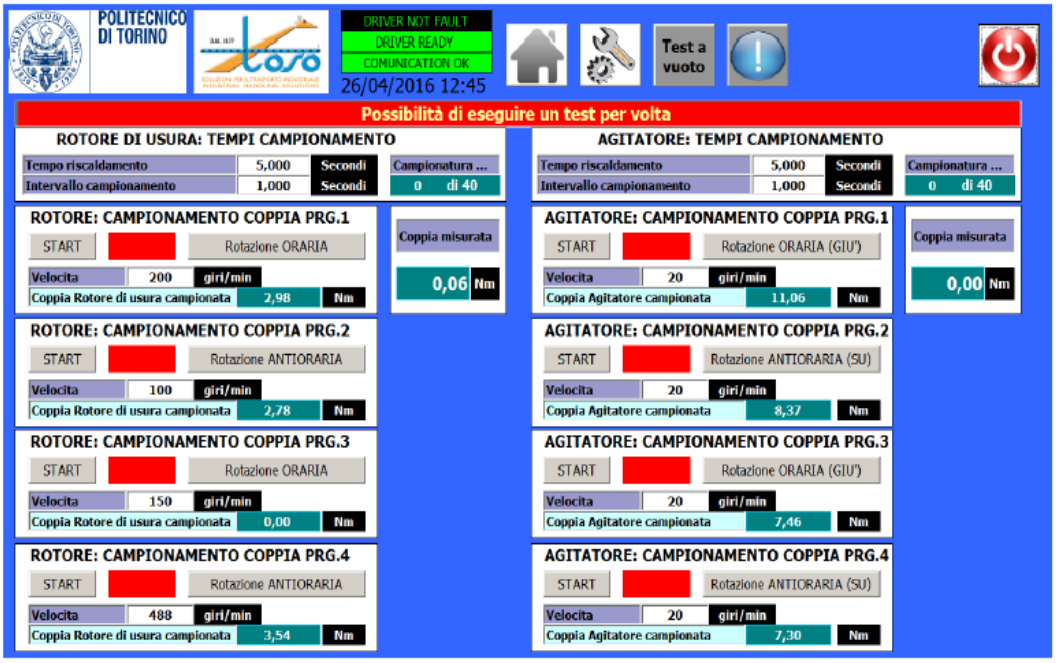

Figure 70. Configuration screen and programs calibration of the software

6.4.1 Test Procedure

In this thesis, a preliminary pilot assessment using the circular discs from the Wear Disc Test and the modified Wear Disc Test (Figure 51) was performed to test the machine.

The procedure to carry out the Pressurized Rotating Mixer test is as follows:

1. Weighing the test disc: Before the test, the disc is washed, dried and weighed, and the w_1 value is recorded.
2. Fixing the disc on the wear rotor axis using bolts (Figure 71).
3. Machine calibration: The system includes the "Vacuum test" to calibrate all torque values before testing. The system can configure 4 test programs for the agitator and the wear rotor, varying the direction and speed of rotation. The calibration program is used to calculate the mean torque of the rotating blades and the wear rotor induced by internal mechanical frictions.
4. Preparation of about 145 dm^3 of soil (particle size less than 20 mm). According to the test to be performed, natural soil, soil with different percentages of water added or soil conditioned with foaming agents and/or anti-wear agents shall be used.
5. Filling the cylinder with soil sample: with 150 dm3, about 90% of the container volume is filled.
6. Sealing the upper part of the tank by affixing the closing plate and the required hydraulic lines (air, water and foam) connections as shown in Figure 67;

7. Activation of the propeller and, after one minute, activation of the wear rotor. This prior agitation is carried out to initiate the motion of the soil inside the tank. Preliminary tests were performed to ensure this one minute period did not affect the disc wear result. If the test is performed under pressure, the one-minute period can be used to bring the chamber pressure from 0 bar to the desired pressure.
8. For these tests, the propeller has been programmed to rotate counterclockwise at 20 rpm for 11 minutes, moving the material upwards, while the wear rotor rotates counterclockwise at 160 rpm for 10 minutes, moving the disc against ground flow. Therefore, the wear test lasts 10 minutes, as the Wear Disc Test and the modified Wear Disc Test.
9. Throughout the test, the agitator and wear rotor torques shall be measured.
10. Empty the cylinder and retract the wear disc.
11. Disc weighing: After the test, the disc is washed, dried and weighed, and the w_2 value is recorded.
12. Determination of disc weight loss with $\Delta w = w_1 - w_2$.
13. Study of torque trends and calculation of the average torque are made.

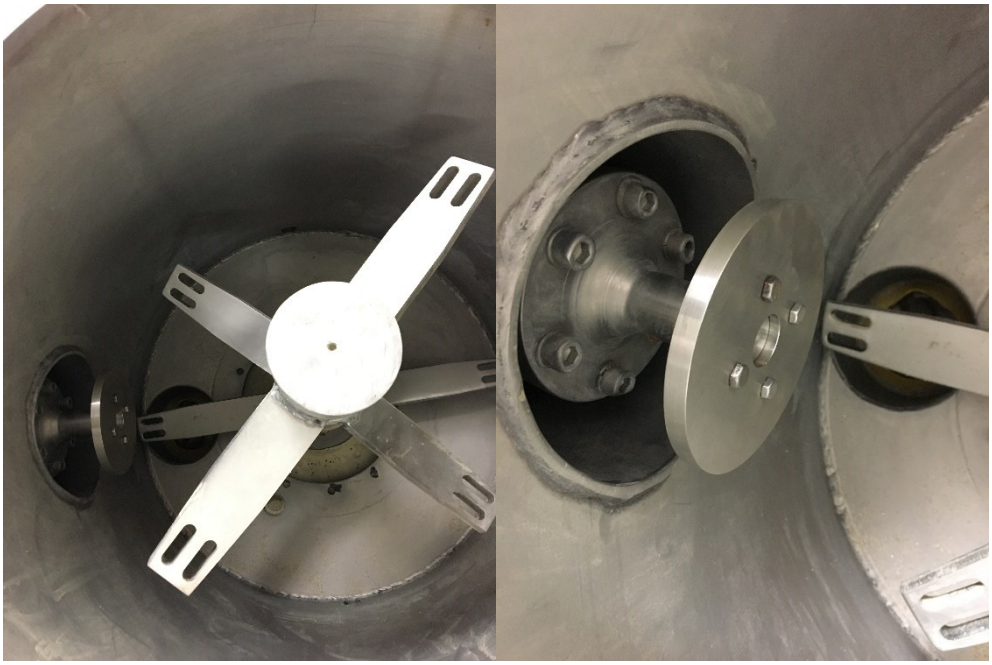

Figure 71. Fixing the disc on the wear rotor axis

Chapter 7

Performed laboratory tests

Wear tests were performed using the previously existing methodology from the Politecnico di Torino and all those methodologies that were developed especially for this thesis work (described in Chapter 6).

Preliminary analyses of soils and metals are performed prior to testing. In the case of reference soils, these analyses were more comprehensive compared to soils from excavations, where a general classification was made.

7.1 Studied soils

7.1.1 Quartz sand

In this work, quartz sand was the soil chosen as the primary reference for wear testing due to the high abrasive potential of quartz. In Figure 72, a picture of quartz sand sample is displayed. In Figure 73, it is observed a microscopic imaging of this sand.

Figure 72. Quartz sand sample.

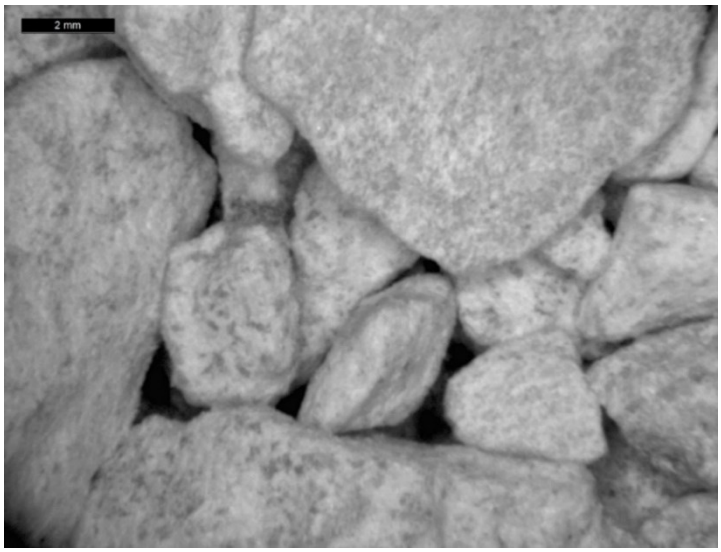

Figure 73. Microscopic imaging of quartz sand, obtained by using a video-microscope LEICA VZ85R (magnification: 40x).

Since this soil comes from an industrial quartzite quarry and samples are obtained by means of a crushing process, the soil samples received in the laboratory were often different from one another. For this reason, a reference granulometry was chose and replicated each time a different soil sample was received. Prior to this process, the soil was divided into different granulometric classes (Figure 74). The chosen grain size distribution is shown in Figure 75. The quartz sand has a grain size at the percentage of 10%, D_{10} = 0.9 mm; a grain size at the percentage of 60%, D_{60} = 6.5 mm and a Uniformity coefficient, $C_u = d_{60}/d_{10}$ = 7.22. The natural water content of the soil is w = 2% by weight and the specific weight is γ = 1.6 kg/dm^3.

Figure 74. Different granulometric size distribution of Quartz sand.

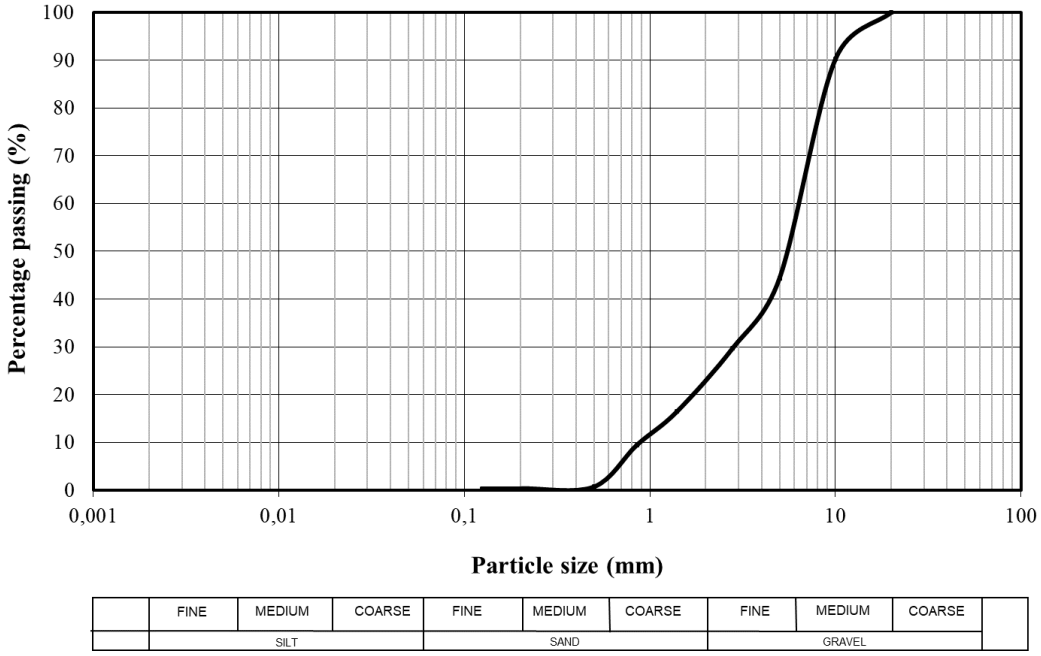

Figure 75. Grain size distribution of tested quartz sand

For a better wear process characterization microscopic analyses were carried out in order to define the quartz content inside ground sample. Leica DMPL microscopy was used for performing analysis taking into account grain size smaller than 0.5mm. Outcomes showed that quartz content is about 98% of the sample and there are also feldspar and iron impurities with percentage of about 2%.

In the phase contrast image (methodology widely used for asbestos analysis) quartz grains show a blue colour and feldspars show a lighter coloration (Figure 76 and Figure 77). The microscope slide was arranged by using a refraction liquid of 1.550.

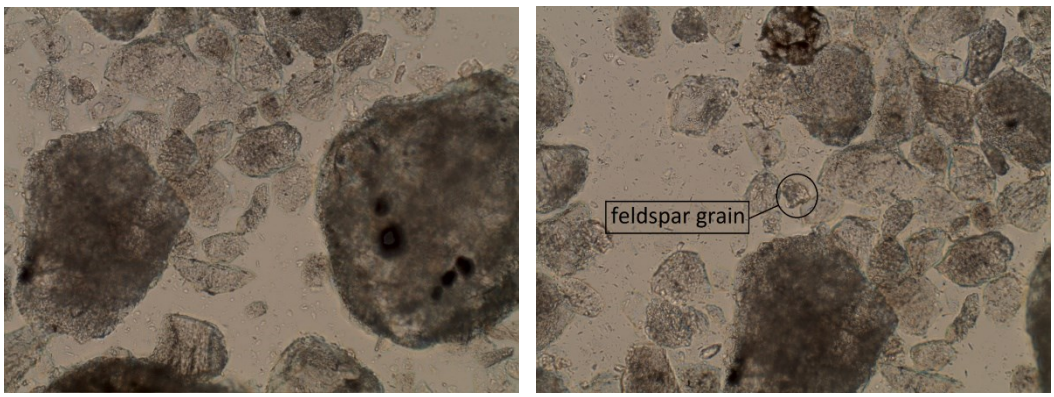

Figure 76. Quartz sand (Magnification 10 x) – Phase contrast view. Quartz grains look clearly in the pictures. Feldspar grains are indicated.

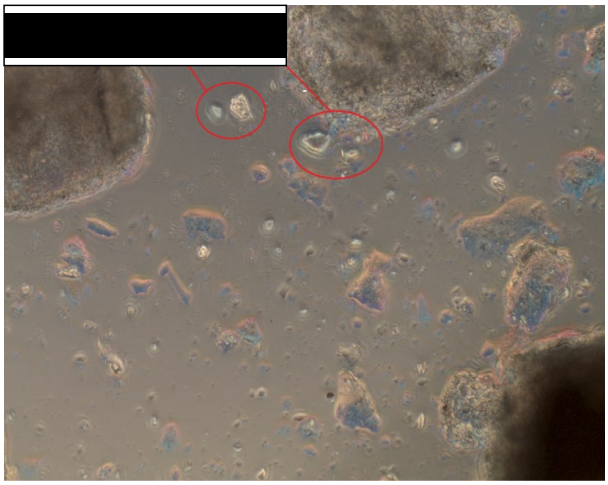

Figure 77. Phase contrast picture of quartz sand (magnification: 10×) - Quartz grains appear clear – detail of feldspar at top of the image.

For quartz sand, a study of grain shape was performed to determine sphericity and roundness: The soil was divided into 15 granulometric classes and each of them was analyzed under a microscope (macroscopically for grains larger than 0.710 mm), taking at least 30 grain images to be subsequently studied.

In order to classify the shape of each soil grain, the chart proposed by Krumbein & Sloss (1956) is usually used as a reference (Figure 78). For the purposes of this work, a software (ImageJ, National Institutes of Health) that provides sphericity and roundness values, among other values, was used.

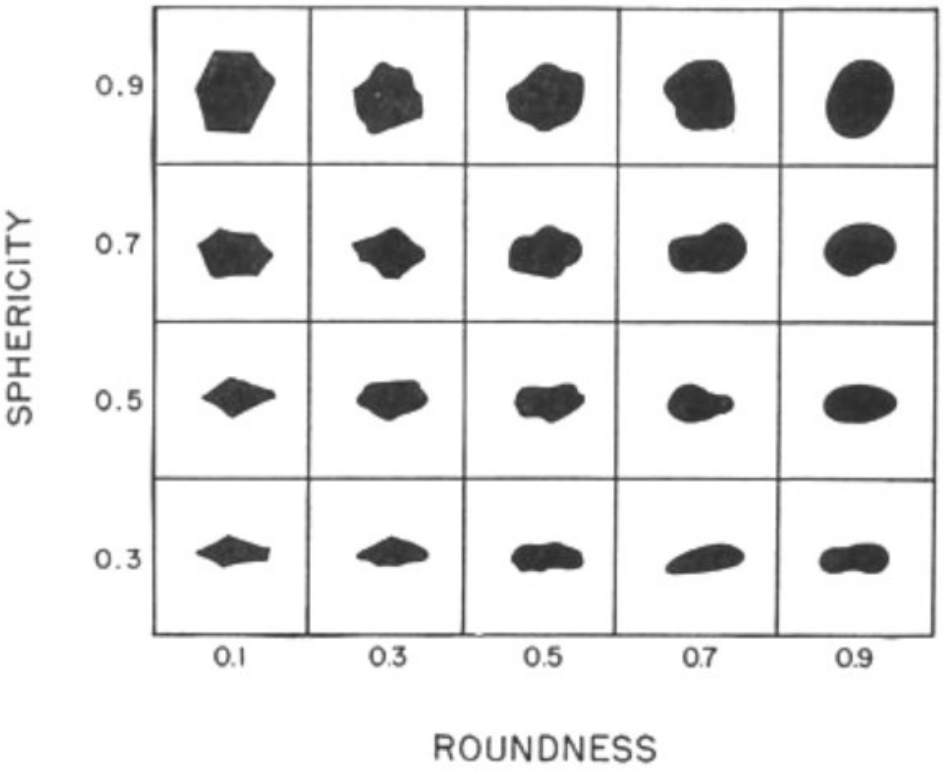

Figure 78. Reference chart for estimating the roundness and sphericity of sand grains (Krumbein & Sloss, 1956).

Sphericity is an indicator of particle shape. A sphericity value of 1.0 indicates a perfect circle and as the value approaches 0.0, it indicates an increasingly elongated shape. Roundness is considered to be the measurement of surface roughness.

Figure 79 some examples of grain pictures obtained during this research are displayed. In Table 5, it is shown a summary of the sphericity and roundness values measured for each granulometric class with an average of 30 values per class.

Another performed characterization was the Modified Proctor compaction test, following the procedure described in the standard UNI EN 13286-2:2010. The obtained curve is shown in Figure 80. In Table 6, maximum compaction values are displayed.

The optimal conditioning set used in wear tests with quartz sand is summarized in Table 7.

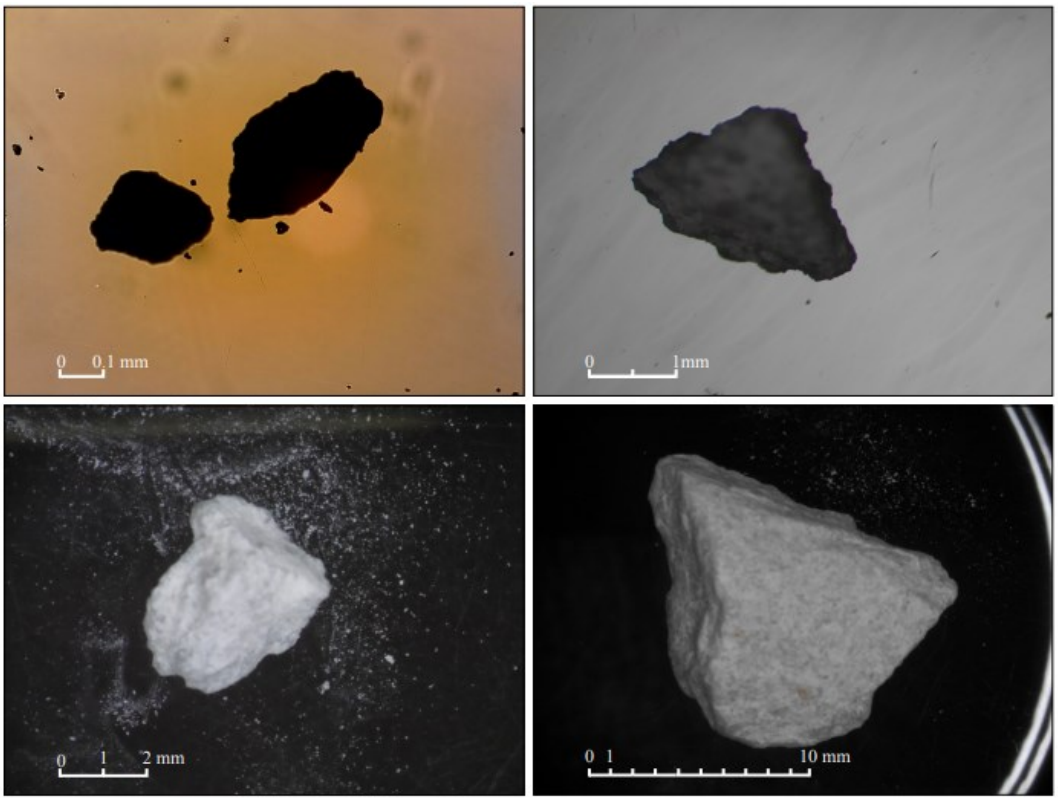

Figure 79. Photographs of quartz sand grains.

Table 5. Sphericity and Roundness values obtained for each granulometric class.

Grain size (mm)	Sphericity	Roundness
> 10.00	0.444	0.755
6.30 - 10.00	0.482	0.717
4.75 - 6.30	0.400	0.701
2.80 - 4.75	0.372	0.706
2.00 - 2.80	0.422	0.739
1.40 - 2.00	0.350	0.713
1.00 - 1.40	0.489	0.617
0.85 - 1.00	0.567	0.692
0.71 - 0.85	0.726	0.856
0.60 - 0.71	0.614	0.719
0.425 - 0.60	0.667	0.740
0.30 - 0.425	0.679	0.699
0.18 - 0.30	0.644	0.722
0.125 - 0.18	0.654	0.750
0.104 - 0.125	0.646	0.728

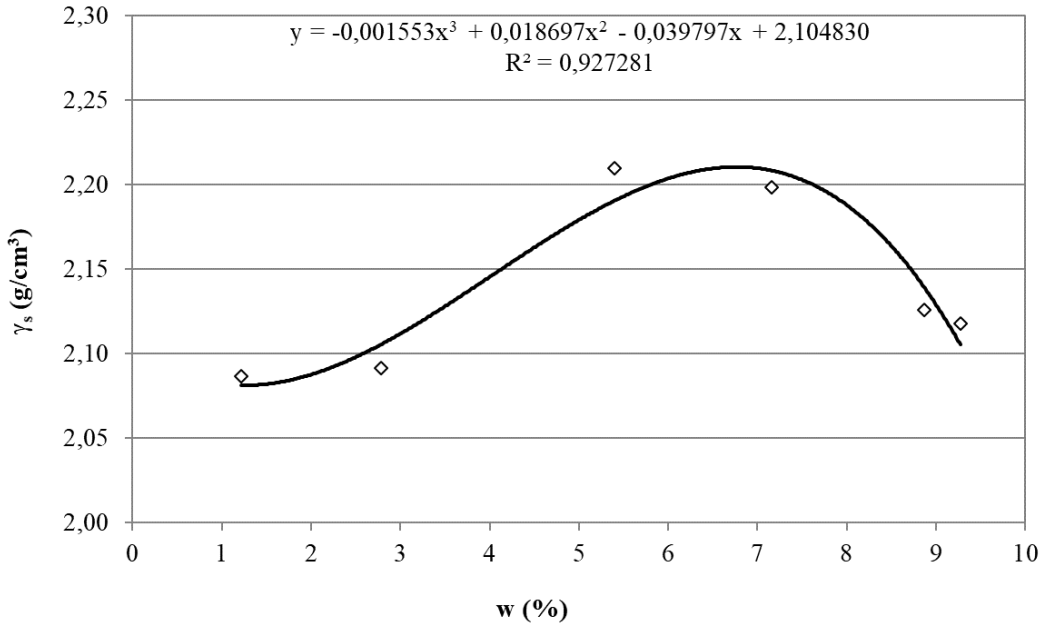

Figure 80. Proctor compaction curve for quartz sand.

Table 6. Maximum compaction values of Quartz sand.

a	-0,001553
b	0,018697
c	-0,039797
d	2,104830
a'	-0,004659
b'	0,037394
c'	-0,039797
w_{opt} (%)	6,8
$\gamma_{s,max}$ (g/cm^3)	2,210

Table 7. The optimal conditioning set for quartz sand

water content (% by weight on natural soil)	5
Foam	Polyfoamer FP
c_{foam} (% by volume on foam generator liquid)	2
FER	10
FIR (%)	40

7.1.2 CC sand

CC sand was the second soil chosen as reference for wear testing in this work. It is an artificial soil and the idea of producing it came from the availability of large quantities of monogranular quartz sand in the Hydraulics Lab. In Figure 81, a photograph of CC sand sample is displayed.

CC sand consists of 75% by weight of monogranular sand and 25% of river sand. It was developed with the aim of having an abrasive and cohesive soil. The grain size distribution is shown in Figure 82. The CC sand has a grain size at the percentage of 10%, D_{10} = 0.23 mm; a grain size at the percentage of 60%, D_{60} = 0.9 mm and a Uniformity coefficient, $C_u = d_{60}/d_{10}$ = 3.91. The natural water content of the soil is w = 0.8% by weight and the specific weight is γ = 1.8 kg/dm^3.

Figure 81. CC sand sample.

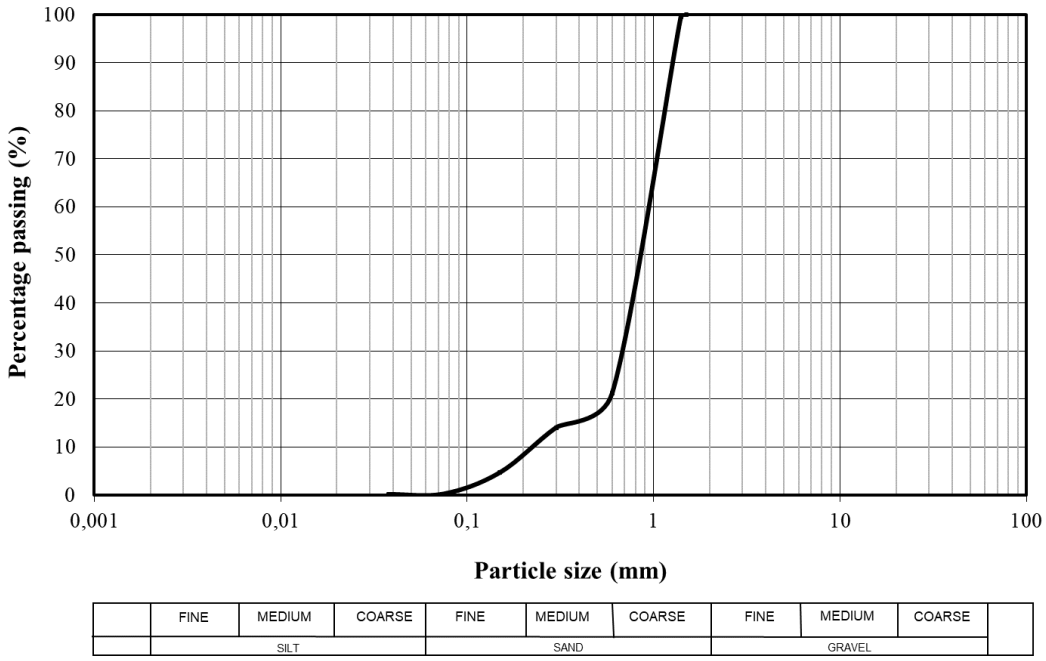

Figure 82. Grain size distribution of CC sand.

For a better wear process characterization microscopic analyses were carried out in order to define the quartz content inside river sand. Leica DMPL microscopy was used for performing analysis taking into account grain size smaller than 0.5mm. Outcomes showed that quartz content in river sand is about 30% and there are also feldspar and iron impurities with percentage of 70%. By considering that single grained sand has quartz content of 99%, CC ground has approximately a quartz content of 80%. In the phase contrast image (methodology widely used for asbestos analysis) quartz grains show a blue colour and feldspars show a lighter coloration (Figure 83). The microscope slide was arranged by using a refraction liquid of 1.550. By using petrographic method and the crossed polarizer, quartz looks like rainbow colours (Figure 84).

River sand it is not “mature” material because its mineralogical composition is characterized by weak minerals. These minerals are weaker than quartz and they will have a desegregation process that will destroyed themselves with the time.

Another performed characterization was the Proctor compaction test. The obtained curve is shown in Figure 85. In Table 8, maximum compaction values are displayed. This atypical behaviour of the Proctor curve has been found in uniformly graded fine sands (Rollings, 1996) , (Figure 86).

The optimal conditioning set used in wear tests with CC sand is summarized in Table 9.

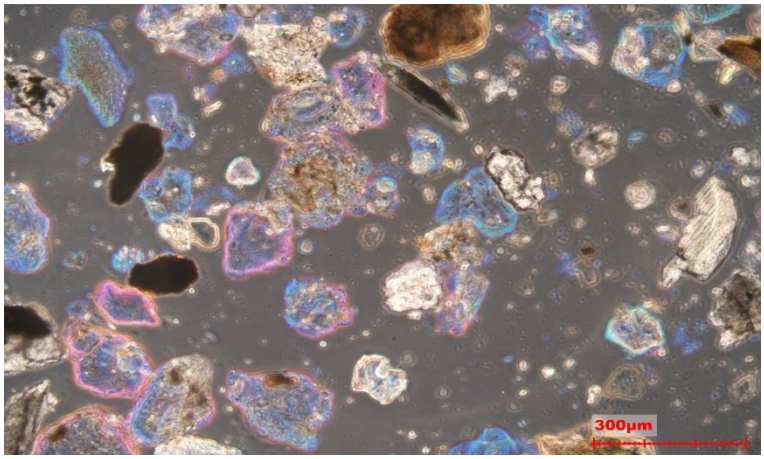

Figure 83. Image in phase contrast, CC sand.

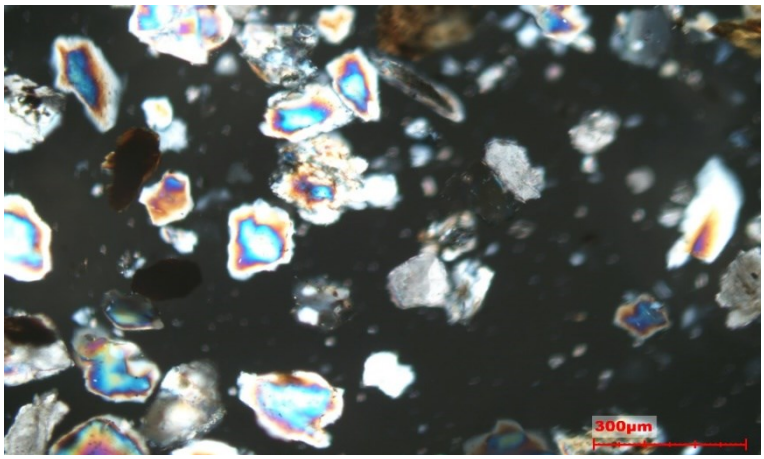

Figure 84. Image obtained using the petrographic method. Quartz produces a rainbow colouring in the grain.

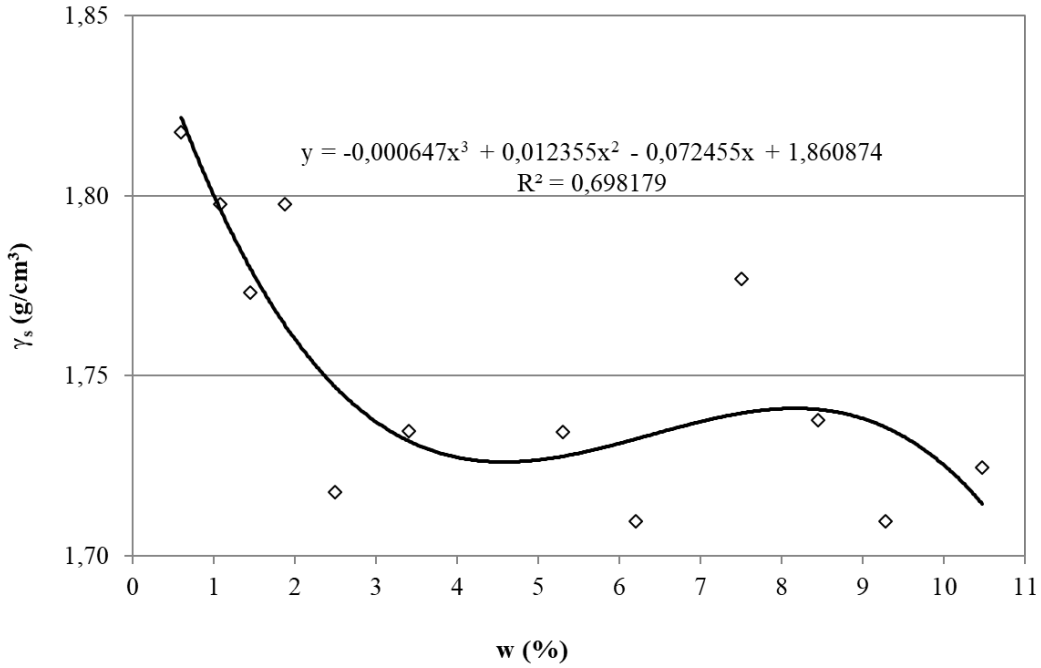

Figure 85. Proctor compaction curve for CC sand.

Table 8. Maximum compaction values of CC sand

a	-0,000647
b	0,012355
c	-0,072455
d	1,860874
a'	-0,001941
b'	0,024710
c'	-0,072455
w_{opt} (%)	8,2
$\gamma_{s,max}$ (g/cm^3)	1,741

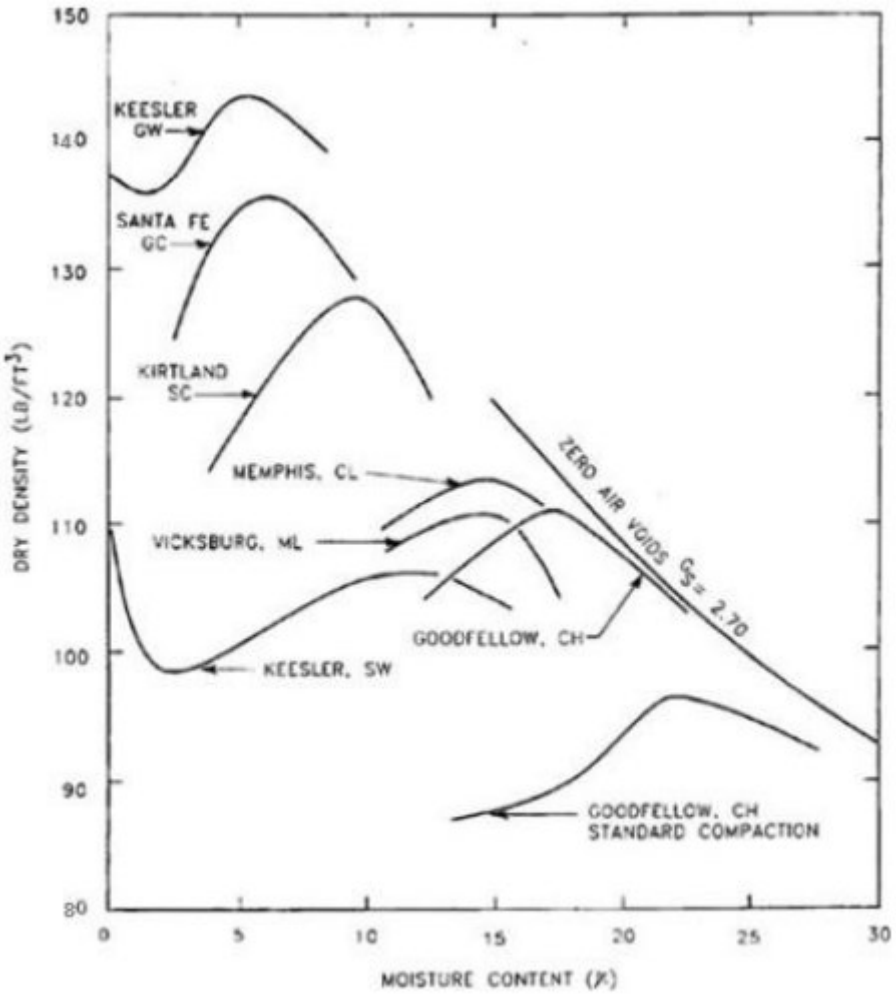

Figure 86. Typical compaction curves for different kind of soils (Rollings, 1996).

Table 9. The optimal conditioning set for CC sand

water content (% by weight on natural soil)	8,8	
Foam	Polyfoamer ECO/100 Pluss	
c $_{foam}$ (% by volume on foam generator liquid)	2	
FER	15	
FIR (%)	30	

7.1.3 Volcanic sand

This kind of sand is obtained from excavations of the Catania subway (Figure 87). The grain size distribution is shown in Figure 88. The volcanic sand has a grain size at the percentage of 10%, D_{10} = 0.11 mm; a grain size at the percentage of 60%, D_{60} = 2.2 mm and a Uniformity coefficient, $C_u = d_{60}/d_{10} = 20$. The natural water content is w = 5% by weight and the specific weight is $\gamma = 1.6$ kg/dm^3.

The optimal conditioning set used in wear tests with volcanic sand is summarized in Table 10.

Figure 87. Volcanic sand sample

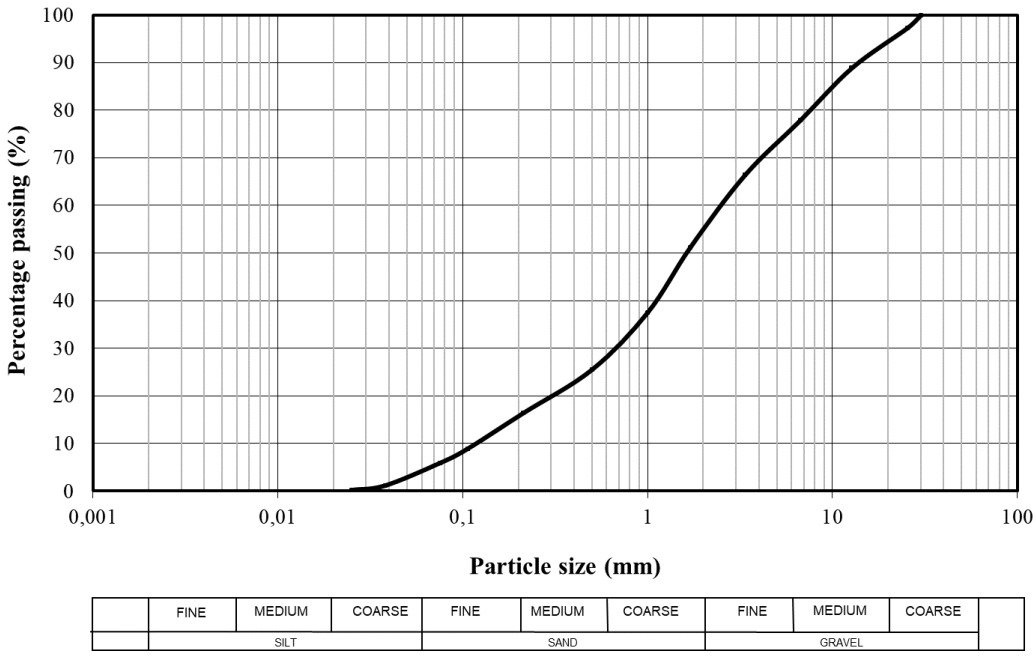

Figure 88. Grain size distribution for volcanic sand.

Table 10. The optimal conditioning set for volcanic sand

water content (% by weight on natural soil)	10	
Foam	Polyfoamer FP	
c $_{foam}$ (% by volume on foam generator liquid)	2	
FER	16	
FIR (%)	30	

7.1.4 Crushed volcanic rock

This ground is obtained from the crushing of porphyry excavated in the Catania subway (Figure 89). The grain size distribution is shown in Figure 90. The crushed volcanic rock has a grain size at the percentage of 10%, D_{10} = 2 mm; a grain size at the percentage of 60%, D_{60} = 8 mm and a Uniformity coefficient, $C_u = d_{60}/d_{10} = 4$. The natural water content of the soil range from w = 0% to w = 1% by weight; specific weight is $\gamma = 1.6$ kg/dm^3.

The optimal conditioning set used in wear tests is summarized in Table 11.

Figure 89. Crushed volcanic rock sample.

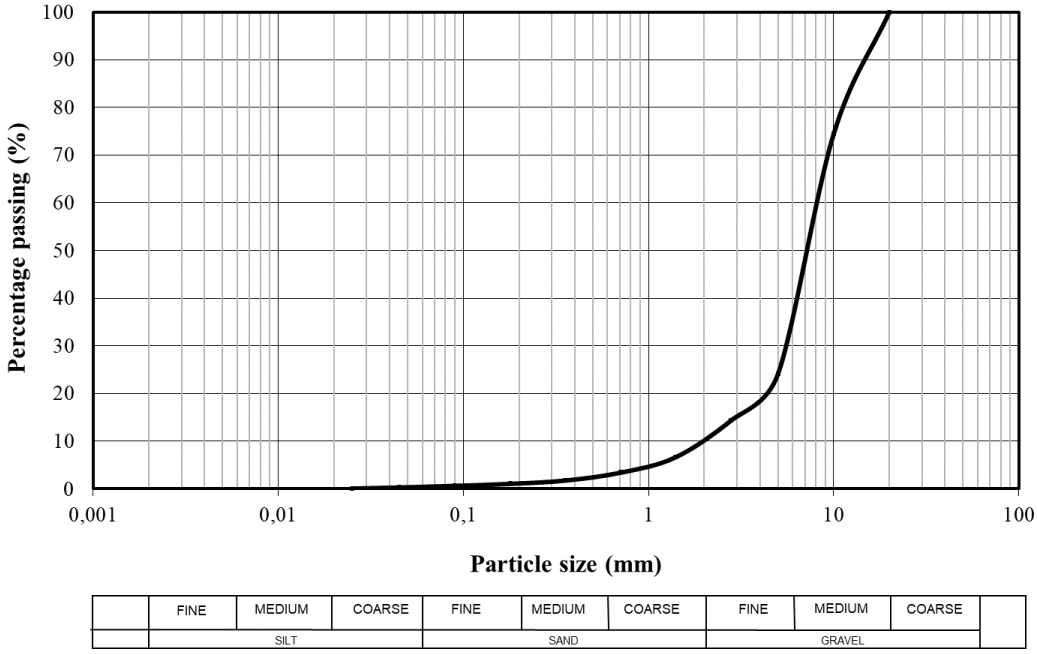

Figure 90. Grain size distribution of crushed volcanic rock.

Table 11. The optimal conditioning set for crushed volcanic rock

water content (% by weight on natural soil)	2,5
Foam	Polyfoamer ECO/100 Pluss
c $_{foam}$ (% by volume on foam generator liquid)	2
FER	15
FIR (%)	40

7.1.5 Moraine soil

This soil sample is obtained from the drilling process performed for the study of the ground that will be excavated for a tunnel construction (Figure 91). The grain size distribution is shown in Figure 92. The moraine soil has a grain size at the percentage of 10%, D_{10} = 0.004 mm; a grain size at the percentage of 60%, D_{60} = 2.17 mm and a Uniformity coefficient, $C_u = d_{60}/d_{10} = 542$. The natural water content of the soil is w = 1% by weight and specific weight is $\gamma = 1.75$ kg/dm^3. Another performed characterization was the Proctor compaction test. The obtained curve is shown in Figure 93. In Table 12, maximum compaction values are displayed.

The optimal conditioning set used in wear tests is summarized in Table 13.

Figure 91. Moraine soil sample.

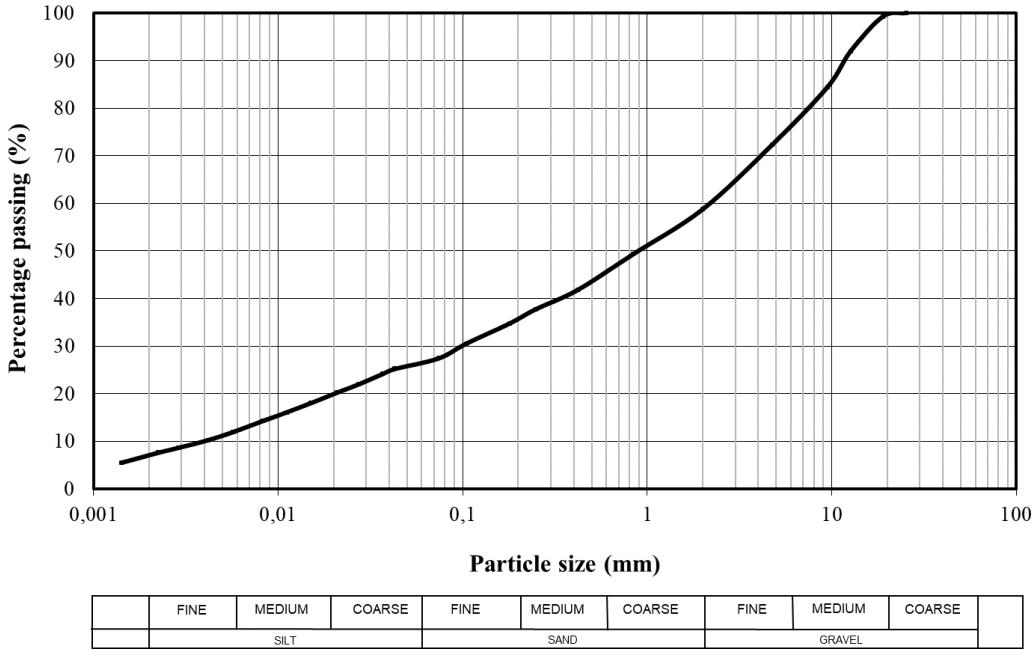

Figure 92. Grain size distribution of moraine soil.

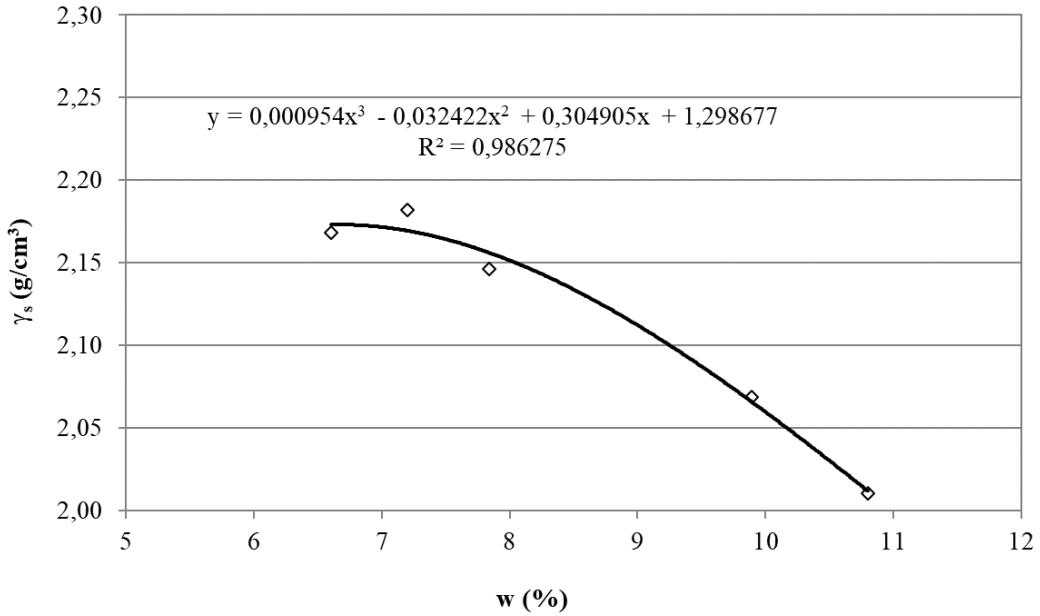

Figure 93. Proctor compaction curve for moraine soil.

Table 12. Maximum compaction values of moraine soil.

a	0,000954
b	-0,032422
c	0,304905
d	1,298677
a'	0,002862
b'	-0,064844
c'	0,304905
w_{opt} (%)	6,7
$\gamma_{s.max}$ (g/cm^3)	2,173

Table 13. The optimal conditioning set for moraine soil

water content (% by weight on natural soil)	12
Foam	Polyfoamer ECO/100
c_{foam} (% by volume on foam generator liquid)	2,2
FER	16
FIR (%)	30

7.1.6 Gneiss

This soil sample is obtained from the drilling process performed for the study of the ground that will be excavated for a tunnel construction. (Figure 94). The grain size distribution is shown in Figure 95. The Gneiss has a grain size at the percentage of 10%, D_{10} = 0.3 mm; a grain size at the percentage of 60%, D_{60} = 4.2 mm and a Uniformity coefficient, $C_u = d_{60}/d_{10} = 14$. The natural water content of the soil is w = 4% by weight and specific weight is $\gamma = 1.75$ kg/dm^3.

Figure 94. Gneiss sample.

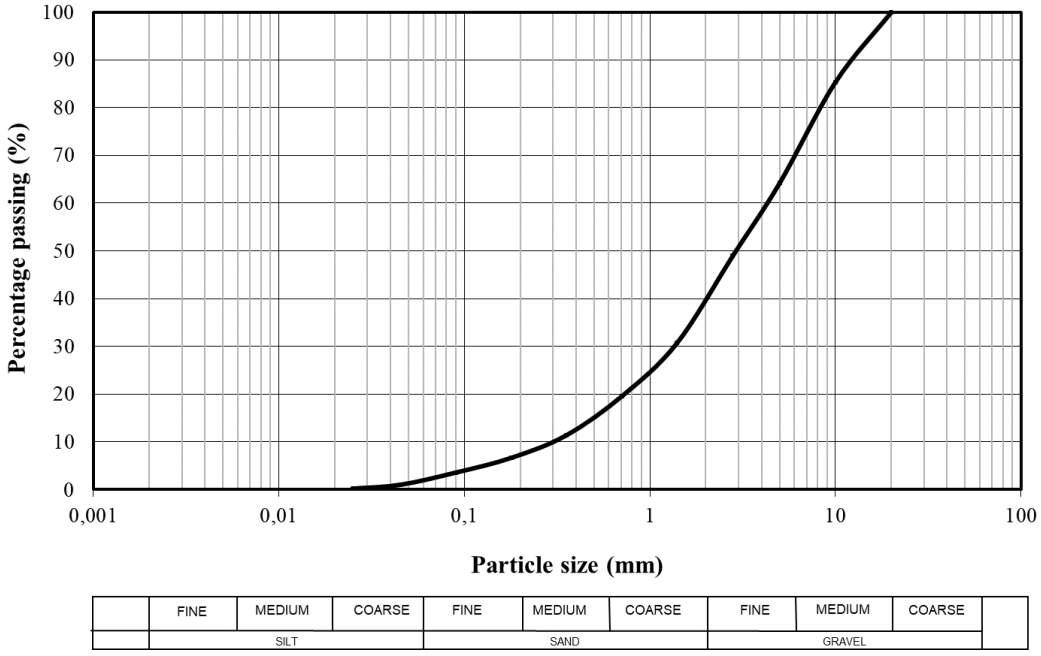

Figure 95. Grain size distribution of Gneiss sample.

7.2 Studied metals

To perform the laboratory tests two different tool geometries were used. For the Wear Disc Test, Modified Wear Disc Test and Pressurized Rotating Mixer circular discs are used while for the Sharp Cutter Test triangular prisms are used.

7.2.1 Circular discs

In this work, three different disc materials are implemented: aluminium, conventional steel and steel obtained from a TBM disc (Figure 96). In Table 14, Vickers hardness values for each kind of disc are displayed, these values are calculated using the HV 10 (10 kg load) program.

The aluminium disc is considered as the reference disc since it allows to better show the wear produced in order to simplify subsequent analyses.

7.2.2 Triangular prisms

The main goal of the Sharp Cutter test which uses triangular prisms is to study the behaviour of hard metals regarding the wear caused by the excavated ground. For this reason, six commercial grades of cemented carbides were studied. In Table 15, a list of the cemented carbide grades used with different binder weight fraction and their grain size is displayed. Carbide grades were selected for their high wear and corrosion resistance properties that are suitable for EPB shield tunnelling. By using a sintering process, cemented carbides consolidation was accomplished. This process was aided by Air pressure by means of an industrial furnace with temperatures from 1410 to 1460°C and pressures from 5 to 10 MPa. According to Bosio, et al. (2018), the higher the binder content the lower is the sintering temperature to be applied, e.g. M6 and K40, were sintered at 1415°C while M1 at 1460°C. As shown in Table 16, a Liquid Phase Sintering mechanism in which solid grains coexist with a wetting liquid occurs and an adequate densification of materials is reached.

To define the density values of sintered samples the Archimede's method was used. Subsequently, to classify porosity size and shape the ISO 4505:1978 standard was used. After processing, the sintered compacts were tangentially machined by a numerical controlled machine and their surface roughness was measure with a Marsurf M400, getting roughness values of about 0.05 µm, which are particularly low. Table 16 also provides basic mechanical properties, e.g. hardness and cross-section rupture strength of the selected materials. HRA and TRS measurements were respectively carried out according to ISO 6508-1:2005 and ISO 3327:2009 standardized procedures (Bosio, et al., 2018). Additionally, a conventional steel of common use called 2 CD 15 with a Vicker hardness of 160 HV and an average carbon content of 0.15% was used for comparative purposes.

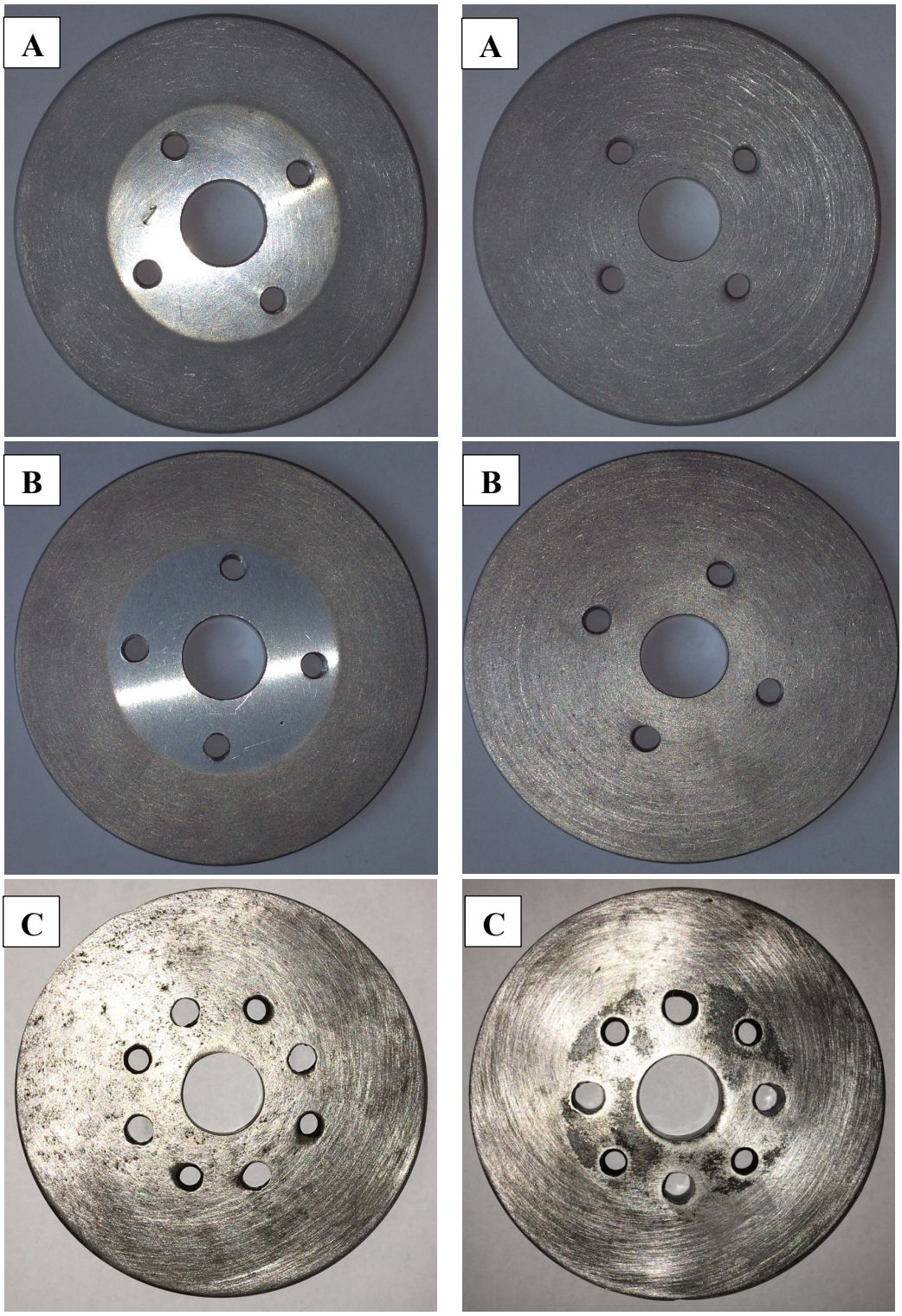

Figure 96. Circular discs of different materials - A: aluminium, B: conventional steel and C: steel obtained from a TBM disc.

Table 14. Vickers hardness of the discs

Conventional steel disc			Aluminium disc			Steel TBM disc		
Points	Hardness (HV)	Average	Points	Hardness (HV)	Average	Points	Hardness (HV)	Average
1	194		1	123		1	161	
2	196		2	118		2	164	
3	191	**189,2**	3	114	**115,6**	3	161	**161,8**
4	179		4	114		4	159	
5	186		5	109		5	164	

Table 15. List of cemented carbide grades used in the study (Bosio, et al., 2018).

Material Code [a]	Binder	f_{binder} [wt%]	Grain size[b]	ρ_{th} [g/cm^3]
M1	Cobalt	6.5	0.8	14.90
M4	Cobalt	11.0	1.7	14.40
M5	Cobalt	9.5	3.6	14.55
M6	Cobalt	13.0	1.1	14.20
K40	Cobalt	12.0	1.0	14.25
N10	Nickel	10.0	–	14.41

[a,b] Material code and grain size as derived by the coercive force values given by Sandvik Hyperion grade list data sheets; NPL methodology [29] was used to derive such values.

Table 16. Mechanical properties and porosities results of the sintered cemented carbide grade (Bosio, et al., 2018).

Material Code	ρ_{Sint} [g/cm^3]	Relative density, $\frac{\rho Sint}{\rho th}$ [%]	Porosity[a]	HRA	E [GPa]	TRS [MPa]
M1	14.85 ± 0.02	99.66	a00 b00 c00	90.4 ± 0.2	457 ± 21	2786 ± 184
M4	14.36 ± 0.02	99.72	a00 b00 c00	87.7 ± 0.5	416 ± 12	2961 ± 148
M5	14.50 ± 0.03	99.66	a00 b00 c00	86.9 ± 0.1	414 ± 11	2468 ± 86
M6	14.05 ± 0.03	98.94	a00 b00 c00	88.6 ± 0.3	395 ± 9	3371 ± 96
K40	14.20 ± 0.04	99.65	a00 b00 c00	89.0 ± 0.1	423 ± 10	3458 ± 150
N10	14.42 ± 0.02	100	a04 b00 c00	89.7 ± 0.1	423 ± 16	2967 ± 214

[a] Estimation according to ISO 4505:1978.

Chapter 8

Results of the Tests

A number of 474 wear tests were performed using a total of about 26200 kg of soil. All test results are summarized in Table 17 and explained in further detail in this chapter.

Table 17. Summary of tests performed.

Method	Soil	Disc	"Bell" Behaviour on natural soil	Maximun average weight loss / Water content for maximum weight loss						Maximum average torque / Water content for maximum torque						Performed tests	Amount of soil
				without foam		with foam (optimal conditioning)		with anti-wear polymer		without foam		with foam (optimal conditioning)		with anti-wear polymer			
				Weight loss (g)	w (%)	Weight loss (g)	w (%)	Weight loss (g)	w (%)	Torque (Nm)	w (%)	Torque (Nm)	w (%)	Torque (Nm)	w (%)		
Wear Disc Test	Quartz sand	Aluminium	YES	0,583	10	0,403	5	0,540	7	1,059	7	0,787	5	1,016	7	143	3575
		Steel	YES	0,503	10	-	-	0,357	7	1,349	10	-	-	1,127	7		
		TBM steel	YES	0,887	10	-	-	-	-	1,679	10	-	-	-	-		
	CC sand	Aluminium	NOT	0,267	0,8	0,073	8,8	-	-	1,293	0,8	0,260	8,8	-	-	27	675
	Volcanic sand	Aluminium	NOT	0,177	5	0,117	10	-	-	0,566	5	0,533	10	-	-	30	750
		TBM steel	YES	0,237	10	0,103	10	-	-	0,572	15	0,543	10	-	-		
	Crushed volcanic rock	TBM steel	NOT	0,478	20	0,230	3	-	-	1,905	20	0,760	3	-	-	27	675
	Moraine	Aluminium	YES	0,247	9	0,032	12	-	-	1,488	13	0,651	12	-	-	38	950
		Steel	YES	0,140	13	0,035	12	-	-	1,899	13	0,717	12	-	-		
	Gneiss soil	Aluminium	YES	0,437	10	-	-	-	-	0,695	10	-	-	-	-	24	600

Method	Soil	Disc	"Bell" Behaviour on natural soil	Maximum average weight loss / Water content for maximum weight loss						Maximum average torque / Water content for maximum torque						Performed tests	Amount of soil
				without foam		with foam (optimal conditioning)		with anti-wear polymer		without foam		with foam (optimal conditioning)		with anti-wear polymer			
				Weight loss (g)	w (%)	Weight loss (g)	w (%)	Weight loss (g)	w (%)	Torque (Nm)	w (%)	Torque (Nm)	w (%)	Torque (Nm)	w (%)		
Modified Wear Disc Test	Quartz sand	Aluminium	YES	9,847	4	0,303	5	-	-	4,215	4	0,206	5	-	-	27	675
	CC sand	Aluminium	YES	1,073	3,6	0,043	8,8	0,977	1,7	2,21	0,8	0,231	8,8	2,01	1,3	76	1900

Method	Soil	Tool	Pressure	Maximum radius of curvature / Water content						Maximum volume loss / Water content						Performed tests	Amount of soil
				without foam		with foam (optimal conditioning)		with anti-wear polymer		without foam		with foam (optimal conditioning)		with anti-wear polymer			
				Curvature radius (mm)	w (%)	Curvature radius (mm)	w (%)	Curvature radius (mm)	w (%)	Volume loss (mm^3)	w (%)	Volume loss (mm^3)	w (%)	Volume loss (mm^3)	w (%)		
Sharp Cutter Test	Quartz sand	Steel	-	2,095	2	1,232	5	-	-	0,080	2	0,025	5	-	-	3	75
		Cemented carbides	-	0,586	2	0,301	5	-	-	12,725	2	6,953	5	-	-	9	225

Method	Soil	Disc	Pressure (bar)	Maximum average weight loss / Water content for maximum weight loss						Maximum average rotor torque / Water content for maximum torque						Performed tests	Amount of soil
				without foam		with foam (optimal conditioning)		with anti-wear polymer		without foam		with foam (optimal conditioning)		with anti-wear polymer			
				Weight loss (g)	w (%)	Weight loss (g)	w (%)	Weight loss (g)	w (%)	Torque (Nm)	w (%)	Torque (Nm)	w (%)	Torque (Nm)	w (%)		
Pressurized Rotating Mixer	Quartz sand	Aluminium	0	5,297	5	0,093	5	-	-	2,251	10	0,234	5	-	-	15	3450
			4	4,743	5	0,273	5	-	-	1,956	10	1,075	5	-	-	15	3450
	CC sand		0	0,383	4	0,047	8,8	-	-	1,122	4	0,355	8,8	-	-	12	2760
			3	0,477	4	0,127	8,8	-	-	1,537	0,8	1,454	8,8	-	-	28	6440
														TOTAL		474	26200

8.1 Wear Disc Test

The Wear Disc Test provides a disc weight loss value and a torque trend that is recorded in order to obtain an average value. For each test configuration, at least three assessments are performed and the average of them is then calculated.

In this thesis work, a total of **289 tests** were executed using the Wear Disc Test method, studying about **7225 kg** of soil. Due to the large amount of data, summary tables and charts of the results will be presented. In Figure 97, an example of the torque record for all three assessments performed in one of the test configurations is shown.

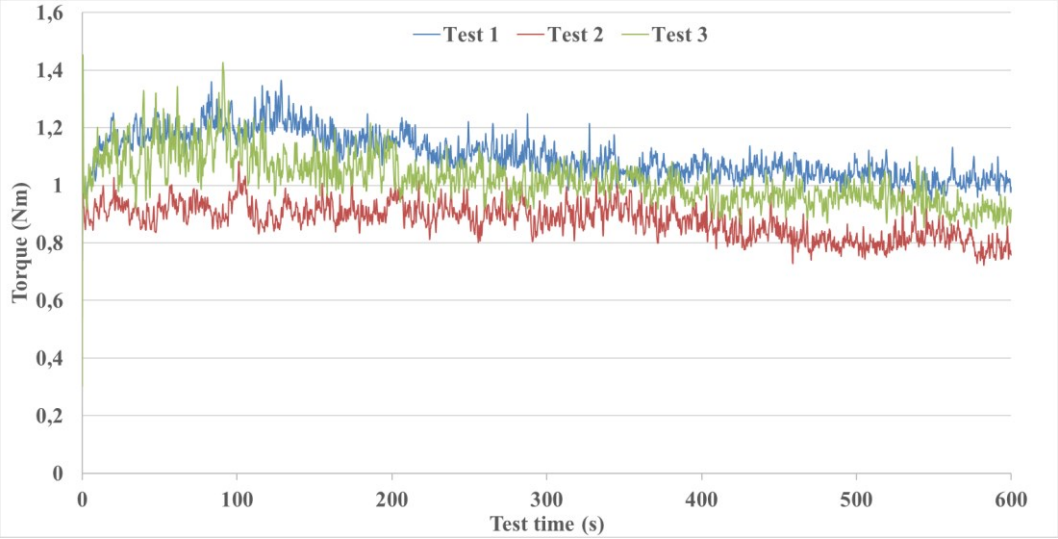

Figure 97. Example of torque record for all three assessments performed in one of the test configurations

8.1.1 Quartz sand

a) Variability in water content of soils

This assessment allows studying the influence of soil water content on discs wear. The used range was between 2% and 15% (between the natural and the saturation limit). All available different disc materials were studied: Aluminium, Steel and Steel from a TBM disc (Paragraph 7.2.1). Results of weight loss and torque trends using different water contents in Quartz sand are summarized in Table 18, Table 19 and Table 20, and illustrated in Figure 98 and Figure 99.

Table 18. Test results for different water contents of quartz sand using an aluminium disc.

Total water content (% by weight)	Weight loss (g)	Average Weight loss (g)	Torque (Nm)	Average Torque (Nm)
2	0,400	0,443	1,102	1,000
	0,420		0,879	
	0,510		1,018	
5	0,400	0,473	0,615	0,706
	0,430		0,611	
	0,590		0,892	
7	0,360	0,338	0,819	1,059
	0,410		1,777	
	0,380		1,809	
	0,310		0,467	
	0,240		0,939	
	0,330		0,544	
10	0,540	0,583	1,119	0,791
	0,560		0,631	
	0,650		0,622	
12	0,600	0,556	0,690	0,598
	0,530		0,525	
	0,590		0,540	
	0,520		0,608	
	0,540		0,626	
15	0,510	0,370	0,714	0,579
	0,360		0,513	
	0,240		0,510	

Table 19. Test results for different water contents of quartz sand using a conventional steel disc.

Total water content (% by weight)	Weight loss (g)	Average Weight loss (g)	Torque (Nm)	Average Torque (Nm)
2	0,280	0,265	1,086	1,101
	0,140		0,830	
	0,280		1,096	
	0,210		1,046	
	0,420		1,419	
	0,260		1,129	
5	0,370	0,433	0,882	1,003
	0,480		1,079	
	0,450		1,048	
7	0,420	0,400	1,134	1,094
	0,400		1,169	
	0,380		0,981	
10	0,660	0,503	1,520	1,349
	0,420		1,272	
	0,430		1,254	
12	0,430	0,347	1,030	0,909
	0,320		0,904	
	0,290		0,793	
15	0,170	0,183	0,753	0,823
	0,230		0,954	
	0,150		0,764	

Table 20. Test results for different water contents of quartz sand using a TBM steel disc.

Total water content (% by weight)	Weight loss (g)	Average Weight loss (g)	Torque (Nm)	Average Torque (Nm)
5	0,420	0,440	0,787	1,021
	0,420		1,057	
	0,480		1,219	
10	0,950	0,887	1,826	1,679
	0,860		1,632	
	0,850		1,579	
12	0,580	0,550	1,254	1,120
	0,520		1,003	
	0,550		1,104	
15	0,200	0,173	0,629	0,658
	0,170		0,660	
	0,150		0,685	

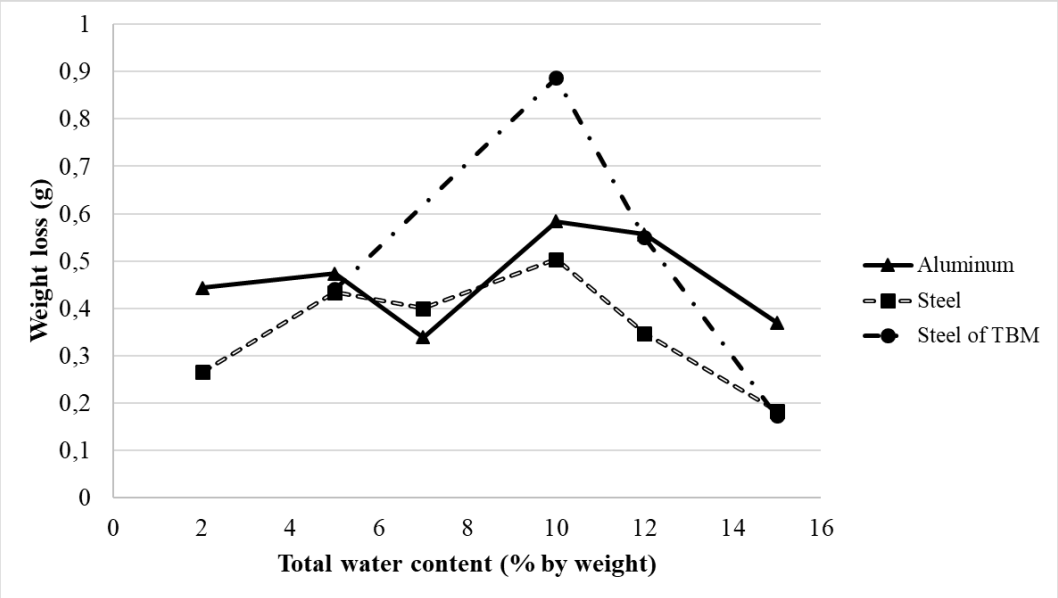

Figure 98. Weight loss average correlated to different water contents for the three available discs.

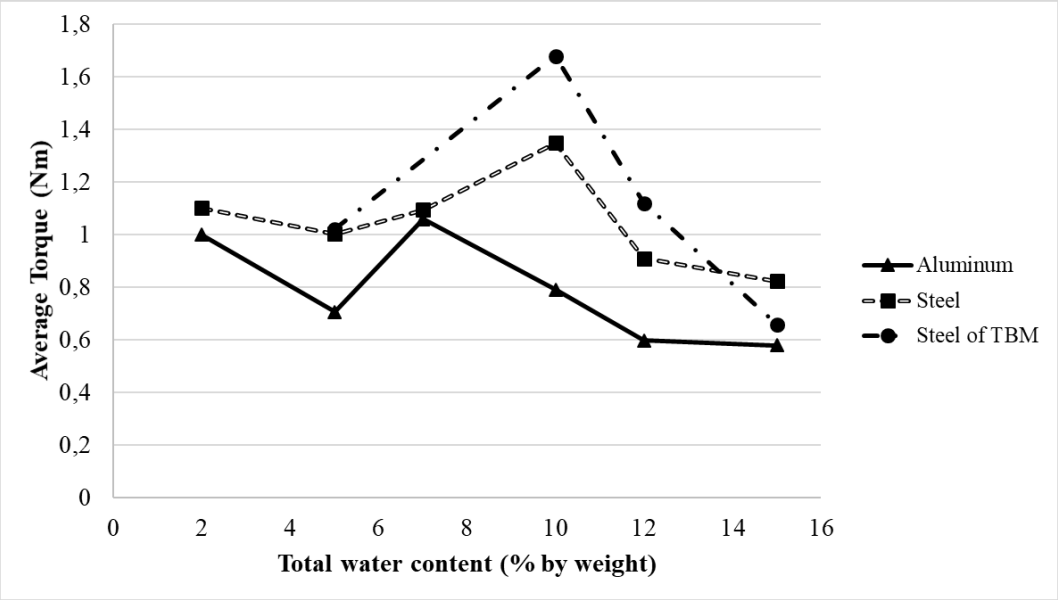

Figure 99. Average torque correlated to different water contents for the three available discs.

b) Use of anti-wear polymer

The anti-wear polymer is an experimental additive prototype developed by MAPEI SpA specifically targeted to reduce wear. It is known as MAPEDRILL F.R.A. 02C (herein called ease FRA02C).

According to Oñate Salazar, et al. (2016), by using this additive, particles are covered by thin polymeric layer that should decrease friction strengths between ground and tools. Examinations using a macroscope have been carried out in order to observe the behaviour of the grains when the additive is in contact with the quartz grain surface. Some images are shown in Figure 100.

Mapei SpA technicians recommended concentration is from 2% to 5% by the weight of water. For a prior assessment on the effect of this polymer, the water percentage that corresponds to the weight loss highest value obtained in the study of variability in water content was considered: 10% of total water content. A different analysis for a total water content of 5% was performed.

For preliminary studies the aluminium disc was used and the results are summarized in Table 21 and displayed in Figure 101 and Figure 102.

Based on these results, it can be observed that a 2% FRA02C concentration produce yet a significant wear reduction and an insignificant torque increase. Torque increase is caused by the increased viscosity of the soil. Since this is the most cost effective option, other two different wear “bells” were performed by using both the discs (aluminium and steel).

In Table 22 and Table 23, a summary of tests results using 2% of FRA02C by the weight of water is presented. In Figure 103 and Figure 104, a graphic representation of these results compared to the control curve (no polymer added) is shown.

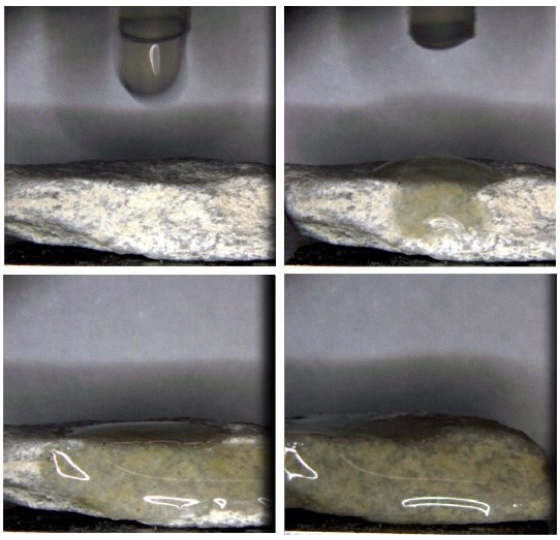

Figure 100. Drop of the solution of water and FRA02C (2% by weight of water) on quartz grain surface (Oñate Salazar, et al., 2016).

Table 21. Test Results of different doses of FRA02C using the aluminium disc.

Total water content (% by weight)	c FRA02C (% by weight on added water)	Weight loss (g)	Average Weight loss (g)	Torque (Nm)	Average Torque (Nm)
5%	0	0,400	0,473	0,615	0,706
		0,430		0,611	
		0,590		0,892	
	2	0,360	0,383	0,756	0,891
		0,410		1,011	
		0,380		0,906	
	3,5	0,380	0,367	0,939	0,923
		0,350		0,911	
		0,370		0,919	
	5	0,390	0,407	1,005	0,949
		0,430		0,894	
		0,400		0,947	
10%	0	0,540	0,583	1,119	0,791
		0,560		0,631	
		0,650		0,622	
	2	0,560	0,492	0,882	0,839
		0,470		0,920	
		0,470		0,859	
		0,330		0,620	
		0,490		0,802	
		0,630		0,951	
	3,5	0,410	0,443	1,073	0,931
		0,450		0,922	
		0,470		0,799	
	5	0,230	0,307	0,634	0,773
		0,340		0,765	
		0,350		0,919	

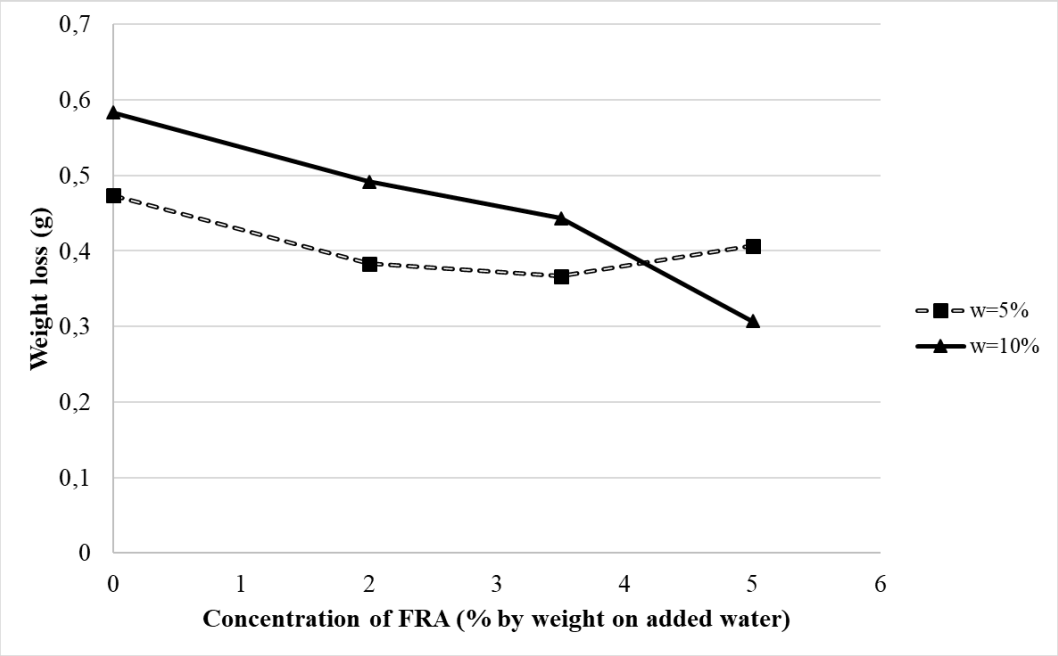

Figure 101. Weight loss average correlated to FRA02C concentration using aluminium disc and total water content of 10% and 5 %.

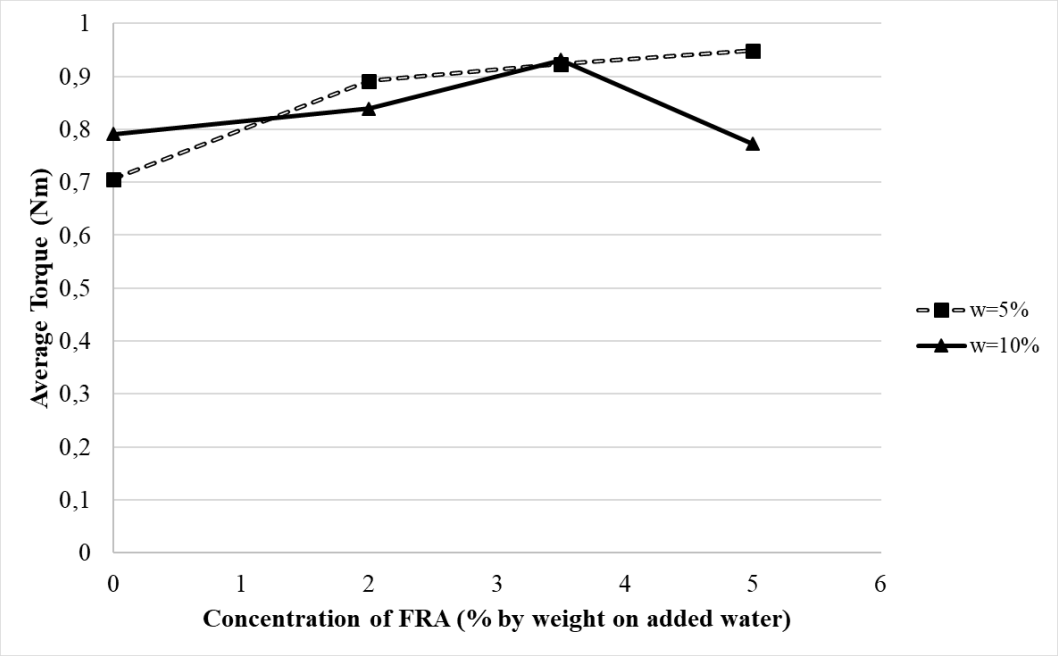

Figure 102. Average Torque correlated to FRA02C concentration using aluminium disc and total water content of 10% and 5 %.

Table 22. Test results obtained with 2% FRA02C concentration using the aluminium disc and varying total water content.

Total water content (% by weight)	c FRA02C (% by weight on added water)	Weight loss (g)	Average Weight loss (g)	Torque (Nm)	Average Torque (Nm)
5	2%	0,360	0,383	0,756	0,891
		0,410		1,011	
		0,380		0,906	
7		0,330	0,540	0,832	1,016
		0,540		1,219	
		0,750		0,998	
10		0,560	0,492	0,882	0,839
		0,470		0,920	
		0,470		0,859	
		0,330		0,620	
		0,490		0,802	
		0,630		0,951	
12		0,450	0,467	0,913	0,850
		0,610		0,859	
		0,340		0,778	
15		0,480	0,497	0,782	0,843
		0,460		0,970	
		0,550		0,778	

Table 23. Test results obtained with 2% FRA02C concentration using the steel disc and varying total water content.

Total water content (% by weight)	c FRA02C (% by weight on added water)	Weight loss (g)	Average Weight loss (g)	Torque (Nm)	Average Torque (Nm)
5	2%	0,230	0,227	0,988	1,039
		0,230		1,073	
		0,220		1,055	
7		0,370	0,357	1,306	1,127
		0,350		1,008	
		0,350		1,068	
10		0,340	0,323	0,985	0,869
		0,380		0,933	
		0,250		0,690	
12		0,280	0,290	0,807	0,786
		0,260		0,773	
		0,330		0,779	
15		0,400	0,330	1,035	0,839
		0,330		0,779	
		0,260		0,702	

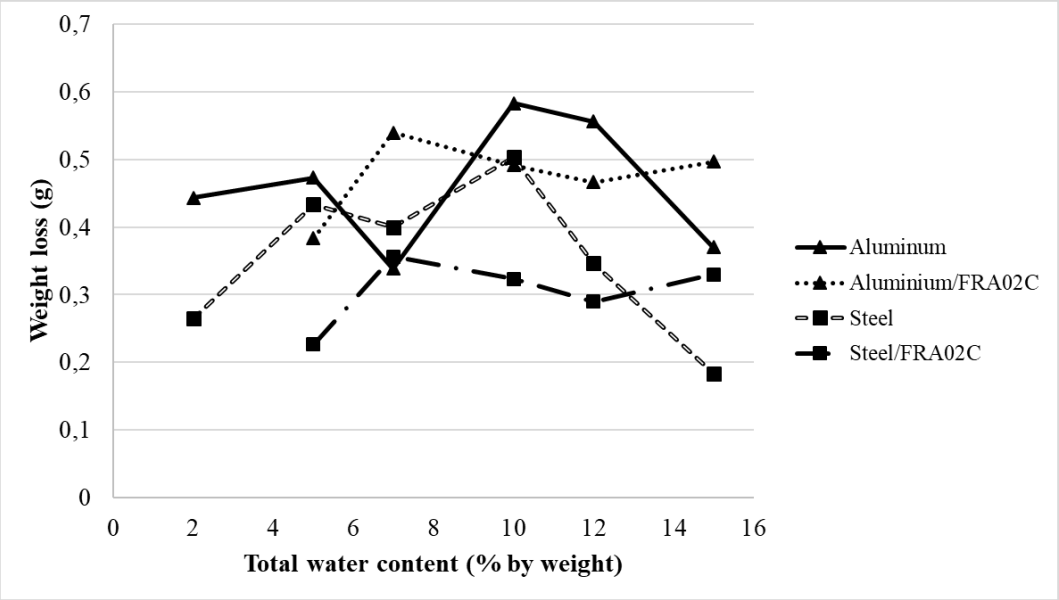

Figure 103. Weight loss average correlated to soil water content using aluminium and steel discs with or without adding anti-wear polymer.

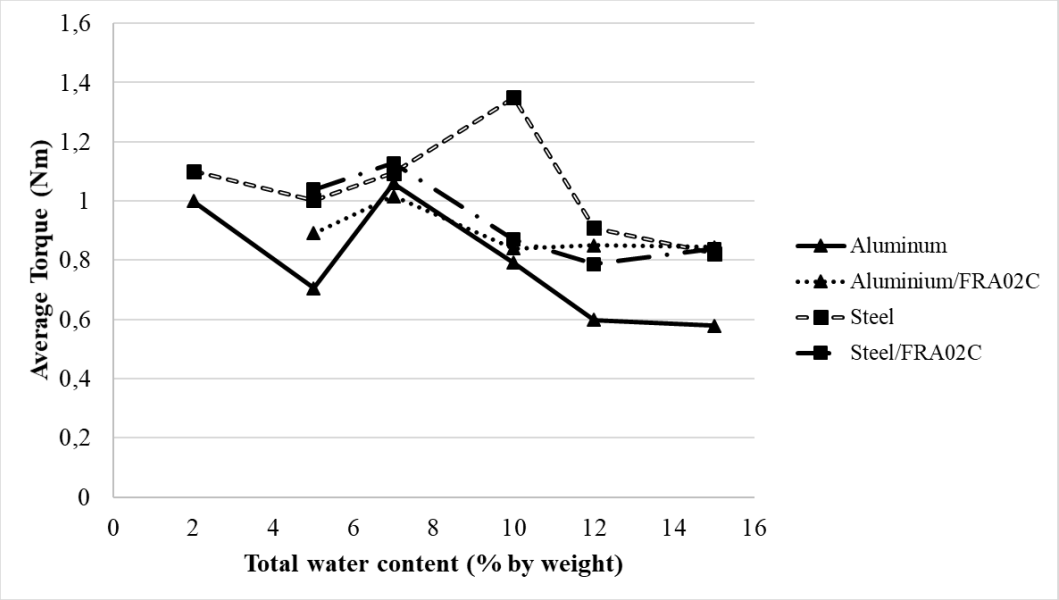

Figure 104. Average Torque correlated to soil water content using aluminium and steel discs with or without adding anti-wear polymer.

c) Use of foams

Different conditioning sets were studied including the optimal conditioning one. For some established total water contents and FER the amount of foam used was modified. The obtained results are summarized in Table 24 and illustrated in Figure 105 and Figure 106, using as reference the wear value that corresponds to the total water content of a FIR = 0%.

d) Comments

It can be observed a "bell" behaviour obtained from different water contents of the soil when correlated to weight loss and torque. The highest wear value for the three studied discs was obtained when the total water content was equal to 10%. It was observed an atypical reduction in weight loss with 7% of total water content that might be related to the test configuration.

The anti-wear polymer was useful in reducing disc weight loss especially for low water contents (with the exception of the atypical value observed in this test previously mentioned).

In general, using foams led to a reduction in disc wear although this decrease was not linear.

Table 24. Tests Results for quartz sand conditioned with foam.

Total water content (% by weight)	FER	FIR (%)	Weight loss (g)	Average Weight loss (g)	Torque (Nm)	Average Torque (Nm)
5	10	20	0,240	0,260	0,497	0,569
		20	0,290		0,673	
		20	0,250		0,537	
		30	0,190	0,250	0,546	0,661
		30	0,250		0,725	
		30	0,270		0,586	
		30	0,290		0,788	
		40	0,400	0,403	0,763	0,787
		40	0,410		0,808	
		40	0,400		0,789	
10	10	10	0,140	0,170	0,398	0,532
		10	0,200		0,681	
		10	0,170		0,517	
		20	0,310	0,313	0,690	0,681
		20	0,330		0,687	
		20	0,300		0,664	
		30	0,390	0,393	0,758	0,820
		30	0,420		0,891	
		30	0,370		0,812	
		40	0,270	0,283	0,743	0,764
		40	0,300		0,794	
		40	0,280		0,755	
10	12	10	0,420	0,363	0,869	0,735
		10	0,400		0,769	
		10	0,270		0,568	
		15	0,450	0,383	0,820	0,666
		15	0,330		0,532	
		15	0,370		0,647	
		20	0,200	0,263	0,679	0,646
		20	0,430		0,824	
		20	0,160		0,436	

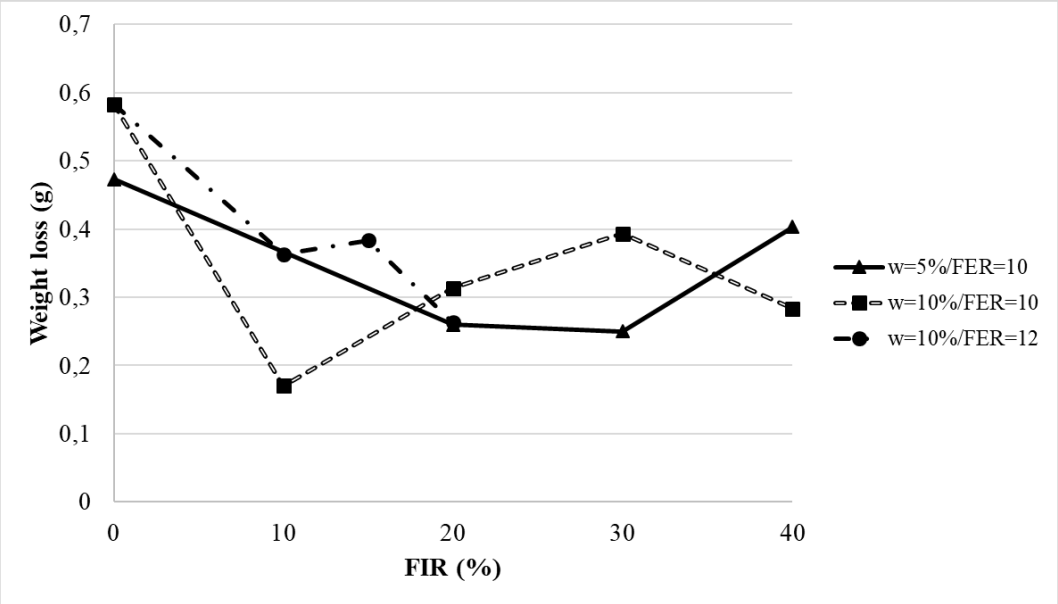

Figure 105. Weight loss average correlated to FIR

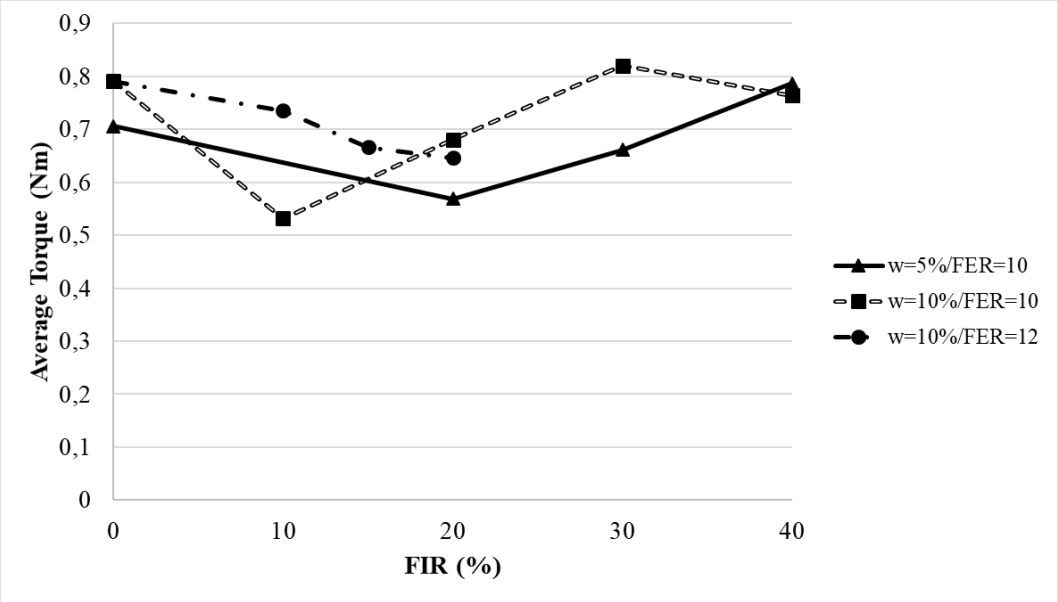

Figure 106. Average torque correlated to FIR.

8.1.2 CC sand

CC sand tests were carried out using different water contents and optimal conditioning set to establish a behavioural comparison to quartz sand in order to evaluate the validity of the method.

a) Variability in water content of soils

The used range was between 0.8% and 18% (between the natural and the saturation limit). CC sand tests were performed using the aluminium disc

(Paragraph 7.2.1). The obtained results are summarized in Table 25 and illustrated in Figure 107 and Figure 108.

b) Use of foams

Only optimal conditioning set was evaluated in order to compare conditioned CC sand to this test method. The obtained results are summarized in Table 26 and illustrated in Figure 107 and Figure 108.

c) Comments

In CC sand tests the typical "bell" behaviour with different water contents wasn't observed. Furthermore, conditioned soil wear values were higher than unconditioned soil ones. It is important to mention that CC sand did not present a standard behaviour when tested with the Proctor compaction method (Paragraph 7.1.2), therefore, it should be assessed whether this test methodology is feasible for soils with particular characteristics.

Table 25. Test results in CC sand using an aluminium disc.

Total water content (% by weight)	Weight loss (g)	Average Weight loss (g)	Torque (Nm)	Average Torque (Nm)
0,8	0,270	0,267	1,254	1,293
	0,260		1,378	
	0,270		1,248	
2,7	0,100	0,077	0,251	0,214
	0,050		0,176	
	0,080		0,216	
4,6	0,020	0,033	0,078	0,068
	0,040		0,070	
	0,040		0,057	
6,5	0,020	0,010	0,074	0,070
	0,000		0,066	
	0,010		0,071	
8	0,020	0,023	0,124	0,141
	0,020		0,111	
	0,030		0,188	
10	0,040	0,033	0,127	0,130
	0,030		0,131	
	0,030		0,133	
12	0,030	0,027	0,210	0,212
	0,030		0,225	
	0,020		0,201	
18	0,170	0,147	0,688	0,660
	0,140		0,647	
	0,130		0,643	

Table 26. Test results in CC sand conditioned with foam.

Total water content (% by weight)	FER	FIR (%)	Weight loss (g)	Average Weight loss (g)	Torque (Nm)	Average Torque (Nm)
8,8	15	30	0,070	0,073	0,264	0,260
		30	0,060		0,245	
		30	0,090		0,271	

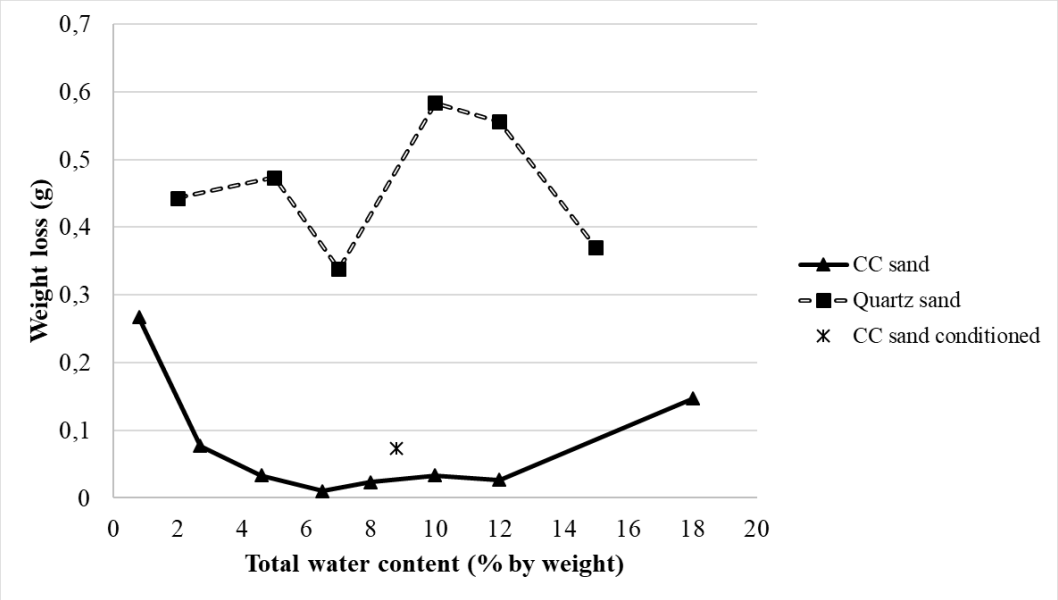

Figure 107. Weight loss average correlated to water content in CC sand and Quartz sand.

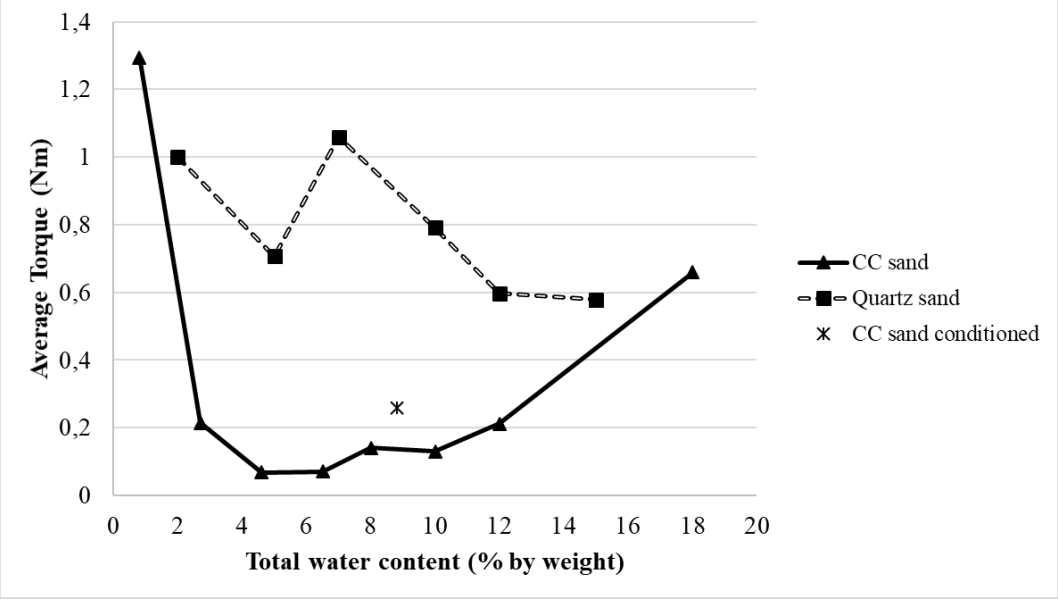

Figure 108. Average Torque correlated to water content in CC sand and Quartz sand.

8.1.3 Volcanic sand

Tests were performed with different water contents and optimal conditioning dosage using aluminium and TBM steel discs. This study was carried out to establish a behavioural comparison between volcanic sand sample and reference quartz sand in order to evaluate the abrasivity of this kind of soil that will be excavated with the same TBM steel tested.

a) Variability in water content of soils

The used range was between 5% and 15% (between the natural and the saturation limit). Volcanic sand tests were performed using the aluminium and TBM steel discs (Paragraph 7.2.1). The obtained results are summarized in Table 27 and Table 28, and illustrated in Figure 109 and Figure 110.

In Figure 111 and Figure 112, comparisons between volcanic sand and quartz sand wear tests are shown.

b) Use of foams

Only optimal conditioning set was evaluated in order to compare the behaviour between both conditioned and unconditioned volcanic sand. Tests were performed using the same type of discs (aluminium and TBM steel) studied in the water content test. The obtained results are summarized in Table 29 and illustrated in Figure 109 and Figure 110.

Table 27. Tests results in Volcanic sand using an aluminium disc.

Total water content (% by weight)	Weight loss (g)	Average Weight loss (g)	Torque (Nm)	Average Torque (Nm)
5	0,160	0,177	0,582	0,566
	0,160		0,486	
	0,210		0,630	
10	0,160	0,113	0,387	0,507
	0,090		0,523	
	0,090		0,611	
12	0,120	0,110	0,416	0,487
	0,100		0,515	
	0,110		0,531	
15	0,120	0,133	0,741	0,638
	0,120		0,494	
	0,160		0,677	

Table 28. Tests results in Volcanic sand using a TBM steel disc.

Total water content (% by weight)	Weight loss (g)	Average Weight loss (g)	Torque (Nm)	Average Torque (Nm)
5	0,130	0,137	0,559	0,567
	0,140		0,572	
	0,140		0,569	
10	0,600	0,237	0,356	0,357
	0,060		0,346	
	0,050		0,370	
12	0,080	0,073	0,451	0,447
	0,070		0,476	
	0,070		0,413	
15	0,120	0,137	0,545	0,572
	0,100		0,589	
	0,190		0,584	

Table 29. Results of conditioned volcanic sand tests

Disc	Total water content (% by weight)	FER	FIR (%)	Weight loss (g)	Average Weight loss (g)	Torque (Nm)	Average Torque (Nm)
Aluminium	10	16	30	0,100	0,117	0,431	0,533
			30	0,130		0,627	
			30	0,120		0,541	
Steel of TBM	10	16	30	0,060	0,103	0,453	0,543
			30	0,160		0,632	
			30	0,090		0,543	

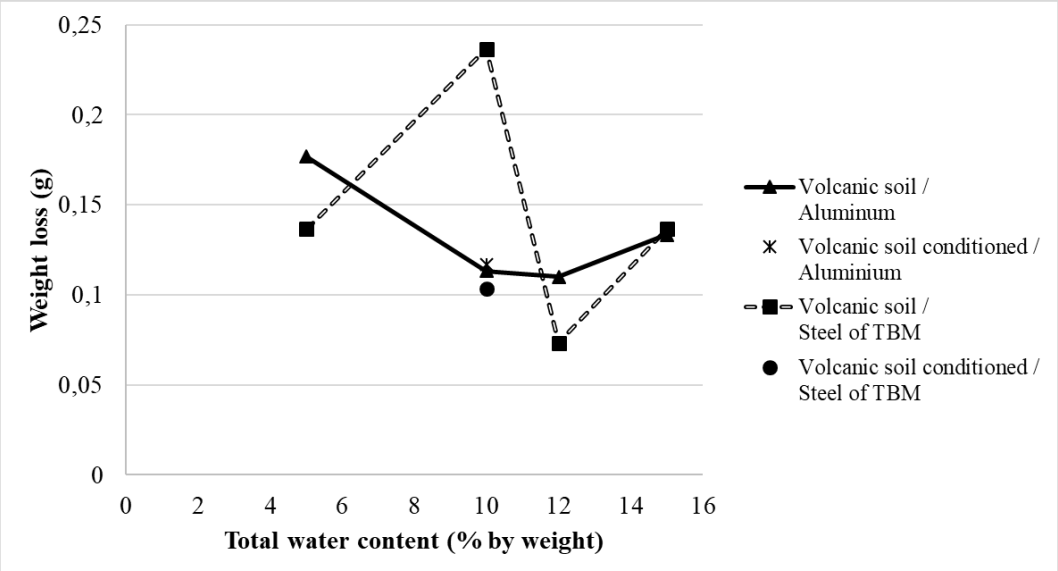

Figure 109. Weight loss average correlated to water content in volcanic sand for aluminium and TBM steel discs.

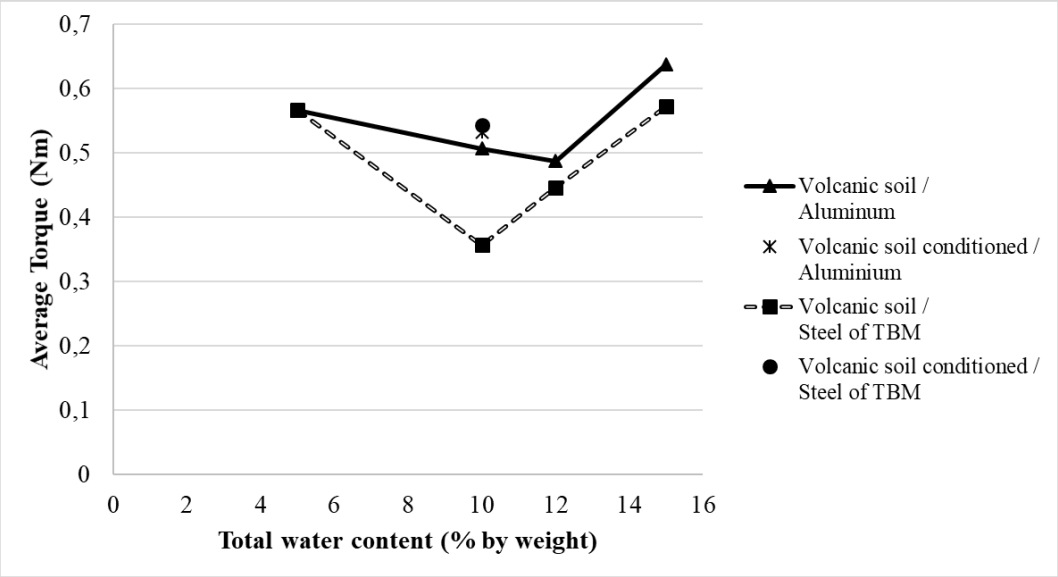

Figure 110. Average torque correlated to water content in volcanic sand for aluminium and TBM steel discs.

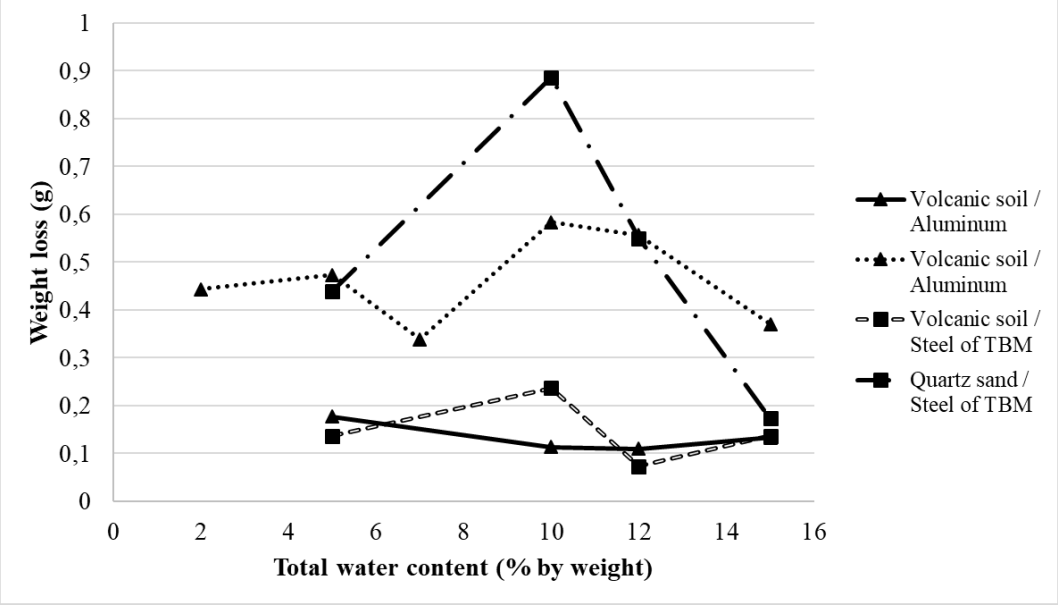

Figure 111. Weight loss average correlated to water content of volcanic and quartz sands for aluminium and TBM steel discs.

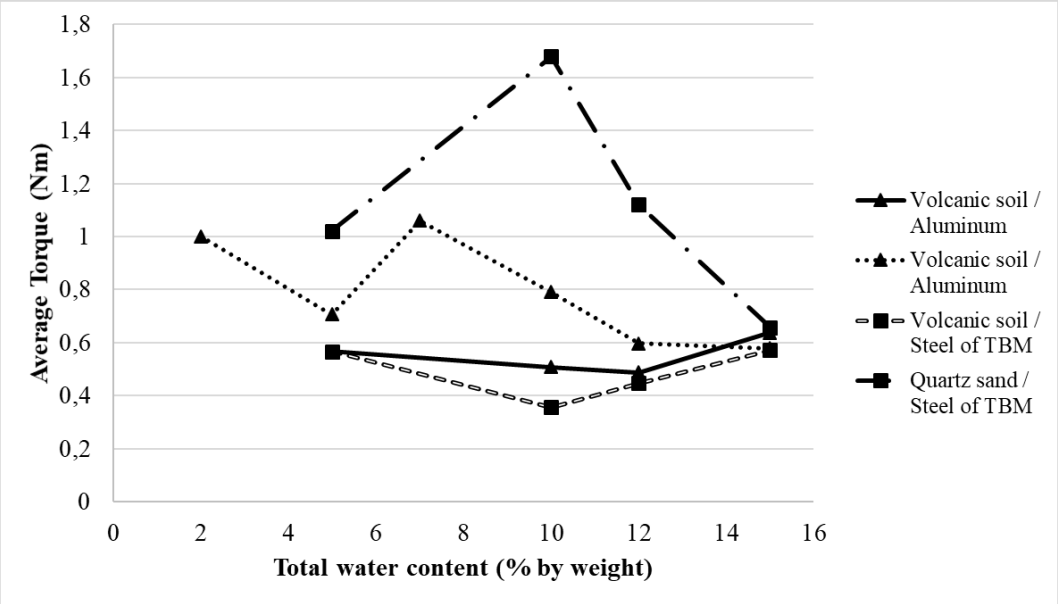

Figure 112. Average torque correlated to water content of volcanic and quartz sands for aluminium and TBM steel discs.

c) Comments

In volcanic sand tests a "bell" behaviour was observed when using the TBM steel disc (highest wear with 10% of total water content), but using the aluminium disc a different behaviour was shown. It is clearly that volcanic soil produces less discs wear, than quartz sand.

It wasn't possible to observe any improvement with conditioned soil. These atypical results can be attributed to a phenomenon seen when water contents are present. In Figure 113 it is shown the aluminium disc after being tested; it is demonstrated that not enough contact took place between the soil sample and the disc due to the high compaction of soil under disc level, leaving a vacuum in the middle. However, this vacuum is not present when soil have been conditioned, justifying the missing of the expected improvement when the conditioned soil sample is used.

Figure 113. Disc condition after testing (Left: top view, right: bottom view)

8.1.4 Crushed volcanic rock

Tests were performed with different water contents and optimal conditioning dosage using the TBM steel disc only. This study was carried out to establish a behavioural comparison between crushed volcanic rock sample and reference quartz sand in order to evaluate the abrasivity of this kind of soil that will be excavated with the same TBM steel tested.

a) Variability in water content of soils

The used range was between 1% and 20% (between the natural and the saturation limit). Crushed volcanic rock tests were performed using the TBM steel disc (Paragraph 7.2.1). The obtained results are summarized in Table 30 and illustrated in Figure 114 and Figure 115 along with quartz sand results for comparison purposes.

b) Use of foams and polymers

10 different conditioning sets including polymers were evaluated. Tests were performed with the TBM steel disc. The obtained results are summarized in Table 31 and illustrated in Figure 116 and Figure 117 along with the wear control curve of unconditioned soil values.

Table 30. Results of crushed volcanic rock tests using TBM steel disc.

Total water content (% by weight)	Weight loss (g)	Average Weight loss (g)	Torque (Nm)	Average Torque (Nm)
1	0,280	0,237	1,540	1,243
	0,220		1,259	
	0,210		0,929	
6	0,180	0,183	0,935	0,918
	0,180		0,868	
	0,190		0,951	
11	0,250	0,243	1,143	1,063
	0,200		1,102	
	0,280		0,942	
16	0,210	0,197	1,194	1,158
	0,160		1,159	
	0,220		1,122	
20	0,560	0,478	2,038	1,905
	0,240		1,254	
	0,530		2,362	
	0,520		1,950	
	0,540		1,921	

Table 31. Results of conditioned crushed volcanic rock tests using TBM steel disc.

n°	Total water content (% by weight)	c Polymer (% by weight on added water)	FER	FIR (%)	Weight loss (g)	Torque (Nm)
1	3	-	15	50	0,230	0,760
2	3	0,20	15	50	0,610	1,454
3	5	0,10	15	50	0,410	1,185
4	5	0,40	15	40	0,300	0,998
5	5	0,40	18	60	0,240	0,797
6	10	0,10	15	60	0,210	1,494
7	10	0,20	15	20	0,410	1,111
8	10	0,40	18	60	0,090	0,527
9	10	0,48	18	60	0,160	1,152
10	20	0,43	18	60	0,050	0,796

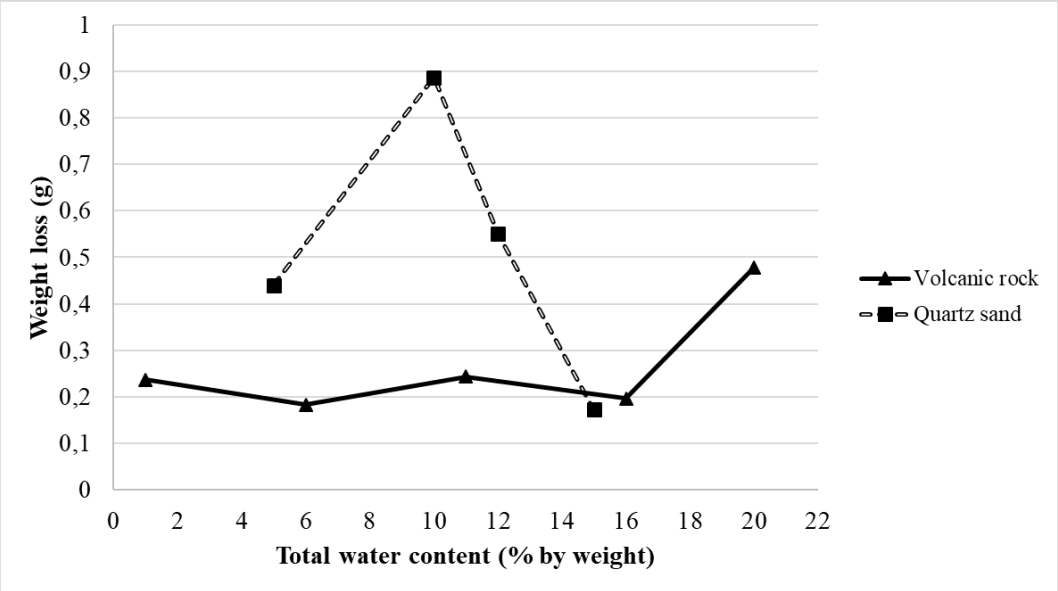

Figure 114. Weight loss average correlated to water content of crushed volcanic rock and quartz sand for TBM steel disc.

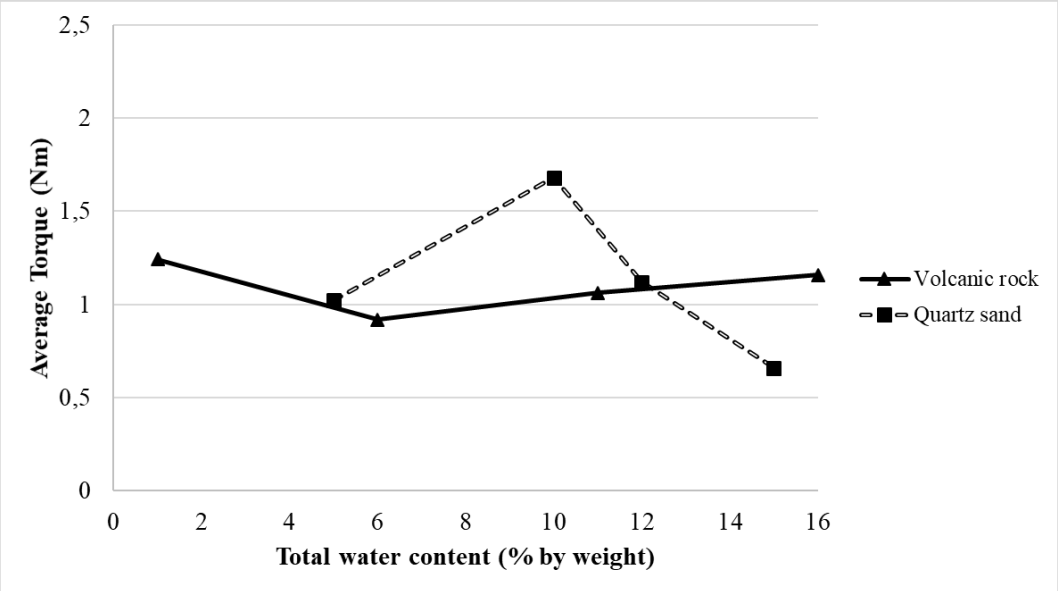

Figure 115. Average torque correlated to water content of crushed volcanic rock and quartz sand for TBM steel disc.

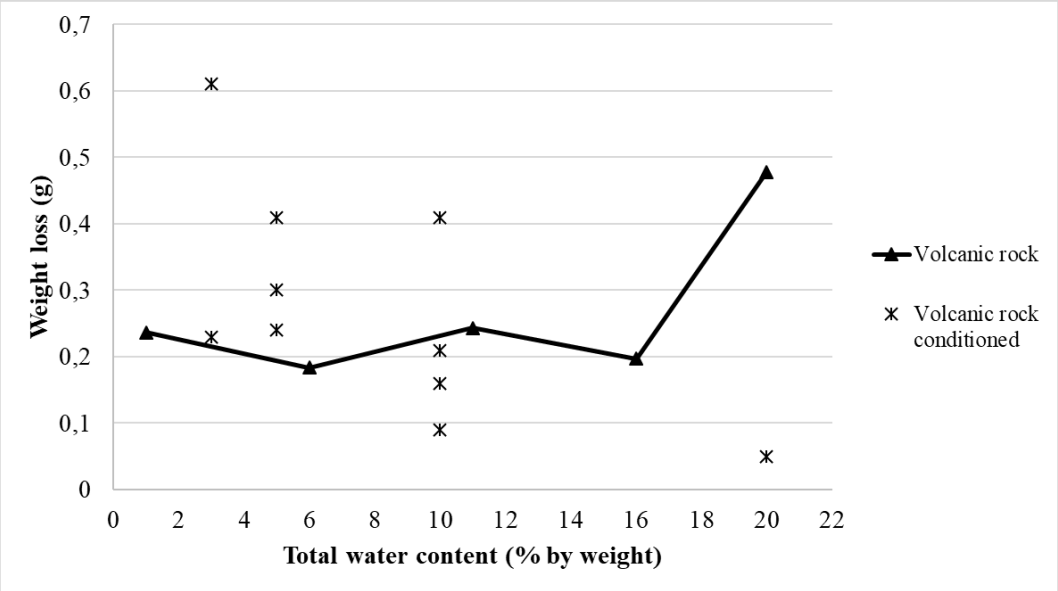

Figure 116. Weight loss average correlated to water content of conditioned and unconditioned crushed volcanic rock.

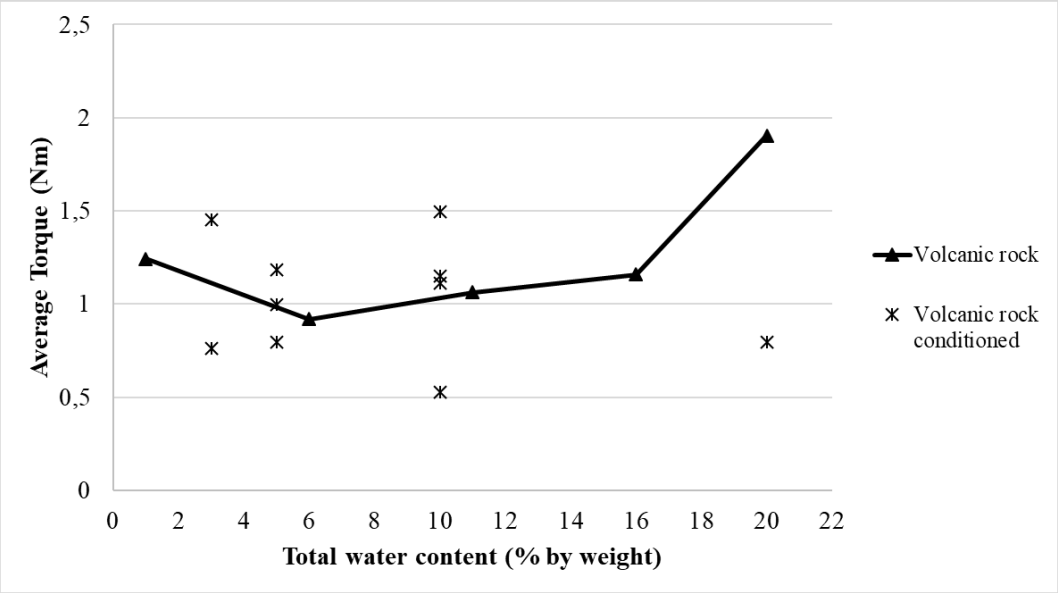

Figure 117. Average torque correlated to water content of conditioned and unconditioned crushed volcanic rock.

c) Comments

It was observed that wear produced by the crushed volcanic rock did not display a “bell” behaviour. However, the abrasive impact was less than the Quartz sand one, except in the saturation value. The torque behavior also did not exhibit a “bell” behavior and the values obtained are comparable to those obtained with Quartz sand.

Different conditioning sets used resulted in very variable values: some of them were high and others were low when compared to the unconditioned soil ones.

8.1.5 Moraine soil

Tests were performed with different water contents and two conditioning sets using the aluminium and TBM steel discs. This study was carried out to establish a behavioural comparison between moraine soil sample and reference quartz sand in order to evaluate the abrasivity of this soil.

a) Variability in water content of soils

The used range was between 1% and 16% (between the natural and the saturation limit). Moraine soil tests were performed using the aluminium and TBM steel discs (Paragraph 7.2.1). The obtained results are summarized in Table 32 and Table 33 and illustrated in Figure 118 and Figure 119.

In Figure 120 and Figure 121, comparisons between moraine soil and quartz sand wear tests are shown.

b) Use of foams

Only optimal conditioning set was evaluated in order to compare the behaviour between both conditioned and unconditioned moraine soil. Tests were performed using the same type of discs (aluminium and steel) studied in the water content test. The obtained results are summarized in Table 34 and illustrated in Figure 118 and Figure 119.

Table 32. Results of Moraine soil tests using aluminium disc

Total water content (% by weight)	Weight loss (g)	Average Weight loss (g)	Torque (Nm)	Average Torque (Nm)
1	0,490	0,340	1,023	0,865
	0,210		0,866	
	0,320		0,706	
5	0,090	0,230	0,653	1,142
	0,290		1,112	
	0,310		1,661	
9	0,370	0,247	0,734	0,637
	0,200		0,656	
	0,170		0,521	
13	0,160	0,153	1,377	1,488
	0,090		0,859	
	0,210		2,229	
16	0,050	0,023	0,260	0,416
	0,010		0,538	
	0,010		0,449	

Table 33. Results of Moraine soil tests using steel disc

Total water content (% by weight)	Weight loss (g)	Average Weight loss (g)	Torque (Nm)	Average Torque (Nm)
1	0,320	0,143	0,939	0,880
	0,090		0,808	
	0,020		0,892	
5	0,090	0,033	0,779	0,854
	0,010		1,047	
	0,000		0,735	
9	0,070	0,067	0,463	0,558
	0,060		0,600	
	0,070		0,610	
13	0,180	0,140	2,253	1,899
	0,060		0,980	
	0,180		2,465	
16	0,020	0,013	0,520	0,593
	0,000		0,528	
	0,020		0,732	

Table 34. Results of conditioned moraine soil tests

Disc	Total water content (% by weight)	FER	FIR (%)	Weight loss (g)	Average Weight loss (g)	Torque (Nm)	Average Torque (Nm)
Aluminium	12	16	30	0,030	0,032	0,601	0,651
			30	0,030		0,657	
			30	0,050		0,644	
			30	0,020		0,702	
Steel	12	16	30	0,070	0,035	0,738	0,715
			30	0,010		0,796	
			30	0,040		0,710	
			30	0,020		0,616	

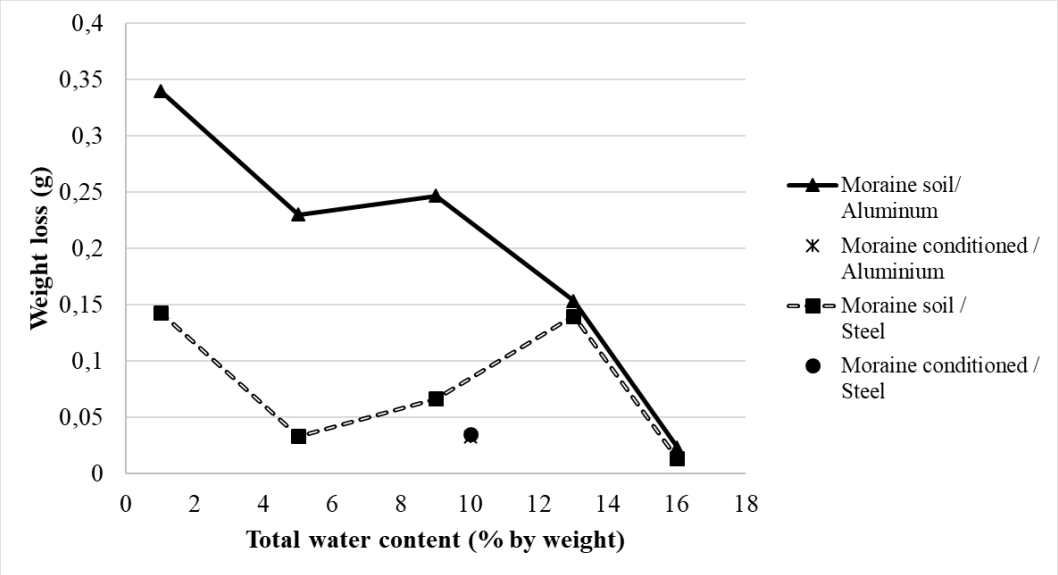

Figure 118. Weight loss average correlated to water content of moraine soil using aluminium and TBM steel discs.

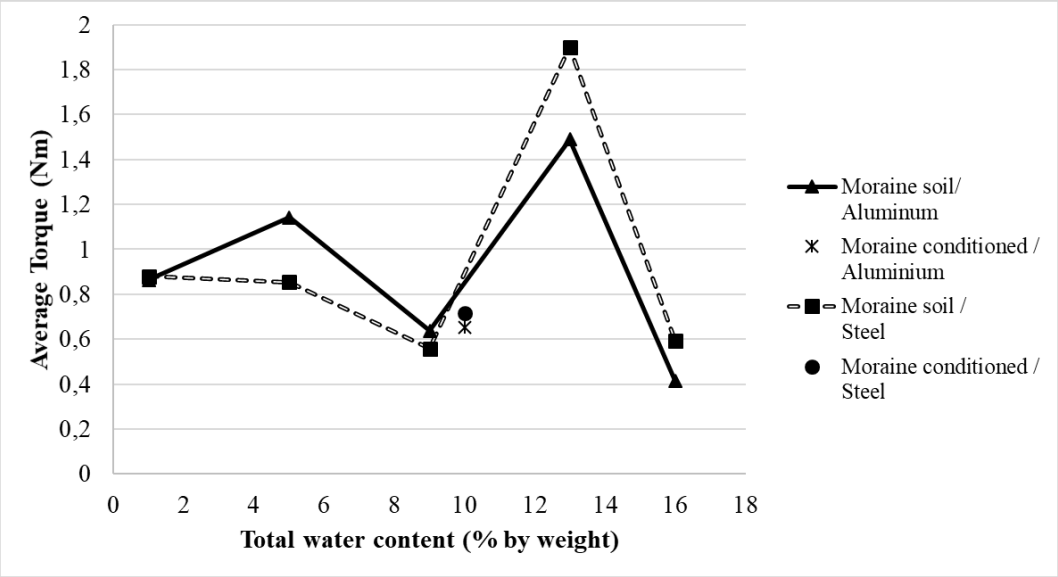

Figure 119. Average torque correlated to water content of moraine soil using aluminium and TBM steel discs.

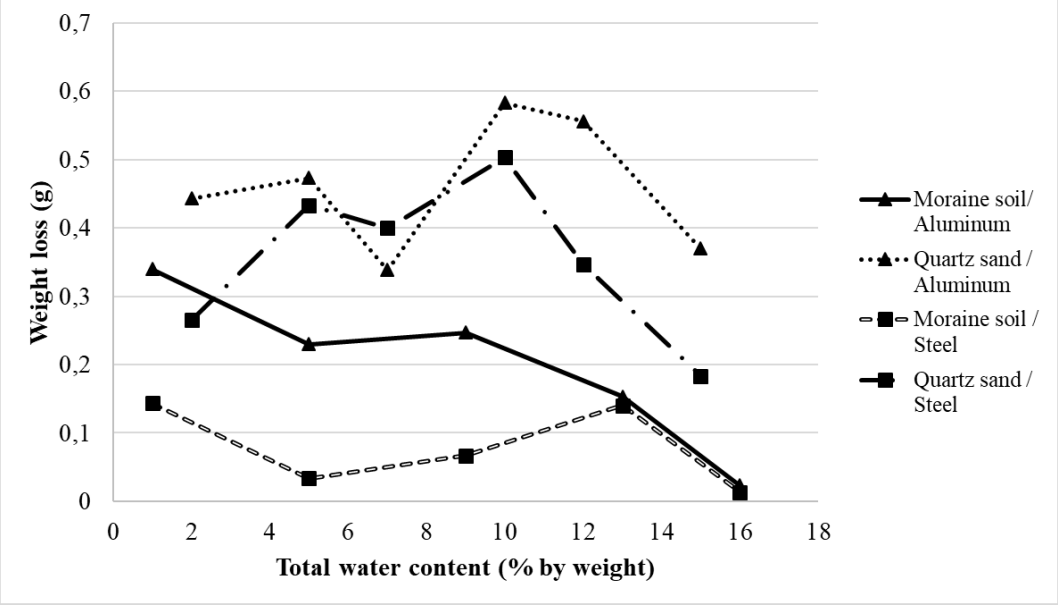

Figure 120. Weight loss average correlated to water content of moraine soil and quartz sand.

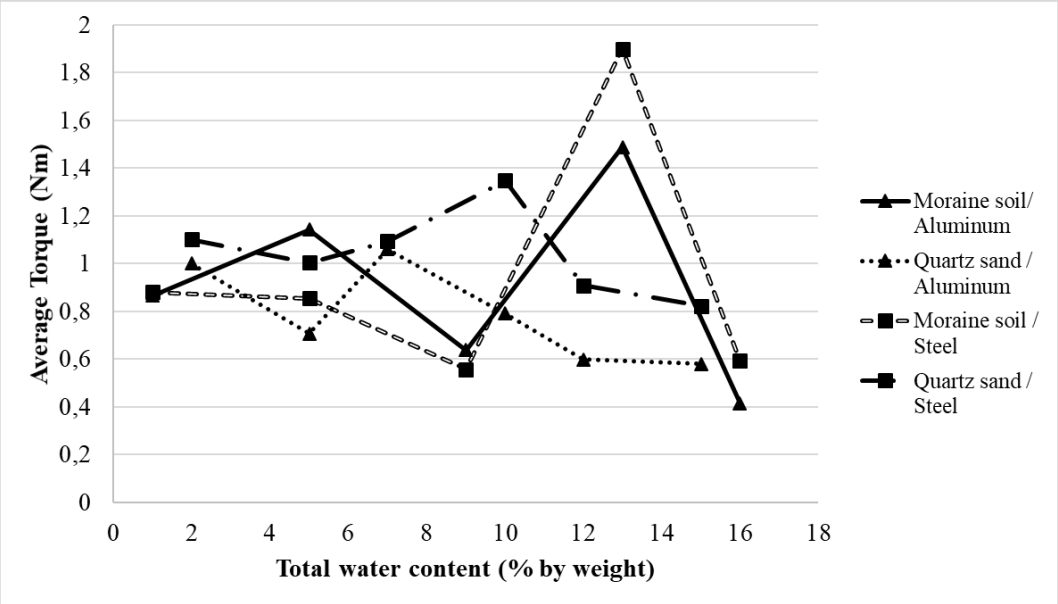

Figure 121. Average torque correlated to water content of moraine soil and quartz sand.

c) Comments

Disregarding the first water content increase, it's possible to say that moraine soil displays a "bell" behaviour for weight loss, with maximum values ranging from 9% to 13% by water content, according to the disc used. "bell" behaviour is more evident in torque testing, showing an inflexion point at 9% but the maximum value, equal to 13% of water content for both discs, was reached. Conditioned moraine soil shows lower wear and torque values for both discs studied.

Moraine soil presents lower disc wear values than quartz sand but torque values are similar.

8.1.6 Gneiss soil

a) Variability in water content of soils

The used range was between 4% and 19% (between the natural and the saturation limit). Savona soil tests were performed using the aluminium disc (Paragraph 7.2.1). The obtained results are summarized in Table 35 and illustrated in Figure 122 and Figure 123 along with quartz sand results for comparison purposes.

Table 35. Tests results in Gneiss soil using an aluminium disc.

Total water content (% by weight)	Weight loss (g)	Average Weight loss (g)	Torque (Nm)	Average Torque (Nm)
4	0,250	0,260	0,386	0,401
	0,280		0,431	
	0,250		0,387	
6	0,060	0,060	0,290	0,293
	0,050		0,285	
	0,070		0,303	
8	0,140	0,237	0,270	0,355
	0,290		0,394	
	0,280		0,402	
10	0,510	0,437	0,781	0,695
	0,370		0,614	
	0,430		0,689	
12	0,410	0,407	0,581	0,583
	0,400		0,573	
	0,410		0,594	
14	0,040	0,080	0,297	0,311
	0,080		0,314	
	0,120		0,321	
16	0,100	0,087	0,286	0,266
	0,080		0,270	
	0,080		0,241	
19	0,040	0,050	0,187	0,194
	0,060		0,231	
	0,050		0,164	

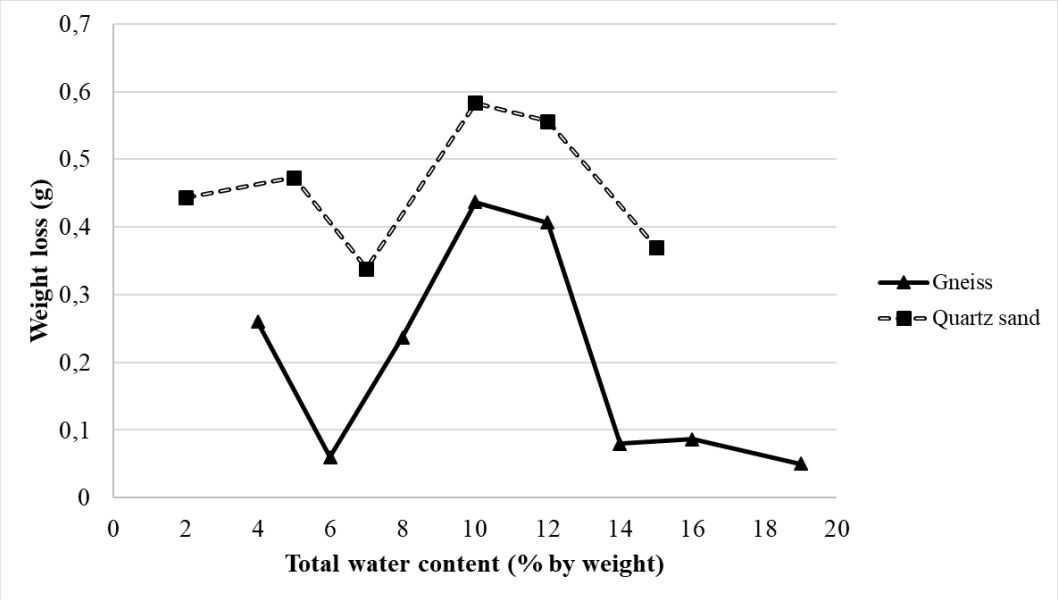

Figure 122. Weight loss average correlated to water content in Gneiss and Quartz sand.

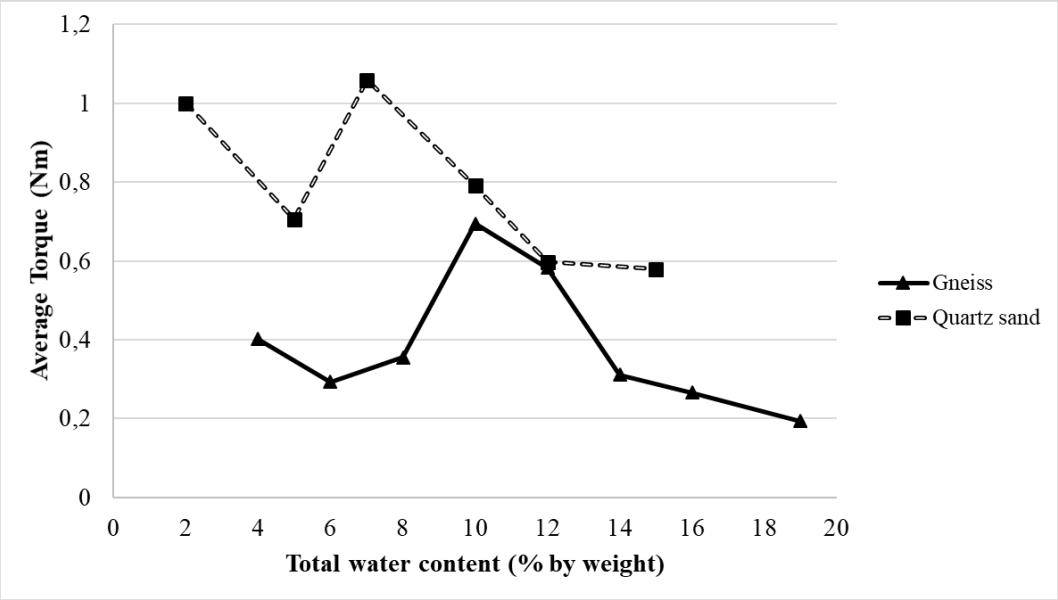

Figure 123. Average torque correlated to water content in Gneiss and Quartz sand

b) Comments

Gneiss sand has an extremely similar behaviour to the Quartz sand one. It is possible to observe the "bell" behaviour obtained with the different water contents of the soil correlated to weight loss and torque. The highest wear and torque values were obtained when total water content was 10%.

8.2 Modified Wear Disc Test

The Modified Wear Disc Test provides a disc weight loss value and a torque trend that is recorded in order to obtain an average value. For each test configuration, at least three assessments are performed and the average of them is then calculated. For this work, two reference soil samples were used as reference (Quartz sand and used in a particular mode, the CC sand). All tests were performed with the aluminium disc in order to calibrate this new methodology.

In this thesis work, a total of **103 tests** were executed using the Modified Wear Disc Test method, studying about **2575 kg** of soil. Due to the large amount of data, summary tables and charts of the results will be presented. In Figure 124, an example of the torque record for all three assessments performed in one of the test configurations is shown.

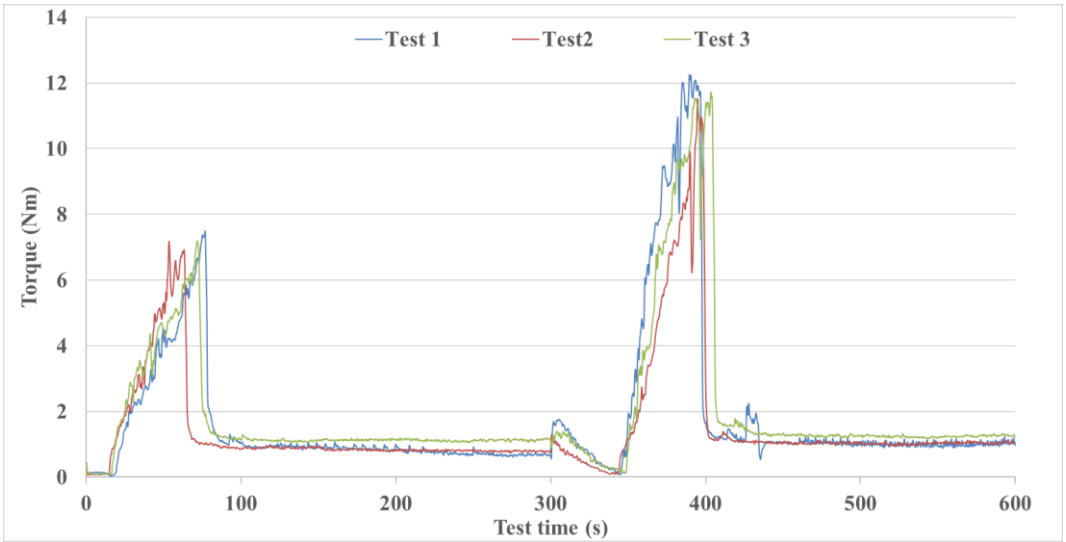

Figure 124. Example of torque record for all three assessments performed in one of the test configurations

8.2.1 Quartz sand

a) Variability in water content of soils

This assessment allows studying the influence of soil water content on discs wear. The used range was between 2% and 15% (between the natural and the saturation limit). All tests were performed using the aluminium disc (Paragraph 7.2.1). Results of weight loss and torque trends using different water contents and are summarized in Table 36 and illustrated in Figure 125 and Figure 126.

b) Use of foams

Two suitable conditioning sets were evaluated in order to compare conditioned quartz sand to this new test method. The obtained results are summarized in Table 37 and illustrated in Figure 125 and Figure 126.

c) Comments

The “bell” behaviour of disc weight loss values in relation to water content corresponds to the typical behaviour of these curves, except for the wear produced by natural water content of the soil that is very high. This sample has high abrasive capacity and there is a greater contact created between the disc and the soil with this new test method.

Table 36. Test results for different water contents of quartz sand.

Total water content (% by weight)	Weight loss (g)	Average Weight loss (g)	Torque (Nm)	Average Torque (Nm)
0	8,260	11,830	5,670	5,354
	17,130		5,152	
	10,100		5,240	
2	2,810	3,907	2,951	2,733
	5,930		2,497	
	2,980		2,753	
4	14,160	9,847	4,187	4,215
	5,960		4,787	
	9,420		3,669	
6	5,020	5,433	3,622	3,439
	6,480		3,971	
	4,800		2,724	
10	0,260	0,197	2,246	2,034
	0,180		1,842	
	0,150		2,014	
12	0,090	0,080	0,489	0,473
	0,080		0,501	
	0,070		0,430	
15	0,020	0,023	0,279	0,280
	0,040		0,314	
	0,010		0,246	

Table 37. Test results of quartz sand conditioned with foam.

Total water content (% by weight)	FER	FIR (%)	Weight loss (g)	Average Weight loss (g)	Torque (Nm)	Average Torque (Nm)
5	10	40	0,390	0,303	0,236	0,206
		40	0,270		0,197	
		40	0,250		0,184	
10	10	20	0,090	0,103	0,154	0,139
		20	0,140		0,128	
		20	0,080		0,134	

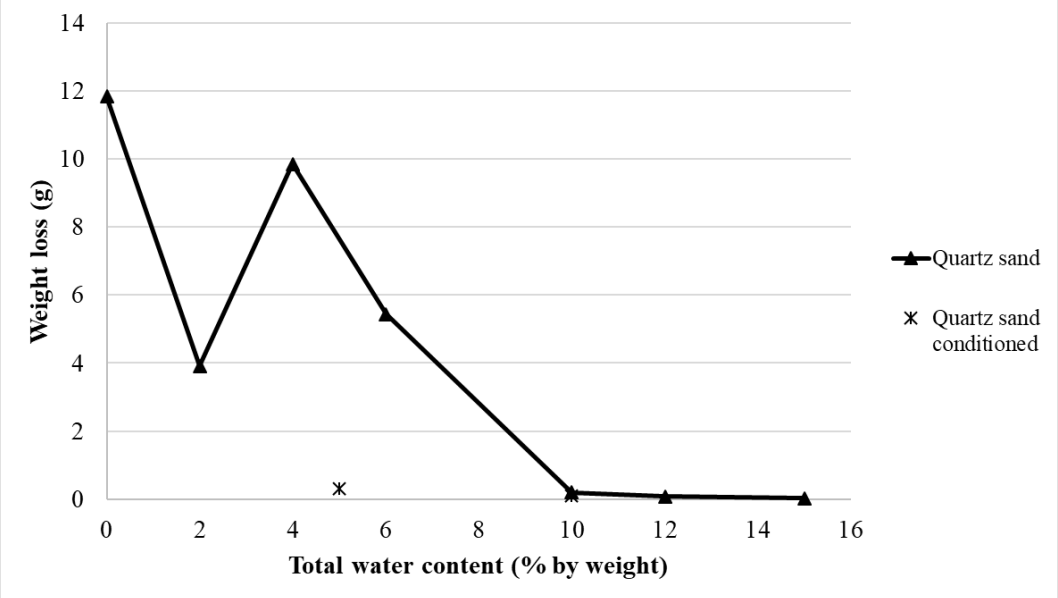

Figure 125. Weight loss average correlated to water content of quartz sand

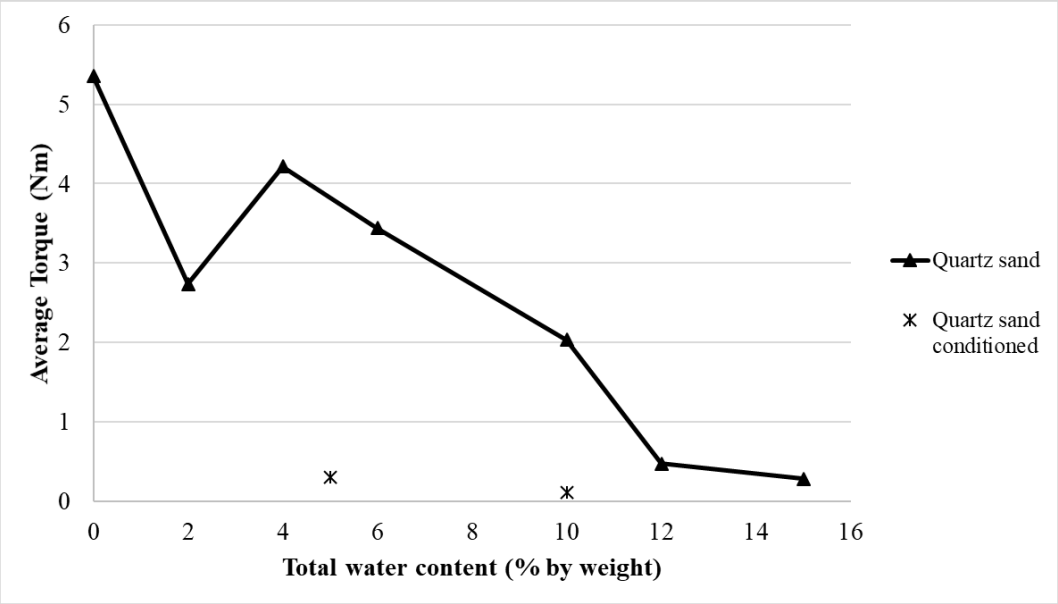

Figure 126. Average torque correlated to water content of quartz sand.

8.2.2 CC sand

a) Variability in water content of soils

The used range was between 0.8% and 18% (between the natural and the saturation limit). CC sand tests were performed using the aluminium disc (Paragraph 7.2.1). The obtained results are summarized in Table 38 and illustrated in Figure 127 and Figure 128.

In Figure 129 and Figure 130, comparisons between CC sand and quartz sand wear tests are shown.

b) Use of anti-wear polymer

The selected dose for preliminary tests with the MAPEDRILL F.R.A. 02C (herein called ease FRA02C) product in the Wear Disc Test was used as reference for this test, using 2% FRA02C by weight on added water. The study was performed with the aluminium disc (Paragraph 7.2.1). The obtained results are summarized in Table 39. In Figure 131 and Figure 132 a graphic representation of these results compared to the control curve (no polymer added) is shown.

Table 38. Test results for different water contents of CC sand.

Total water content (% by weight)	Weight loss (g)	Average Weight loss (g)	Torque (Nm)	Average Torque (Nm)
0,8	0,600	0,808	1,798	2,210
	1,070		2,666	
	0,840		2,408	
	0,720		1,968	
1,7	1,030	1,060	1,791	1,874
	1,370		2,296	
	1,140		1,978	
	0,870		1,531	
	0,890		1,774	
2,7	1,020	1,070	1,562	1,648
	1,100		1,741	
	1,090		1,639	
3,6	1,090	1,073	1,530	1,519
	1,060		1,507	
	1,070		1,519	
4,6	1,120	0,977	1,567	1,429
	0,720		1,108	
	1,080		1,534	
	0,990		1,507	
5,5	0,850	0,850	1,384	1,381
	0,860		1,438	
	0,840		1,321	
6,5	0,790	0,733	1,392	1,292
	0,670		1,196	
	0,740		1,287	
8	0,660	0,677	1,293	1,349
	0,680		1,341	
	0,690		1,411	
10	0,600	0,620	1,309	1,322
	0,530		1,172	
	0,730		1,486	
12	0,590	0,597	1,298	1,318
	0,560		1,267	
	0,640		1,389	
18	0,300	0,287	1,066	0,987
	0,270		0,916	
	0,290		0,978	

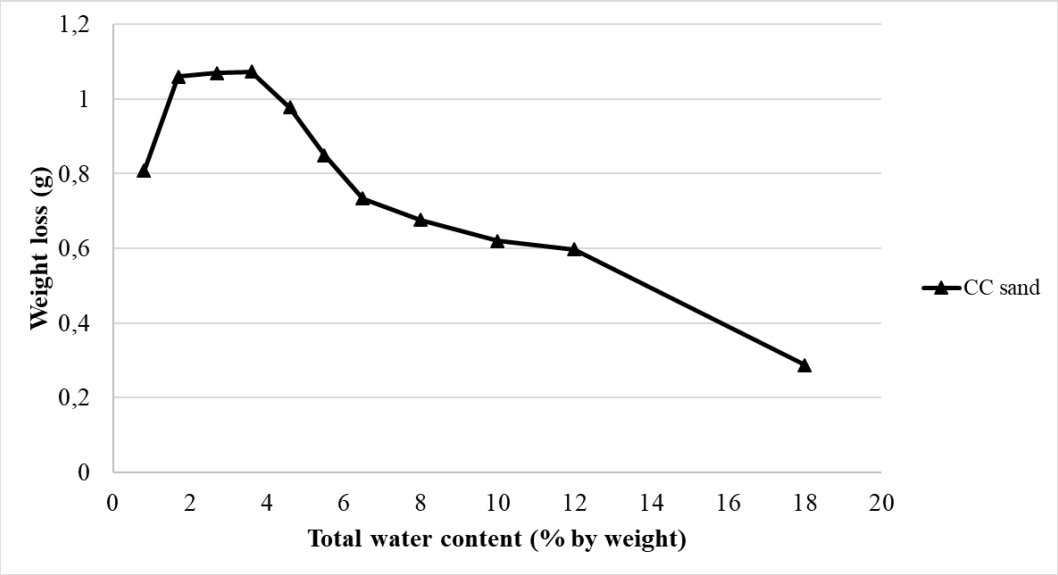

Figure 127. Weight loss average correlated to water content in CC sand.

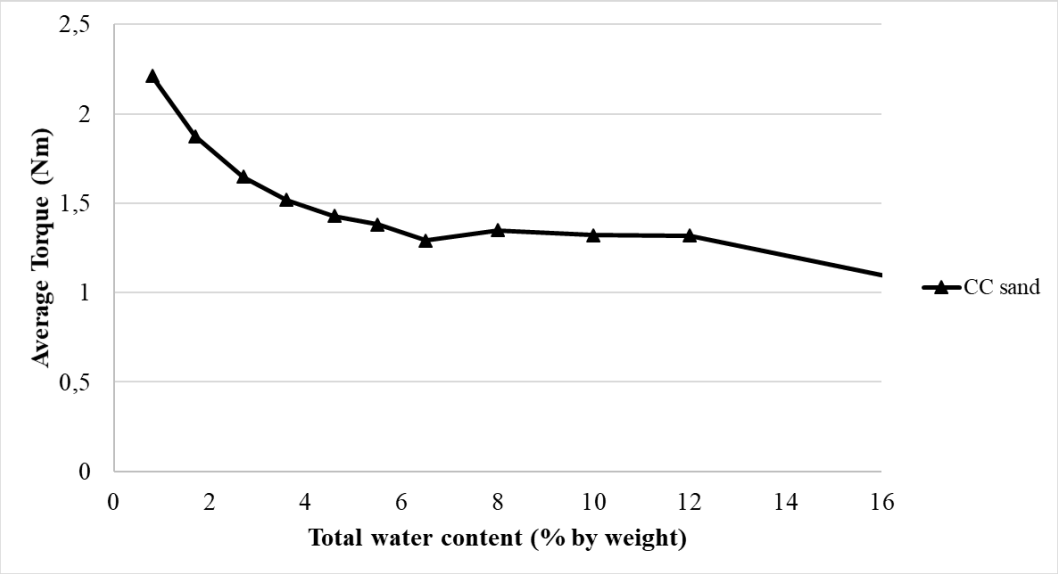

Figure 128. Average torque correlated to water content in CC sand.

.

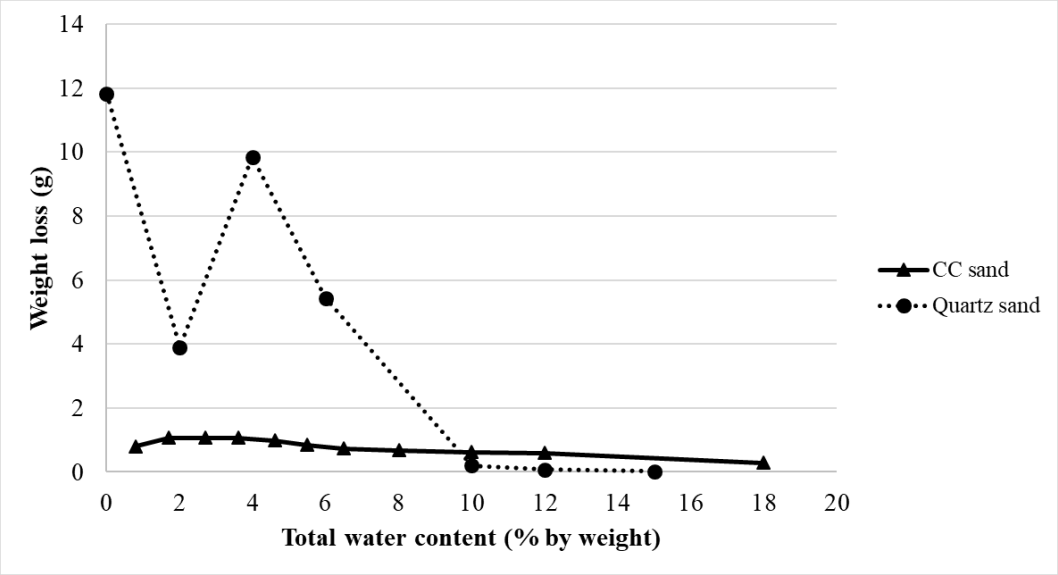

Figure 129. Weight loss average correlated to water content in CC sand and Quartz sand

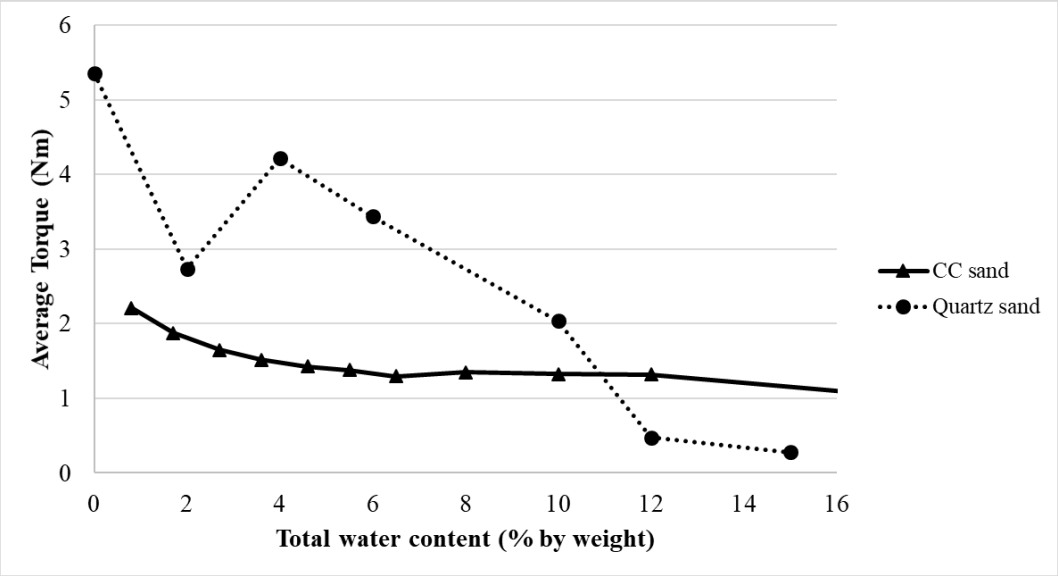

Figure 130. Average torque correlated to water content in CC sand and Quartz sand.

Table 39. Tests results obtained with 2% FRA02C concentration varying total water content.

Total water content (% by weight)	c FRA02C (% by weight on added water)	Weight loss (g)	Average Weight loss (g)	Torque (Nm)	Average Torque (Nm)
1,3	2%	0,710	0,847	1,874	2,010
		0,930		2,055	
		0,900		2,099	
1,7		1,110	0,977	2,129	1,954
		0,880		1,909	
		0,940		1,822	
2,8		0,880	0,920	1,663	1,722
		1,040		1,787	
		0,840		1,716	
3,6		0,760	0,947	1,475	1,655
		1,000		1,593	
		1,080		1,898	
4,6		0,750	0,757	1,354	1,350
		0,940		1,507	
		0,580		1,190	
5,5		1,000	0,847	1,654	1,548
		0,690		1,440	
		0,850		1,549	
6,5		0,850	0,857	1,634	1,646
		0,810		1,731	
		0,910		1,572	
8		0,660	0,753	1,490	1,529
		0,760		1,537	
		0,840		1,560	

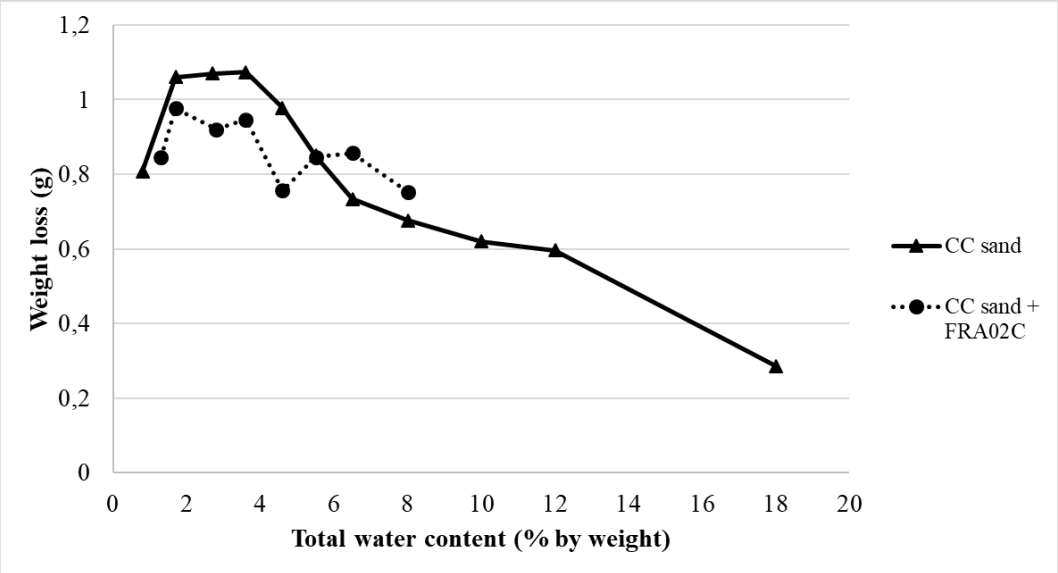

Figure 131. Weight loss average correlated to soil water content with or without adding anti-wear polymer

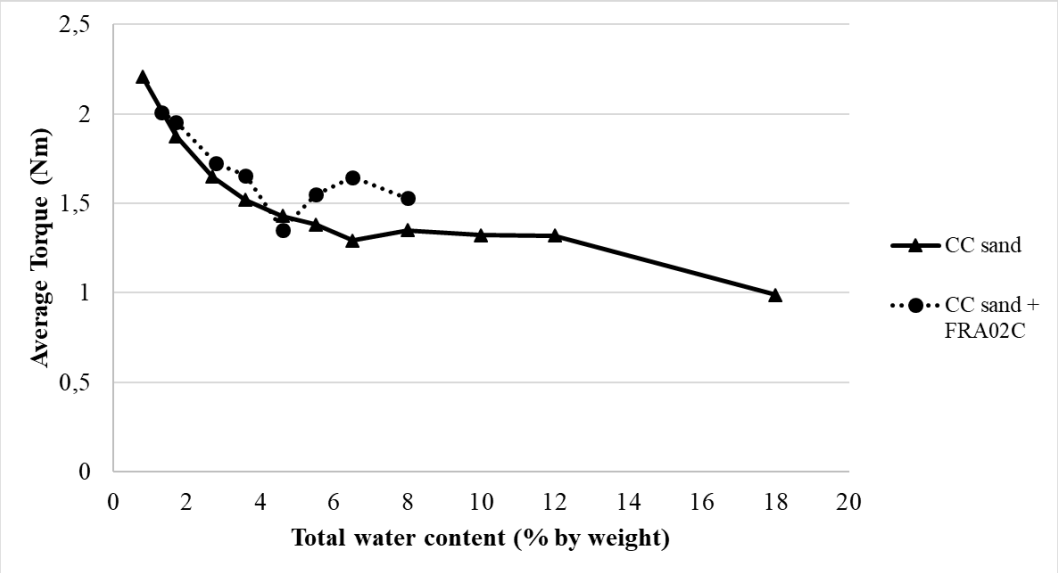

Figure 132. Average torque correlated to soil water content with or without adding anti-wear polymer.

c) Use of foams

From optimal conditioning set the amount of added foam (FIR) was modified in order to evaluate the influence of conditioning using this test methodology. The obtained results are summarized in Table 40 and illustrated in Figure 133 and Figure 134, using as reference the wear value that corresponds to the total water content of a FIR = 0%.

Table 40. Tests Results for quartz sand conditioned with foam.

Total water content (% by weight)	FER	FIR (%)	Weight loss (g)	Average Weight loss (g)	Torque (Nm)	Average Torque (Nm)
8	15	0	0,660	0,677	1,293	1,349
		0	0,680		1,341	
		0	0,690		1,411	
		10	0,200	0,177	0,603	0,597
		10	0,150		0,588	
		10	0,180		0,599	
		20	0,130	0,137	0,487	0,492
		20	0,140		0,526	
		20	0,140		0,463	
		30	0,060	0,067	0,301	0,311
		30	0,070		0,320	
		30	0,070		0,313	
		40	0,040	0,043	0,214	0,231
		40	0,050		0,292	
		40	0,040		0,187	

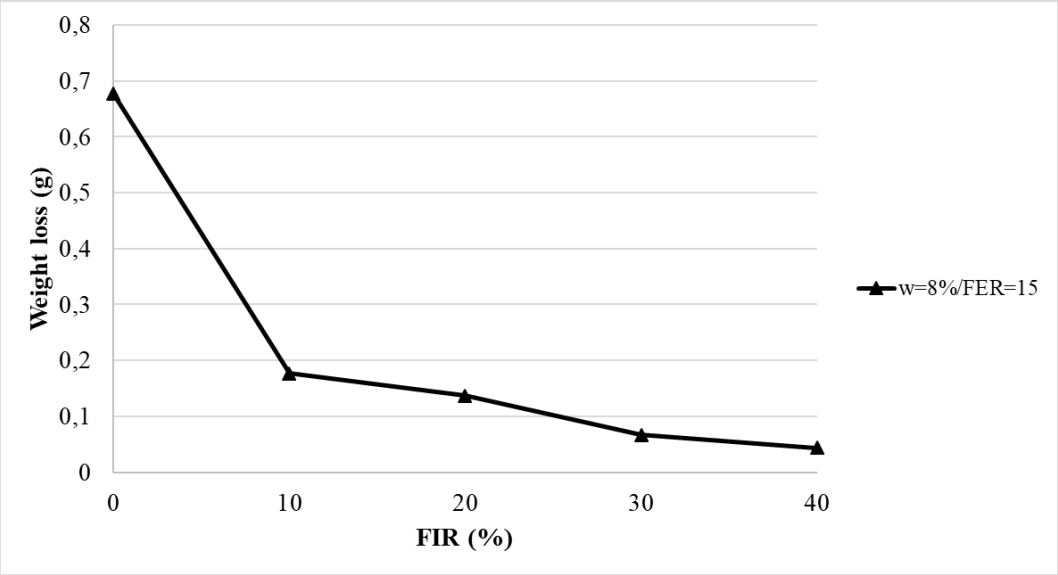

Figure 133. Weight loss average correlated to FIR

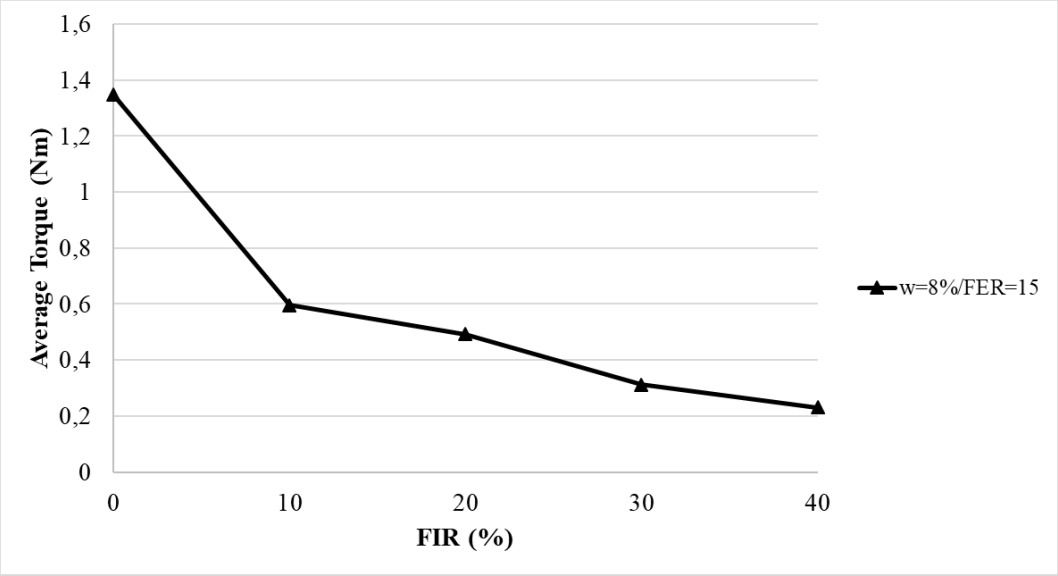

Figure 134. Average torque correlated to FIR

d) Comments

The wear curve obtained for quartz sand corresponds to the typical "bell" behaviour for these tests. However, torque curve doesn't exhibit this behavior (nor did this soil in the Wear Disc Test).

Disc wear produced by this soil is significantly less than Quartz sand one. This test methodology highlights even more the wear differences between these two soils compared to the Wear Disc Test.

The use of the anti-wear polymer was found to be useful in reducing disc weight loss, especially for lower water contents, as occurred in the Wear Disc Test.

Foams adoption in this test led to a significant reduction in disc wear and torque, maintaining this improvement while the amount of foam added was increased.

8.3 Sharp Cutter Test

Preliminary tests for the Sharp Cutter Test were performed using the Quartz sand and metals described in Paragraph 7.2.2. The purpose of this test method is to study in depth the influence of soil conditioning and the difference between hard metals and conventional steel. Conditioning used is described in Paragraph 7.1.1.

For each element (tool material) three consecutive test cycles were performed in order to measure the variation of tool profiles. Each wear test cycle (described in Paragraph 6.3.1) corresponds of a tool path length of about 1200m (considering the point of the wear tool at the maximum distance from the rotation axis, i.e. the external edge of the test device).

In this thesis work, a total of **12 tests** were executed using the Wear Disc Test method, studying about **300 kg** of soil. The test configurations used for this method are described in Table 41.

Measurements of torque were performed showing a great difference in torque levels achieved in conditioned and unconditioned soils. In Figure 135, an example of torque measurements is provided as reference; it clearly displays the difference between both soils. According to Oñate Salazar, et al. (2018), taking into account the lower position of the carrier (see Chapter 6, position 2 in Figure 54), the natural soil torque is ranging between 12 to 16 Nm while for conditioned soil torque values are ranging around 1.5 Nm. The conditioning decreases the torque of an order of magnitude.

The study of profiles and volumes of each tool was performed as described in Paragraph 6.3.2. An example of these measurements is shown in Figure 136.

Table 41. Configuration of tests performed with the Sharp Cutter Test Method

Test	Soil Condition	Type of tool wear material	Number of wear cycles	Tool path length (km)
#1	Conditioned	cemented carbide	1	1,2
#2	Conditioned	steel	1	1,2
#3	Natural	cemented carbide	1	1,2
#4	Natural	steel	1	1,2
#5	Conditioned	cemented carbide	2	2,4
#6	Conditioned	steel	2	2,4
#7	Natural	cemented carbide	2	2,4
#8	Natural	steel	2	2,4
#9	Conditioned	cemented carbide	3	3,6
#10	Conditioned	steel	3	3,6
#11	Natural	cemented carbide	3	3,6
#12	Natural	steel	3	3,6

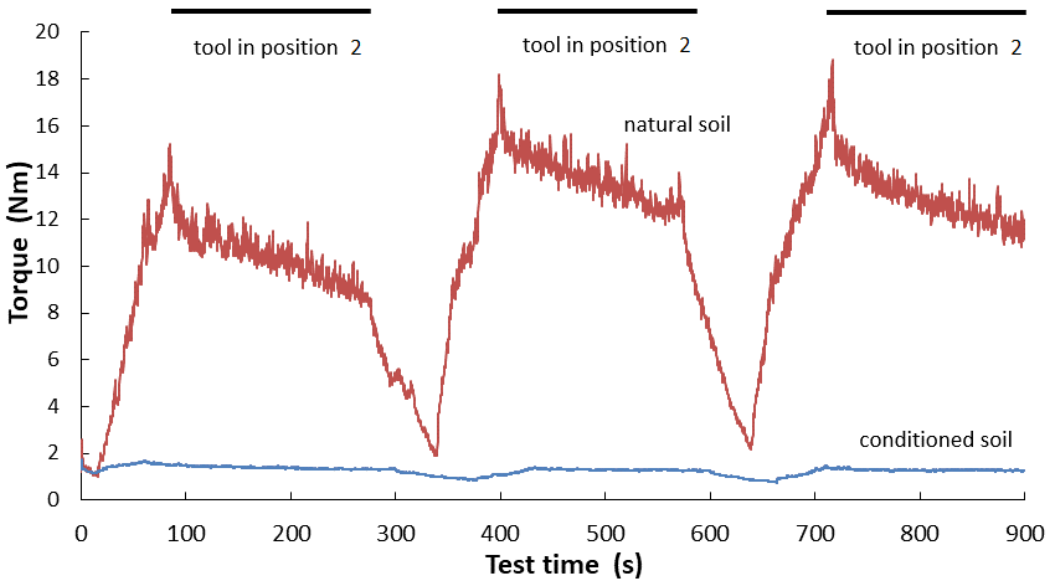

Figure 135. Reference comparison between the torques measured for natural and conditioned soils.

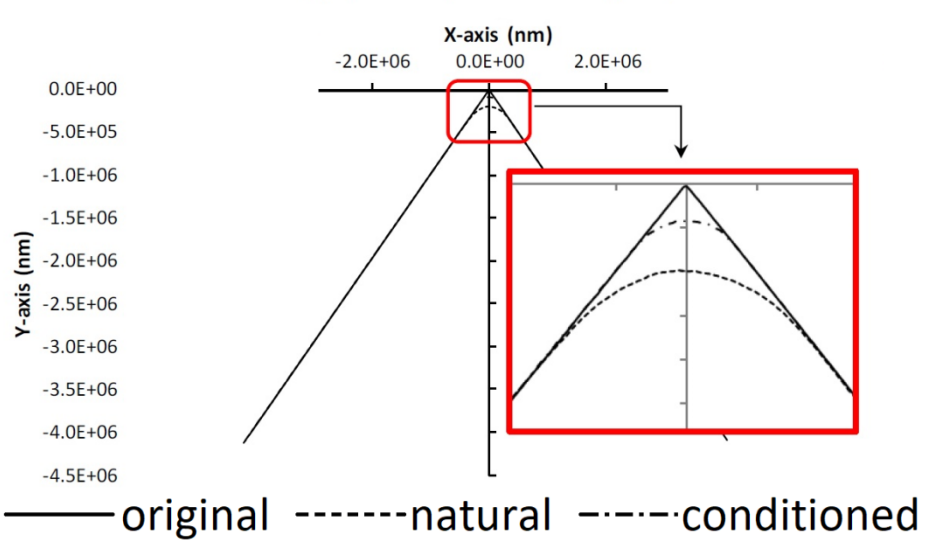

Figure 136. Example of measurement performed on the wear located in the blade of the tool for the cemented carbide tool (Oñate Salazar, et al., 2018).

a) Radius of curvature:

According to tools profiles obtained after each cycle, the values corresponding to radius of curvature were measured in the predetermined sections of the cemented carbides and conventional steel. Final values (after three cycles) are summarized in Table 42. In Figure 137 and Figure 138, radiuses of curvature for all tools studied in unconditioned and conditioned soils, respectively, are shown. In Figure 139 and Figure 140 the same previous curves are presented but excluding the results for conventional steel in order to better appreciate cemented carbides curves.

In Figure 141 a comparison between the cemented carbide with the highest curvature radius (M5) value and conventional steel is shown. This comparison is made using natural and conditioned soil values.

Table 42. Curvature Radius measured after three wear cycles.

Tool	Distance from mounting area (mm)	Curvature radius (mm)		Tool	Distance from mounting area (mm)	Curvature radius (mm)	
		Natural soil	Conditined soil			Natural soil	Conditined soil
M1	0	0,1142	0,0523	M6	0	0,1245	0,0652
	5	0,1395	0,0678		5	0,1668	0,0830
	10	0,1593	0,0753		10	0,2075	0,0998
	15	0,1740	0,0758		15	0,2239	0,1064
	20	0,1993	0,0843		20	0,2641	0,1164
	25	0,2118	0,0971		25	0,3004	0,1382
	29	0,2554	0,1312		29	0,3978	0,1940
M4	0	0,2056	0,0653	K40	0	0,1666	0,0517
	5	0,2445	0,0769		5	0,1989	0,0603
	10	0,2879	0,0905		10	0,2305	0,0656
	15	0,3202	0,0936		15	0,2666	0,0706
	20	0,3394	0,1111		20	0,2800	0,0831
	25	0,3856	0,1714		25	0,3184	0,1361
	29	0,4775	0,2428		29	0,4283	0,2015
M5	0	0,2229	0,0974	N10	0	0,1252	0,0501
	5	0,2787	0,1265		5	0,1648	0,0620
	10	0,3280	0,1497		10	0,1887	0,0730
	15	0,3812	0,1695		15	0,2048	0,0826
	20	0,4347	0,1887		20	0,2389	0,0918
	25	0,4889	0,2237		25	0,2644	0,1019
	29	0,5855	0,3007		29	0,3253	0,1310
Steel	0	0,8579	0,4769				
	5	0,9105	0,5494				
	10	0,9947	0,5338				
	15	1,1038	0,5371				
	20	1,2104	0,6100				
	25	1,3722	0,7932				
	29	2,0949	1,2316				

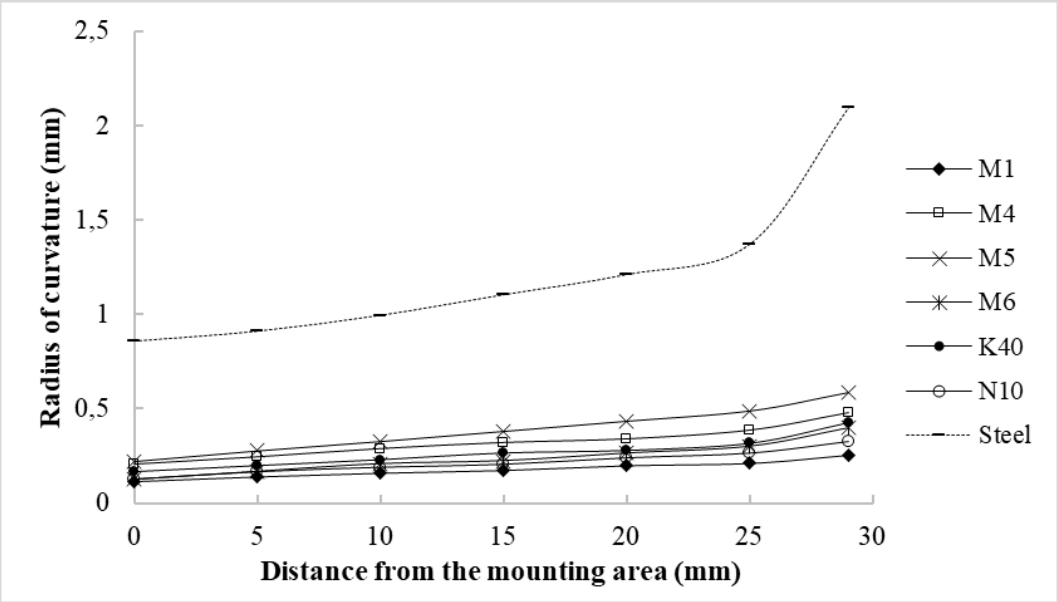

Figure 137. Curvature radius measured after three wear cycles in natural soil.

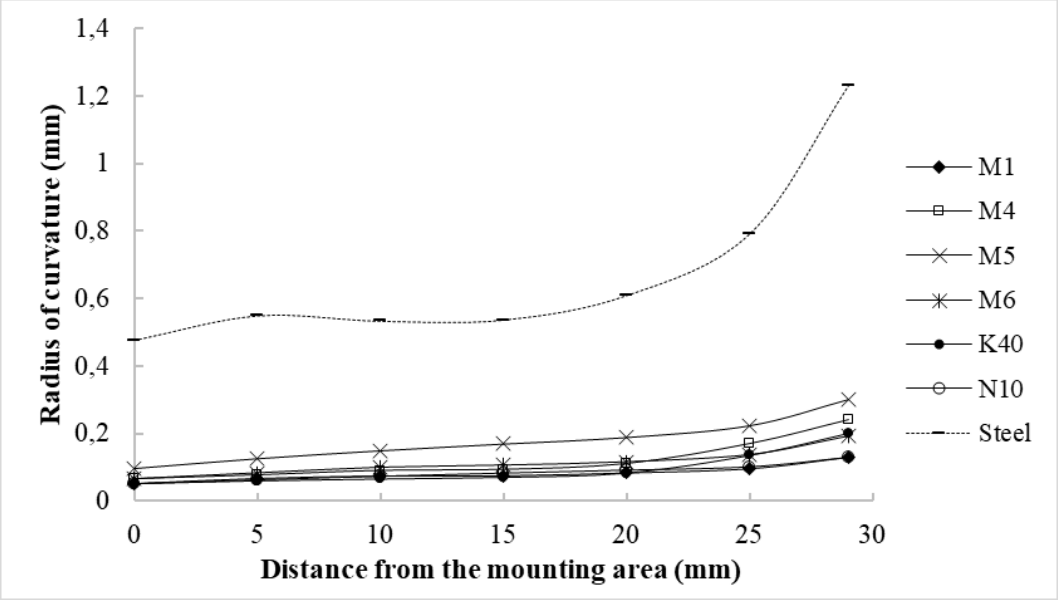

Figure 138. Curvature radius measured after three wear cycles in conditioned soil.

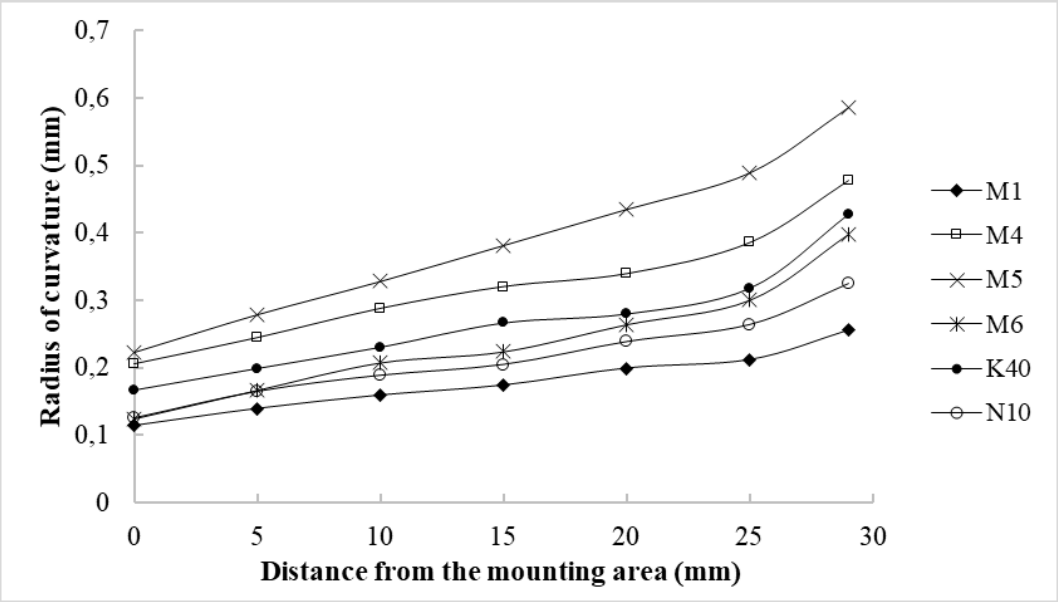

Figure 139. Curvature radius measured after three wear cycles in natural soil for cemented carbides.

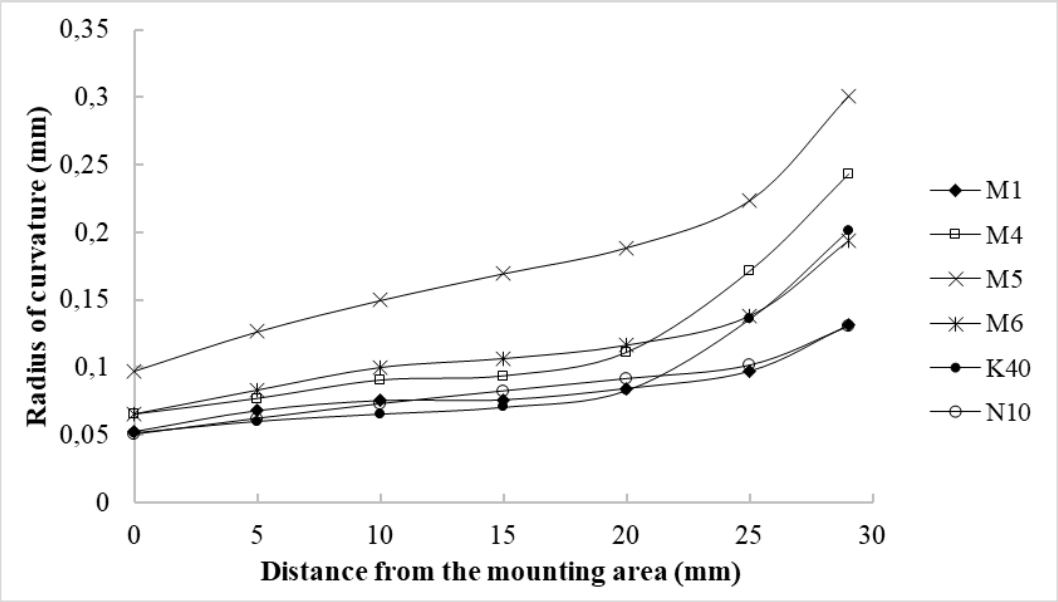

Figure 140. Curvature radius measured after three wear cycles in conditioned soil for cemented carbides.

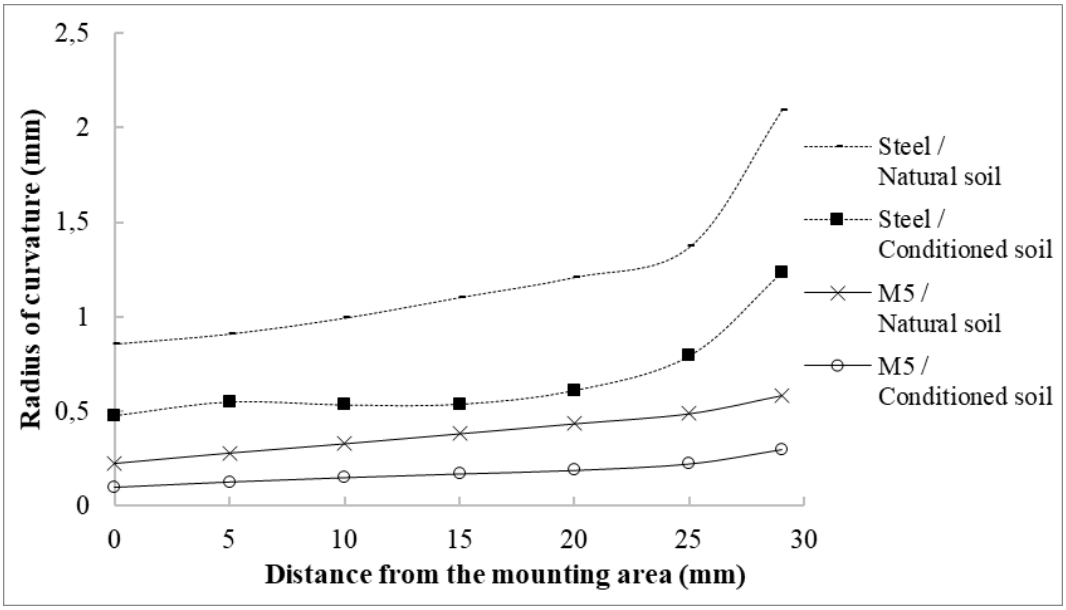

Figure 141. Curvature radius measured after three wear cycles in natural and conditioned soil, for M5 and conventional steel tools.

b) Area and Volume Loss

Area loss of all studied tools was calculated using the same test principle of curvature radius for tool sections. Final values corresponding to area loss after three cycles are summarized in Table 43. In Figure 142 and Figure 143, area loss of cemented carbide tools in natural and conditioned soil, respectively, is shown. In Figure 144 and Figure 145, the results for conventional steel are presented.

In Figure 146 and Figure 147, a comparison between the tests carried out in natural and conditioned soil for the cemented carbide that have the highest area loss (M5) and conventional steel, respectively. The cemented carbide and conventional steel values were not plotted together since there is a scale gap and the results are not correctly appreciated.

Considering the area of each section and the separation between them, volumes before and after the tests were calculated. The tool volume loss in each cycle was obtained. The values of the volume loss will be presented subsequently in Table 44.

These obtained results match with the images of the tool cutting edge observed by the video-microscope (Figure 148) that show changes in geometry after three wear cycles. It is possible to observe that the maximum wear occurs near the tool edge where three wear surfaces are present. In hard metals limited signs of lateral faces wear are detected, but rounding of the edge is observed especially for the tools studied in natural soil. A comparison between M5 cemented carbide (having the highest wear values in all tests) and conventional steel photographs was performed. This comparison is presented in Figure 149. It's possible to note that conventional steel tools show a stronger wear both on the

edge and on the lateral faces where the formation of pitting and of important wear zones can be detected.

Based on the results obtained from worn areas and considering the worn profile at maxima, the percentages of reduction in area loss with the use of conditioned soil compared to natural soil were calculated (Table 45). Similarly, the percentages of reduction in volume loss due to the use of conditioned soil compared to natural soil were computed (Table 46).

In both cases it is observed that the use of foam improves wear reduction of cemented carbide tools by 70% to 85% and conventional steel by approximately 50%.

Table 43. Area loss results after three wear cycles.

Tool	Distance from mounting area (mm)	Area Loss (mm^2)		Tool	Distance from mounting area (mm)	Area Loss (mm^2)	
		Natural soil	Conditined soil			Natural soil	Conditined soil
M1	0	0,0036	0,0005	**M6**	0	0,0051	0,0019
	5	0,0060	0,0011		5	0,0059	0,0040
	10	0,0062	0,0012		10	0,0100	0,0046
	15	0,0094	0,0011		15	0,0107	0,0052
	20	0,0097	0,0019		20	0,0159	0,0037
	25	0,0118	0,0020		25	0,0204	0,0049
	29	0,0162	0,0038		29	0,0382	0,0095
M4	0	0,0112	0,0019	**K40**	0	0,0064	0,0007
	5	0,0178	0,0026		5	0,0092	0,0010
	10	0,0182	0,0029		10	0,0119	0,0020
	15	0,0226	0,0028		15	0,0160	0,0013
	20	0,0303	0,0047		20	0,0185	0,0022
	25	0,0401	0,0072		25	0,0248	0,0048
	29	0,0530	0,0154		29	0,0428	0,0084
M5	0	0,0106	0,0018	**N10**	0	0,0051	0,0007
	5	0,0176	0,0050		5	0,0063	0,0009
	10	0,0262	0,0061		10	0,0087	0,0013
	15	0,0317	0,0060		15	0,0114	0,0019
	20	0,0433	0,0114		20	0,0145	0,0018
	25	0,0540	0,0125		25	0,0169	0,0028
	29	0,0800	0,0245		29	0,0223	0,0048
Steel	0	1,5220	1,2505				
	5	2,4890	1,9296				
	10	4,4185	1,3984				
	15	4,4365	1,5222				
	20	5,5871	1,9599				
	25	6,2058	2,3846				
	29	12,7253	6,9533				

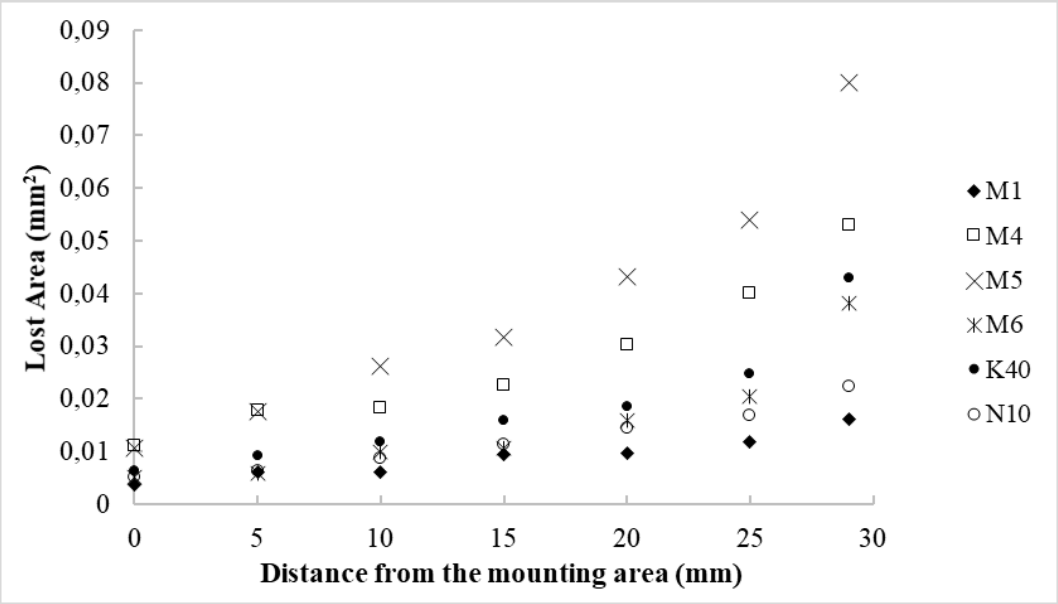

Figure 142. Area losses according to location of the measurement linescan for the natural soil using the cemented carbides tools after three wear cycles.

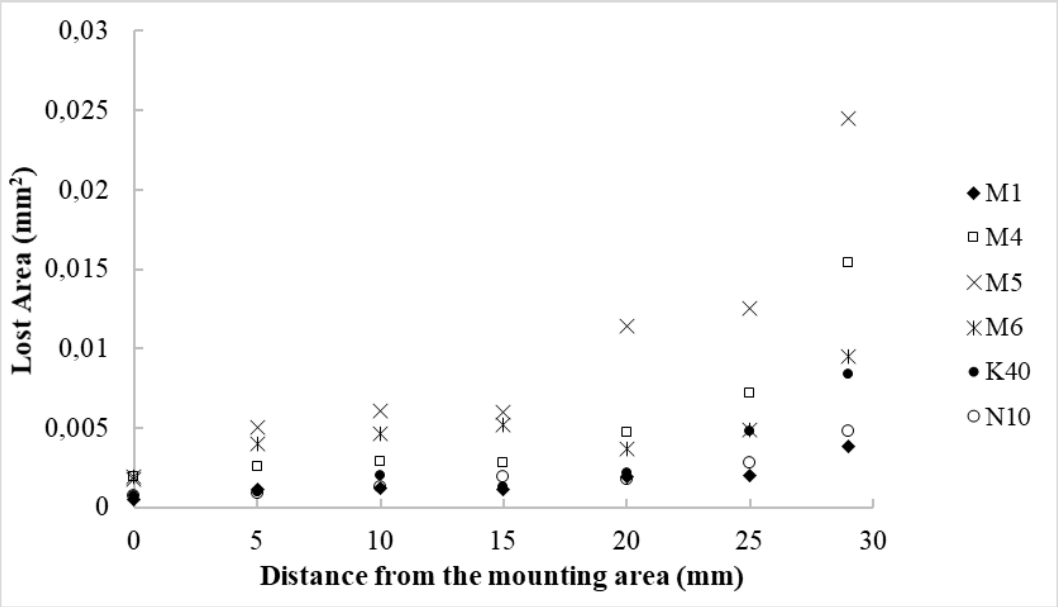

Figure 143. Area losses according to location of the measurement linescan for the conditioned soil using the cemented carbides tools after three wear cycles.

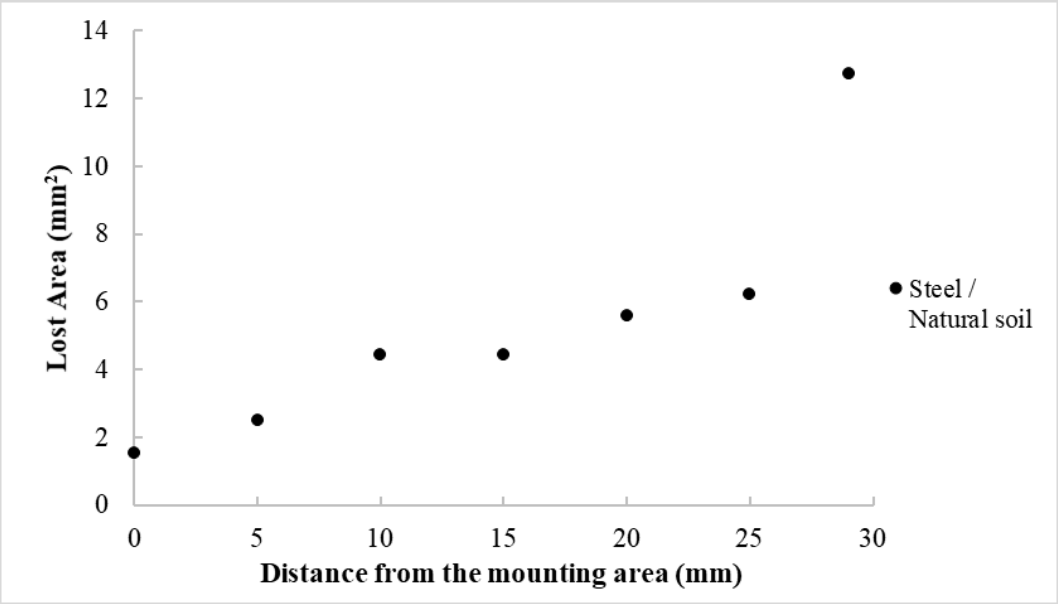

Figure 144. Area losses according to location of the measurement linescan for the natural soil using the conventional steel tools after three wear cycles.

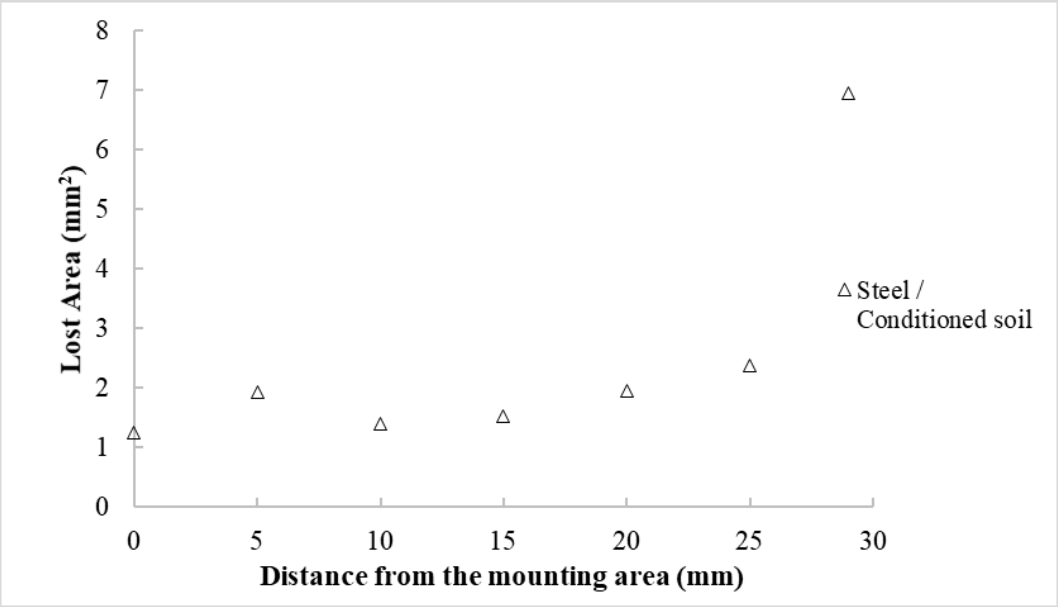

Figure 145. Area losses according to location of the measurement linescan for the conditioned soil using the conventional steel tools after three wear cycles.

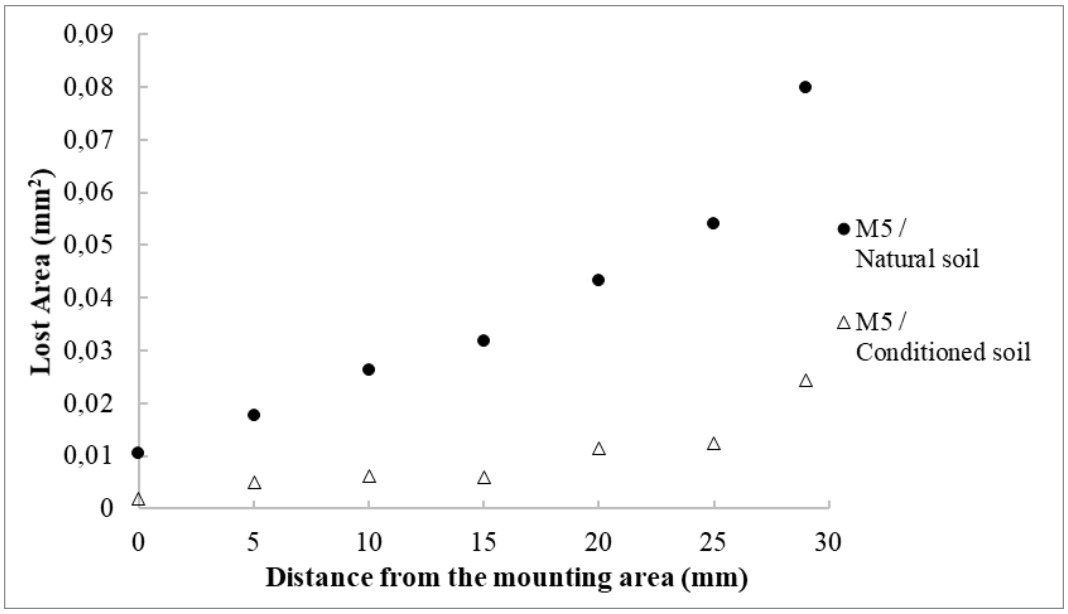

Figure 146. Area losses according to location of the measurement linescan for the natural and conditioned soil using the M5 cemented carbide tool after three wear cycles.

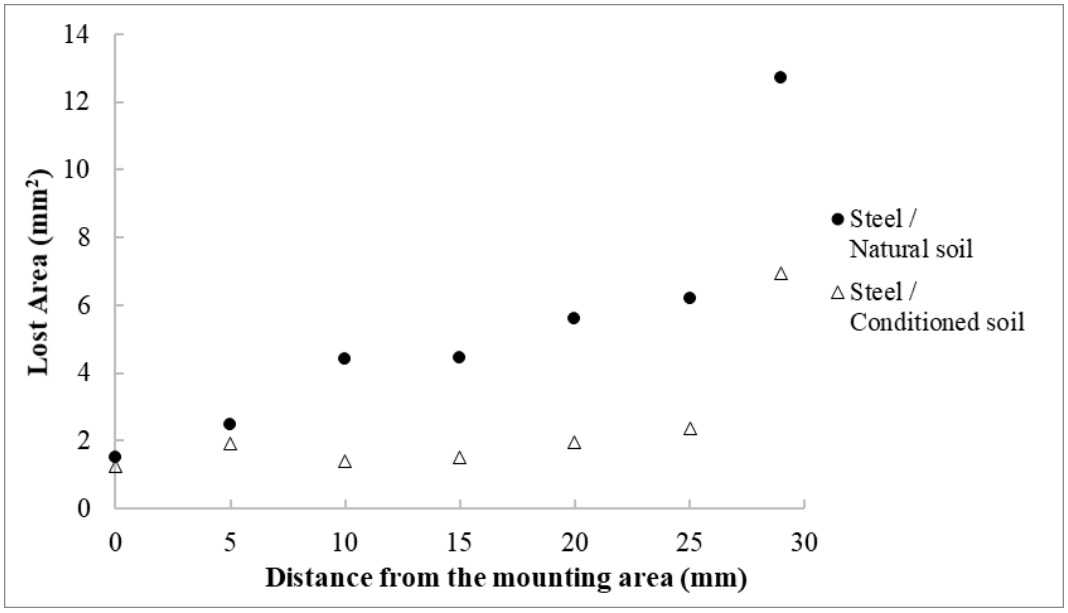

Figure 147. Area losses according to location of the measurement linescan for the natural and conditioned soil using the M5 cemented carbide tool after three wear cycles.

Table 44. Volume losses after each wear cycle.

Tool	Tool path length (km)	Soil conditiom	ΔV (mm^3)
M1	1,2	Natural	0,17
	2,4		0,18
	3,6		0,25
	1,2	Conditioned	0,03
	2,4		0,03
	3,6		0,04
M6	1,2	Natural	0,18
	2,4		0,26
	3,6		0,39
	1,2	Conditioned	0,04
	2,4		0,08
	3,6		0,13
M4	1,2	Natural	0,33
	2,4		0,52
	3,6		0,76
	1,2	Conditioned	0,04
	2,4		0,08
	3,6		0,13
K40	1,2	Natural	0,29
	2,4		0,33
	3,6		0,49
	1,2	Conditioned	0,03
	2,4		0,04
	3,6		0,07
M5	1,2	Natural	0,46
	2,4		0,74
	3,6		1,02
	1,2	Conditioned	0,09
	2,4		0,19
	3,6		0,25
N10	1,2	Natural	0,16
	2,4		0,22
	3,6		0,34
	1,2	Conditioned	0,03
	2,4		0,04
	3,6		0,05
Steel	1,2	Natural	29,05
	2,4		64,40
	3,6		148,81
	1,2	Conditioned	16,45
	2,4		29,71
	3,6		66,48

Table 45. Reduction of Area Loss by soil conditioning

Tool	Distance from mounting area (mm)	Area Loss (mm^2)		Reduction of Area Loss (%)
		Natural soil	Conditioned soil	
M1	29	0,0162	0,0038	76,54
M6	29	0,0382	0,0095	75,13
M4	29	0,0530	0,0154	70,94
K40	29	0,0428	0,0084	80,39
M5	29	0,0800	0,0245	69,38
N10	29	0,0223	0,0048	78,48
Steel	29	12,7253	6,9533	45,36

Table 46. Reduction of Volume Loss by soil conditioning

Tool	ΔV (mm^3)		Reduction of Volume Loss (%)
	Natural soil	Conditoined soil	
M1	0,2510	0,0444	82,31
M6	0,3935	0,1333	66,12
M4	0,7590	0,1330	82,48
K40	0,4913	0,0727	85,20
M5	1,0235	0,2523	75,35
N10	0,3379	0,0535	84,17
Steel	148,8100	66,4800	55,33

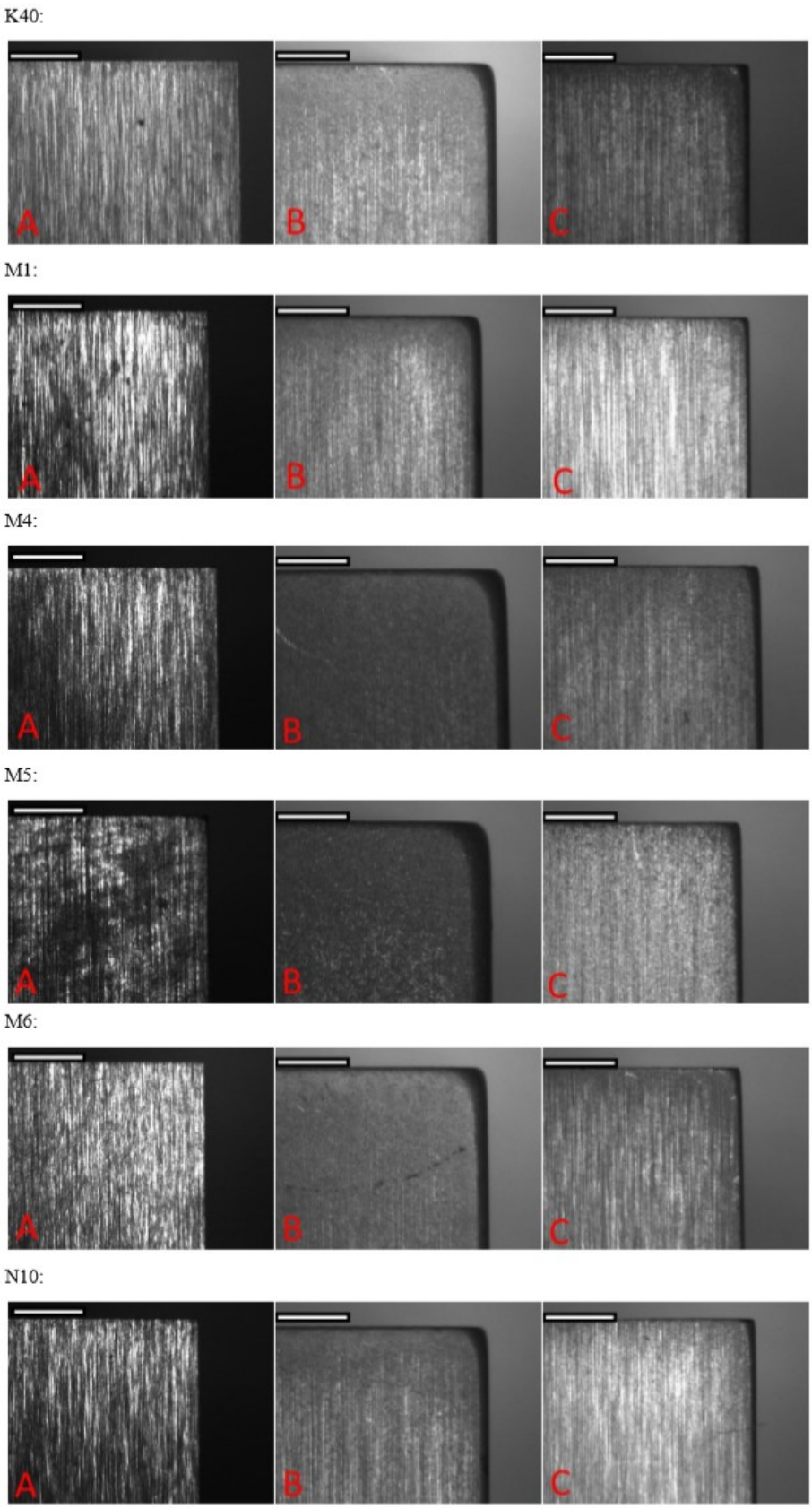

Figure 148. Tools cutting edge scanned by video-microscope Leica VZ85R. A: Original tool, B: tool wore in natural soil, C: tool wore in conditioned soil. Magnification: 200×. Scale bar: 1 mm.

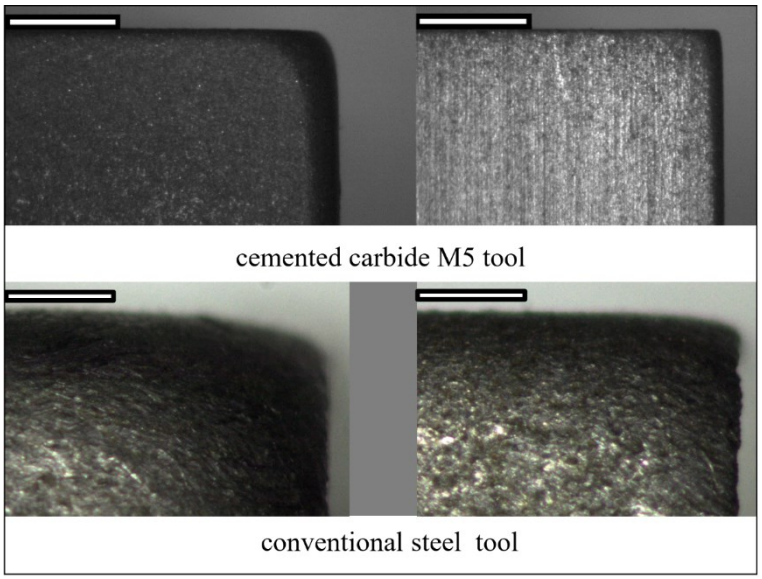

Figure 149. Comparison between the cemented carbide and conventional steel tools. Tools cutting edge scanned by video-microscope Leica VZ85R. Natural soil (left) and conditioned soil (right). Magnification: 200×. Scale bar: 1 mm (Oñate Salazar, et al., 2018).

c) Proposed Indexes

To quantify the effect of tools wear three indexes are proposed:

- ΔV index (expressed in mm^3)

The volume lost after 3 wear cycles (ΔV) expressed by the difference between the shape of the worn tool and the original one. It is feasible to use this value as index since it takes into account the global wear that can occur both on the sharp angle and along the tool faces and the tool blade. These values were already presented in Table 44.

- I_{cr} index (expressed in mm/km)

The curvature radius index (I_{cr}) is expressed as the ratio of the mounting area of the wear tool at the tool edge divided by the distance carried by the tool (after 3 wear cycles). The obtained results for this index are displayed in Table 47. As expected, conventional steel index values are higher than cemented carbide ones, which present congruent results among them. It is also observed that the index decreases in the conditioned soil for all tools tested.

Table 47. The curvature radius index (I_{cr})

Tool	Tool path length (km)	Soil conditiom	Curvature radius (mm)	I_{cr} (mm/km)
M1	3,6	Natural	0,26	0,07
	3,6	Conditioned	0,13	0,04
M6	3,6	Natural	0,40	0,11
	3,6	Conditioned	0,19	0,05
M4	3,6	Natural	0,48	0,13
	3,6	Conditioned	0,24	0,07
K40	3,6	Natural	0,43	0,12
	3,6	Conditioned	0,20	0,06
M5	3,6	Natural	0,59	0,16
	3,6	Conditioned	0,30	0,08
N10	3,6	Natural	0,33	0,09
	3,6	Conditioned	0,13	0,04
Steel	3,6	Natural	2,09	0,58
	3,6	Conditioned	1,23	0,34

- I_{WeC} index (expressed in (mm^3/mm^3)/km)

The wear index (I_{WeC}) is defined as the slope of the line interpolating the specific volume loss ($\Delta V/V_{Original}$) after each wear cycle. This index was calculated after the three fixed cycles in all performed tests.

Calculations of specific volume loss are summarized in Table 48 and graphic representations of the slope that best adapts to the values obtained after each wear cycle for all tools tested are shown in Figure 150. The I_{WeC} indexes are shown in Table 49. In wear index calculations it can be observed that numerical values are congruent to the wear analysis previously performed. Higher values of wear index correspond to worn tools tested in natural soils and indexes obtained in conventional steel are significantly higher that cemented carbides ones.

Table 48. Specific volume loss ($\Delta V/V_0 * 10^{-4}$)

Tool	Tool path length (km)	Soil condition	ΔV (mm^3)	$\Delta V/V_0 * 10^{-4}$ (-)
M1	1,2	Natural	0,17	0,50
	2,4		0,18	0,53
	3,6		0,25	0,86
	1,2	Conditioned	0,03	0,08
	2,4		0,03	0,08
	3,6		0,04	0,15
M6	1,2	Natural	0,18	0,66
	2,4		0,26	0,95
	3,6		0,39	1,35
	1,2	Conditioned	0,04	0,12
	2,4		0,08	0,21
	3,6		0,13	0,46
M4	1,2	Natural	0,33	1,11
	2,4		0,52	1,73
	3,6		0,76	2,60
	1,2	Conditioned	0,04	0,11
	2,4		0,08	0,20
	3,6		0,13	0,46
K40	1,2	Natural	0,29	1,03
	2,4		0,33	1,17
	3,6		0,49	1,69
	1,2	Conditioned	0,03	0,10
	2,4		0,04	0,15
	3,6		0,07	0,25
M5	1,2	Natural	0,46	1,79
	2,4		0,74	2,91
	3,6		1,02	3,51
	1,2	Conditioned	0,09	0,27
	2,4		0,19	0,55
	3,6		0,25	0,87
N10	1,2	Natural	0,16	0,55
	2,4		0,22	0,74
	3,6		0,34	1,16
	1,2	Conditioned	0,03	0,09
	2,4		0,04	0,12
	3,6		0,05	0,18
Steel	1,2	Natural	29,05	83
	2,4		64,40	184
	3,6		148,81	425
	1,2	Conditioned	16,45	47
	2,4		29,71	85
	3,6		66,48	189

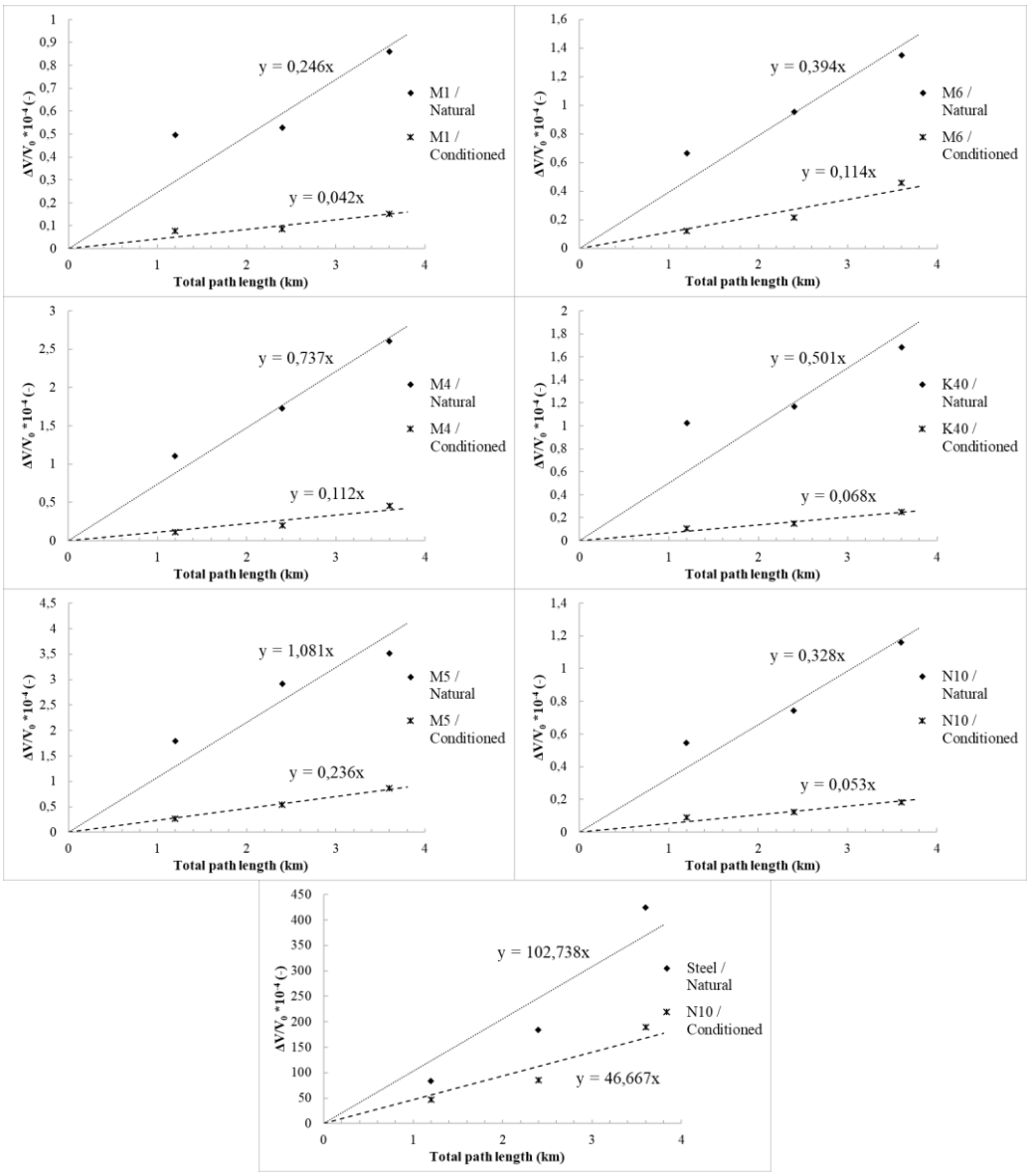

Figure 150. Specific volume loss correlated to total path length of the wear tool for all tools tested.

Table 49. IWeC Indexes

Tool	Tool path length (km)	Soil condition	Curvature radius (mm)	ΔV (mm^3)	$\Delta V/V_0*10^{-4}$ (-)	I_{WeC}
M1	3,6	Natural	0,26	0,25	0,86	0,246
	3,6	Conditioned	0,13	0,04	0,15	0,042
M6	3,6	Natural	0,40	0,39	1,35	0,394
	3,6	Conditioned	0,19	0,13	0,46	0,114
M4	3,6	Natural	0,48	0,76	2,60	0,737
	3,6	Conditioned	0,24	0,13	0,46	0,112
K40	3,6	Natural	0,43	0,49	1,69	0,501
	3,6	Conditioned	0,20	0,07	0,25	0,068
M5	3,6	Natural	0,59	1,02	3,51	1,081
	3,6	Conditioned	0,30	0,25	0,87	0,236
N10	3,6	Natural	0,33	0,34	1,16	0,328
	3,6	Conditioned	0,13	0,05	0,18	0,053
Steel	3,6	Natural	2,09	148,81	425	102,738
	3,6	Conditioned	1,23	66,48	189	46,667

d) Comments

This test methodology demonstrated to be extremely useful studying the influence of soil conditioning and use of hard metals compared to conventional steels. It was observed in detail the difference between the wear caused by soil conditioned with foams and unconditioned regarding the shape and volume loss of the tool (cemented carbides and conventional steels).

By performing this test procedure it was possible to establish 3 predictive indexes that can be used to evaluate wear phenomenon and compare results under different conditions.

8.4 Pressurized Rotating Mixer

Preliminary wear tests with the Pressurized Rotating Mixer were performed using the two reference soils (Quartz sand and CC sand) and the aluminium disc (Paragraph 7.2.1). The purpose of this test method is to study the influence of confining pressures on the wear process by better simulating the wear mechanisms exhibited by the discs in the TBM.

In this thesis work, a total of **70 tests** were executed using the Pressurized Rotating Mixer method, studying about **16100 kg** of soil.

For each test, agitator and wear rotor torque values are recorded. In Figure 151 and Figure 152, examples of the charts obtained with the mentioned torque values in unconditioned and conditioned soil, respectively, are shown.

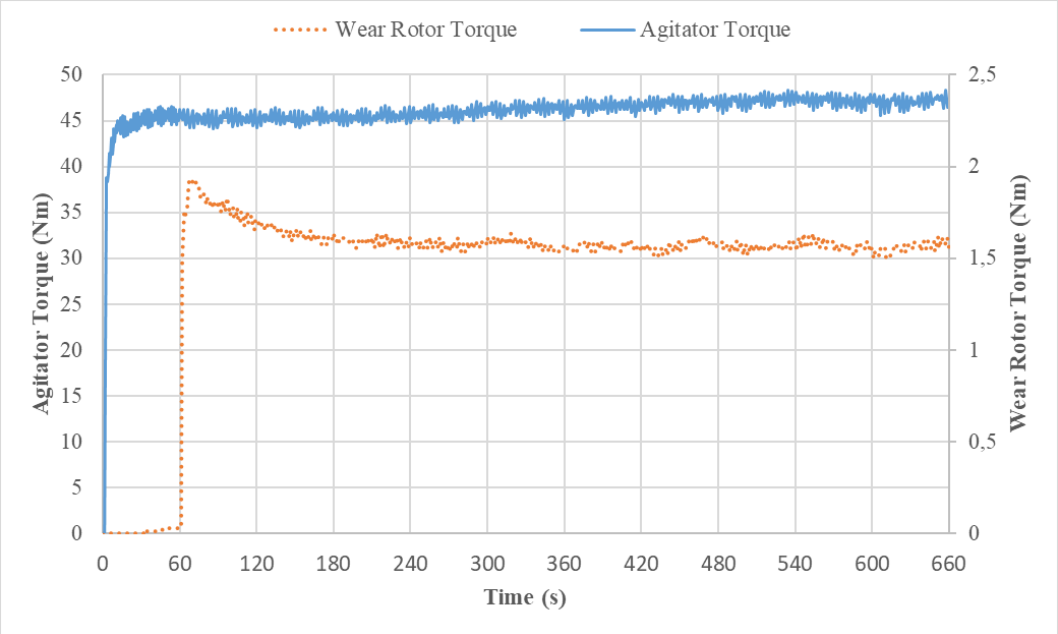

Figure 151. Example of agitator and wear rotor torque values obtained with the Pressurized Rotating Mixer method for an unconditioned soil.

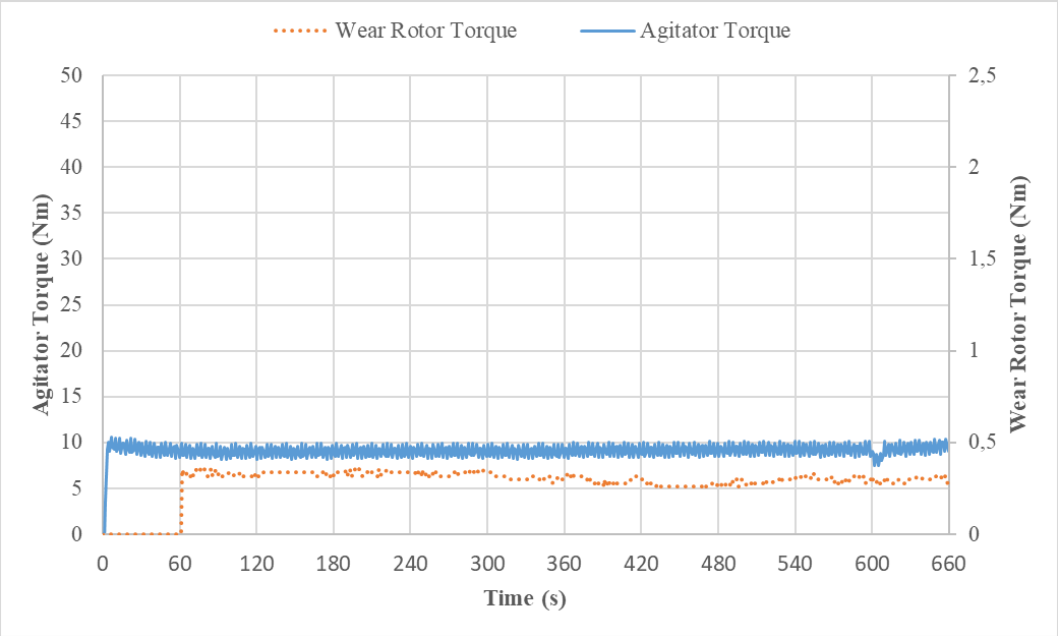

Figure 152. Example of agitator and wear rotor torque values obtained with the Pressurized Rotating Mixer method for a conditioned soil.

8.4.1 Quartz sand

a) Variability in water content of soils

This assessment allows studying the influence of soil water content on discs wear. The used range was between 2% and 15% (between the natural and the saturation limit). The procedure was performed using two soil confinement pressures: 0 and 4 bar. Results of all measurements using different water contents in Quartz sand are summarized in Table 50. In Figure 153, the disc weight loss results are illustrated. In Figure 154 and Figure 155, the agitator and wear rotor torque values are shown, respectively.

b) Use of foam

The optimal conditioning set (Paragraph 7.1.1) was evaluated in order to compare the conditioned soil behaviour at different pressures with this test method. The obtained results are summarized in Table 51 and are plotted along with the unconditioned soil results in Figure 153, Figure 154 and Figure 155

Table 50. Test results for different water contents of Quartz sand.

Pressure (bar)	Total water content (% by weight)	Weight loss (g)	Average Weight loss (g)	Agitator Torque (Nm)	Average Agitator Torque (Nm)	Wear Rotor Torque (Nm)	Average Wear Rotor Torque (Nm)
0	2	3,220	3,297	64,068	65,933	1,671	1,684
		3,370		67,517		1,586	
		3,300		66,214		1,794	
	5	4,940	5,297	91,141	90,909	1,432	1,335
		5,300		90,678		1,317	
		5,650		90,908		1,255	
	10	1,190	1,227	30,578	30,038	2,147	2,251
		1,440		30,373		2,506	
		1,050		29,163		2,099	
	15	0,440	0,447	19,619	17,556	0,474	0,510
		0,500		16,871		0,564	
		0,400		16,179		0,492	
4	2	3,260	3,153	68,178	68,335	1,647	1,549
		3,300		70,853		1,971	
		2,900		65,974		1,030	
	5	4,970	4,743	96,613	93,534	1,644	1,438
		4,500		80,346		1,087	
		4,760		103,644		1,582	
	10	0,510	0,497	21,725	20,072	2,208	1,956
		0,480		18,377		1,624	
		0,500		20,113		2,037	
	15	0,220	0,213	17,317	15,447	0,634	0,620
		0,200		14,496		0,911	
		0,220		14,528		0,317	

Table 51. Test results for different water contents of conditioned Quartz sand.

Pressure (bar)	Weight loss (g)	Average Weight loss (g)	Agitator Torque (Nm)	Average Agitator Torque (Nm)	Wear Rotor Torque (Nm)	Average Wear Rotor Torque (Nm)
0	0,090	0,093	8,373	8,838	0,284	0,234
	0,090		9,128		0,190	
	0,100		9,014		0,229	
4	0,300	0,273	15,970	15,594	1,183	1,075
	0,280		15,737		1,044	
	0,240		15,074		0,997	

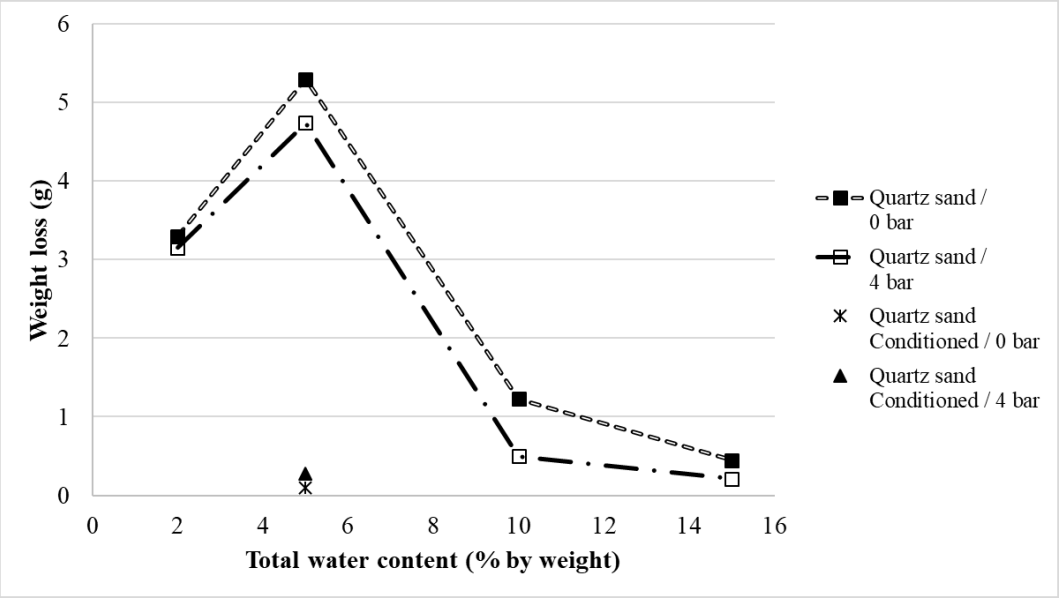

Figure 153. Weight loss average correlated to water content of Quartz sand.

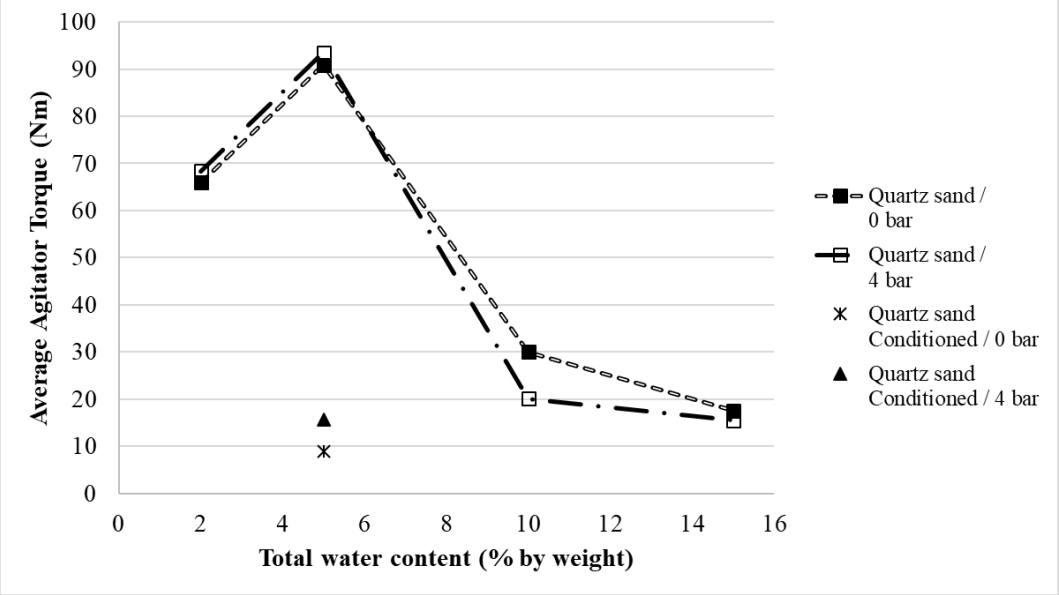

Figure 154. Average Agitator Torque correlated to water content of Quartz sand.

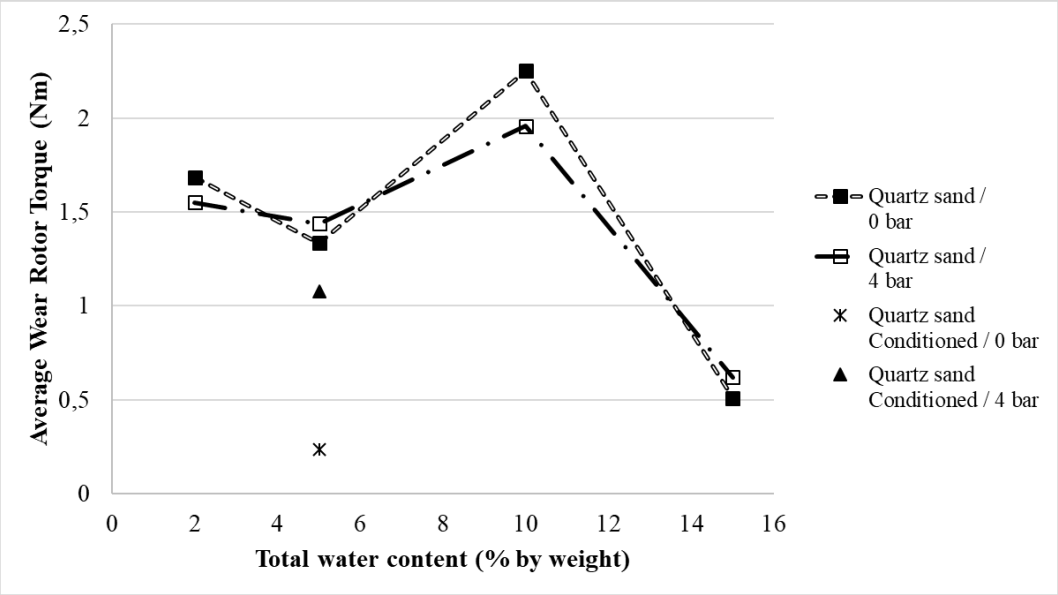

Figure 155. Average Wear Rotor Torque correlated to water content of Quartz sand.

c) Study of Pressures

In order to evaluate the influence of pressure, values obtained from Table 50 and Table 51 were plotted as a function of the applied pressures. Graphic representations are shown in Figure 156, Figure 157 and Figure 158.

The weight loss shows a slight reduction for the unconditioned soil while a slight increase for the conditioned soil is observed. In any case, these small variations are not numerically significant and can therefore be considered as invariant.

In most cases, when the ground pressure grows, there is a small increment in the agitator and wear rotor torque values in relation to the recorded average value. Therefore, these torque values are also considered as numerically insignificant, with the exception of wear rotor torque for the conditioned soil that increases more than twice and so it is considered significant.

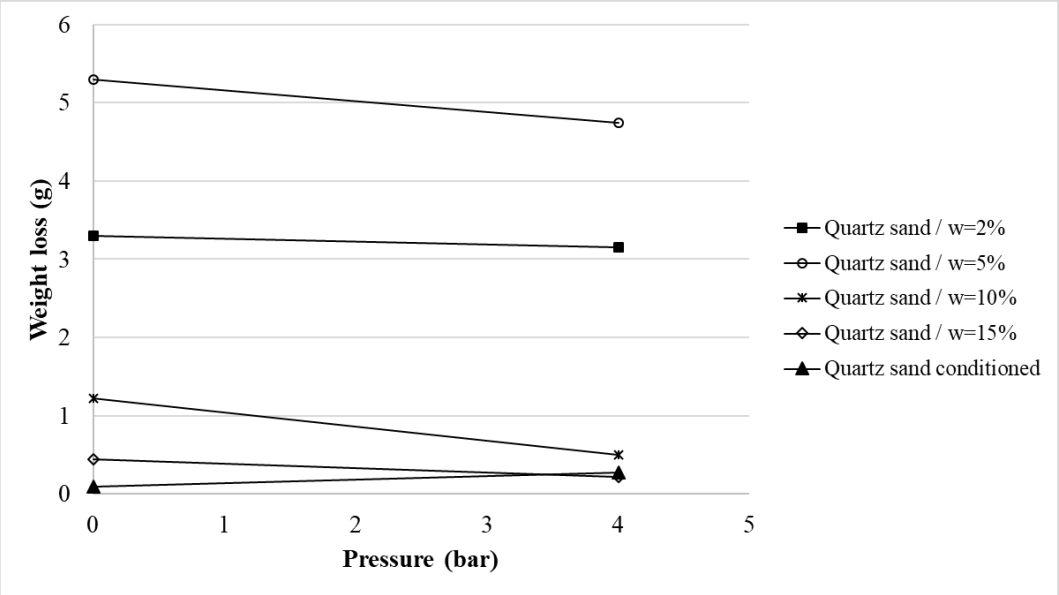

Figure 156. Weight loss average correlated to confinement pressure of Quartz sand.

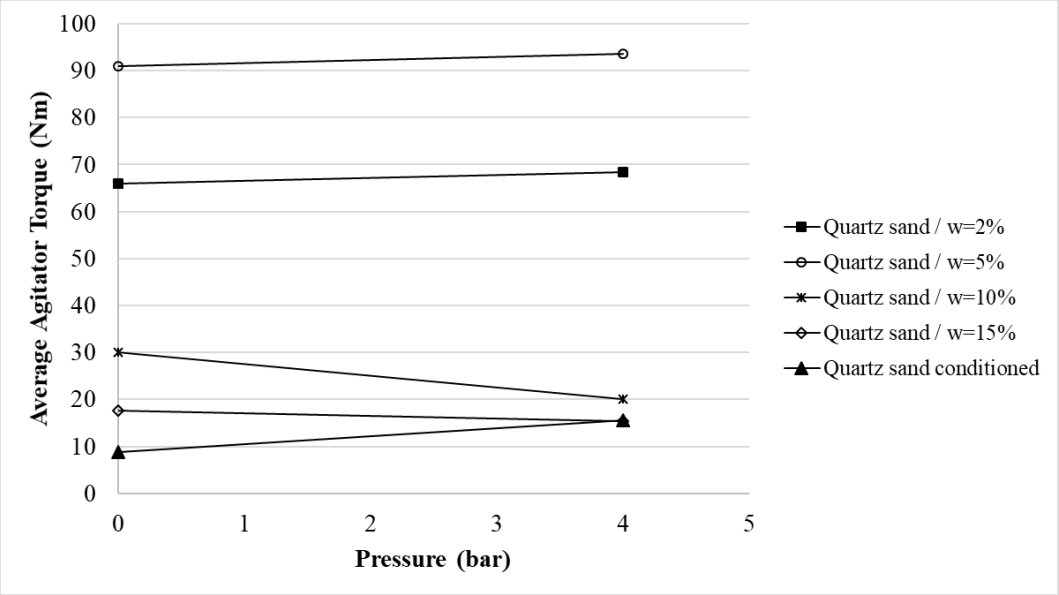

Figure 157. Average Agitator Torque correlated to confinement pressure of Quartz sand.

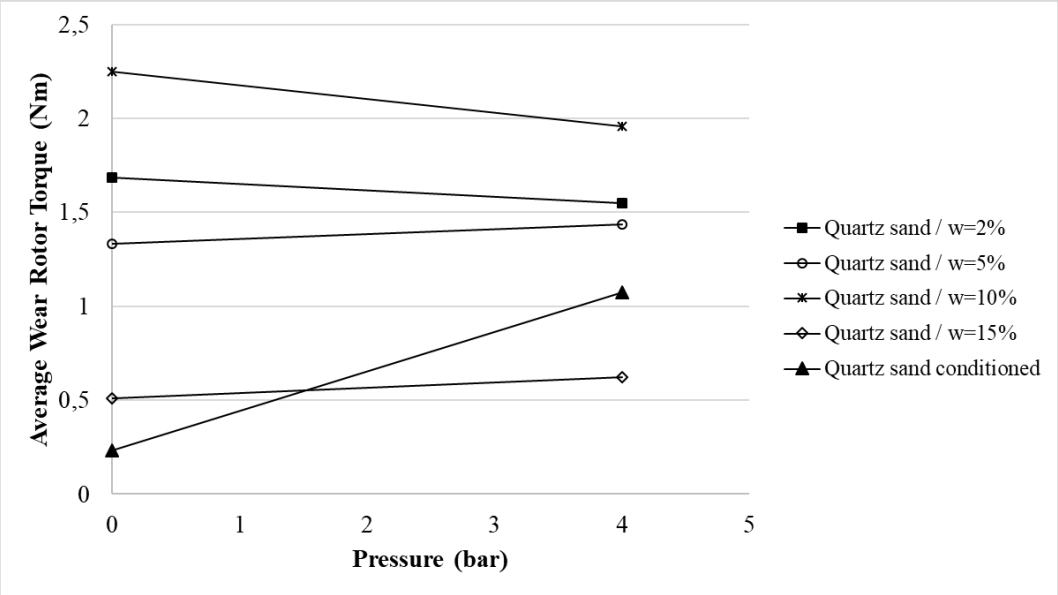

Figure 158. Average Wear Rotor Torque correlated to confinement pressure of Quartz sand.

8.4.2 CC sand

a) Variability in water content of soils

This assessment allows studying the influence of soil water content on discs wear. The used range was between 0.8% and 8%. The procedure was performed using two soil confinement pressures: 0 and 3 bar. Results of all measurements using different water contents in CC sand are summarized in Table 52. In Figure 159, the disc weight loss results are illustrated. In Figure 160 and Figure 161, the agitator and wear rotor torque values are shown, respectively.

b) Use of foam

The optimal conditioning set (Paragraph 7.1.2) was evaluated in order to compare the conditioned soil behaviour at different pressures with this test method. The obtained results are summarized in Table 53 and are plotted along with the unconditioned soil results in Figure 159, Figure 160 and Figure 161.

Table 52. Test results for different water contents of CC sand

Pressure (bar)	Total water content (% by weight)	Weight loss (g)	Average Weight loss (g)	Agitator Torque (Nm)	Average Agitator Torque (Nm)	Wear Rotor Torque (Nm)	Average Wear Rotor Torque (Nm)
0	0,8	0,400	0,377	40,690	41,852	1,114	0,996
		0,360		44,181		0,909	
		0,370		40,684		0,964	
	4	0,330	0,383	42,370	44,159	0,954	1,122
		0,390		43,161		1,089	
		0,430		46,947		1,324	
	8	0,350	0,330	42,314	44,886	0,855	0,834
		0,300		46,530		0,943	
		0,340		45,815		0,706	
3	0,8	0,370	0,370	44,256	45,357	1,482	1,537
		0,360		45,788		1,594	
		0,380		46,029		1,534	
	4	0,440	0,477	45,318	47,595	1,541	1,513
		0,480		49,147		1,397	
		0,510		48,319		1,601	
	8	0,340	0,347	51,098	50,453	1,344	1,381
		0,400		50,569		1,540	
		0,300		49,693		1,259	

Table 53. Test results for different water contents of conditioned CC sand

Pressure (bar)	Weight loss (g)	Average Weight loss (g)	Agitator Torque (Nm)	Average Agitator Torque (Nm)	Wear Rotor Torque (Nm)	Average Wear Rotor Torque (Nm)
0	0,040	0,047	5,958	7,022	0,407	0,355
	0,060		9,091		0,307	
	0,040		6,018		0,351	
0,5	0,100	0,103	20,873	21,042	0,991	1,004
	0,090		25,155		1,076	
	0,120		17,098		0,944	
1,5	0,090	0,097	30,965	31,822	1,467	1,393
	0,100		32,853		1,319	
	0,100		31,648		1,394	
2	0,098	0,103	35,137	35,793	1,390	1,454
	0,100		36,028		1,440	
	0,110		36,214		1,531	
3	0,150	0,127	36,396	40,448	1,402	1,454
	0,140		32,414		1,581	
	0,100		47,118		1,479	
	0,120		45,863		1,353	
4,5	0,100	0,097	32,401	32,384	1,971	1,905
	0,090		31,056		1,772	
	0,100		33,696		1,974	
6	0,130	0,113	45,336	39,627	1,513	1,556
	0,100		37,403		1,618	
	0,110		36,143		1,537	

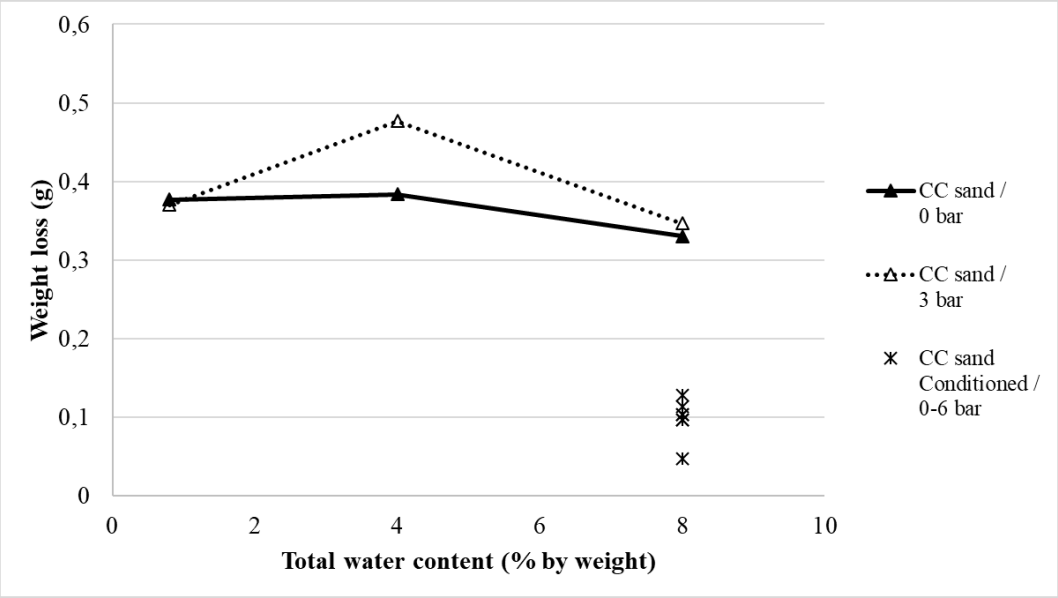

Figure 159. Weight loss average correlated to water content of CC sand.

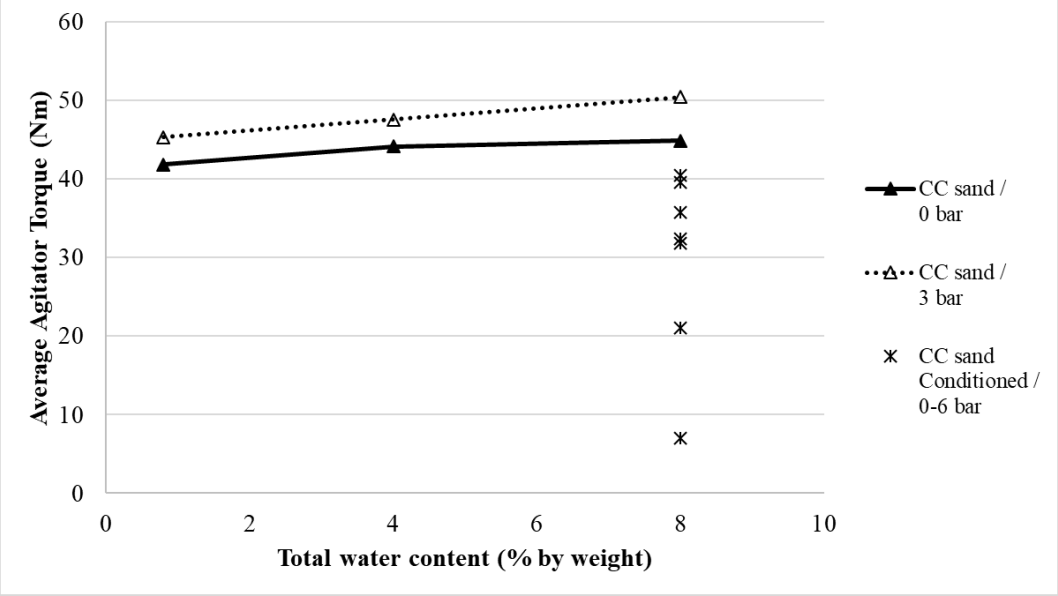

Figure 160. Average Agitator Torque correlated to water content of CC sand.

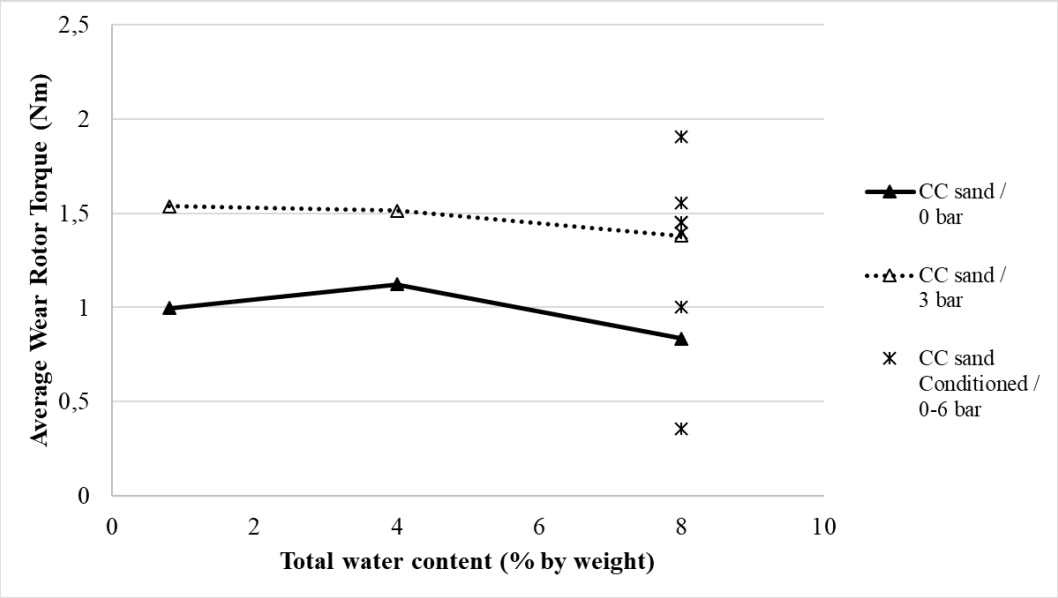

Figure 161. Average Wear Rotor Torque correlated to water content of CC sand.

c) Study of Pressures

In order to evaluate the influence of pressure, values obtained from Table 52 and Table 53 were plotted as a function of the applied pressures. Graphic representations are shown in Figure 162, Figure 163 Figure 164.

In general, the weight loss shows a slight increase when soil pressure is incremented.

It is important to mention that this increase in weight loss remains almost constant in the conditioned soil for the different pressures applied once they have been increased from 0 bar to 0.5 bar. In other words, there is a growth of about twice in weight loss with the application of pressure, regardless its magnitude.

On the other hand, for unconditioned or conditioned soil, the agitator and wear rotor torques increase while the soil pressure rises.

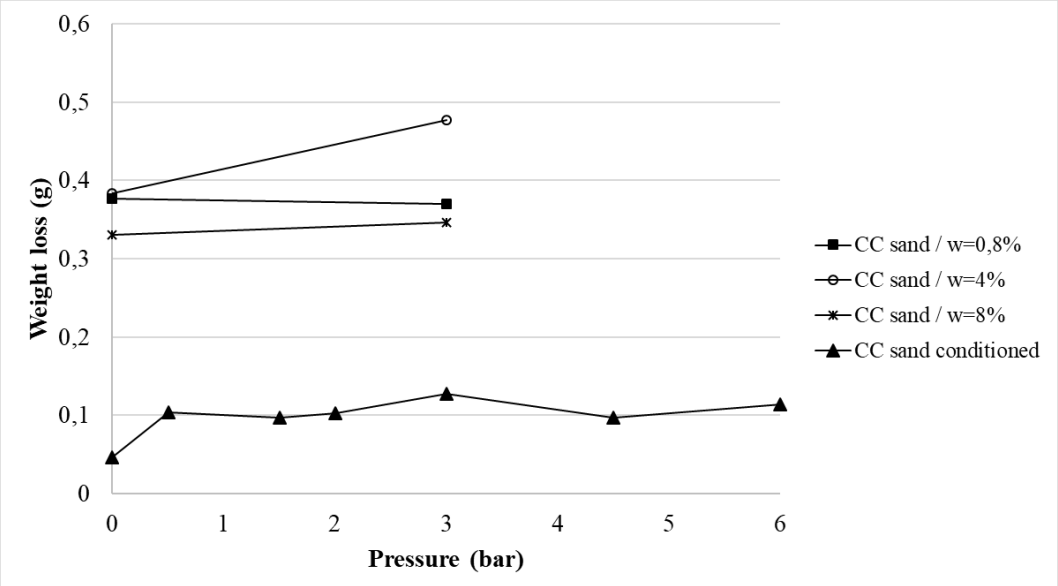

Figure 162. Weight loss average correlated to confinement pressure of CC sand.

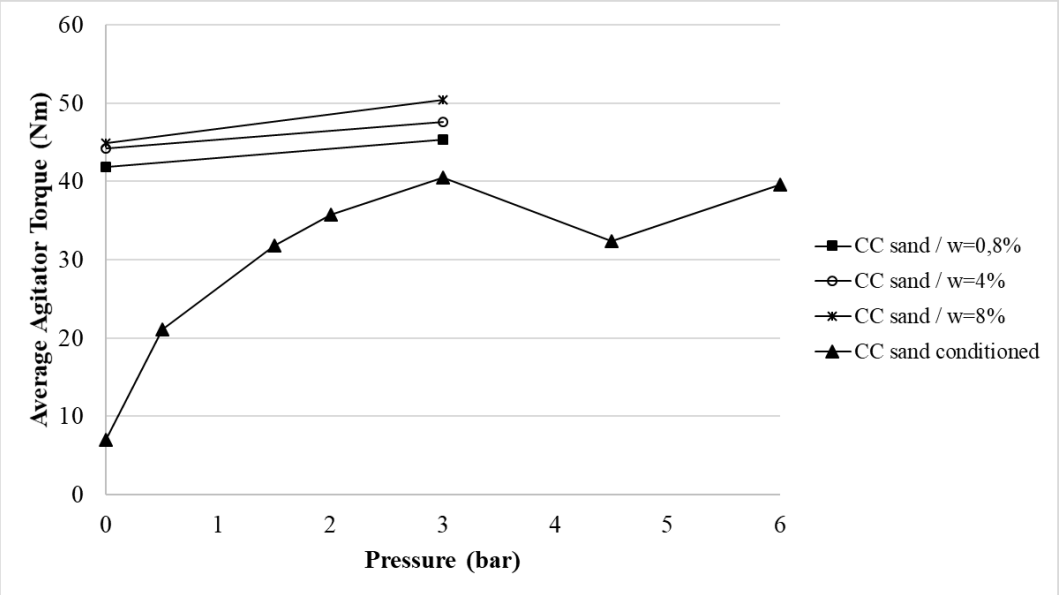

Figure 163. Average Agitator Torque correlated to confinement pressure of CC sand.

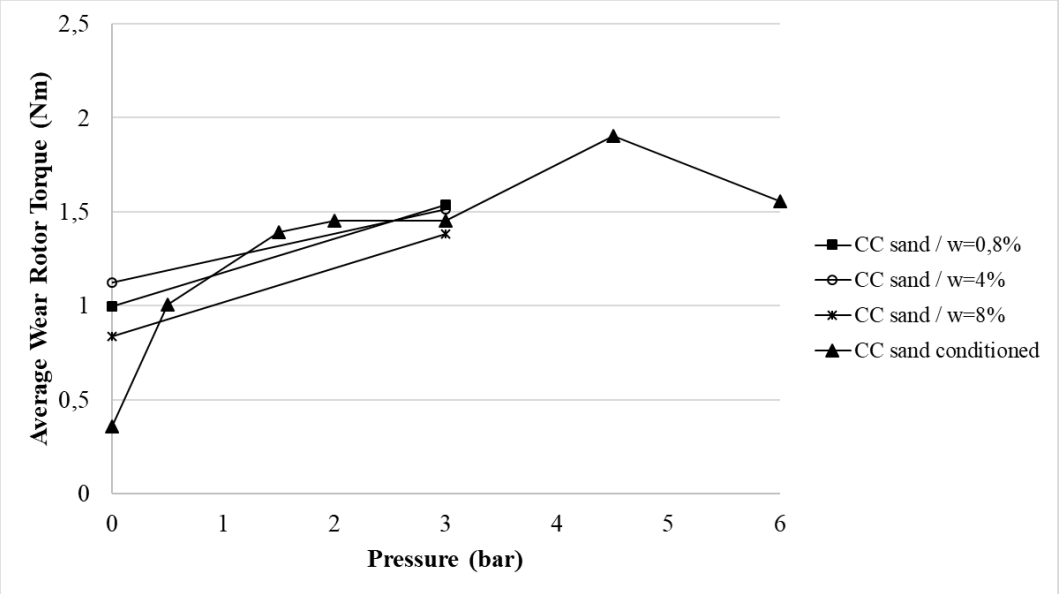

Figure 164. Average Wear Rotor Torque correlated to confinement pressure of CC sand.

Chapter 9

Conclusions

In tunnels construction with EPB machines there are innumerable factors limiting their productivity and efficiency. One of these factors is metallic parts wear, since it involves machine downtimes for replacement or repair of the worn elements, that are typically slow work practices and sometimes can represent a risk for operators. For this reason, wear phenomenon study is essential for the design stage of new projects, since it allows to select the most convenient products and to plan the construction schedule and the related costs with higher effectiveness.

Today a standard procedure for the study of wear phenomenon caused by the ground in the excavation machines or TBM doesn't exist. Therefore, in different research centers around the world, studies are carried out in order to propose test methodologies that can be used for wear prognosis. For this thesis work, six different soils used in 474 tests (for a total of about 26200 kg) have been studied and four test methodologies have been proposed. Each methodology has different benefits, limitations and scope, but provides valuable data.

Wear Disc Test allows a swift wear analysis, being a test of easy execution that requires a relatively slight amount of time for results examination. Nevertheless, for some kind of soils this is not the most suitable methodology due to the stationary rotation of the disc and risk that voids between the disc and the soil can be formed. Due to those voids, in most of the cases the comparison between natural and conditioned soils are not consistent.

By using the Wear Disc Test, it was possible to validate the "bell" behaviour that is obtained by correlating soil water content increases to tool weight loss. Maximum wear values are found at around 10% by weight of soil water content. For all the studies performed, quartz sand exhibited the highest wear values and, as a result, it can be used as the reference material for executing the comparative method between soils.

The second method proposed and studied was the Modified Wear Disc Test. It is also a simple method that although requires more control during execution. This test allowed to solve the problem found in the Wear Disc Test (stationary rotation of the disc and formation of void). The obtained results confirmed this is a valid methodology to study wear using soils with different water contents and conditioned soils.

The use of Mapedrill FRA02C a specifically designed anti-wear polymer was studied with these first two test methodologies and demonstrated to be useful in reducing disc wear, especially for lower water contents.

The Sharp Cutter Test was developed for studying the influence of conditioning on hard metals wear. Although this is not a test of difficult execution, the data processing is demanding. By using this methodology, it is possible to observe in depth the difference between wear caused by soil conditioned with foams or unconditioned, as well as to obtain concrete and significant results in the study of wear on hard metals.

The application of execution and evaluation procedures of the Sharp Cutter Test allowed to obtain three indexes that are very useful for wear prediction and serve to compare results under different conditions. For future works, these values should be correlated to real data obtained from the excavation machines in the work field in order to improve the validity of the method.

The last proposed methodology is the use of the Pressurized Rotating Mixer. This device is difficult and demanding to implement due to the large quantities of soil needed to run the test, but it is the ideal method to study the influence of soil confinement pressures, particularly in conditioned soils.

According on the results obtained from the performed tests, it is possible to confirm that using conditioning agents have a positive effect in reducing tool wear. Furthermore, the addition of water to the soil must be studied and controlled in order to avoid reaching the ratio that corresponds to the highest wear, considering the wear curve “bell” behaviour.

Finally, the research that has been developed allowed to provide a contribution to discussion of the effects of conditioning on the wear of metallic parts of an EPB machine.

Further research could allow to compare the real site data with the laboratory ones in order to provide a result able to give a forecast of the wear on the machine even if this tests can be demanding due to the large numbers of parameters included in a real tunnel.

References

Abu Bakar, M. Z., Majeed, Y. & Rostami, J., 2016. Effects of rock water content on CERCHAR Abrasivity Index. *Wear,* p. 132–145.

Alber, M., 2017. Stress dependency of the Cerchar abrasivity index (CAI) and its effects on wear of selected rock cutting tools. *ScienceDirect,* pp. 351-359.

Alber, M. et al., 2014. ISRM Suggested Method for Determining the Abrasivity of Rock by the CERCHAR Abrasivity Test. *ROCK MECHANICS AND ROCK ENGINEERING,* pp. 261-266.

ASM, I., 1992. *ASM Handbook: Friction, Lubrication, and Wear Technology.* s.l.:s.n.

ASTM International C 143/C 143M , 2003. *Standard Test Method for Slump of Hydraulic Cement Concrete.* s.l.:s.n.

Barbero, M. et al., 2012. Procedura sperimentale per la valutazione dell'effetto del condizionamento del terreno sull'abrasione degli utensili nello scavo con EPB. *GEAM. Geoingegneria Ambientale e Mineraria,* 135(1), pp. 13-19.

Blindheim, O. T. & Bruland, A., 1998. Boreability testing. *Norwegian TBM Tunnell,* Issue 11, pp. 21-27.

Borio, L. & Peila, D., 2011. Laboratory test for EPB tunnelling assessment: results of test campaign on two different granular soils. *Gospodarka Surowcami Mineralnymi,* Issue 27, pp. 85-100.

Bosio, F. et al., 2018. The influence of microstructure on abrasive wear resistance of selected cemented carbide grades operating as cutting tools in dry and foam conditioned soil. *Wear,* Volume 394–395, pp. 203-216.

Büchi, E., Mathier, J. F. & Wyss, C., 1995. Rock abrasivity–a significant cost factor for mechanical tunnelling in loose and hard rock. *Tunnel,* 5(95), pp. 38-44.

Cerchar, 1986. The Cerchar Abrasivity Index. *Centre d'Études et des Recherches des Charbonages de France.*

Deliormanli, A. H., 2011. Cerchar abrasivity index (CAI) and its relation to strength and abrasion test methods for stones. *Construction and Building Materials,* pp. 16-21.

EcuRed, n.d. [Online]
Available at: https://www.ecured.cu/Ensayo_a_la_dureza_Vickers
[Accessed 2018].

EFNARC, 2003. The European Guidelines for Self-Compacting Concrete.

EFNARC, 2005. The European Guidelines for Self-Compacting Concrete.

Gharahbagh, E. A., Rostami, J. & Palomino, A. M., 2011. New soil abrasion testing method for soft ground tunneling applications. *Tunnelling and Underground Space Technology,* 26(5), pp. 604-613.

Herrenknecht, M., Thewes, M. & Budach, C., 2011. The development of earth pressure shields: from the beginning to the present / Entwicklung der Erddruckschilde: Von den Anfängen bis zur Gegenwart. *Geomechanics and Tunnelling,* 4(1), pp. 11-35.

Jakobsen, P. D., Bruland, A. & Dahl, F., 2013a. Review and assessment of the NTNU/SINTEF Soil Abrasion Test (SAT™) for determination of abrasiveness of soil and soft ground. *Tunnelling and underground space technology,* Issue 37, pp. 107-114.

Jakobsen, P. D., Langmaack, L., Dahl, F. & Breivik, T., 2012. Predicting the abrasivity of in situ like soils. *Tunnels & Tunnelling International,* p. 41–44.

Jakobsen, P. D., Langmaack, L., Dahl, F. & Breivik, T., 2013b. Development of the Soft Ground Abrasion Tester (SGAT) to predict TBM tool wear, torque and thrust. *Tunnelling and Underground Space Technology,* Volume 38, pp. 398-408.

Jakobsen, P. D. & Lohne, J., 2013. Challenges of methods and approaches for estimating soil abrasivity in soft ground TBM tunnelling. *Wear,* 308(1), pp. 166-173.

Käsling, H. & Thuro, K., 2010. Determining rock abrasivity in the laboratory. *Proceedings of the European Rock Mechanics Symposium EUROROCK 2010,* p. 4.

Kato, K. & Adachi, K., 2000. *MODERN TRIBOLOGY HANDBOOK.* s.l.:B. Bhushan Editor.

KEY, M., 2016. *MUSCULOSKELETAL KEY.* [Online]
Available at: https://musculoskeletalkey.com/tribology-of-the-artificial-hip-joint/
[Accessed 2018].

Khna, Z., 2015. *YourArticleLibrary.com: The Next Generation Library.* [Online]
Available at: http://www.yourarticlelibrary.com/soil/flow-of-water-through-soil-permeability-and-factors-affecting-permeability/45420/
[Accessed 2018].

Kovari, K., 2004. Safety Systems in Urban Tunnelling–The Zimmerberg Tunnel. *Int. Congress on Mechanized Tunnelling Challenging Case Histories.*

Krumbein, W. C. & Sloss, L. L., 1956. *Stratigraphy and Sedimentation.* San Francisco: Freeman and Company.

Langmaack, L. & Feng, Q., 2005. *Soil conditioning for EPB machines: balance of functional and ecological properties.* Istanbul, s.n.

Martinelli, D., 2016. *Mechanical behaviour of conditioned material for EPBS tunnelling. Phd Thesis.* s.l.:Politecnico di Torino.

Martinelli, D., Peila, D. & Campa, E., 2015. Feasibility study of tar sands conditioning for earth pressure balance tunnelling. *Journal of Rock Mechanics and Geotechnical Engineering,* 7(6), p. 684–690.

Milligan, G., 2000. State of the art review: Lubrification and Soil Conditioning. *Technical report, Geotechnical Consulting Group.*

Milligan, G., 2001. Lubrication and soil conditioning in tunnelling, pipe jacking and microtunnelling. State of the art review. *Geotechnical consulting group.*

Mosleh, M., Atnafu, N. D., Belk, J. H. & Nobles, O. M., 2009. Modification of sheet metal forming fluids with dispersed nanoparticles for improved lubrication. *Wear,* 267(5-8), pp. 1220-1225.

Naitoh, K., 1985. The development of earth pressure balanced shields in Japan. *Tunnels & tunnelling,* 17(5), p. 15–18.

Namin, F. S., Ghafari, H. & Diana, A., 2014. New model for environmental impact assessment of tunneling projects. *Journal of Environmental Protection,* 5(06), p. 530.

Nilsen, B., Dahl, F., Holzhäuser, J. & Raleigh, P., 2006a. Abrasivity of soils in TBM tunnelling. *Tunnels & Tunnelling International,* pp. 36-38.

Nilsen, B., Dahl, F., Holzhäuser, J. & Raleigh, P., 2006b. Abrasivity testing for rock and soils. *Tunnels & Tunnelling International,* pp. 47-49.

Nilsen, B., Dahl, F., Holzhäuser, J. & Raleigh, P., 2006c. SAT: NTNU's new soil abrasion test. *Tunnels & Tunnelling International,* pp. 43-45.

Nilsen, B., Dahl, F., Holzhäuser, J. & Raleigh, P., 2007. New test methodology for estimating the abrasiveness of soils for TBM tunneling. *Proceedings of the rapid excavation and tunneling conference (RETC),* pp. 104-106.

Nishitake, S., 1990. Advanced technology realize high-performance earth pressure balanced shield. *Franchissements souterrains pour l'Europe,* pp. 291-302.

Oñate Salazar, C. G. et al., 2016. Preliminary study of wear induced by granular soil on metallic parts of EPB tunnelling machines. *GEAM: Geoingegneria Ambientale e Mineraria,* pp. 67-70.

Oñate Salazar, C. G. et al., 2018. A new test device for the study of metal wear in conditioned granular soil used in EPB shield tunneling. *Tunnelling and Underground Space Technology,* Volume 73, pp. 212-221.

Ozdemir, L. & Nilsen, B., 1999. Recommended laboratory rock testing for TBM projects. *AUA News,* 14(2), pp. 21-35.

Peila, D., Oggeri, C. & Borio, L., 2009. Using the slump test to assess the behavior of conditioned soil for EPB tunneling. *Environmental & Engineering Geoscience,* 15(3), pp. 167-174.

Peila, D., Oggeri, C. & Vinai, R., 2007. Screw conveyor device for laboratory tests on conditioned soil for EPB tunneling operations. *Journal of Geotechnical and Geoenvironmental Engineering,* 133(12), pp. 1622-1625.

Peña Duarte, M. Á., 2007. *Foam as a soil conditioner in tunnelling: physical and mechanical properties of conditioned sands. PhD Thesis.* s.l.:University of Oxford.

Psomas, S., 2001. *Properties of foam/sand mixtures for tunnelling applications. Master's thesis.* s.l.:University of Oxford Michaelmas.

Psomas, S. & Houlsby, G. T., 2002. Soil conditioning for EPBM tunnelling: compressibility behaviour of foam/sand mixtures. *Geotechnical Aspects of Construction in Soft Ground, Balkema,* pp. 215-220.

Rollings, M. P., 1996. *Geotechnical materials in construction.* s.l.:McGraw-Hill Professional Publishing.

Rostami, J., Gharahbagh, E. A., Palomino, A. M. & Mosleh, M., 2012. Development of soil abrasivity testing for soft ground tunneling using shield machines. *Tunn. Undergr. Space Technol.,* Issue 28, p. 245–256.

Sowers, G. B., 1979. *Introductory soil mechanics and foundations geotehnical engineering.* 4th a cura di Ne York: Macmillan.

substech, n.d. [Online]
Available at:
http://www.substech.com/dokuwiki/doku.php?id=mechanisms_of_wear&s=wear
[Accessed 2018].

theconstructor.org, n.d. *theconstructor.org.* [Online]
Available at: https://theconstructor.org/concrete/concrete-slump-test/1558/
[Accessed 2018].

Thewes, M., Budach, C. & Bezuijen, A., 2012. Foam conditioning in EPB tunnelling. *Geotechnical Aspects of Underground Construction in Soft Ground,* p. 127.

Thewes, M., Budach, C. & Galli, M., 2010. Laboratory tests with various conditioned soils for tunnelling with earth pressure balance shield machines. *Tunnel International Journal For Subsurface Use,* 6(21).

Thuro, K. & Käsling, H., 2009. Classification of the abrasiveness of soil and rock. Klassifikation der Abrasivität von Boden und Fels. *Geomechanics and Tunnelling,* 2(2), pp. 179-188.

Thuro, K., Singer, J., Kasling, H. & Bauer, M., 2006. Soil Abrasivity assessment using the LCPC testing device. *Felsbau,* 24(6), pp. 37-45.

Thuro, K., Singer, J., Kasling, H. & Bauer, M., 2007. Determining abrasivity with the LCPC test. In 1st Canada-US Rock Mechanics Symposium. *American Rock Mechanics Association.*

Young, B. B. & Millman, A. P., 1964. Microhardness and deformation characteristics of ore minerals. *Inst. Mining Metall. Trans,* Volume 73, pp. 437-466.

Zum Gahr, K. H., 1987. Microstructure and wear of materials. *Elsevier,* Volume 10.